

Single- and Multi-Carrier CDMA
Multi-User Detection, Space-Time Spreading,
Synchronisation and Standards

by

L. Hanzo, L-L. Yang, E-L. Kuan and K. Yen

*We dedicate this monograph to the numerous contributors of this field, many
of whom are listed in the Author Index*

Title Page - for Wiley to do

Copyright Page - for Wiley to do

About the Authors



Lajos Hanzo received his degree in electronics in 1976 and his doctorate in 1983. During his career in telecommunications he has held various research and academic posts in Hungary, Germany and the UK. Since 1986 he has been with the Department of Electronics and Computer Science, University of Southampton, UK, where he holds the chair in telecommunications. He has co-authored 10 books on mobile radio communications, published about 400 research papers, organised and chaired conference sessions, presented overview lectures and has been awarded a number of distinctions. Currently he heads an academic research team, working on a range of research projects in the field of wireless multimedia communications sponsored by industry, the Engineering and Physical Sciences Research Council (EPSRC) UK, the European IST Programme and the Mobile Virtual Centre of Excellence (VCE), UK. He is an enthusiastic supporter of industrial and academic liaison and he offers a range of industrial courses. He is also an IEEE Distinguished Lecturer. For further information on research in progress and associated publications please refer to <http://www-mobile.ecs.soton.ac.uk>

Lie-Liang Yang

Other Wiley and IEEE Press Books on Related Topics ¹

- R. Steele, L. Hanzo (Ed): *Mobile Radio Communications: Second and Third Generation Cellular and WATM Systems*, John Wiley-IEEE Press, 2nd edition, 1999, ISBN 07 273-1406-8, p 1064
- L. Hanzo, W. Webb, and T. Keller, *Single- and Multi-Carrier Quadrature Amplitude Modulation: Principles and Applications for Personal Communications, WLANs and Broadcasting*. IEEE Press, 2000.
- L. Hanzo, F.C.A. Somerville, J.P. Woodard: *Voice Compression and Communications: Principles and Applications for Fixed and Wireless Channels*; IEEE Press-John Wiley, 2001, p 642
- L. Hanzo, P. Cherriman, J. Streit: *Wireless Video Communications: Second to Third Generation and Beyond*, IEEE Press, 2001, p 1093
- L. Hanzo, T.H. Liew, B.L. Yeap: *Turbo Coding, Turbo Equalisation and Space-Time Coding*, John Wiley - IEEE Press, 2002, p 751
- J.S. Blogh, L. Hanzo: *Third-Generation Systems and Intelligent Wireless Networking: Smart Antennas and Adaptive Modulation*, John Wiley - IEEE Press, 2002, p408
- L. Hanzo, C.H. Wong, M.S. Yee: *Adaptive wireless transceivers: Turbo-Coded, Turbo-Equalised and Space-Time Coded TDMA, CDMA and OFDM systems*, John Wiley - IEEE Press, 2002, p 737
- L. Hanzo, M. Münster, T. Keller, B-J. Choi: *OFDM and MC-CDMA for for Broadband Multi-user Communications, WLANs and Broadcasting*, John Wiley - IEEE Press, 2003

¹For detailed contents please refer to <http://www-mobile.ecs.soton.ac.uk>

Contents

About the Authors	v
Other Wiley and IEEE Press Books on Related Topics	viii
Acknowledgments	1
1 Prologue - Intelligent Broadband Wireless Transceivers	3
1.1 Motivation of the Book	3
1.2 Organisation and Novel Contributions of the Book	4
1.3 Introduction to Flexible Transceivers	13
1.4 FH/MC DS-CDMA	14
1.5 Characteristics of the FH/MC DS-CDMA Systems	16
1.6 Adaptive Rate Transmission	20
1.6.1 Why Adaptive Rate Transmission?	20
1.6.2 What Is Adaptive Rate Transmission?	21
1.6.3 Adaptive Rate Transmission in FH/MC DS-CDMA System	24
1.7 Software Defined Radio Assisted FH/MC DS-CDMA	24
1.8 Chapter Summary and Conclusions	28
I Multi-User Detection for Adaptive Single-Carrier CDMA	29
2 CDMA Overview	35
2.1 Introduction to Code Division Multiple Access	35
2.2 DS-CDMA transmission model	39
2.3 DS-CDMA transmitter	39
2.4 DS-CDMA receiver	39
2.4.1 Recovery of the information signal	40
2.4.2 Recovery of the information signal in multiple access interference	42
2.5 Frequency-domain representation	44
2.6 Spreading sequences	46
2.6.1 Correlation of sequences	46

2.6.2	<i>m</i> -sequences	48
2.6.3	Gold sequences	48
2.6.4	Kasami sequences	51
2.7	DS-CDMA system performance	52
2.7.1	Theoretical BER performance of asynchronous BPSK/DS-CDMA over Gaussian channels	54
2.7.2	Theoretical BER performance of bit-synchronous BPSK/DS-CDMA systems over Gaussian channels	58
2.8	Simulation results and discussion	61
2.8.1	Estimation of E_b/N_0	63
2.8.2	Simulated DS-CDMA BER performance over Gaussian channels for synchronous users	64
2.8.3	Simulated DS-CDMA BER performance versus the number of users over Gaussian channels	66
2.8.4	Simulated DS-CDMA BER performance versus spreading code length over Gaussian channels	66
2.8.5	Simulated DS-CDMA BER performance for spreading code sets having different cross-correlation values over Gaussian channels	67
2.9	Discussion	68
2.10	Multuser detection	70
2.10.1	Survey of multuser receivers	72
2.11	Chapter Summary and Conclusions	79

List of Symbols in Part I 34

3	Joint Detection of CDMA Signals	81
3.1	Basic equalizer theory	81
3.1.1	Zero-forcing equalizer	83
3.1.2	Minimum mean square error equalizer	85
3.1.3	Decision feedback equalizers	87
3.1.4	Equalizer modifications for joint detection	88
3.2	System model	89
3.3	Joint detection techniques	98
3.3.1	Whitening filter	98
3.3.2	Matched filter	99
3.3.3	Whitening matched filter	100
3.3.4	Zero Forcing Block Linear Equalizer	102
3.3.5	Minimum Mean Square Error Block Linear Equalizer	104
3.3.6	Zero Forcing Block Decision Feedback Equalizer	108
3.3.7	Minimum Mean Square Error Block Decision Feedback Equalizer	111
3.4	Complexity calculations	113
3.4.1	Whitening matched filter	114
3.4.2	Zero Forcing Block Linear Equalizer	115
3.4.3	Minimum Mean Square Error Block Linear Equalizer	118
3.4.4	Zero Forcing Block Decision Feedback Equalizer	119
3.4.5	Minimum Mean Square Error Block Decision Feedback Equalizer	120

3.5	Advantages and disadvantages of joint detection receivers	123
3.6	Experimental work on joint detection receivers	123
3.6.1	Experimental conditions	123
3.6.2	Comparison of joint detection receivers in different channels	125
3.6.3	Effect of multipath diversity	128
3.6.4	Effect of increasing the number of users, K	129
3.6.5	Joint detection and channel coding	130
3.6.6	Effect of channel estimation errors	131
3.7	Chapter Summary and Conclusions	135
4	Adaptive-Rate Joint Detection Aided CDMA	137
4.1	Introduction	137
4.2	Adaptive Quadrature Amplitude Modulation	140
4.3	Joint detection assisted AQAM based CDMA	144
4.3.1	System model	146
4.3.2	Output SINR for the joint detection receiver	147
4.3.3	Output SINR of the MMSE-BDFE	151
4.3.4	Numerical analysis of the JD-CDMA system performance	155
4.3.5	Simulation parameters	156
4.3.6	Performance of a two-user, twin-mode AQAM/JD-CDMA system	157
4.3.7	Performance comparisons of a twin-mode AQAM/JD-CDMA system for various number of users	161
4.3.8	Performance of a two-user, triple-mode AQAM/JD-CDMA system	162
4.3.9	Performance comparisons of a triple-mode AQAM/JD-CDMA sys- tem for various number of users	164
4.3.10	Performance of a five-mode AQAM/JD-CDMA system	166
4.3.11	Effect of imperfect SINR estimation on AQAM performance	170
4.3.12	Discussion	176
4.4	Variable Spreading Factor based adaptive-rate CDMA	178
4.4.1	System model	180
4.4.2	Simulation results	182
4.5	Comparison of AQAM/JD-CDMA and VSF/JD-CDMA	184
4.6	Combining AQAM and VSF with JD-CDMA	187
4.7	Chapter Summary and Conclusions	189
5	Adaptive-Rate Interference Cancellation Assisted CDMA	191
5.1	Successive interference cancellation	191
5.1.1	Complexity calculations	193
5.1.2	BER performance of SIC-CDMA	194
5.1.3	Adaptive-rate SIC-CDMA	198
5.1.4	AQAM/SIC-CDMA	200
5.1.5	VSF/SIC-CDMA	206
5.2	Parallel interference cancellation	208
5.2.1	Complexity calculations	209
5.2.2	BER performance of PIC-CDMA	211
5.2.3	Adaptive-rate PIC-CDMA	212

5.2.4	AQAM/PIC-CDMA	214
5.3	Comparison of JD, SIC and PIC CDMA receivers for AQAM transmission	216
5.4	Comparison of JD, SIC and PIC CDMA receivers for VSF transmission	221
5.5	Chapter Summary and Conclusions	223
6	Blind Per-Survivor Processing Aided CDMA	225
6.1	Blind PSP for bit-synchronous CDMA data detection and multipath CIR estimation	227
6.2	Tree-search algorithm for data sequence detection	228
6.3	Metric calculation	229
6.4	Adaptive Recursive Least Squares multipath CIR estimator	231
6.5	Blind PSP receiver performance	236
6.6	PSP with turbo coding	240
6.7	Chapter Summary and Conclusions	243
7	Space-Time Spreading Aided Single-Carrier Wideband CDMA	247
7.1	Motivation	247
7.2	System Model	249
7.2.1	Transmitted Signal	249
7.2.2	Channel Model	252
7.2.3	Receiver Model	254
7.3	Detection of Space-Time Spreading W-CDMA Signals	254
7.4	BER Performance	257
7.4.1	BER Analysis	257
7.4.2	Numerical Results and Discussions	259
7.5	Adaptive Space-time Spreading	262
7.6	Chapter Summary and Conclusions	268
II	Genetic Algorithm Assisted Multiuser Detection	271
8	Overview of Genetic Algorithms Invoked for Multiuser Detection	277
8.1	An Introduction to Genetic Algorithms	278
8.2	Genetic Algorithms at Work	282
8.3	Why do GA work?	285
8.3.1	Optimisation from a Human's Perspective	286
8.3.2	Optimisation from a GA's Perspective	287
8.3.2.1	Effects of Selection on the Schemata	288
8.3.2.2	Effects of Crossover on the Schemata	289
8.3.2.3	Effects of Mutation on the Schemata	290
8.4	Elements of Genetic Algorithms	291
8.4.1	Representation	291
8.4.1.1	Binary Encoding	291
8.4.1.2	Gray Encoding	291
8.4.2	Selection	292
8.4.2.1	Fitness-proportionate Selection	293
8.4.2.2	Sigma Scaling	293

8.4.2.3	Linear Ranking Selection	294
8.4.2.4	Tournament Selection	294
8.4.2.5	Incest Prevention	294
8.4.3	Crossover	295
8.4.3.1	Single-point Crossover	295
8.4.3.2	Double-point Crossover	295
8.4.3.3	Uniform Crossover	296
8.4.4	Mutation	296
8.4.4.1	Mutation of binary decision variables	297
8.4.4.2	Mutation of real-valued decision variables	297
8.4.5	Elitism	297
8.4.6	Termination Criterion	298
8.5	Survey of Genetic Algorithm-Assisted CDMA Multiuser Detection	298
8.6	Chapter Summary and Conclusions	301
List of Symbols in Part II		302
9	GA-Assisted Multiuser Detection for Synchronous CDMA	303
9.1	Introduction	303
9.2	Synchronous CDMA System Model	304
9.3	Discrete-Time Synchronous CDMA Model	307
9.4	Optimum Multiuser Detector for Synchronous CDMA Systems	308
9.5	Experimental Results	310
9.5.1	Effects of the Population Size	311
9.5.2	Effects of the Probability of Mutation	313
9.5.3	Effects of the Choice of Crossover Operation	314
9.5.4	Effects of Incest Prevention and Elitism	316
9.5.5	Effects of the Choice of Selection Schemes	317
9.5.6	Effects of a Biased Generated Population	320
9.6	Simulation Results	325
9.6.1	AWGN Channel	325
9.6.2	Single-path Rayleigh Fading Channel	327
9.7	Chapter Summary and Conclusions	331
10	Joint GA-Assisted Channel Estimation and Symbol Detection	335
10.1	Introduction	335
10.2	System Model	336
10.3	Joint GA-assisted Multiuser Channel Estimation and Symbol Detection	339
10.3.1	Initialisation	340
10.3.2	Effects of the Mating Pool Size	341
10.3.3	Effects of the Mutation Size	344
10.4	Simulation Results	348
10.5	Chapter Summary and Conclusions	351

11 GA-Assisted, Antenna Diversity Aided Multiuser Detection	357
11.1 Introduction	357
11.2 System Model	358
11.3 GA-Assisted Diversity-Aided Multiuser Detection	360
11.3.1 Direct Approach	362
11.3.2 Pareto Optimality Approach	362
11.4 Simulation Results	363
11.5 Chapter Summary and Conclusions	367
12 GA-Assisted Multiuser Detection for Asynchronous CDMA	371
12.1 Introduction	371
12.2 Asynchronous CDMA System Model	373
12.3 GA-Assisted Multiuser Detection in Asynchronous CDMA Systems	378
12.3.1 Matched Filter-Assisted EEB Estimation	380
12.3.2 GA-Assisted EEB Estimation	381
12.3.3 Complexity Issues	382
12.4 Simulation Results	382
12.4.1 Effects of the Mating Pool Size	383
12.5 Chapter Summary and Conclusions	388
III M-ary Single-Carrier CDMA	393
13 Non-Coherent M-ary Orthogonal Modulation in CDMA	395
13.1 Background	395
13.2 Introduction to M -ary Orthogonal Modulation	396
13.3 Fundamentals of M -ary CDMA	400
13.4 System Model	400
13.4.1 The Transmitter Model	400
13.4.2 Channel Model	402
13.4.3 The Receiver Model	402
13.5 Performance Analysis	407
13.5.1 Noise analysis	408
13.5.2 Self-interference analysis	408
13.5.3 MAI analysis	409
13.5.4 Decision Statistic and Error Probability	409
13.6 Bandwidth Efficiency in M -ary modulated CDMA	413
13.7 Numerical Simulation Results	413
13.7.1 Summary of Performance Results	419
13.8 Chapter Summary and Conclusions	420
14 RS Coded Non-coherent M-ary Orthogonal Modulation in CDMA	421
14.1 Motivation	421
14.2 System Description and Channel Model	423
14.2.1 The Transmitted Signals	423
14.2.2 The Channel Model	424
14.3 The Detection Model	425

14.3.1	Equal Gain Combining	427
14.3.2	Selection Combining	429
14.4	Average Error Probability without FEC	430
14.4.1	Equal Gain Combining	431
14.4.2	Selection Combining	431
14.5	Performance using RS forward error-correction codes	431
14.5.1	Error-Correction-Only Decoding	432
14.5.2	Errors-and-Erasures Decoding	432
14.6	Numerical Results	437
14.7	Chapter Summary and Conclusions	441
15	Residue Number System Arithmetic Invoked for M-ary CDMA	447
15.1	Introduction	447
15.2	Residue Number System Transform and Its Inverse	448
15.3	Redundant Residue Number System	453
15.4	Error-Detection and Error-Correction in RRNS	455
15.5	Chapter Summary and Conclusions	464
16	Redundant Residue Number System Coded M-ary DS-CDMA	467
16.1	State of the Art	467
16.2	Performance in AWGN channels	469
16.2.1	Communication Model	469
16.2.2	Performance of Coherent Receiver	472
16.2.2.1	Receiver Model	472
16.2.2.2	Coherent RNS-CDMA System's Probability of Error	472
16.2.2.3	Numerical Results and Analysis	477
16.2.3	Performance of Noncoherent Receiver	479
16.2.3.1	Receiver Model	479
16.2.3.2	The Noncoherent Receiver's Probability of Error	479
16.2.3.3	Numerical Results	483
16.3	Performance in Multipath Fading channels	485
16.3.1	Multipath Slow-Fading Channel Model	486
16.3.2	Performance of the Coherent RNS-Based CDMA Receiver Using Maximum Ratio Combining	487
16.3.2.1	Receiver Model	487
16.3.2.2	Decision Statistics	490
16.3.2.3	Upper-Bound of the Average Probability of Error	492
16.3.2.4	Numerical Results	493
16.3.3	Performance of Noncoherent RNS-Based DS-CDMA Receiver Us- ing Equal Gain Combining and Selection Combining	495
16.3.3.1	Receiver Model	497
16.3.3.2	Decision Statistics	500
16.3.3.3	Average Probability of Error	504
16.3.3.4	Numerical Results	506
16.4	Performance of RRNS Coded Systems	508
16.4.1	Introduction	508

16.4.2	Ratio Statistic Test	509
16.4.2.1	Probability Density Function of the Ratio Using EGC	511
16.4.2.2	Probability Density Function of the Ratio Using SC	514
16.4.3	Decoding Error Probability	519
16.4.3.1	'Error-Correction-Only' Decoding	520
16.4.3.2	'Error-Dropping-Only' Decoding	521
16.4.3.3	'Error-Dropping-and-Correction' Decoding	523
16.4.4	Numerical Results	525
16.5	Performance of Concatenated RS-RRNS Coded Systems	528
16.5.1	Concatenated RS-RRNS codes	528
16.5.2	Decoding Error Probability of RS-RRNS codes	531
16.5.3	Numerical Results	533
16.6	Chapter Summary and Conclusions	536

IV Multi-Carrier CDMA 539

17	Overview of Multicarrier CDMA	541
17.1	Introduction	541
17.2	Overview of Multicarrier CDMA Systems	542
17.2.1	Frequency-Domain Spreading Assisted Multicarrier CDMA Scheme	543
17.2.2	Orthogonal Multicarrier DS-CDMA scheme – Type I	546
17.2.3	Orthogonal Multicarrier DS-CDMA Scheme – Type II	550
17.2.4	Multitone DS-CDMA Scheme	553
17.2.5	Adaptive Frequency-Hopping Assisted multicarrier DS-CDMA scheme	556
17.2.6	Adaptive Subchannel Allocation Assisted Multicarrier DS-CDMA	558
17.2.7	Slow Frequency-Hopping Multicarrier DS-CDMA	561
17.2.8	Summary	564
17.3	Channel Model	564
17.4	Performance of MC-CDMA System	565
17.4.1	System Description	565
17.4.1.1	The Transmitter	565
17.4.1.2	Receiver	568
17.4.2	Performance Analysis	571
17.4.2.1	Noise and Interference Analysis	571
17.4.2.2	Decision Statistics and Error Probability	573
17.5	Performance of Overlapping Multicarrier DS-CDMA Systems	577
17.5.1	Preliminaries	577
17.5.2	System Description	579
17.5.2.1	Transmitted Signal	579
17.5.2.2	Receiver Model	581
17.5.3	Interference Analysis	584
17.5.4	Performance Analysis	588
17.6	Performance of Multicarrier DS-CDMA-I Systems	593
17.6.1	Decision Variable Statistics	593
17.6.2	Performance Analysis	596

17.7	Performance of AMC DS-CDMA Systems	597
17.8	Performance of SFH/MC DS-CDMA Systems	604
17.8.1	System Description	605
17.8.1.1	The Transmitted Signal	605
17.8.1.2	Channel Description	605
17.8.1.3	Receiver Model	606
17.8.2	Performance of SFH/MC DS-CDMA Using Hard-Detection	608
17.8.2.1	Probability of Error	608
17.8.2.2	Numerical Results	610
17.8.3	Blind Joint Detection of the SFH/MC DS-CDMA Signals	613
17.8.3.1	Maximum Likelihood Detection	614
17.8.3.2	Approach I	616
17.8.3.3	Approach II	616
17.8.4	Performance of SFH/MC DS-CDMA Using Soft-Detection	617
17.8.4.1	Approach I	619
17.8.4.2	Approach II	621
17.8.4.3	Numerical Results	622
17.9	Chapter Summary and Conclusions	625
18	Space-Time Spreading Assisted Broadband Multicarrier DS-CDMA	627
18.1	Motivation and Outline	627
18.2	Comparison of CDMA, MC-CDMA and MC DS-CDMA	629
18.2.1	Motivation	629
18.2.2	Introduction	629
18.2.3	Overview of CDMA Schemes Using No Frequency-Hopping	630
18.2.3.1	SC DS-CDMA	630
18.2.3.2	MC-CDMA	631
18.2.3.3	MC DS-CDMA	632
18.2.3.4	Flexibility Comparison	633
18.2.4	Broadband Wireless Communications Based on CDMA	634
18.2.4.1	Deficiencies of Broadband SC DS-CDMA and Broadband MC-CDMA	634
18.2.4.2	Using Broadband MC DS-CDMA for Supporting Ubiqui- tous Wireless Communications	637
18.2.5	Transmit Diversity Assisted MC DS-CDMA Based on STS	639
18.2.6	Capacity Improvement Based on TF-domain Spreading	642
18.2.7	Conclusions	645
18.3	Space-Time Spreading Assisted Multicarrier DS-CDMA	647
18.3.1	Introduction	647
18.3.2	System Description	649
18.3.2.1	Transmitter Model	649
18.3.2.2	Channel Model and System Parameter Design	654
18.3.2.3	Receiver Model	656
18.3.3	Bit Error Rate Analysis	657
18.3.4	Capacity Extension Using Time-Frequency-Domain Spreading	660
18.3.4.1	System Description	661

18.3.4.2	Signal Detection	663
18.3.4.3	BER Performance	666
18.3.5	Conclusions	668
18.4	Performance of Generalized MC-CDMA over Nakagami- m Channels	669
18.4.1	Motivation	669
18.4.2	Introduction	670
18.4.3	Generalized Multicarrier DS-CDMA Systems	672
18.4.3.1	Transmitted Signal	672
18.4.3.2	Channel Model	674
18.4.3.3	Receiver Model	676
18.4.4	Decision Variable Statistics	677
18.4.5	Performance Analysis	682
18.4.6	Numerical Results	685
18.4.7	Conclusions	690
18.5	Chapter Summary and Conclusions	692
19	Initial Synchronization of DS-CDMA and MC-CDMA Systems	695
19.1	Introduction	695
19.2	System Model	697
19.2.1	The Transmitted Signal	697
19.2.2	The Channel model and The Received Signal	697
19.3	Acquisition Procedure Description	699
19.3.1	Serial Search Acquisition Scheme	702
19.3.2	Parallel Acquisition Scheme	703
19.4	Asymptotic Mean Acquisition Time	704
19.4.1	Mean Acquisition Time of Serial Acquisition	704
19.4.2	Parallel Acquisition Scheme	707
19.5	Detection Performance over AWGN Channels	709
19.5.1	Statistics of the Decision Variables	710
19.5.2	Probabilities of False-Alarm and Overall Missing for the Serial Search Acquisition Scheme	714
19.5.3	Overall Detection, Missing and False-Alarm Probabilities of The Parallel Acquisition Scheme	717
19.6	Detection Performance over Multipath Fading Channels	722
19.6.1	Statistics of Decision Variables	722
19.6.2	Probabilities of Overall Missing and False-Alarm for the Serial Acquisition Scheme	727
19.6.3	Probabilities of Overall Successful Detection, Overall Missing and Overall False-Alarm for the Parallel Search Based Acquisition Scheme	731
19.7	Serial Search Using Multicell Joint Detection	735
19.7.1	Joint Two-Cell Detection Model	736
19.7.2	Detection Performance over AWGN Channels	739
19.7.3	Detection Performance over Dispersive Multipath Rayleigh Fading Channels	747
19.7.3.1	Conditional Probability Density Functions	747

19.7.3.2	Probabilities of Overall Missing and False-Alarm for Joint Two-Cell Detection	749
19.8	Code-Acquisition in Multi-Carrier DS-CDMA System	757
19.8.1	System Model	758
19.8.1.1	The transmitter	758
19.8.1.2	Code-Acquisition Description	760
19.8.2	Decision Variable Statistics	762
19.8.2.1	Equal Gain Combining	764
19.8.2.2	Selection Combining	764
19.8.3	Probability of Detection, Missing and False-Alarm	765
19.8.3.1	Equal Gain Combining	765
19.8.3.2	Selection Combining	766
V	Standards and Networking	773
20	Third-Generation CDMA Systems	775
20.1	Introduction	775
20.2	Third-Generation Systems	776
20.2.1	Introduction	776
20.2.2	UMTS Terrestrial Radio Access (UTRA)	777
20.2.2.1	Characteristics of UTRA	778
20.2.2.2	Transport Channels	781
20.2.2.3	Physical Channels	782
20.2.2.3.1	Dedicated Physical Channels	783
20.2.2.3.2	Common Physical Channels	784
20.2.2.3.2.1	Common Physical Channels of the FDD Mode	784
20.2.2.3.2.2	Common Physical Channels of the TDD Mode	788
20.2.2.4	Service Multiplexing and Channel Coding in UTRA	790
20.2.2.4.1	CRC Attachment	791
20.2.2.4.2	Transport Block Concatenation	791
20.2.2.4.3	Channel-Coding	794
20.2.2.4.4	Radio Frame Padding	794
20.2.2.4.5	First Interleaving	794
20.2.2.4.6	Radio Frame Segmentation	794
20.2.2.4.7	Rate Matching	794
20.2.2.4.8	Discontinuous Transmission Indication	795
20.2.2.4.9	Transport Channel Multiplexing	795
20.2.2.4.10	Physical Channel Segmentation	795
20.2.2.4.11	Second Interleaving	795
20.2.2.4.12	Physical Channel Mapping	795
20.2.2.4.13	Mapping Several Multirate Services to the UL Dedicated Physical Channels in FDD Mode	796

20.2.2.4.14	Mapping of a 4.1 Kbps Data Service to the DL DPDCH in FDD Mode	797
20.2.2.4.15	Mapping Several Multirate Services to the UL Dedicated Physical Channels in TDD Mode	798
20.2.2.5	Variable-Rate and Multicode Transmission in UTRA	798
20.2.2.6	Spreading and Modulation	801
20.2.2.6.1	Orthogonal Variable Spreading Factor Codes	802
20.2.2.6.2	Uplink Scrambling Codes	805
20.2.2.6.3	Downlink Scrambling Codes	805
20.2.2.6.4	Uplink Spreading and Modulation	805
20.2.2.6.5	Downlink Spreading and Modulation	807
20.2.2.7	Random Access	808
20.2.2.7.1	Mobile-Initiated Physical Random Access Procedures	808
20.2.2.7.2	Common Packet Channel Access Procedures	809
20.2.2.8	Power Control	809
20.2.2.8.1	Closed-Loop Power Control in UTRA	809
20.2.2.8.2	Open-Loop Power Control in TDD Mode	810
20.2.2.9	Cell Identification	810
20.2.2.9.1	Cell Identification in the FDD Mode	810
20.2.2.9.2	Cell Identification in the TDD Mode	813
20.2.2.10	Handover	814
20.2.2.10.1	Intra-Frequency Handover or Soft Handover	814
20.2.2.10.2	Inter-Frequency Handover or Hard Handover	815
20.2.2.11	Intercell Time Synchronisation in the UTRA TDD Mode	816
20.2.3	The cdma2000 Terrestrial Radio Access	816
20.2.3.1	Characteristics of cdma2000	818
20.2.3.2	Physical Channels in cdma2000	819
20.2.3.3	Service Multiplexing and Channel Coding	821
20.2.3.4	Spreading and Modulation	822
20.2.3.4.1	Downlink Spreading and Modulation	822
20.2.3.4.2	Uplink Spreading and Modulation	823
20.2.3.5	Random Access	823
20.2.3.6	Handover	827
20.2.4	Performance-Enhancement Features	828
20.2.4.1	Downlink Transmit Diversity Techniques	828
20.2.4.1.1	Space Time Block Coding-Based Transmit Di- versity	828
20.2.4.1.2	Time-Switched Transmit Diversity	828
20.2.4.1.3	Closed-Loop Transmit Diversity	829
20.2.4.2	Adaptive Antennas	829
20.2.4.3	Multi-User Detection/Interference Cancellation	829
20.3	Chapter Summary and Conclusions	830

21 Adaptive Rate DS-CDMA Networks Using VSFs	839
21.1 Motivation	839
21.2 Introduction	840
21.3 System Overview	841
21.4 Adaptive Transmission Scheme	845
21.5 Throughput and BER Analysis	847
21.6 Numerical Results and Discussions	852
21.7 Chapter Summary and Conclusions	856
22 Book Summary and Conclusions	859
22.1 Part I	859
22.2 Part II	869
22.3 Part III	871
22.4 Part IV	873
22.5 Part V	874
A Appendix of Chapter 13	875
A.1 Derivation of Equations 13.26 and 13.27	875
A.1.1 In-phase channel	875
A.1.2 Quadrature channel	877
A.2 Derivation of Equation 13.42	877
B Appendix of Chapter 14	881
C Appendix of Chapter 19	883
D Appendix of Chapter 16	885
D.1 Probability Density Function of the λ -th Maximum	885
D.2 Decision PDFs under the hypotheses of H_1 and H_2	886
D.2.1 PDFs under the hypothesis H_1	887
D.2.2 PDFs under the hypothesis H_0	888
Glossary	891
Bibliography	896

Acknowledgments

We are indebted to our many colleagues who have enhanced our understanding of the subject, in particular to Prof. Emeritus Raymond Steele. These colleagues and valued friends, too numerous to be mentioned, have influenced our views concerning various aspects of wireless multimedia communications. We thank them for the enlightenment gained from our collaborations on various projects, papers and books. We are grateful to Steve Braithwaite, Jan Brecht, Jon Blogh, Marco Breiling, Marco del Buono, Sheng Chen, Peter Cherriman, Stanley Chia, Byoung Jo Choi, Joseph Cheung, Sheyam Lal Dhomeja, Dirk Didascalou, Lim Dongmin, Stephan Ernst, Peter Fortune, Eddie Green, David Greenwood, Hee Thong How, Thomas Keller, Ee Lin Kuan, W. H. Lam, C. C. Lee, Xiao Lin, Chee Siong Lee, Tong-Hooi Liew, Matthias Münster, Vincent Roger-Marchart, Jason Ng, Michael Ng, M. A. Nofal, Jeff Reeve, Redwan Salami, Clare Somerville, Rob Stedman, David Stewart, Jürgen Streit, Jeff Torrance, Spyros Vlahoyiannatos, William Webb, Stephan Weiss, John Williams, Jason Woodard, Choong Hin Wong, Henry Wong, James Wong, Lie-Liang Yang, Bee-Leong Yeap, Mong-Suan Yee, Kai Yen, Andy Yuen, and many others with whom we enjoyed an association.

We also acknowledge our valuable associations with the Virtual Centre of Excellence (VCE) in Mobile Communications, in particular with its chief executive, Dr Walter Tuttlebee, and other leading members of the VCE, namely Dr Keith Baughan, Prof. Hamid Aghvami, Prof. Ed Candy, Prof. John Dunlop, Prof. Barry Evans, Prof. Peter Grant, Dr Mike Barnard, Prof. Joseph McGeehan, Prof. Steve McLaughlin and many other valued colleagues. Our sincere thanks are also due to the EPSRC, UK for supporting our research. We would also like to thank Dr Joao Da Silva, Dr Jorge Pereira, Dr Bartholome Arroyo, Dr Bernard Barani, Dr Demosthenes Ikonomou, Dr Fabrizio Sestini and other valued colleagues from the Commission of the European Communities, Brussels, Belgium.

We feel particularly indebted to Denise Harvey for her skilful assistance in correcting the final manuscript in LaTeX. Without the kind support of Mark Hammond, Sarah Hinton, Zöe Pinnock and their colleagues at the Wiley editorial office in Chichester, UK this monograph would never have reached the readers. *Finally, our sincere gratitude is due to the numerous authors listed in the Author Index — as well as to those whose work was not cited owing to space limitations — for their contributions to the state of the art, without whom this book would not have materialised.*

Lajos Hanzo, Lie-Liang Yang, Ee-Lin Kuan and Kai Yen
*Department of Electronics and Computer Science
University of Southampton*

Chapter 1

Prologue - Introduction to Intelligent Broadband Wireless Transceivers

1.1 Motivation of the Book

Against the back-cloth of the explosive expansion of the Internet and the continued dramatic increase in demand for high-speed multimedia wireless services, there is an urging demand for flexible, bandwidth-efficient transceivers. Multi-standards operation is also an important requirement for the future generations of wireless systems. In this introductory chapter we present a versatile broadband multiple access scheme, combining frequency-hopping (FH) with multicarrier DS-CDMA (FH/MC DS-CDMA). The proposed FH/MC DS-CDMA system framework is capable of meeting the requirements of future mobile wireless systems, by supporting the existing 2nd- and 3rd- generation systems, while also introducing more advanced techniques facilitated by the employment of Software Defined Radios (SDR) [1–3], and with the aid of efficient adaptive base-band algorithms [4,5]. **This generic system design framework will be used throughout the monograph as the unifying backbone of the various intelligent algorithms and systems proposed. No doubt that the concrete solutions proposed constitute only a miniscule fraction of the set of potential solutions to wireless communications problems. Our hope is however that the book will be motivational, inspiring further research and leading to more advanced wireless system solutions.**

The design of attractive wireless transceivers hinges on a range of contradictory factors, which are summarised in Figure 1.1. The essence of this illustration is that of contrasting the conflicting design factors of wireless systems from different perspectives. For example, given a certain wireless channel, it is always feasible to design a transmission scheme capable of further increasing the achievable transmission integrity at the cost of invoking 'smarter' and hence more sophisticated signal processing. Alternatively, the transmission integrity may be increased even without increasing the system's complexity, provided that for example the

turbo channel coding/interleaving delay can be further extended. Naturally, this is only possible in the context of delay-insensitive, ie. non-interactive data communications, but not in delay-sensitive interactive speech or video systems. It is also realistic to increase the system's integrity by invoking a more robust but lower throughput modulation scheme, as it will be demonstrated throughout this monograph, again often with the added benefit of reducing the system's complexity. Naturally, diverse system solutions accrue when optimising different features of the system.

By contrast, it is always possible to increase the achievable effective throughput of the system, if the system's target integrity may be relaxed, which facilitates the employment of an increased throughput, but more error-sensitive transmission scheme. As another design alternative to employing more robust modulation schemes when requiring a reduced target BER, the channel coding rate may be reduced, in order to increase the transmission integrity at the cost of sacrificing the effective throughput of the system. as well as increasing the system's complexity. When the fading channel's characteristics and the associated bit error statistics change, different transceiver modes may have to be activated. Furthermore, the channel's impulse response and the associated dispersion varies, as the receiver roams in different environments. The subject of this monograph is that of providing powerful solutions to these problems, with particular emphasis on various CDMA transceivers, which have found favour in all the recent third-generation wireless systems.

Our intention with the book is multi-fold:

- 1) *First, we would like to pay tribute to all researchers, colleagues and valued friends who contributed to the field. Hence this book is dedicated to them, since without their quest for better CDMA transceiver solutions this monograph could not have been conceived. They are too numerous to name here, hence they appear in the author index of the book.*
- 2) *Since at the time of writing no joint treatment of the subjects covered by this book exists, it is timely to compile the most recent advances in the field. Hence it is our hope that the conception of this monograph on the topic will present an adequate portrayal of the community's recent research efforts and spur this innovation process by stimulating further research in the wireless communications research community.*

1.2 Organisation and Novel Contributions of the Book

The book is constituted by four parts and the grade of challenge as well as the amount of knowledge assumed is gradually increasing towards the end of the book. Below, we present the outline and rationale of the monograph:

- Part I provides a detailed discourse on multiuser detection, aiming for furnishing a detailed historical perspective on the topic. Our discussions are embedded in the generic system design framework to be outlined at a later stage in this introductory chapter.
- **Chapter 2:** A basic exposition of the principles of CDMA transmission and reception is presented in this chapter. The conventional CDMA receiver, i.e. the matched filter

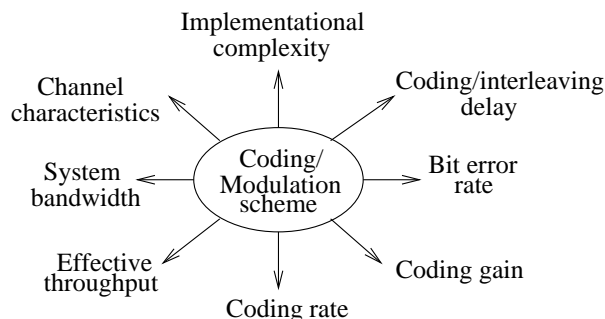


Figure 1.1: Factors affecting the design of wireless transceivers ©John Wiley and IEEE Press, 2002, Hanzo, Liew, Yeap [5]

is investigated and its performance in synchronous Gaussian channels is analyzed. The effects of various spreading sequences on the bit error rate (BER) performance are also considered. Finally, a literature survey of multiuser receivers is discussed and the various receivers are loosely classified.

- **Chapter 3:** Joint detection (JD) receivers, which constitute a class of multiuser receivers are introduced. These multiuser receivers are derived from the well-known single-user equalizers, which are used to equalize signals that have been distorted by inter-symbol interference (ISI) due to multipath channels. The adoption of these single-user equalizers is supported by the fact that the ISI inflicted by a K -path dispersive channel is similar to the multiuser interference due to K users. As a preliminary introduction to joint detection, a brief overview of single-user equalization is presented. This is followed by the portrayal of the theoretical basis of four joint detection receivers, namely the zero-forcing block linear equalizer (ZF-BLE), the minimum mean square error block linear equalizer (MMSE-BLE), zero-forcing block decision feedback equalizer (ZF-BDFE) and the minimum mean square error block decision feedback equalizer (MMSE-BDFE). The implementational complexity of these receivers is estimated and a simple method of reducing the complexity is presented. Finally, the effects of multipath diversity, channel coding and channel estimation errors on the BER performances of the JD receivers are presented and discussed.
- **Chapter 4:** In this chapter, adaptive-rate CDMA techniques are introduced, where the information rate is varied in accordance with the channel quality. The information rate is chosen accordingly, in order to provide the best trade-off between the BER and throughput performance for a given application. The signal to interference plus noise ratio (SINR) at the output of the JD receiver is derived and this parameter is used as the criterion for adapting the information rate. Two different methods of varying the information rate are considered, namely the Adaptive Quadrature Amplitude Modulated (AQAM) JD-CDMA system and the Variable Spreading Factor (VSF) JD-CDMA scheme. AQAM is an adaptive-rate technique, whereby the data modulation mode is chosen according to some criterion related to the channel quality. On the other hand, in VSF transmission, the information rate is varied by adapting the spreading factor of

the CDMA codes used, while keeping the chip rate constant. The performance of the proposed AQAM JD-CDMA and VSF JD-CDMA schemes is evaluated and discussed in relation to fixed-rate schemes. A numerical method for obtaining the BER of the JD receiver is presented, which employs the SINR at the receiver output and the associated semi-analytical performance is compared to the simulation results presented. Finally, a performance comparison between the two different adaptive-rate methods is carried out and a combined AQAM-VSF scheme is investigated.

- **Chapter 5:** Another class of multiuser receivers is considered, namely the family of interference cancellation (IC) receivers. These IC receivers are often divided into three categories, namely successive interference cancellation (SIC), parallel interference cancellation (PIC) and hybrid IC, which is a combination of the former two. Here, the SIC and PIC receivers are analyzed in terms of their BER performance and complexity. The performance of these receivers in adaptive-rate CDMA schemes is also investigated and again, the SINR at the output of each receiver is derived and used as the switching criterion in the adaptive schemes. Finally, performance comparisons between the IC and JD receivers are carried out.
- **Chapter 6:** A joint data detector and channel impulse response (CIR) estimator is proposed in this chapter, namely the blind Per-Survivor Processing (PSP) receiver. This receiver performs joint data detection and CIR estimation at the receiver, without the aid of training sequences. The blind PSP receiver is proposed for the bit-synchronous, multipath, multiuser scenario, where a reduced complexity tree-search-based algorithm is employed for data detection and CIR estimation is performed by adaptive Recursive Least Squares (RLS) estimators. The performance of this receiver is investigated for static, slowly-fading and fast-fading multipath channels. The PSP-CDMA receiver is also combined with error correction techniques, namely turbo convolutional coding, in order to improve the performance of the system. The performance of the turbo-coded, PSP-CDMA receiver is analyzed for various fading scenarios and the performance for various turbo-coded schemes are compared.
- **Chapter 7:** In this chapter we investigate the performance of single-carrier Wideband CDMA (W-CDMA) schemes. Furthermore, we employ space-time spreading (STS) based transmit diversity, when encountering multipath Nakagami- m fading channels, multiuser interference and background noise. Our analysis and the results will demonstrate that the diversity gains achieved by STS and those owing to multipath diversity accruing as a benefit of the channel's frequency-selectivity are independent. Furthermore, we will show that both the STS based transmit diversity and the multipath-induced receiver diversity achieved with the aid of the channel's frequency-selectivity appear to have the same order of importance and hence offer similar potential performance benefits.

We will argue, however that in certain non-dispersive indoor propagation environments the channel may have a single resolvable propagation path and hence no receiver diversity gain may be achieved. Given a fixed chip-rate associated with a constant system bandwidth, such as in the third-generation IMT2000 standard of Chapter 20, in this scenario the number of resolvable multipath components and the associated receiver diversity gain cannot be increased by increasing the chip-rate. We will argue in this

chapter that in this case the intelligent system framework proposed at a later stage in this Prologue is expected to configure itself for attaining a higher transmit diversity gain.

More specifically, based on the time-varying characteristics of the wireless communication channels, in this chapter an adaptive STS based transmission scheme is proposed and investigated, which adapts the mode of operation of its STS scheme and its corresponding data rate according to the near-instantaneous frequency-selectivity information fed back from the mobile receiver to the base station's transmitter. Our numerical results show that this adaptive STS scheme is capable of efficiently exploiting the diversity potential provided by the channel's frequency-selectivity, hence significantly improving the effective throughput of W-CDMA systems.

To elaborate a little further, since W-CDMA signals are subjected to frequency-selective fading, the number of resolvable paths at the receiver may vary over a wide range depending on the transmission environment encountered. It is shown that if the channel's grade of frequency-selectivity is sufficiently high, there is no need to employ transmit diversity. Therefore in this chapter an adaptive STS based transmission scheme is proposed for improving the throughput of W-CDMA systems. Specifically, when the number of resolvable paths is low and hence the resultant BER is higher than the required BER, then a low throughput STS-assisted transmitter mode is activated, which exhibits a high transmit diversity gain. By contrast, when the number of resolvable paths is high and hence the resultant BER is lower than the required BER, then a higher throughput STS-assisted transmitter mode is activated, which has a lower transmit diversity gain. Our numerical results will demonstrate that this adaptive STS-based transmission scheme is capable of significantly improving the effective throughput of W-CDMA systems. Specifically, the studied W-CDMA system's bitrate can be increased by a factor of three at the modest cost of requiring an extra 0.4dB or 1.2dB transmitted power in the context of the investigated urban or suburban areas, respectively.

- **Chapter 8:** Part II of the book commences with Chapter 8, which investigates the potential of genetic algorithm assisted MUD. In this chapter we continue our discourse by assuming that the reader is familiar with the basic CDMA principles. We commence our discourse by giving an overview of GAs, since the concepts of GAs are not widely known in the mobile communications community. We will present the basic functions of a GA in optimising an objective function, with the aid of a flowchart as well as an example. An insight into why a GA constitutes an efficient function optimiser is also given in the context of the schemata and the schema theorem [6]. Some of the more advanced GA processes are also highlighted here, in order to improve the efficiency of our search for the optimum solution. Finally, a survey of the GA-based CDMA multiuser detection schemes found in the current literature is conducted.
- **Chapter 9:** In this chapter, we will invoke the GA-assisted multiuser detector in a symbol-synchronous CDMA system over a simple AWGN channel as well as over a single-path Rayleigh fading channel. While this system model is not practical, it can provide us with a better insight into how certain GA operations and parameters behave in the context of our specific application, without considering the effects of the multi-

path interference and the asynchronism amongst the users. We will first define the objective function for our optimisation by deriving the correlation metric for the optimum multiuser detector. As mentioned above, the complexity of the optimum multiuser detector is exponential to the number of users and hence it is impractical to implement. Hence we will apply GAs in optimising the correlation metric, while achieving a reduction in the associated complexity. Through a series of experiments, we will attempt to find the particular GA configuration that is capable of offering a near-optimum bit error probability (BEP) performance at a reduced computational complexity, compared to that of the optimum multiuser detector. Upon determining the GA configuration that we will be adopting for our GA-assisted multiuser detection scheme, we will then investigate its BEP performance in an AWGN channel as well as in a single-path Rayleigh fading channel.

- **Chapter 10:** In Chapter 9 we have assumed that the Channel Impulse Response (CIR) coefficients are perfectly known by the receiver, which allowed us to detect the users' transmitted bits coherently. In practice, these coefficients must be estimated either blindly or with the aid of pilot symbols. By exploiting the capabilities of the GAs in dealing with both binary and floating point variables, we proposed a joint GA-assisted multiuser channel estimation and symbol detection technique in this chapter. Unlike in traditional systems, where the CIR estimation and symbol detection are usually performed by separate but inter-linked algorithms, such as the Kalman filter used for channel estimation [7] and the decorrelator for symbol detection [8], our proposed technique is capable of performing both the channel estimation and symbol detection concurrently using the same GAs. The achievable MSE of the estimated CIR coefficients as well as the BEP performance of our proposed joint GA-assisted multiuser CIR estimator and symbol detector are then evaluated using computer simulations.
- **Chapter 11:** In order to obtain a BEP performance improvement, in this chapter we evaluated the performance of the GA-assisted multiuser detector in conjunction with antenna diversity. More specifically, we investigated the BEP performance of the GA-assisted multiuser detector using two different diversity selection strategies. According to the first strategy, the so-called mating pool is created by selecting the K -bit GA individuals based on the combined figure of merits of the diversity antennas. On the other hand, we can exploit the population-based optimisation approach of the GAs and invoke the so-called Pareto optimality [9], in order to aid our search. According to this strategy, the mating pool is comprised of all non-dominated individuals. The BEP performance of the antenna diversity aided GA-assisted multiuser detector based on these two strategies is evaluated and compared for various fading scenarios.
- **Chapter 12:** The model that we have adopted in the previous GA-assisted MUD chapters was based on a symbol-synchronous CDMA system and multiuser detection is performed at the centralised base station. Unless strict timing control is employed, it is almost impossible to maintain a symbol-synchronous transmission among the users. Hence in Chapter 12 we will propose a GA-assisted multiuser detector for an asynchronous transmission environment. The correlation metric over a finite observation window is derived. The effects of the so-called edge bits, which placed a limitation on the BEP performance, must be taken into account when detection is considered over a

finite observation window. In our proposed technique, we can reduce the effects of the edge bits by attempting to estimate the tentative decisions concerning these edge bits, while at the same time detecting the desired bits using the same GA. The BEP performance of our proposed scheme is then compared with that of a similar GA-assisted multiuser detector, where the edge bits are estimated using the conventional single-user matched filter.

- **Chapter 13:** The topic of Part III of the book is the investigation of M -ary CDMA schemes, which is introduced in Chapter 13 in the context of non-coherent detection. In general the transmission of known pilot signals is required for providing a coherent reference in support of coherent demodulation in a fading environment [10]. However, in the uplink, an independent pilot signal/symbol would have to be transmitted by each user for coherently demodulating each signal. This clearly reduces the efficiency of the system. Thus a more practical approach is to use non-coherent detection on the uplink, which does not require a pilot signal for estimating the phase reference [10]. This is the case in the IS-95 CDMA system [11].
- **Chapter 14:** This chapter investigates the achievable performance of a RS coded DS-CDMA system, when M -ary orthogonal signaling is employed in conjunction with a Ratio Statistic Test (RTT) based erasure insertion scheme, when communicating over multipath Rayleigh-fading channels. Two different diversity combining schemes [12], [13] - namely equal-gain combining (EGC) and selection combining (SC) - are considered and their performance is evaluated in the context of the proposed RTT based erasure insertion scheme. We derive the probability density function (PDF) of the ratio defined in the RTT conditioned on both the correct detection hypothesis (H_1) and erroneous detection hypothesis (H_0) of the received M -ary signals over multipath Rayleigh fading channels. These PDFs are then used for computing the symbol erasure probability and the random symbol error probability after erasure insertion, and finally to compute the codeword decoding error probability. These analytical results allow us to quantify the performance of the system considered using a numerical approach. Furthermore, with the aid of these analytical results, we gain an insight into the basic characteristics of Viterbi's RTT, and determine the optimum decision threshold for practical systems, since the formulae obtained can be evaluated numerically.
- **Chapter 15:** A deficiency of the previously introduced M -ary CDMA systems is that the number of correlators required at the receiver for detecting the M -ary symbols is increasing exponentially with the number of bits transmitted. In this chapter a classic number representation system, namely the so-called Residue Number System (RNS) is introduced with the intention of invoking it in the next chapter in the design of novel error correction coded M -ary CDMA system.
- **Chapter 16:** The motivation of this chapter is the substantial complexity reduction of the previously discussed M -ary CDMA receivers by decomposing each M -ary message into shorter 'symbols' with the aid of the RNS system. This allows us to use a reduced number of correlators at the receiver. More specifically, our basic approach in this chapter is that the M -ary information symbols are converted to the residue digits of an RNS and all required operations are then carried out in the RNS domain. It is

readily seen in this context that each individual M -ary symbol is mapped to a higher number of residue digits. Hence, this mapping operation can be interpreted as breaking up the M -ary symbols into U number of m_u -ary symbols, where U is the number of moduli in the RNS, where $m_u, u = 1, 2, \dots, U$ represents the moduli of the RNS.

In a somewhat simplistic, but conceptually feasible manner one could argue then that for the transmission of the U number of reduced-size m_u -ary symbols we now need only $\sum_{u=1}^U m_u < M$ correlators at the receiver, which is essentially the motivation of this chapter. Hence, in this chapter, we focus our attention on studying the performance of RNS- and Redundant RNS (RRNS) based parallel direct sequence CDMA (DS-CDMA) systems in the context of M -ary orthogonal modulation, when communicating over both Additive White Gaussian Noise (AWGN) channels and multipath fading channels.

- **Chapter 17:** The subject of Part IV of the book is multicarrier CDMA, which is introduced and classified in Chapter 17. It will be shown that there are a number of trade-offs associated with the design and employment of the various multicarrier CDMA scheme proposed in the literature. The BER performance of the various schemes is also characterised, when communicating over frequency selective Rayleigh fading channels. The chapter is concluded with various novel system design proposals invoking frequency hopping for improving the system's achievable performance.
- **Chapter 18:** Following the philosophy of the generic communications system framework proposed in the Prologue of Chapter 1, in Chapter 7 an adaptive STS-aided W-CDMA system was proposed, which was capable of adapting the mode of operation of its STS scheme and its corresponding data rate according to the near-instantaneous frequency-selectivity information fed back from the mobile receiver to the base station's transmitter. The numerical results of Chapter 7 showed that this adaptive STS scheme is capable of efficiently exploiting the diversity potential provided by the channel's frequency-selectivity, hence significantly improving the effective throughput of W-CDMA systems.

In this chapter our discussions evolve further by initially considering the advantages and disadvantages of single-carrier CDMA, MC-CDMA and MC-DS-CDMA in Section 18.2, with particular attention devoted to communicating in diverse propagation environments exhibiting a time-variant amount of dispersion. More specifically, the benefits and deficiencies of these three systems are analyzed, when aiming for supporting ubiquitous communications over a variety of propagation channels encountered in indoor, open rural, suburban and urban environments. We will demonstrate that, when communicating in such diverse environments, both SC DS-CDMA and MC-CDMA exhibit certain limitations that are hard to circumvent. By contrast, when appropriately selecting the system parameters and using transmit diversity, MC DS-CDMA becomes capable of adapting to such diverse propagation environments at a reasonable detection complexity.

Hence again, following the philosophy of the generic communications system framework proposed in the Prologue of Chapter 1, in Section 18.4 we focus our attention on MC DS-CDMA schemes using STS. Specifically, MC DS-CDMA using STS is investigated in the context of broadband communications over frequency-selective Rayleigh

fading channels. We consider a range of design issues as well as the achievable Bit Error Rate (BER) performance for the down-link (base-to-mobile communications), by assuming synchronous transmission of the user signals. We also consider the attainable capacity extension of broadband MC DS-CDMA with the advent of using Time-Frequency-domain (TF-domain) spreading. Furthermore, the detection issues of broadband MC DS-CDMA using TF-domain spreading are investigated. Our study shows that by appropriately selecting the system parameters, STS assisted broadband MC DS-CDMA is capable of supporting ubiquitous communications over various communication environments including indoor, open rural, suburban and urban areas without BER performance degradation. Furthermore, we demonstrate that STS based transmit diversity schemes can be designed according to the required diversity gain, while maintaining a near-constant BER in various communication environments, as long as frequency-selective Rayleigh fading channels are encountered.

Finally, in the spirit of the generic communications system framework proposed in the Prologue of Chapter 1, in Section 4 a class of generalized MC DS-CDMA schemes is defined and its performance is considered, when communicating over multipath Nakagami- m fading channels. In the generalized MC DS-CDMA schemes considered the spacing between two adjacent subcarriers is a variable, allowing us to gain insight into the effects of the spacing on the BER performance of MC DS-CDMA systems. This generalized MC DS-CDMA scheme includes the subclasses of multi-tone DS-CDMA and orthogonal MC DS-CDMA as special cases. A unified analytical framework is utilized, which determines the exact average BER of the generalized MC DS-CDMA system transmitting over generalized multipath Nakagami- m fading channels. The optimum spacing of the MC DS-CDMA system required for achieving the minimum BER is investigated and the BER performance of the system having optimum spacing is evaluated. The resultant BER is compared with that of both multitone DS-CDMA and orthogonal MC DS-CDMA.

- **Chapter 19:** Accurate and fast synchronization plays a cardinal role in the efficient utilization of any spread-spectrum system. Typically, the first step in the process of synchronization between the received spread pseudo noise (PN) code (sequence) and the locally generated despread code (sequence) is code acquisition [14–16], which is also referred to as initial synchronization. More explicitly, initial synchronization is constituted by a process of successive decisions, wherein the ultimate goal is to bring the two codes into coarse time alignment, namely within one code-chip interval. Once initial code acquisition has been accomplished, usually a code tracking loop [14] is employed for achieving fine alignment of the two codes and for maintaining their alignment during the whole data transmission process. The aim of this chapter, however, is to focus on the task of initial synchronization in the context of direct-sequence code division multiple-access (DS-CDMA) systems.

Initial synchronization has been lavishly treated in the literature [15–53] in recent years. Initial code acquisition in DS-CDMA systems is usually achieved with the aid of non-coherent correlation or matched filtering, since prior to despread the signal-to-noise ratio (SNR) is usually insufficient high for attaining a satisfactory performance with the aid of coherent carrier phase estimators based on carrier-phase tracking loops. Initial code synchronization methods can be broadly classified as serial search acqui-

sition [15, 22, 28, 30, 39, 44] and parallel search acquisition [19, 20, 23–25, 31, 46, 49] techniques. In serial search based initial code synchronization all potentially possible code phases are searched serially, until synchronization is achieved. More explicitly, in serial search based code acquisition each reference phase is evaluated by attempting to despread the received signal. If the estimated code phase is correct, successful despreading will take place, which can be detected. If the code phase is incorrect, the received signal will not be successfully despread, and the local reference code replica will be shifted to a new tentative phase for evaluation. By contrast, in parallel search based code acquisition potentially all of the possible code phases are tested simultaneously. In this chapter both serial and parallel search based acquisition schemes will be investigated.

It is well known that the near-far interference inflicted upon low-power signals by high-power interfering signals may substantially degrade the system's performance. In the context of DS-SS the above-discussed serial and parallel search based code timing acquisition are as interference-limited and as vulnerable to the near-far problem, as conventional matched-filter based single-user detection. Recently, a range of timing acquisition algorithms having a high near-far resistance in multiuser environments have also been proposed [17, 18, 21, 37, 54–56]. These timing-acquisition algorithms can be classified as maximum-likelihood synchronization scheme [21, 55], minimum-mean-square-error (MMSE) timing estimation arrangements [17, 37, 54], per-survivor processing (PSP) based blind acquisition techniques [18] and Multiple Signal Classification Algorithm (MUSIC) based timing estimation scheme [54–56]. In this chapter both serial and parallel search based initial synchronization schemes are considered in the context of both single- and multi-carrier CDMA systems.

- **Chapter 20:** In this chapter we present an overview of the various third-generation terrestrial radio transmission standards recently proposed by ETSI, ARIB, and TTA.
- **Chapter 21:** In this chapter adaptive rate transmissions are investigated in the context of DS-SS systems using variable spreading factors (VSF). In the recently established family of adaptive rate transmission schemes [4] the transmission rate is typically adapted in response to the perceived near-instantaneous channel quality. The perceived channel quality is influenced by numerous factors, such as the variation of the number of users supported, which imposes a time-variant MUI load or the fading-induced channel quality fluctuation of the user considered. In Chapter 4 the impact of both of these channel quality factors was considered in the context of multiuser detection aided adaptive modulation as well as variable spreading factor assisted transmissions. It was found that the system performed best, when both the spreading factors and the modulation modes were controlled in a near-instantaneous fashion.

However, the number of users supported was varied in Chapter 4 on a long-term basis. Hence the average MUI level was constant throughout the simulations. By contrast, in this chapter the individual users' transmission rate is adapted in response to the near-instantaneous MUI fluctuations encountered. Our study will show that by employing the proposed VSF-assisted adaptive rate transmission scheme, the effective throughput may be increased by up to 40%, when compared to that of DS-SS systems using constant spreading factors. This increased throughput is achieved without wasting

power, without imposing extra interference upon other users and without increasing the BER.

1.3 Introduction to Flexible Transceivers

There is a range of activities in various parts of the globe concerning the standardization, research and development of the third-generation (3G) mobile systems [57] known as the Universal Mobile Telecommunications System (UMTS) in Europe, which was termed as the IMT-2000 system by the International Telecommunications Union (ITU) [58, 59]. This is mainly due to the explosive growth of the Internet and the continued dramatic increase in demand for all types of advanced multimedia wireless services including voice and data. However, all the advanced services such as bit-hungry high-resolution multimedia ones, which demands data rate significantly higher than 2Mb/s, are unlikely to be supported by the 3G systems [60–64]. Consequently, the concept of “beyond 3G” has been created in the context of techniques such as broadband access, software defined radio and high-flexible terminals.

In contrast to the 3G systems, the beyond 3G mobile wireless communication systems are expected to employ at least the following three (but without any reason to limit them) typical characteristics. The first is the mobile broadband wireless systems, which implies that the future generation mobile wireless systems must be able to handle a wide range of information bit rates with transmission capability “beyond UMTS” up to more than 100 Mb/s as well as various types of real-time and non-real-time service classes with different traffic characteristics and quality of service guarantees [60]. The objective is that the mobile users are able to access to the range of broadband services available for fixed users of the integrated broadband communication network (IBCN). For an outdoor, cellular scenario, Mobile Broadband Systems (MBS), a concept born in the RACE program, are under consideration, targeting data rates upto 155 Mb/s. The second characteristic is the multi-standards connectable systems, which implies that the beyond 3G mobile terminals are capable of connecting the wireless network with no limitation from the existing wireless communication standards [1, 2, 65–68], which are developed primarily regional rather than worldwide and cause problems with global roaming. The third but not the last typical characteristics is the high-flexible mobile wireless systems, which are not only reflected by the multimode and multiband operation as well as global roaming, but also lies in the high-flexible air-interface capable of achieving the highest spectrum efficiency under the difficult constraints of moving users, dynamic traffic load variations, and highly sensitive wireless links. Therefore, the future generation mobile wireless systems in the long term might belong to the adaptive (or even the intelligent) broadband mobile wireless systems based on the software defined radio (SDR) [1, 2].

In the first part of this treatise a broadband multiple access candidate scheme meeting the above requirements is presented, which is constituted by frequency-hopping (FH) based multicarrier DS-CDMA (FH/MC DS-CDMA) [69–72]. Recent investigations show that rate adaptation in mobile wireless systems is not only the efficient strategy to implement variable rate and multiple rate services, but also the increasingly important approach to achieve higher spectrum efficiency in term of b/s/Hz [73–77]. Hence, in the second part the existing and novel possible adaptive rate transmission (ART) schemes associated with supporting variable rate and multirate services as well as achieving high spectrum efficiency are reviewed. Furthermore, ART techniques are also discussed in the context of the FH/MC

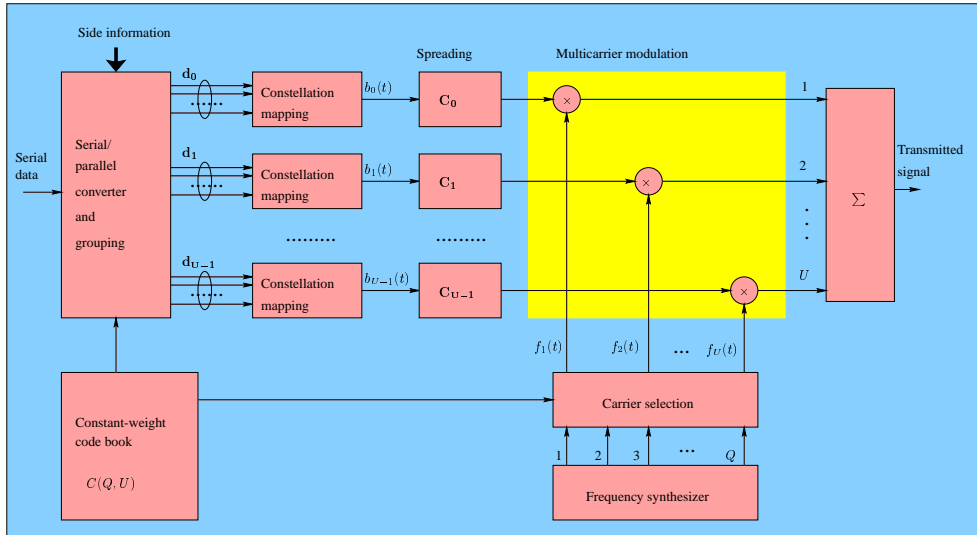


Figure 1.2: Transmitter diagram of the frequency-hopping multicarrier DS-CDMA system using adaptive transmission.

DS-CDMA systems. The standardization worldwide in the field of wireless communications shows that various mobile communication standards will continue to exist even in the future. This causes problems not only with international roaming, but also with multiple standards operation within the same geographical area. Hence, it is important to develop transceivers that will operate with several standards and in several frequency bands on a common hardware platform. SDR are evolving as flexible all-purpose radios and giving rise to the possibility of implementing these kinds of multi-standard, multimode and multiband transceivers. Therefore, in the final part of this chapter, the concept of SDR assisted broadband FH/MC DS-CDMA system is presented and the re-configurable parameters in terms of this system and those associated with connection with the other wireless systems are described.

1.4 FH/MC DS-CDMA

The transmitter schematic of the proposed FH/MC DS-CDMA arrangement is depicted in Fig. 1.2. Each subcarrier of a user is assigned a pseudo-noise (PN) spreading sequence. These PN sequences can be simultaneously assigned to a number of users, provided that only one user activates the same PN sequence on the same subcarrier. These PN sequences produce narrow-band DS-CDMA signals. In Fig. 1.2, $C(Q, U)$ represents a constant-weight code having U number of '1's and $(Q - U)$ number of '0's. Hence the weight of $C(Q, U)$ is U . This code is read from a so-called constant-weight code book, which represents the frequency-hopping patterns. The constant-weight code $C(Q, U)$ plays two different roles. Its first role is that its weight - namely U - determines the number of subcarriers invoked, while its second function is that the positions of the U number of binary '1's determines the selection of a set of U number of subcarrier frequencies from the Q outputs of the frequency

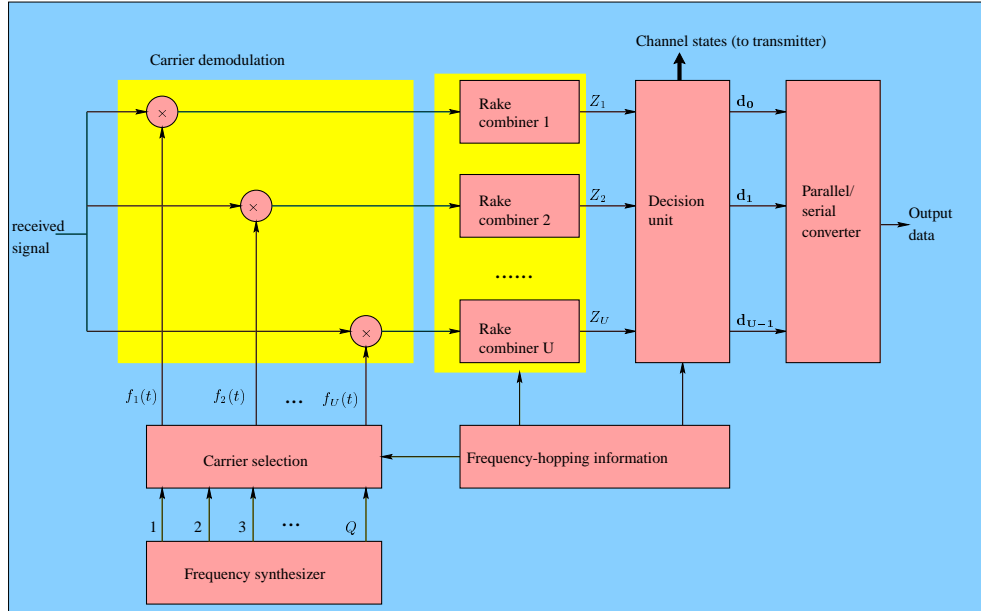


Figure 1.3: Receiver block diagram of the frequency-hopping multicarrier DS-CDMA system using conventional RAKE receiver.

synthesizer. Furthermore, in the transmitter ‘side-information’ reflecting the channel’s instantaneous quality might be employed, in order to control its transmission and coding mode, so that the required target throughput and transmission integrity requirements are met.

As shown in Fig. 1.2, the original bit stream having a bit duration of T_b is first serial-to-parallel (S-P) converted. Then, these parallel bit streams are grouped and mapped to the potentially time-variant modulation constellations of the U active subcarriers. Let us assume that the number of bits transmitted by a FH/MC DS-CDMA symbol is M , and let us denote the symbol duration of the FH/MC DS-CDMA signal by T_s . Then, if the system is designed for achieving a high processing gain and for mitigating the inter-symbol-interference (ISI) in a constant-rate transmission scheme, the symbol duration can be extended to a multiple of the bit duration, i.e., $T_s = MT_b$. By contrast, if the design aims to support multiple transmission rates or channel-quality matched variable information rates, then a constant bit duration of $T_0 = T_s$ can be employed. Both multirate and variable rate transmissions can be implemented by employing a different number of subcarriers associated with different modulation constellations as well as different spreading gains. As seen in Fig. 1.2, after the constellation mapping stage, each branch is DS spread using the assigned PN sequence, and then this spread signal is carrier modulated using one of the active subcarrier frequencies derived from the constant-weight code $C(Q, U)$. Finally, all U active branch signals are multiplexed, in order to form the transmitted signal.

In the FH/MC DS-CDMA receiver of Fig.1.3 the received signal associated with each active subcarrier is detected using for example a RAKE combiner. Alternatively, Multiuser Detection (MUD) can be invoked, in order to approach the single-user bound. In contrast

to the transmitter side, where only U out of Q subcarriers are transmitted by a user, at the receiver different detector structures might be implemented based on the availability [72] or lack [78] of the FH pattern information. During the FH pattern acquisition stage, which usually happens at the beginning of transmission or during hand-over, tentatively all Q subcarriers can be demodulated. The transmitted information can be detected and the FH patterns can be acquired simultaneously by using blind joint detection algorithms exploiting the characteristics of the constant-weight codes [70, 71]. If however, the receiver has the explicit knowledge of the FH patterns, then only U subcarriers have to be demodulated. However, if Fast Fourier Transform (FFT) techniques are employed for demodulation - as often is the case in multicarrier CDMA [79] or OFDM [80] systems, then all Q subcarriers might be demodulated, where the inactive subcarriers only output noise. In the decision unit of Fig.1.3, these noise-output-only branches can be eliminated by exploiting the knowledge of the FH patterns [72, 78]. Hence, the decision unit only outputs the information transmitted by the active subcarriers. Finally, the decision unit's output information is parallel-to-serial converted to form the output data.

At the receiver, the channel states associated with all the subchannels might be estimated or predicted using pilot signals [75, 77]. This channel state information can be utilized for coherent demodulation. It can also be fed back to the transmitter as highly protected side-information, in order to invoke a range of adaptive transmission schemes including power control and adaptive-rate transmission.

1.5 Characteristics of the FH/MC DS-CDMA Systems

In the proposed FH/MC DS-CDMA system the entire bandwidth of future broadband systems can be divided into a number of sub-bands and each sub-band can be assigned a subcarrier. According to the prevalent service requirements, the set of legitimate subcarriers can be distributed in line with the users' instantaneous information rate requirements. FH techniques are employed for each user, in order to evenly occupy the whole system bandwidth available and to efficiently utilize the available frequency resources. In this respect FH/MC DS-CDMA systems exhibit compatibility with the existing 2nd- and 3rd-generation CDMA systems and hence constitute a highly flexible air interface.

Broadband Wireless Mobile System – To elaborate a little further, our advocated FH/MC DS-CDMA system is a broadband wireless mobile system constituted by multiple narrow-band DS-CDMA sub-systems. Again, FH techniques are employed for each user, in order to evenly occupy the whole system bandwidth and to efficiently utilize the available frequency resources. The constant-weight code based FH patterns used in the schematic of Fig.1.2 are invoked, in order to control the number of subcarriers invoked, which is kept constant during the FH procedure. In contrast to single-carrier broadband DS-CDMA systems, such as wide-band CDMA (W-CDMA) [59] exhibiting a bandwidth in excess of 5 MHz - which inevitably results in extremely high-chip-rate spreading sequences and high-complexity - the proposed FH/MC DS-CDMA system does not have to use high chip-rate DS spreading sequences, since each subcarrier conveys a narrow-band DS-CDMA signal. In contrast to broadband OFDM systems [63] - which have to use a high number of subcarriers and usually resulting in a high peak-to-average power fluctuation - due to the associated DS spreading the number

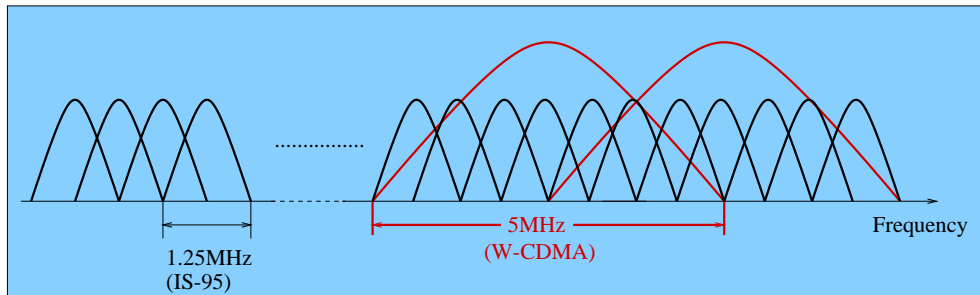


Figure 1.4: Spectrum of FH/MC DS-CDMA signal using subchannel bandwidth of 1.25 MHz and/or 5 MHz.

of subcarriers of the advocated broadband wireless FH/MC DS-CDMA system may be significantly lower. This potentially mitigates the crest-factor problem. Additionally, with the aid of FH, the peak-to-average power fluctuation of the FH/MC DS-CDMA system might be further decreased. In other words, the FH/MC DS-CDMA system is capable of combining the best features of single-carrier DS-CDMA and OFDM systems, while avoiding many of their individual shortcomings. Finally, in comparison to the FH/MC DS-CDMA system, both broadband single-carrier DS-CDMA systems and broadband OFDM systems are less amenable to interworking with the existing 2nd- and 3rd-generation wireless communication systems. Let us now characterize some of the features of the proposed system in more depth.

Compatibility – The broadband FH/MC DS-CDMA system can be rolled out over the bands of the 2nd- and 3rd-generation mobile wireless systems and/or in the band licensed for future broadband wireless communication systems. In FH/MC DS-CDMA systems the sub-bands associated with different subcarriers are not required to be of equal bandwidth. Hence existing 2nd- and 3rd-generation CDMA systems can be supported using one or more subcarriers. For example, Fig. 1.4 shows the spectrum of a frequency hopping, orthogonal multicarrier DS-CDMA signal using a subchannel bandwidth of 1.25 MHz, which constitutes the bandwidth of a DS-CDMA signal in the IS-95 standard [58]. In Fig. 1.4 we also show that seven subchannels, each having a bandwidth of 1.25 MHz can be replaced by one subchannel with a bandwidth of 5 MHz ($= 8 \times 1.25/2$ MHz). Hence, the narrow-band IS-95 CDMA system can be supported by a single subcarrier, while the UMTS and IMT-2000 W-CDMA systems might be supported using seven subchannels' bandwidth amalgamated into one W-CDMA channel. Moreover, with the aid of SDRs, FH/MC DS-CDMA is also capable of embracing other existing standards, such as the Time-Division Multiple-Access (TDMA) based Global System of Mobile communications known as GSM [81].

FH Strategy – In FH/MC DS-CDMA systems both slow FH and fast FH techniques can be invoked, depending on the system's design and the state-of-the-art. In slow FH several symbols are transmitted after each frequency hopping, while in fast FH several frequency hops take place in a symbol duration, i.e. each symbol is transmitted using several subcarriers. Moreover, from a networking point of view, random FH, uniform FH and adaptive FH [72] schemes can be utilized, in order to maximize the efficiency of the network. In the

context of *random* FH [72], the subcarriers associated with each transmission of a user are determined by the set of pre-assigned FH patterns constituting a group of constant-weight codewords [78]. The active subcarriers are switched from a group of frequencies to another without the knowledge of the FH patterns of the other users. By contrast, for the FH/MC DS-CDMA system using *uniform* FH [72], the FH patterns of all users are determined jointly under the control of the base station (BS), so that each subcarrier is activated by a similar number of users. It can be shown that for the down-link (DL) uniform FH can be readily implemented, since the BS has the knowledge of the FH patterns of all users. However, for implementing up-link (UL) transmissions, the FH patterns to be used must be signalled by the BS to each mobile station (MS), in order to be able to implement uniform FH. Finally, if the near-instantaneous channel quality information is available at the transmitter, advanced adaptive FH can be invoked, where information is only transmitted over a group of subchannels exhibiting a satisfactory Signal to Interference Ratio (SIR).

Implementation of Multicarrier Modulation – The multicarrier modulation block in Fig. 1.2 and the multicarrier demodulation block in Fig. 1.3 can be implemented using FFT techniques, provided that each of the subchannels occupies the same bandwidth. Since not all of the subcarriers are activated at each transmission in the proposed FH/MC DS-CDMA system, the deactivated subcarriers can be set to ‘zero’ in the FFT or IFFT algorithm. However, if an unequal bandwidth is associated with the subchannels, multicarrier modulation/demodulation can only be implemented using less efficient conventional, rather than FFT based carrier modulation/demodulation schemes.

Access Strategy – When a new user attempts to access the channel and commences his/her transmission, a range of different access strategies might be offered by the FH/MC DS-CDMA system, in order to minimize the interference inflicted by the new user to the already active users. Specifically, if there are subchannels, which are not occupied by any other users, or there are subchannels that exhibit a sufficiently high SIR, then the new user can access the network using these passive subchannels or the subchannels exhibiting a high SIR. However, if all the subchannels have been occupied and the SIR of each of the subchannels is insufficiently high, then the new user accesses the network by spreading its transmitted energy evenly across the subchannels. This access scheme imposes the minimum possible impact on the QoS of the users already actively communicating. However, the simplest strategy for a new user to access the network is by randomly selecting one or several subchannels.

Multirate and Variable Rate Services – In FH/MC DS-CDMA systems multirate and variable rate services can be implemented using a variety of approaches. Specifically, the existing techniques, such as employing a variable spreading gain, multiple spreading codes, a variable constellation size, variable-rate Forward Error Correction (FEC) coding, etc. can be invoked to provide multirate and variable rate services. Furthermore, since the proposed FH/MC DS-CDMA systems use constant-weight code based FH patterns, multirate and variable rate services can also be supported by using constant-weight codes having different weights, i.e., by activating a different number of subcarriers. Note that the above-mentioned techniques can be implemented either separately or jointly in a system.

Diversity – The FH/MC DS-CDMA system includes frequency hopping, multicarrier mod-

ulation as well as direct-sequence spreading, hence a variety of diversity schemes and their combinations can be implemented. The possible diversity schemes include the following arrangements.

- If the chip-duration of the spreading sequences is lower than the maximum delay spread of the fading channels, then frequency diversity can be achieved on each of the subcarrier signals;
- Frequency diversity can also be achieved by transmitting the same signal using a number of different subcarriers;
- Time diversity can be achieved by using slow frequency hopping in conjunction with error control coding as well as interleaving;
- Time-frequency diversity can be achieved by using fast frequency hopping techniques, where the same symbol is transmitted using several time slots assigned to different frequencies;
- Spatial diversity can be achieved by using multiple transmit antennas, multiple receiver antennas and polarization.

Initial Synchronization – In our FH/MC DS-CDMA system initial synchronization can be implemented by first accomplishing DS code acquisition. The fixed-weight code book index of the FH pattern used can be readily acquired, once DS code acquisition was achieved. During DS code acquisition the training signal supporting the initial synchronization, which is usually the carrier modulated signal without data modulation, can be transmitted using a group of subcarriers. These subcarrier signals can be combined at the receiver using for example equal gain combining (EGC) [82]. Hence, frequency diversity can be employed during the DS code acquisition stage of the FH/MC DS-CDMA system's operation, and consequently the initial synchronization performance can be significantly enhanced. Following the DS code acquisition phase, data transmission can be activated and the index of the FH pattern used can be signalled to the receiver using a given set of fixed subchannels. Alternatively, the index of the FH pattern can be acquired blindly from the received signal with the aid of a group of constant-weight codes having a given minimum distance [71].

Interference Resistance – The FH/MC DS-CDMA system concerned can mitigate the effects of inter-symbol interference encountered during high-speed transmissions, and it readily supports partial-band and multi-tone interference suppression. Moreover, the multiuser interference can be suppressed by using multiuser detection techniques [73], potentially approaching the single-user performance.

Advanced Technologies – The FH/MC DS-CDMA system can efficiently amalgamate the techniques of FH, OFDM and DS-CDMA. Simultaneously, a variety of performance enhancement techniques, such as multiuser detection [83], turbo coding [84], adaptive antennas [85], space-time coding and transmitter diversity [86], near-instantaneously adaptive modulation [74], etc, might be introduced.

Flexibility – The future generation broadband mobile wireless systems will aim to support a wide range of services and bit rates. The transmission rates may vary from voice and low-rate messages to very high-rate multimedia services requiring rates in excess of 100Mb/s [60]. The communications environments vary in terms of their grade of mobility, the cellular infrastructure, the required symmetric and asymmetric transmission capacity, and whether indoor, outdoor, urban or rural area propagation scenarios are encountered, etc. Hence flexible air interfaces are required, which are capable of maximizing the area spectrum efficiency expressed in terms of bits/s/Hz/km² in a variety of communication environments. Future systems are also expected to support various types of services based on ATM and IP, which require various Quality of Service (QoS). As argued before, FH/MC DS-CDMA systems exhibit a high grade of compatibility with existing systems. These systems also benefit from the employment of FH, MC and DS spreading based diversity assisted adaptive modulation [80]. In short, FH/MC DS-CDMA systems constitute a high-flexibility air interface.

1.6 Adaptive Rate Transmission

1.6.1 Why Adaptive Rate Transmission?

There are a range of issues, which motivate the application of adaptive rate transmissions (ART) in the broadband mobile wireless communication systems of the near future. The explosive growth of the Internet and the continued dramatic increase in demand for all types of wireless services are fueling the demand for increasing the user capacity, data rates and the variety of services supported. Typical low-data-rate applications include audio conferencing, voice mail, messaging, email, facsimile, and so on. Medium- to high-data-rate applications encompass file transfer, Internet access, high-speed packet- and circuit-based network access as well as high-quality video conferencing. Furthermore, the broadband wireless systems in the future are also expected to support real-time multimedia services, which provide concurrent video, audio and data services to support advanced interactive applications. Hence, in the future generation mobile wireless communication systems, a wide range of information rates must be provided, in order to support different services, which demand different data rates and different QoS. In short, an important motivation for using ART is to support a variety of services, which we refer to as service-motivated ART (S-ART). However, there is a range of other motivating factors, which are addressed below.

The performance of wireless systems is affected by a number of propagation phenomena: 1) path-loss variation versus distance; 2) random slow shadowing; 3) random multipath fading; 4) Inter-Symbol Interference (ISI), co-channel interference as well as multiuser interference; and 5) background noise. For example, mobile radio links typically exhibit severe multipath fading, which leads to serious degradation in the link's signal-to-noise ratio (SNR) and consequently to a higher bit error rate (BER). Fading compensation techniques such as an increased link budget margin or interleaving with channel coding are typically required to improve the link's performance. However, today's cellular systems are designed for the worst-case channel conditions, typically achieving adequate voice quality over 90-95% of the coverage area for voice users, where the signal to interference plus noise ratio (SINR) is above the designed target [74]. Consequently, the systems designed for the worst-case channel conditions result in poor exploitation of the available channel capacity a good percentage

of time. Adapting the transmitter's certain parameters to the time-varying channel conditions leads to better exploitation of the channel capacity available. This ultimately increases the area spectral efficiency expressed in terms of b/s/Hz/km^2 . Hence, the second reason for the application of ART is constituted by the time-varying nature of the channel, which we refer to as channel quality motivated ART (C-ART).

1.6.2 What Is Adaptive Rate Transmission?

Broadly speaking, ART in mobile wireless communications implies that the transmission rate at both the base stations and the mobile terminals can be adaptively adjusted according to the instantaneous operational conditions, including the communication environment and service requirements. With the expected employment of SDR-based wireless systems, the concept of ART might also be extended to adaptively controlling the multiple access schemes - including FDMA, TDMA, narrow-band CDMA, W-CDMA and OFDM - as well as the supporting network structures - such as Local Area Networks and Wide Area Networks. In this chapter only C-ART and S-ART are concerned in the context of the proposed FH/MC DS-CDMA scheme. Employing ART in response to different service requests indicates that the transmission rate of the base station and the mobile station can be adapted according to the requirements of the services concerned, as well as to meet their different QoS targets. By contrast, employing ART in response to the time-varying channel quality implies that for a given service supported, the transmission rate of the base station and that of the mobile station can be adaptively controlled in response to their near-instantaneous channel conditions. The main philosophy behind C-ART is the real-time balancing of the link budget through adaptive variation of the symbol rate, modulation constellation size and format, spreading factor, coding rate/scheme, etc, or in fact any combination of these parameters. Thus, by taking advantage of the time-varying nature of the wireless channel and interference conditions, the C-ART schemes can provide a significantly higher average spectral efficiency than their fixed-mode counterparts. This takes place without wasting power, without increasing the co-channel interference, or without increasing the BER. We achieve these desirable properties by transmitting at high speeds under favorable interference/channel conditions and by responding to degrading interference and/or channel conditions through a smooth reduction of the associated data throughput. Procedures that exploit the time-varying nature of the mobile channel are already in place for all the major cellular standards worldwide [74], including IS-95 CDMA, cdma2000 and UMTS W-CDMA [81], IS-136 TDMA, the General Packet Radio Service of GSM and in the Enhanced Data rates for Global Evolution (EDGE) schemes. The rudimentary portrayal of a range of existing and future ART schemes is given below. Note that a system may employ a combination of several ART schemes listed below, in order to achieve the desired data rate, BER or the highest possible area spectrum efficiency.

- **Multiple Spreading Codes** – In terms of S-ART, higher rate services can be supported in CDMA based systems by assigning a number of codes. For example, in IS-95B each high-speed user can be assigned one to eight Walsh codes, each of which supports a data rate of 9.6kb/s. By contrast, multiple codes cannot be employed in the context of C-ART in order to compensate for channel fading, path-loss and shadowing, **unless they convey the same information and achieve certain diversity gain**. However, if

the co-channel interference is low - which usually implies in CDMA based systems that the number of simultaneously transmitting users is low - then multiple codes can be transmitted by an active user, in order to increase the user's transmission rate.

- **Variable Spreading Factors** – In the context of S-ART higher rate services are supported by using lower spreading factors without increasing the bandwidth required. For example, in UMTS W-CDMA [58] the spreading factors of 4/8/16/32/64/128/256 may be invoked to achieve the corresponding data rates of 1024/512/ 256/128/64/32/16 kb/s. In terms of C-ART, when the SINR experienced is increased, reduced spreading factors are assigned to users for the sake of achieving higher data rates.
- **Variable Rate FEC Codes** – In a S-ART scenario higher rate services can be supported by assigning less powerful, higher rate FEC codes associated with reduced redundancy. In a C-ART scenario, when the SINR improves, a higher-rate FEC code associated with reduced redundancy is assigned, in an effort to achieve a higher data rate.
- **Different FEC Schemes** – The range of coding schemes might entail different classes of FEC codes, code structures, encoding/decoding schemes, puncturing patterns, interleaving depths and patterns, and so on. In the context of S-ART, higher rate services can be supported by coding schemes having a higher coding rate. In the context of C-ART, usually an appropriate coding scheme is selected, in order to maximize the spectrum efficiency. The FEC schemes concerned may entail block or convolutional codes, block or convolutional constituent code based turbo codes, trellis codes, turbo trellis codes, etc. The implementational complexity and error correction capability of these codes can be varied as a function of the coding rate, code constraint length, the number of turbo decoding iterations, the puncturing pattern, etc. A rule of thumb is that the coding rate is increased towards unity, as the channel quality improves, in order to increase the system's effective throughput.
- **Variable Constellation Size** – In S-ART schemes higher rate services can be supported by transmitting symbols having higher constellation sizes. For example, an adaptive modem may employ BPSK, QPSK, 16QAM and 64QAM constellations [80], which corresponds to 1, 2, 4 and 6 bits per symbol. The highest data rate provided by the 64QAM constellation is a factor six higher than that provided by employing the BPSK constellation. In C-ART scenarios, when the SINR increases, a higher number of bits per symbol associated with a higher order constellation is transmitted for increasing the system's throughput.
- **Multiple Time Slots** – In a S-ART scenario higher rate services can also be supported by assigning a corresponding number of time slots. A multiple time slot based adaptive rate scheme is used in GPRS-136 (1-3 time slots/20 ms) and in Enhanced GPRS (EGPRS) (1-8 time slots/4.615GSM frame) in order to achieve increased data rates. In the context of C-ART, multiple time slots associated with interleaving or frequency

hopping can be implemented for achieving time diversity gain. Hence, C-ART can be supported by assigning a high number of time slots for the compensation of severe channel fading at the cost of tolerating a low data throughput. By contrast, assigning a low number of time slots over benign non-fading channels allows us to achieve a high throughput.

- **Multiple Bands** – In the context of S-ART higher rate services can also be supported by assigning a higher number of frequency bands. For example, in UMTS W-CDMA [58] two 5 MHz bands may be assigned to a user, in order to support the highest data rate of 2 Mb/s ($= 2 \times 1024\text{kb/s}$), which is obtained by using a spreading factor of 4 on each sub-band signal. In the context of C-ART associated with multiple bands, frequency-hopping associated with time-variant redundancy and/or variable rate FEC coding schemes, or frequency diversity techniques might be invoked, in order to increase the spectrum efficiency of the system. For example, in C-ART schemes associated with double-band assisted frequency diversity, if the channel quality is low, the same signal can be transmitted in two frequency bands for the sake of maintaining a diversity order of two. However, if the channel quality is sufficiently high, two independent streams of information can be transmitted in these bands and consequently the throughput can be doubled.
- **Multiple Transmit Antennas** – Employing multiple transmit antennas based on space-time coding [86] is a novel method of communicating over wireless channels, which was also adapted for use in the 3rd-generation mobile wireless systems. ART can also be implemented using multiple transmit antennas associated with different space-time codes. In S-ART schemes higher rate services can be supported by a higher number of transmit antennas associated with appropriate space-time codes. In terms of C-ART schemes, multiple transmit antennas can be invoked for achieving a high diversity gain. Therefore, when the channel quality expressed in terms of the SINR is sufficiently high, the diversity gain can be decreased. Consequently, two or more symbols can be transmitted in each signalling interval and each stream is transmitted by only a fraction of the transmit antennas associated with the appropriate space-time codes. Hence the throughput is increased. However, when the channel quality is poor, all the transmit antennas can be invoked for transmitting one stream of data, hence achieving the highest possible transmit diversity gain of the system, while decreasing the throughput.

Above we have summarized the philosophy of a number of ART schemes, which can be employed in wireless communication systems. A S-ART scheme requires a certain level of transmitted power, in order to achieve the required QoS. Specifically, a relatively high transmitted power is necessitated for supporting high-data rate services, and a relatively low transmitted power is required for offering low-data rate services. Hence, a side-effect of a S-ART scheme supporting high data rate services is the concomitant reduction of the number of users supported due to the increased interference or/and increased bandwidth. By contrast, a cardinal requirement of a C-ART scheme is the accurate channel quality estimation or prediction at the receiver as well as the provision of a reliable side-information feedback

between the channel quality estimator or predictor of the receiver and the remote transmitter [75, 77], where the modulation/coding mode requested by the receiver is activated. The parameters capable of reflecting the channel quality may include BER, SINR, transmission frame error rate, received power, path loss, Automatic Repeat Request (ARQ) status, etc. A C-ART scheme typically operates under the constraint of constant transmit power and constant bandwidth. Hence, without wasting power and bandwidth, or without increasing the co-channel interference compromising the BER performance, C-ART schemes are capable of providing a significantly increased average spectral efficiency by taking advantage of the time-varying nature of the wireless channel, when compared to fixed-mode transmissions.

1.6.3 Adaptive Rate Transmission in FH/MC DS-CDMA System

Above we have discussed a range of ART schemes, which were controlled by the prevalent service requirements and the channel quality. Future broadband mobile wireless systems are expected to provide a wide range of services characterized by highly different data rates, while achieving the highest possible spectrum efficiency. The proposed FH/MC DS-CDMA based broadband mobile wireless system constitutes an attractive candidate system, since it is capable of efficiently utilizing the available frequency resources, as we discussed previously, and simultaneously achieving a high grade of flexibility by employing ART techniques. More explicitly, the FH/MC DS-CDMA system can provide a wide range of data rates by combining the various ART schemes discussed above. At the same time, for any given service, the FH/MC DS-CDMA system may also invoke a range of adaptation schemes, in order to achieve the highest possible spectrum efficiency in various propagation environments, such as indoor, outdoor, urban, rural scenarios at low to high speeds. Again, the system is expected to support different services at a variety of QoS, including voice mail, messaging, email, file transfer, Internet access, high-speed packet- and circuit-based network access, real-time multimedia services, and so on. As an example, a channel-quality motivated burst-by-burst ART assisted FH/MC DS-CDMA system is shown in Fig. 1.5, where we assume that the number of subcarriers is three, the bandwidth of each subchannel is 5 MHz and the channel quality metric is the SINR. In response to the SINR experienced, the transmitter may transmit a frame of symbols selected from the set of BPSK, QPSK, 16QAM or 64QAM constellations, or simply curtail transmitting information, if the SINR is too low.

1.7 Software Defined Radio Assisted FH/MC DS-CDMA

The range of existing wireless communication systems is shown in Fig.1.6. Different legacy systems will continue to coexist, unless ITU - by some miracle - succeeds in harmonizing all the forthcoming standards under a joint framework, while at the same time ensuring compatibility with the existing standards. In the absence of the 'perfect' standard, the only solution is employing multiband, multimode, multi-standard transceivers based on the concept of Software Defined Radios (SDR) [1–3].

In SDRs the digitization of the received signal is performed at some stage downstream from the antenna, typically after wideband filtering, low-noise amplification, and down-conversion to a lower frequency. The reverse processes are invoked by the transmitter. In contrast to most wireless communication systems which employ Digital Signal Processing

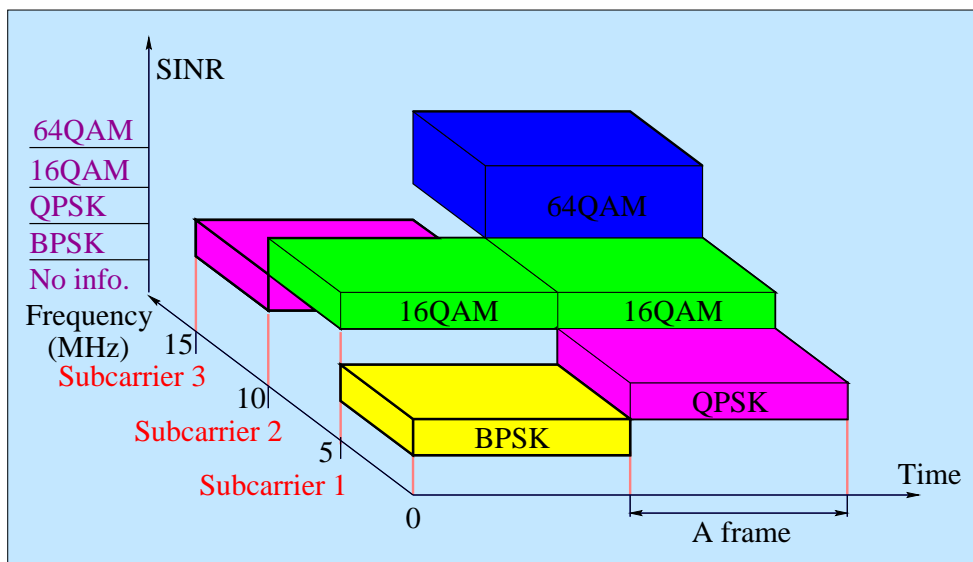


Figure 1.5: A frame structure of burst-by-burst adaptive modulation in multicarrier DS-CDMA systems.

(DSP) only at baseband, SDRs are expected to implement the DSP functions at an intermediate frequency (IF) band. A SDR defines all aspects of the air interface, including RF channel access and waveform synthesis in software. In SDRs wide-band analog-to-digital and digital-to-analog converters (ADC and DAC) transform each RF service band from digital and analogue forms at IF. The wideband digitized receiver stream of bandwidth W_s accommodates all subscriber channels, each of which has a bandwidth of W_c ($W_c \ll W_s$). Thanks to using programmable DSP chips at both the intermediate frequency as well as at baseband, SDRs are sufficiently to efficiently support multiband and multi-standard communications. A SDR employs one or more reconfigurable processors embedded in a real-time multiprocessing fabric, permitting flexible reprogramming and reconfiguration using software downloaded for example with the aid of a signalling channel from the base-station. Hence, SDRs offer an elegant solution to accommodating various modulation formats, coding and radio access schemes. They also have the potential of reducing the cost of introducing new technology superseding legacy systems, and are amenable to future software upgrades, potentially supporting sophisticated future signal processing functions such as array processing, multi-user detection and as yet unknown coding techniques.

FH/MC DS-CDMA systems will be designed, in order to provide the maximum grade of compatibility with the existing CDMA based systems, such as IS-95 and W-CDMA based systems. For example, the frequency bands of the IS-95 CDMA system in North America are 824-849 MHz (uplink) and 869-894 MHz (downlink), respectively. The corresponding frequency bands for the UMTS-FDD wideband CDMA system are 1850-1910 MHz (uplink) and 1930-1990 MHz (downlink) in North America, while 1920-1980 MHz (uplink) and 2110-2170 MHz (downlink) in Europe. In order to ensure compatibility with these systems, the proposed FH/MC DS-CDMA system's spectrum can be assigned according to Fig.1.7.

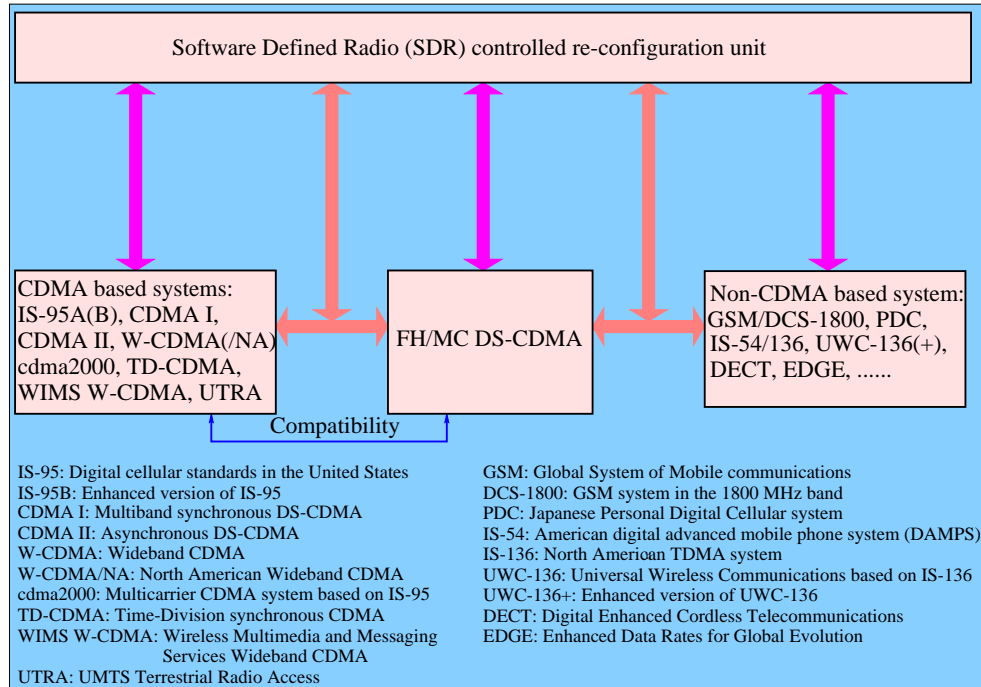


Figure 1.6: Software defined radio assisted FH/MC DS-CDMA and its re-configuration modes.

Specially, in the frequency band of IS-95, 39 orthogonal subcarriers are assigned, each having a bandwidth of 1.25 MHz, while in the frequency band of UMTS-FDD W-CDMA, 23 orthogonal subcarriers are allocated, each with a bandwidth of 5 MHz. The multicarrier modulation used in the FH/MC DS-CDMA system obeying the above spectrum allocation can be readily implemented using two IFFT sub-systems at the transmitter and two FFT sub-systems at the receiver, where a pair of IFFT-FFT sub-systems carries out modulation/demodulation in the IS-95 band, while another pair of IFFT-FFT sub-systems transmits and receives in the UMTS-FDD band. If the chip rate for the 1.25 MHz bandwidth subcarriers is 1.2288M chips per second (cps) and for the 5 MHz bandwidth subcarriers is 3.84 Mcps, then the FH/MC DS-CDMA system will be compatible with both the IS-95 and the UMTS-FDD W-CDMA systems.

However, the terminals of future broadband mobile wireless systems are expected not only to support multimode and multi-standard communications, but also to possess the highest possible grade of flexibility, while achieving a high spectrum efficiency. Hence, these systems are expected to be capable of software re-configuration both between different standards as well as within a specific standard. In contrast to re-configuration between different standards invoked, mainly for the sake of compatibility, the objective of re-configuration within a specific standard is to support a variety of services at the highest possible spectrum efficiency. The SDR assisted broadband FH/MC DS-CDMA system is operated under the control of the software re-configuration unit shown in Fig.1.6. The set of reconfigured parameters of the broadband FH/MC DS-CDMA system may include:

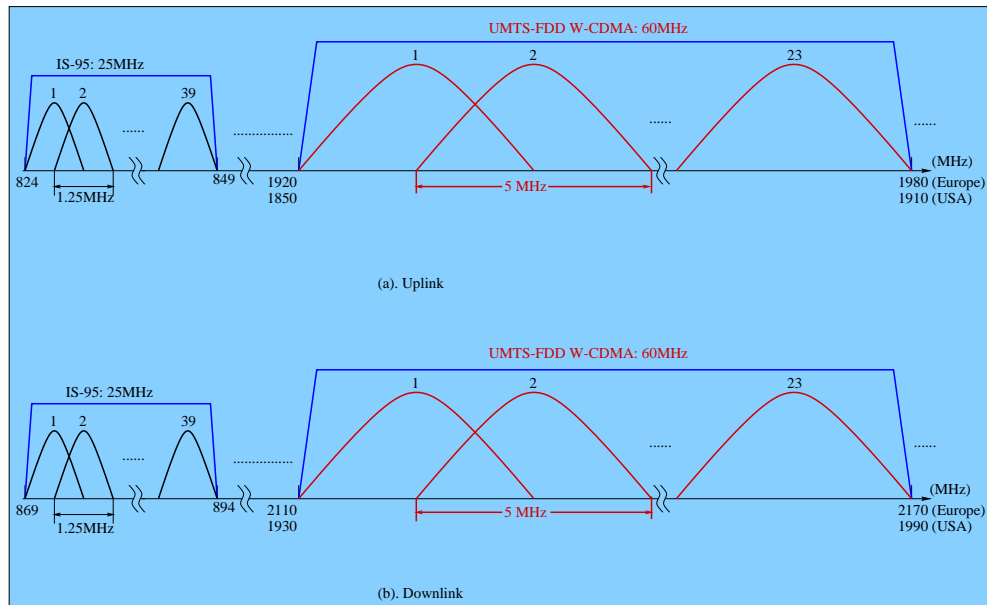


Figure 1.7: Exhibition of spectrum compatibility of the broadband FH/MC DS-CDMA system with IS-95 and UMTS-FDD wideband CDMA systems.

- **Services:** Data rate, QoS, real-time or non-real-time transmission, encryption/decryption schemes and parameters;
- **Error Control:** CRC, FEC codes, coding/decoding schemes, coding rate, number of turbo decoding steps, interleaving depth and pattern;
- **Modulation:** Modulation schemes, signal constellation, partial response filtering;
- **PN Sequence:** Spreading sequences (codes), chip rate, chip waveform, spreading factor, PN acquisition and tracking schemes;
- **Frequency Hopping:** FH schemes (slow, fast, random, uniform and adaptive), FH patterns, weight of constant-weight codes;
- **Detection:** Detection schemes (coherent or non-coherent, etc.) and algorithms (maximum likelihood sequence detection (MLSD) or minimum mean square estimation (MMSE), etc.), parameters associated with space/time as well as frequency diversity, beam-forming, diversity combining schemes, equalization schemes as well as the related parameters (such as the number of turbo equalization iterations, etc.) and channel quality estimation algorithms, parameters;
- **Others:** Subchannel bandwidth, power control parameters.

In the context of different standards - in addition to the parameters listed above - the transceiver parameters that must be re-configurable have to include the clock rate, the radio frequency (RF) bands and air interface modes.

1.8 Chapter Summary and Conclusions

We have presented a flexible broadband mobile wireless communication system based on FH/MC DS-CDMA and reviewed a variety of existing as well as a range of forthcoming techniques, which might be required for developing broadband mobile wireless systems exhibiting a high flexibility and high communications efficiency. We argued that this broadband FH/MC DS-CDMA system exhibits a high grade of compatibility with the existing CDMA based systems, since it is capable of incorporating a wide range of techniques developed for the 2nd- and 3rd-generation mobile systems. At the time of writing research is well under way towards the SDR-based implementation of a range of existing systems. It is expected that these efforts will soon encompass a generic scheme not too different from the FH/MC DS-CDMA scheme advocated here. The rest of this monograph will provide an overview of various communications techniques, which may be accommodated by the system framework introduced in this Prologue.

Part I

Multi-User Detection for Adaptive Single-Carrier CDMA

Chapter 2

CDMA Overview

2.1 Introduction to Code Division Multiple Access

Spread spectrum communications have long been used in military systems [87]. The distinguishing feature of spread spectrum communications is that the transmission bandwidth is significantly higher than that required by the information rate, resulting in the “spread” terminology. Typically, a pseudo-random code is used to ‘spread’ the information signal to the allocated frequency bandwidth.

Multiple access systems designed for mobile communications have traditionally employed Time Division Multiple Access (TDMA) [81] and Frequency Division Multiple Access (FDMA) [81] techniques. In FDMA, the allocated spectrum is divided into frequency slots, while in TDMA the time-domain transmission frame is periodically divided into time slots. Thus each user accesses its own slot in either the time-domain or frequency-domain and hence they are thus orthogonal to each other either in time or frequency, respectively. from Qualcomm Inc. was one of the first to propose using Code Division Multiple Access (CDMA) [88] for civilian mobile communications, which eventually led to the North American IS-95 standard [89, 90]. CDMA is a multiple access technique that allows multiple users to transmit independent information within the same bandwidth simultaneously. Each user is assigned a pseudo-random code that is either orthogonal to the codes of all the other users or the code possesses appropriate cross-correlation properties that minimize the multiple access interference (MAI). This code is superimposed on the information signal, making the signal appear noise-like to all the other users. Only the intended receiver has a replica of the same code and uses it to extract the information signal. This then allows the sharing of the same spectrum by multiple users without causing excessive MAI. It also ensures message privacy, since only the intended user is able to “decode” the signal. This code is also known as a spreading code, since it spreads the bandwidth of the original data signal into a much higher bandwidth before transmission. Therefore the term Spread Spectrum Multiple Access (SSMA) is also used interchangeably with the term CDMA. These aspects are explained in further detail later in this chapter.

Figure 2.1 shows a classification tree of the various types of CDMA techniques. These

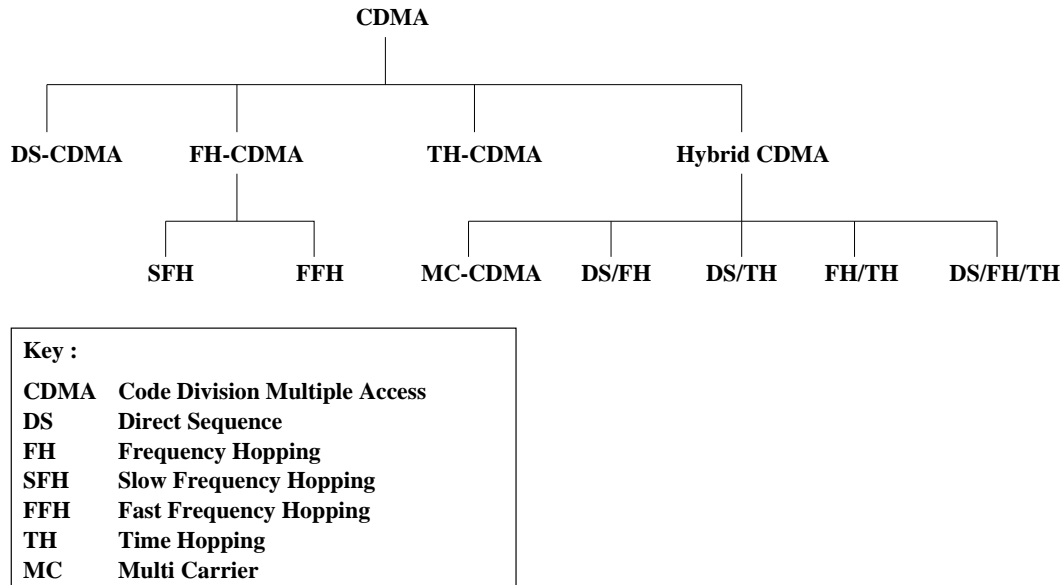


Figure 2.1: Classification of CDMA schemes according to the modulation method used to obtain the spread spectrum signal

techniques differ from each other in the way that the information signal is transformed to produce a high-bandwidth spread signal. In Direct Sequence CDMA (DS-CDMA), a pseudo-random sequence having a higher bandwidth than the information signal is used to modulate the information signal directly. The resultant signal has a significantly higher bandwidth than the original signal. In Frequency Hopping CDMA (FH-CDMA), the transmission bandwidth is divided into frequency sub-bands, where the bandwidth of each sub-band is equal to the bandwidth of the information signal. A pseudo-random code is then used to select the sub-band, in which the information signal is transmitted and this sub-band changes periodically according to the code. There are two sub-categories of FH-CDMA, namely Slow Frequency Hopping (SFH) [91] and Fast Frequency Hopping (FFH) [91]. In FFH, the frequency sub-band used to transmit one bit of information is changed multiple times within the bit-duration, while in SFH, the sub-band is changed only after multiple bits have been transmitted. Time Hopping CDMA (TH-CDMA) [91] transmits the information signal in short bursts. These short bursts render the transmission bandwidth high. The start of each burst for one user is determined by a pseudo-random code. Hybrid CDMA [91] encompasses a group of techniques that combine two or more of the other techniques already described. One of these hybrid techniques is known as Multi-Carrier CDMA (MC-CDMA) [91]. There are many variations of this technique, which were summarized, for example, by [79, 91], but their common characteristic is that a spreading code is used to spread a user's signal either in the time or frequency domain, and that more than one carrier frequency is used for transmission. This thesis discusses DS-CDMA only. For more detailed information on the other multiple access schemes, the reader is referred to the excellent monographs by [88], [91], and [92],

as well as and [93].

CDMA as a multiple access scheme has advantages and disadvantages over the more traditionally employed FDMA and TDMA. [94] has provided an insightful comparison of CDMA, FDMA and TDMA. If all three multiple access schemes are compared under the hypothetical conditions of a Gaussian channel and all the users are perfectly orthogonal to each other, then all three schemes are equivalent with respect to Shannon's channel capacity [95]. However, mobile communications are usually conducted over radio channels that are more hostile than the ideal Gaussian channel and these radio channels lead to performance differences amongst the three multiple access schemes. In comparison to FDMA and TDMA systems, CDMA systems suffer more severe multiple access interference (MAI) due to the often imperfect cross-correlation properties of the spreading codes used. The user signals in FDMA and TDMA are inherently orthogonal to each other due to the orthogonal frequency and time slots used. However, FDMA and TDMA are primarily dependent on the availability of bandwidth, which is a costly resource, and the capacities of both these schemes are therefore bandwidth-limited. CDMA, on the other hand is only interference-limited. In second generation CDMA systems, specifically, in the Qualcomm IS-95 CDMA standard [11, 88], the multiple access interference (MAI) is treated as noise. We note, however that upon exploiting the extra knowledge of the users' spreading sequences and their associated channel impulse responses (CIR) the MAI can be substantially reduced, resulting in corresponding user capacity gains.

One of the effects of the mobile radio channel is dispersive multipath propagation. This is due to the reflections and scattering of the signal by objects present in the propagation environment. The multipath channel destroys the orthogonality between spreading codes, thus further increasing the cross-correlation between the users. The multipath spreading of the signal results in inter-symbol interference (ISI), which severely degrades the performance of the system. However, an advantage of CDMA schemes is that the multipath propagation can be exploited to give multipath diversity gains. With the aid of multipath receivers, namely RAKE receivers [96, 97], the correlation properties of the spreading codes can be exploited and the energy from the different paths can be coherently combined, in order to provide a multipath diversity gain. A detrimental effect of the mobile channel is its time-varying property, more commonly known as fading. This time-varying property is caused by the movements of mobile stations and other objects in the propagation environment. This results in the received signal having a large variance about its mean, again resulting in a degraded performance. These effects will be explained in more detail in our further discussions. Other advantages of CDMA include the privilege of privacy through the use of unique spreading codes for different users and diversity techniques to combat multipath fading [98, 99]. Some of these diversity techniques include multipath diversity combining [100], cell-site antenna diversity combining [100] and "soft-handoff" combining, where signals from two or more cell sites are combined [100]. Another advantage of CDMA is that it is well suited to support variable bit rate transmission and data rates can be chosen individually for each user, as proposed for example by Baier [101]; and [102]; and [103]. Further discussions on variable bit rate and adaptive-rate transmissions are provided in Chapter 4.

A disadvantage of CDMA is that multiple access interference (MAI) is the main limiting factor imposed by the cross-correlation between spreading codes. Additionally, even when the spreading codes are designed to be perfectly orthogonal, the wideband mobile channel destroys this orthogonality between the codes. Traditionally, powerful error-correcting

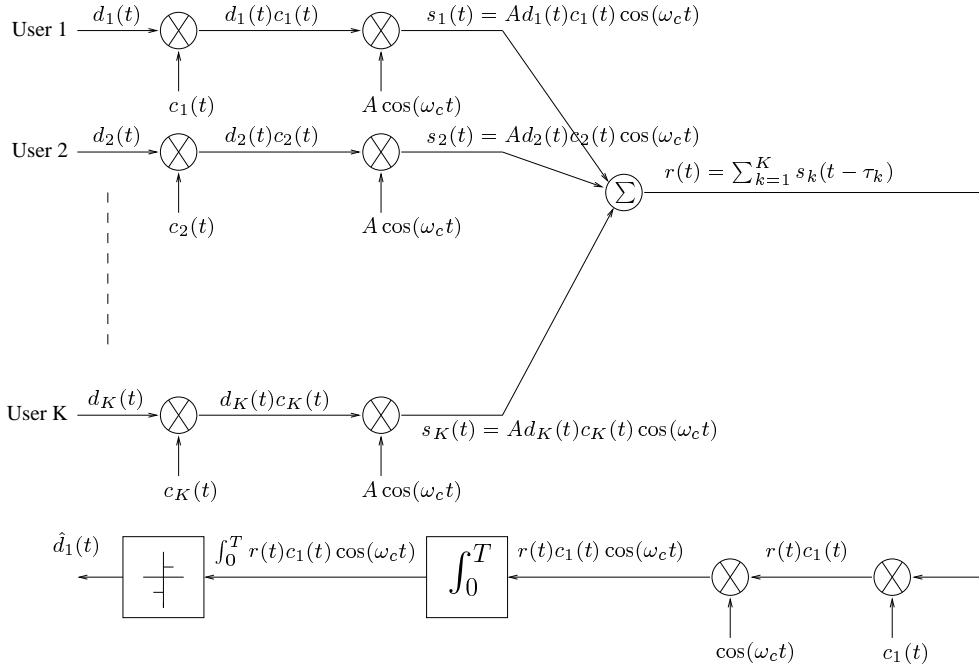


Figure 2.2: Block diagram of a simple asynchronous DS-CDMA system in a noiseless channel. The signals from all the K users arrive at the receiver with different propagation delays, τ_k . Only the receiver for user 1 is shown. The despreading and demodulation processes shown in the figure assume perfect synchronization.

codes [104] are used to overcome this problem. Other interference reduction techniques used in CDMA are voice activity-based bit rate control [98, 99] and cell-site sectorization [98, 99]. Current research on CDMA receivers includes multiuser detection [83] that exploits the available information about the spreading sequences and CIR estimates, in order to reduce the MAI. An introduction to the basic principles of these receivers was given, for example by [91] and [83]. Multiuser receivers are dealt with in Chapters 3 to 5. Furthermore, due to the time-varying nature of the mobile radio channel, the powers of the received signals vary widely among the users. This results in the phenomenon commonly termed as the “near-far” effect, where the stronger signals “swamp” the weaker signals. Therefore, stringent power control [98] is required to ensure that the signals from all the different users arrive at the receiver with relatively similar strengths.

Following the above brief introduction to CDMA, let us now consider the basics of this multiple access technique and the foundations of conventional DS-CDMA receivers in a little more depth.

2.2 DS-CDMA transmission model

This section explains the basic principles of operation in a DS-CDMA scheme. For a more detailed discussion, the reader is referred to the monographs by [88], [91], and [92] as well as and [93]. The block diagram of a simple asynchronous CDMA modem in a noiseless channel is shown in Figure 2.2. This system supports K users, each transmitting its own information. The users are identified by $k = 1, 2, \dots, K$. The modulation scheme used is Binary Phase Shift Keying (BPSK). Each user's data signal is denoted by $d_k(t)$ and each user is assigned a unique pseudo-random code also known as a spreading code denoted by $c_k(t)$. There are two classes of spreading codes in general, binary and complex. For simplicity, the following discussion considers only binary codes. Each spreading code consists of Q pulses, commonly known as chips. Spreading codes are discussed in more detail in Section 2.6.

In this discussion, the wanted signal is the signal of user $k = 1$ and all the other $(K - 1)$ signals are considered to be interfering signals.

2.3 DS-CDMA transmitter

At the transmitter of user k , each data bit of user k is first multiplied by the spreading code $c_k(t)$. This causes the spectrum of the information signal to be spread across the allocated bandwidth. Next, the signal is modulated onto its carrier before it is transmitted. The transmitted signal is given by :

$$s_k(t) = Ad_k(t)c_k(t) \cos(\omega_c t), \quad (2.1)$$

where ω_c is the carrier frequency in rad/sec and A is the amplitude of the carrier signal. Let us now consider the recovery of the DS-CDMA signal at the receiver.

2.4 DS-CDMA receiver

At the receiver, the composite of all the K user signals is received, consisting of the transmitted signal from user 1 and the other $(K - 1)$ interfering signals. Ignoring the noise, the received signal is given by :

$$r(t) = \sum_{k=1}^K s_k(t - \tau_k), \quad (2.2)$$

where τ_k is the propagation delay from the transmitter to the receiver of the k -th user. Let us now concentrate on the recovery of the information signal.

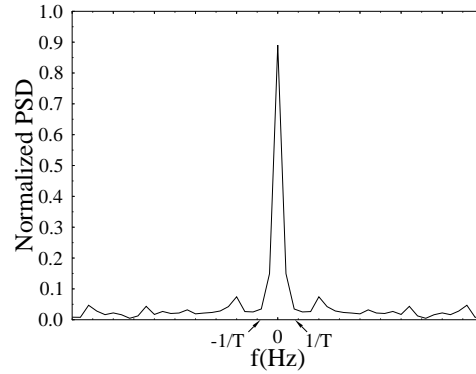


Figure 2.3: The power spectral density (PSD) plot of a despread signal in the presence of interfering users, normalized to the total power in the signal. The received signal consists of the superposition of the signals from more than one user. The PSD values are normalized to the PSD value at frequency 0. The despread signal has a bandwidth of approximately $1/T$ compared to the other signals, which remain spread and have bandwidths of $1/T_c$, where T_c is the duration of one chip in the spreading sequence. The ratio of T/T_c is 128.

2.4.1 Recovery of the information signal

Let us first consider the simplest case, where $K = 1$, yielding :

$$r(t) = s_1(t - \tau_1) \quad (2.3)$$

$$= Ad_1(t - \tau_1)c_1(t - \tau_1) \cos(\omega_c t + \theta'), \quad (2.4)$$

where the propagation delay-induced carrier shift is given by $\theta' = -\omega_c \tau_1$.

In order to recover the original information of user 1, the received signal is despread by multiplying the received signal with a synchronized replica of the spreading code of user 1, as follows :

$$\hat{s}_1(t) = r(t)c_1(t - \tau') \quad (2.5)$$

$$= Ad_1(t - \tau_1)c_1(t - \tau_1)c_1(t - \tau') \cos(\omega_c t + \theta'), \quad (2.6)$$

where τ' is the delay estimate. This despreads the spread signal of user 1 back to its original bandwidth, as illustrated in Figure 2.3.

In order to demodulate the signal, it is then multiplied by the carrier and passed through a correlator followed by a thresholding device, as demonstrated in Figure 2.2. At the correlator

output, we then have :

$$z_1 = \int_{t_1}^{t_1+T} \hat{s}_1(t) \cos(\omega_c t + \theta' + \varphi) dt, \quad (2.7)$$

where t_1 is the time of commencement for the data bit, T is the period of one data bit and φ is the phase synchronization error.

If we assume that the replica of the spreading code at the receiver is perfectly synchronized to the code used to spread the signal at the transmitter, then $\tau_1 = \tau'$ and we can set $\tau_1 = 0$, yielding :

$$\hat{s}_1(t) = A d_1(t) c_1^2(t) \cos(\omega_c t). \quad (2.8)$$

Substituting Equation 2.8 into Equation 2.7 and assuming that there is no phase synchronization error, i.e. $\varphi = 0$, we then have :

$$z_1 = \int_{t_1}^{t_1+T} A d_1(t) c_1^2(t) \cos^2(\omega_c t) \quad (2.9)$$

$$= \frac{A}{2} \int_{t_1}^{t_1+T} d_1(t) c_1^2(t) [\cos 2(\omega_c t) + 1] dt. \quad (2.10)$$

The high frequency term $\cos 2(\omega_c t)$ tends to zero after the correlator-based receiver, since the frequency ω_c is significantly higher than that of $d_1(t) c_1^2(t)$, resulting in an equal number of positive and negative terms in the integral, yielding :

$$z_1 = \frac{A}{2} \int_{t_1}^{t_1+T} d_1(t) c_1^2(t) dt. \quad (2.11)$$

Since it is assumed that there is no timing error, $d_1(t)$ is BPSK demodulated, giving $d_1(t) = \pm 1$, and $\int_0^T c_1^2(t) dt = T$, hence we have :

$$z_1 = \pm \frac{AT}{2}. \quad (2.12)$$

The above derivation assumes that there is accurate phase and timing synchronization. If these assumptions are invalid, then we arrive at :

$$z_1 = \int_{t_1}^{t_1+T} A d_1(t - \tau_1) c_1(t - \tau_1) c_1(t - \tau') \cos(\omega_c t + \theta') \cos(\omega_c t + \theta' + \varphi) dt, \quad (2.13)$$

$$= \int_{t_1}^{t_1+T} \frac{A}{2} d_1(t - \tau_1) c_1(t - \tau_1) c_1(t - \tau') \cos(\varphi) dt, \quad (2.14)$$

where we used the identity that $\cos A \cos B = \frac{1}{2}[\cos(A+B) + \cos(A-B)]$ and we exploited

again that the high-frequency term of $\frac{1}{2} \cos[2(\omega_c t + \theta') + \varphi]$ tends to 0 after the correlator. Since $d_1(t - \tau_1) = \pm 1$, the following ensues :

$$z_1 = \pm \frac{A}{2} \cos(\varphi) \int_{t_1}^{t_1+T} c_1(t - \tau_1) c_1(t - \tau') dt \quad (2.15)$$

$$= \pm \frac{AT}{2} \cos(\varphi) R_{cc}(\tau_1 - \tau'), \quad (2.16)$$

where $R_{cc}(\tau_1 - \tau')$ is the auto-correlation of the spreading code $c_1(t)$ given by :

$$R_{cc}(\tau_1 - \tau') = \int_0^T c_1(\tau_1) c_1(\tau') d\tau. \quad (2.17)$$

Therefore $|z_1|$ is maximum, when $(\tau_1 - \tau') = 0$ and $\varphi = 0$. Synchronization errors will result in lower $|z_1|$ values, leading to lower signal-to-noise ratios (SNR) and hence higher bit-error-rates (BER). When inaccurate synchronization occurs, we have $\tau_1 \neq \tau'$ and hence the high values of out-of-phase autocorrelation contributions due to $R_{cc}(\tau_1 - \tau')$ result in high BERs. Therefore, the spreading codes have to be carefully designed in order to have low out-of-phase autocorrelation values, an issue to be addressed in Section 2.6 in greater depth.

2.4.2 Recovery of the information signal in multiple access interference

In the case where there are several users, i.e. $K > 1$, the received signal is given by :

$$r(t) = \sum_{k=1}^K s_k(t - \tau_k). \quad (2.18)$$

After multiplying the received signal, $r(t)$, with the spreading code, $c_1(t)$, the information signal of user 1, $d_1(t)$, is despread into its original bandwidth. However, the signals of all the other $K - 1$ users remain spread, since $c_1(t)$ is orthogonal to the other spreading codes, resulting in :

$$\hat{s}_1(t) = \sum_{k=1}^K s_k(t - \tau_k) c_1(t - \tau_1'). \quad (2.19)$$

Next the signal is demodulated and passed through a correlator as well as the thresholding

device, as seen in Figure 2.2. The output of the correlator is formulated as :

$$z_1(t) = \int_{t_1}^{t_1+T} \sum_{k=1}^K s_k(t - \tau_k) c_1(t - \tau'_1) \cos(\omega_c t + \theta') dt \quad (2.20)$$

$$= \int_{t_1}^{t_1+T} \left[s_1(t - \tau_1) c_1(t - \tau'_1) + s_2(t - \tau_2) c_2(t - \tau'_1) + \dots + s_K(t - \tau_K) c_1(t - \tau'_1) \right] \cos(\omega_c t + \theta') dt. \quad (2.21)$$

In a synchronous system, the start of each data bit of a user coincides with the start of the data bits of all the other users. Assuming that there are no phase or timing synchronization errors, i.e. $\tau_k = 0$ and $\theta' = 0$, we have :

$$z_1(t) = \int_{t_1}^{t_1+T} \sum_{k=1}^K s_k(t) c_1(t) \cos(\omega_c t) dt \quad (2.22)$$

$$= \int_{t_1}^{t_1+T} \sum_{k=1}^K A d_k(t) c_k(t) c_1(t) \cos^2(\omega_c t) dt \quad (2.23)$$

$$= \frac{A}{2} \int_{t_1}^{t_1+T} \sum_{k=1}^K d_k(t) c_k(t) c_1(t) dt \quad (2.24)$$

$$= \frac{A}{2} \int_{t_1}^{t_1+T} \left[d_1(t) c_1^2(t) + d_2(t) c_2(t) c_1(t) + \dots + d_K(t) c_K(t) c_1(t) \right] dt \quad (2.25)$$

where again, the high frequency term of $\cos(2\omega_c t)$ integrates to zero.

If the spreading sequences are designed such that they constitute an orthogonal set, where

$$\int_0^T c_i(t) c_j(t) dt = \begin{cases} T & \text{for } i = j \\ 0 & \text{for } i \neq j \end{cases}, \quad (2.26)$$

then all the interference terms integrate to zero, leaving only the data bits of the wanted user, namely user 1. Since $d_1(t) = \pm 1$ and $\int_0^T c_1^2(t) dt = T$, we have :

$$z_1 = \pm \frac{AT}{2}, \quad (2.27)$$

as seen for a single user in Equation 2.12.

Thus, under the assumption of perfect synchronization the data bits of user 1 can be recovered despite the other interfering users. In practice, it is difficult to design a large set of spreading codes that are perfectly orthogonal, since two different demands have to be satisfied. Firstly, zero out-of-phase correlation is required, i.e. $\int_0^T c_i(t - \tau) c_i(t) dt = 0$, for $\tau \neq 0$. Secondly, Equation 2.26 has to be satisfied. In addition, a range of other practical code design constraints have to be satisfied, as we will see in Section 2.6. The result is

usually a compromise by approximating the ideal conditions, where the spreading codes are not perfectly uncorrelated with each other, but the cross-correlation values are kept as small as possible. These cross-correlations result in multiple access interference (MAI) that degrades the performance of the system. These correlations are given by :

$$\int_0^T c_i(t)c_j(t)dt = \begin{cases} T & \text{for } i = j \\ R_{ij} \neq 0 & \text{for } i \neq j \end{cases} \quad (2.28)$$

Considering Equation 2.25 again in conjunction with the correlation constraints of Equation 2.28, we have :

$$z_1(t) = \frac{A}{2} \int_{t_1}^{t_1+T} \left[d_1(t)c_1^2(t) + d_2(t)c_2(t)c_1(t) + d_K(t)c_K(t)c_1(t) \right] dt \quad (2.29)$$

$$= \frac{A}{2} \left[\pm T \pm TR_{12} + \dots \pm TR_{1K} \right]. \quad (2.30)$$

The first term is the wanted data and all the other terms contribute to the MAI.

Let us now consider the corresponding operations in the frequency domain.

2.5 Frequency-domain representation

The spreading and despreading of the information signal is more easily represented in the frequency domain. If the information signal, $d_k(t)$, is BPSK-modulated, having an amplitude of ± 1 and a bit rate of $1/T$ bits/sec, then the power spectral density (PSD) of the information signal is given by :

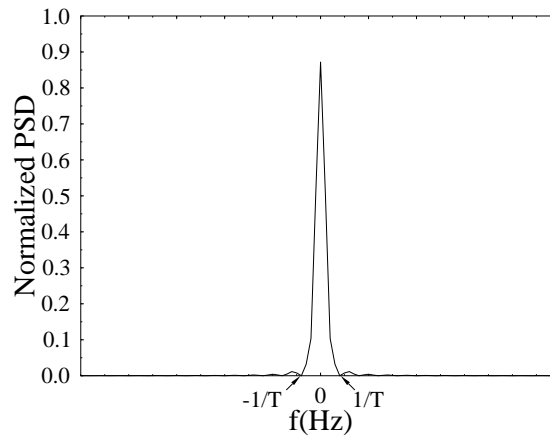
$$S(f) = T \text{sinc}^2(fT). \quad (2.31)$$

This is shown in Figure 2.4(a). The frequencies of the first nulls of the spectrum are at $\pm 1/T$, giving an approximate bandwidth of $1/T$.

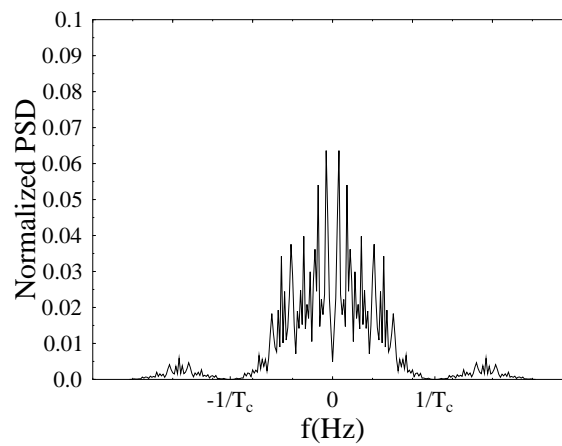
The spreading signal, $c_k(t)$, has a chip rate of $1/T_c$. If the chip amplitudes are also ± 1 , then the spreading signal has a PSD of :

$$S_c(f) = T_c \text{sinc}^2(fT_c). \quad (2.32)$$

If the spread time-domain signal is given by the product $d_k(t)c_k(t)$, the resulting frequency-domain PSD is that of the corresponding convolved spectra, which is shown in Figure 2.4(b). Since the T_c/T ratio is typically high, the PSD of Equation 2.31 is a 'near-Dirac' impulse and hence the PSD of Figure 2.4(b) is similar to $S_c(f)$ in Equation 2.32. Therefore, for conventional receivers, the bandwidth of the original information signal is spread by the ratio of T/T_c . The ratio of the spread bandwidth to the information bandwidth is known as the *processing gain*. Historically, the term *processing gain* was used in jamming systems, which employed the principles of spread spectrum to protect a signal against jamming interference from an unknown or hostile source. The term *processing gain* was used



(a) PSD of the information signal before spreading. The first nulls are at $\pm 1/T$, where T is the bit rate of the signal.



(b) PSD of the information signal after spreading. The first PSD nulls are at $\pm 1/T_c$, where T_c is the chip rate of the signal.

Figure 2.4: Power spectral density (PSD) plot of the signal before and after spreading, normalized to the total power in the signal. The PSD values are normalized to the PSD value at frequency 0. Note that the frequency scales in (a) and (b) are different for simple graphical representation reasons, since $T/T_c = 128$.

to quantify the factor of advantage of a signal that had been spread over the jammer interference. In DS-CDMA systems, the spread bandwidth is approximately the spreading code chip rate, $1/T_c$ and the information bandwidth is approximately $1/T$. This thus gives a processing gain of T/T_c . The term *spreading factor* is also used interchangeably with *processing gain* to convey a similar meaning.

If at the receiver, the spread signal, $d_k(t)c_k(t)$, is multiplied by the spreading signal, $c_k(t)$, again, the spread signal is then despread into its original bandwidth and will have a PSD of :

$$S(f) = T \text{sinc}^2(fT), \quad (2.33)$$

while all the other signals remain spread. Figure 2.3 shows the PSD of a despread signal in the presence of interfering users, which corresponds to the convolution of the received signal spectrum with that of the spreading code for an arbitrary T/T_c ratio of 128.

In the next section, a few examples of spreading sequences will be considered.

2.6 Spreading sequences

In Section 2.4.2, we noted that the multiple access interference (MAI) of Equation 2.30 is largely dependent on the cross-correlation (CCL) between the spreading code of the wanted user and the spreading codes of all the other interfering users. The ideal CCL value is zero for all values of $t \neq 0$. Ideally, the out-of-phase auto-correlation (ACL) of the spreading sequences should also be zero, in order to tolerate inaccurate synchronization of the spreading sequences. Therefore, for the conventional CDMA receiver, the design of the set of spreading sequences to be used in a CDMA system is very important as to its performance. The design is usually based on a set of criteria which will be the topic of the forthcoming sections. Let us commence by considering the correlation properties of the spreading sequences.

2.6.1 Correlation of sequences

The periodic ACL of a complex spreading sequence, $c^{(k)}$, is defined as:

$$R_{kk}(q) = \sum_{i=1}^Q c_i^{(k)} c_{(q+i) \circledast Q}^{(k)*}, \quad (2.34)$$

for $q = -(Q-1), \dots, Q$; where the expression $[(q+i) \circledast Q]$ represents the remainder after dividing $(q+i)$ by Q , $c^{(k)*}$ is the complex conjugate of $c^{(k)}$ and Q is the length of the sequence. The periodic CCL of two different sequences, $c^{(j)}$ and $c^{(k)}$ is defined as :

$$R_{jk}(q) = \sum_{i=1}^Q c_i^{(j)} c_{q+i}^{(k)*}, \quad (2.35)$$

for $q = -(Q-1), \dots, Q$.

A user's signal that has been spread has to appear noise-like to all the other users. This can be achieved by using a random spreading code, having an infinite repetition time. However, if the code is truly random, the original data signal cannot be recovered at the receiver by correlation techniques. For the spreading code to be useful, it has to be deterministic, but known only to the transmitter and the intended receiver. However, it still has to appear like random noise to non-intended receivers. Therefore, the spreading codes are generally known as pseudo-random or pseudo-noise (PN) sequences. These codes have a length of Q and are repeated periodically with a period of Q . Each spreading code set has a family size of K , i.e. there are K codes in the set. This will be explained later in the following sections. There are basically two classes of spreading sequences, namely the binary and the non-binary sequences also known as polyphase sequences [105]. The latter are complex-valued sequences.

Traditionally, the measure used to compare different code sets was defined as R_{max} , where :

$$R_{max} = \max |R_a, R_c|, \quad (2.36)$$

and

$$\begin{aligned} R_a &= \max |R_{kk}(q)| \quad \text{for } 1 \leq k \leq K; & -(Q-1) < q \leq Q, q \neq 0 \\ R_c &= \max |R_{jk}(q)| \quad \text{for } 1 \leq j, k \leq K, j \neq k; & -(Q-1) < q \leq Q. \end{aligned} \quad (2.37)$$

The value of the periodic CCL or out-of-phase periodic ACL that has the highest magnitude is taken to be the R_{max} of a particular code set. A low out-of-phase periodic ACL allows easier code acquisition or synchronization, while a low periodic CCL reduces the MAI. A measure of "goodness" of R_{max} is how well it compares with the well-known Welch [87] or Sidelnikov [87] bounds. For a set of K sequences having a period of Q , the Welch bound is defined as [87] :

$$R_{max} \geq Q \sqrt{\frac{K-1}{KQ-1}}. \quad (2.38)$$

This value is dependent on the number, K , of codes in the set, and the length, Q , of the codes. Therefore, for a code set to be optimum, according to Welch, it had to achieve the minimum value given by Equation 2.38.

For the same set of sequences, the Sidelnikov bound is defined as [87] :

$$R_{max} > (2Q-2)^{\frac{1}{2}}. \quad (2.39)$$

A code set is optimum according to these criteria, if its performance measure, R_{max} , approaches the Welch or Sidelnikov lower bounds, given by Equations 2.38 and 2.39, respectively. Some numerical examples will be given in Sections 2.6.3 and 2.6.4 in the context of Gold sequences and Kasami sequences, respectively.

The criterion of family size, K , is important because large families of good codes enable more users to be accommodated in the same bandwidth, thus increasing the user capacity of the system. Since a CDMA system is interference-limited, as it will be shown in Section

2.7, the larger the code set having low CCL values, the higher the capacity. The difficulty in designing spreading codes lies in achieving a large family size having good CCL values for a specific value of spreading code length, Q . These issues will be demonstrated in Sections 2.6.2, 2.6.3 and 2.6.4 using various examples, namely the m -sequences [87], Gold codes [106] and Kasami sequences [107], respectively.

2.6.2 m -sequences

An important class of binary sequences is the binary maximal-length shift register sequences, commonly known as m -sequences [87]. Sequences can be generated using the well-known linear generator polynomials of degree m , where :

$$g(x) = g_m x^m + g_{m-1} x^{m-1} + g_{m-2} x^{m-2} + \dots + g_1 x + g_0. \quad (2.40)$$

In order to generate m -sequences, the generator polynomial, $g(x)$, must be from the class of polynomials known as primitive polynomials, which implies in simple terms, that $g(x)$ cannot be factorized into lower-order polynomials. For a more detailed discussion on primitive polynomials, the reader is referred to 's excellent monograph on error correction coding [104], where generator polynomials are used extensively. The m -sequence generated has a period of $Q = 2^m - 1$, where m is the degree of the generator polynomial. By contrast, a sequence generated by a non-primitive generator polynomial, $g(x)$, may have a period of less than $2^m - 1$ and hence this sequence is not an m -sequence.

One of the properties of m -sequences is that the ACL of these sequences can be calculated as :

$$\begin{aligned} R_{kk}(0) &= Q \\ R_{kk}(q) &= -1 \quad \text{for } q \neq 0, \end{aligned} \quad (2.41)$$

which accrues from the simple binary nature of the sequences. Explicitly, when a Q -chip sequence is perfectly aligned with itself, corresponding to a shift of $q = 0$ chip intervals, there are Q number of $+1$ terms in the autocorrelation sum of Equation 2.34. By contrast, for $q \neq 0$, the summation always consists of one extra -1 value compared to the number of $+1$ values. These ACL properties are near-ideal for code acquisition or synchronization, where the perfectly aligned condition of $q = 0$ between the received and locally stored sequences has to be detected. As an additional constraint, in multi-user communications, a large set of spreading sequences exhibiting low CCL values is needed. The m -sequences do not satisfy this requirement, since some m -sequence pairs have large CCL values. Let us now consider the family of Gold codes.

2.6.3 Gold sequences

One of the best-known binary sequences having relatively good correlation values is the Gold sequence set [106]. A set of Gold sequences is constructed from a preferred pair of m -sequences, \underline{x} and \underline{y} , having identical length Q . In 1967, Gold proved that these preferred pairs of m -sequences of length Q have only three possible CCL values, which are shown in

Equations 2.43, 2.44 and 2.45. The period of the Gold sequences generated by \underline{x} and \underline{y} is also Q . Each Gold sequence in a set is generated by a modulo-2 sum of \underline{x} and cyclic shifts of \underline{y} . The set also includes the m -sequences \underline{x} and \underline{y} . The entire set of Gold sequences having a period of Q is given by :

$$S_g = \left\{ \underline{x}, \underline{y}, \underline{x} \oplus \underline{y}, \underline{x} \oplus T^{-1}\underline{y}, \underline{x} \oplus T^{-2}\underline{y}, \dots, \underline{x} \oplus T^{-(Q-1)}\underline{y} \right\} \quad (2.42)$$

where $T^{-q}\underline{y}$ for $q = 0, 1, \dots, Q - 1$, represents a cyclic shift of \underline{y} by q chip intervals; and the symbol \oplus represents modulo-2 addition.

The family size of a Gold sequence set having a period of Q is $K = Q + 2$. A property of Gold sequences, as stated earlier, is that the CCLs and out-of-phase ACLs have only three possible values, which are given by :

$$R_{kk}(q) = \begin{cases} Q & \text{for } q = 0 \\ \{-1, -t(m), t(m) - 2\} & \text{for } q \neq 0 \end{cases} \quad (2.43)$$

$$R_{jk}(q) = \{-1, -t(m), t(m) - 2\} \quad \text{for all } q \text{ and } j \neq k, \quad (2.44)$$

where

$$\begin{aligned} t(m) &= 2^{(m+1)/2} + 1 & m \text{ is odd} \\ t(m) &= 2^{(m+2)/2} + 1 & m \text{ is even.} \end{aligned} \quad (2.45)$$

Since Gold sequences are constructed from preferred pairs of m -sequences, the ACL is given by Q , as seen in Equation 2.41. The detailed derivation of the CCL values and out-of-phase ACL values was given by Simon *et al* [87]. In order to compute the correlation values, the binary bits 0 and 1 are mapped to +1 and -1, respectively. From the correlation values, it can be seen that for a set of Gold sequences, $R_{max} = t(m)$. Consider a Gold sequence set of period $Q = 63$, corresponding to $m = 6$. Then from Equation 2.45 we have :

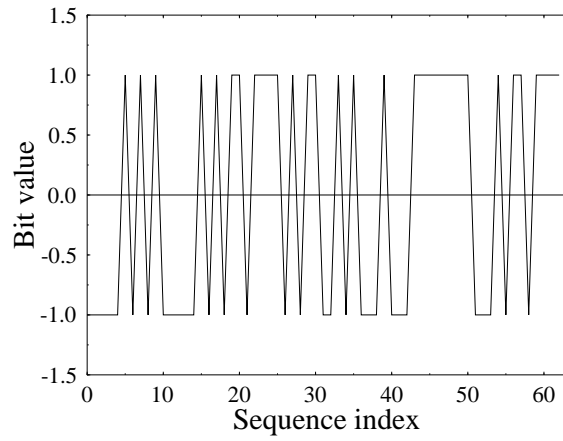
$$R_{max} = t(m) = 2^{(6+2)/2} + 1 = 17. \quad (2.46)$$

The Welch bound of Equation 2.38 for this Gold sequence set, which has a family size of $K = Q + 2 = 65$, is computed as follows :

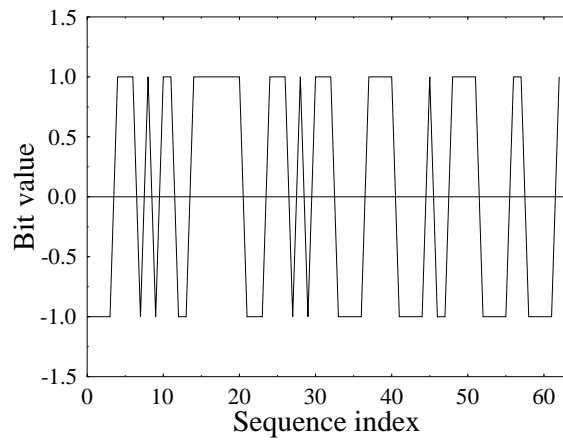
$$R_{max} \geq 63 \sqrt{\frac{65 - 1}{63(65) - 1}} \approx 7.88. \quad (2.47)$$

Note that the Welch bound is as low as 46% of $|R_{max}| = 17$ in Equation 2.46, computed for our example of a code set of $Q = 63$ and $K = 65$. Two examples of Gold sequences are shown in Figure 2.5.

The periodic CCL of these two sequences was calculated using Equation 2.35 and the CCL is plotted in Figure 2.6. The binary bits 0 and 1 were mapped to +1 and -1, respectively. It can be seen from Figure 2.6 that the CCL has three values, i.e. -1, -17 and +15. This set of spreading sequences yields comparatively high CCLs, where the spikes are located in the



(a) A Gold sequence from the code set of $Q = 63$.



(b) A different Gold sequence from code set of $Q = 63$.

Figure 2.5: Examples of Gold sequences

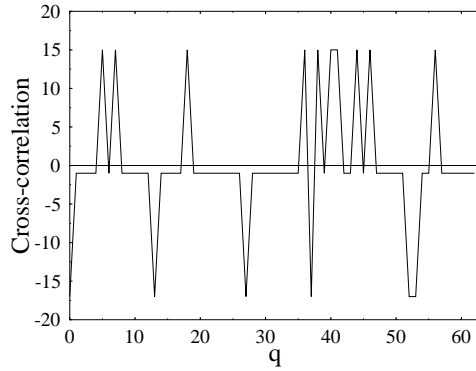


Figure 2.6: Cross-correlation values between two pairs of Gold sequences versus q as specified in Equation 2.35. The binary bits 0 and 1 were mapped to +1 and -1 respectively to compute the correlation values. The CCL values are -1, -17 or 15.

figure.

Following the above brief notes on Gold codes, let us now consider Kasami sequences.

2.6.4 Kasami sequences

A set of binary sequences that are near-optimum with respect to the Welch bound is the Kasami sequence family [107]. Each sequence set is generated from one m -sequence, \underline{x} , which has a period of Q . The m -sequence \underline{x} is decimated by sampling it periodically. Then, a second sequence, \underline{y} , is formed by concatenating the decimated sequence repeatedly, until a sequence of length \bar{Q} is obtained. The entire Kasami set is then generated by the modulo-2 addition of the sequence \underline{x} and the sequences generated by cyclic shifts of \underline{y} .

The generator polynomial of \underline{x} is of degree m and \underline{x} has a period of $Q = 2^m - 1$. Kasami sequences can only be generated for even values of m . The decimation factor used to decimate \underline{x} is given by $s(m) = 2^{m/2} + 1$. The decimated sequence, \underline{y} , has a shorter period of $(2^m - 1)/s(m) = 2^{m/2} - 1$. Hence, the set of Kasami sequences is given by :

$$S_k = \left\{ \underline{x}, \underline{x} \oplus \underline{y}, \underline{x} \oplus T^{-1}\underline{y}, \underline{x} \oplus T^{-2}\underline{y}, \dots, \underline{x} \oplus T^{-(2^{m/2}-2)}\underline{y} \right\}. \quad (2.48)$$

The correlation values of a Kasami sequence set are also ternary, similar to those of the Gold sequences, but the values are lower for sequences of the same length, which are given

by :

$$R_{kk}(q) = \begin{cases} Q & \text{for } q = 0 \\ \{-1, -s(m), s(m) - 2\} & \text{for } q \neq 0 \end{cases} \quad (2.49)$$

$$R_{jk}(q) = \{-1, -s(m), s(m) - 2\} \quad \text{for all } q \text{ and } j \neq k. \quad (2.50)$$

The number of Kasami sequences is now reduced to $K = 2^{m/2}$, which is lower than that of the m -sequences. More explicitly, the usage of a decimated sequence reduces the number of sequences in a set, compared to the Gold sequence set, having the same period. For example, a Gold sequence set having a period of $Q = 63$ has a family size of $K = 65$, while Kasami sequences of the same length have a set size of $K = 8$. However, due to the reduced set size, the high CCL sequences can be eliminated and hence the Kasami sequences have lower CCL values, which is essentially due to the usage of a decimated sequence. This is explained in more depth by *et al* [87]. These lower CCL values result in Kasami sequences being nearer to achieving the optimum Welch lower bound compared to Gold sequences of the same length. The Welch bound of Equation 2.38 for the Kasami set of $Q = 63$ and $K = 8$ is given by :

$$R_{max} \geq 63 \sqrt{\frac{8-1}{63(8)-1}} \approx 7.43, \quad (2.51)$$

while

$$|s(m)| = 2^{(6/2)} + 1 = 9. \quad (2.52)$$

Therefore, the optimum Welch lower bound is now 83% of R_{max} , compared to the previous 46% for the equivalent Gold sequence set. Having considered a range of spreading sequences, let us now concentrate our discussions on the performance of the DS-CDMA system.

2.7 DS-CDMA system performance

In this section, a model for a DS-CDMA system using BPSK modulation is presented and a theoretical analysis of its performance is obtained. The model shown in Figure 2.7 is similar to the model shown in Figure 2.2, the difference being that the noise signal $n(t)$ is now added to the received signal. From this model, an expression for the bit-error-rate (BER) performance of the system is derived. The conditions under which this model is presented are :

- BPSK modulation is used for the information signal. The carrier signal has a frequency of ω_c and amplitude of $A = \sqrt{P}$, where P is the average power of the signal. This gives an energy per bit of $E_b = A^2 T = PT$.
- The length of the spreading code used is Q .

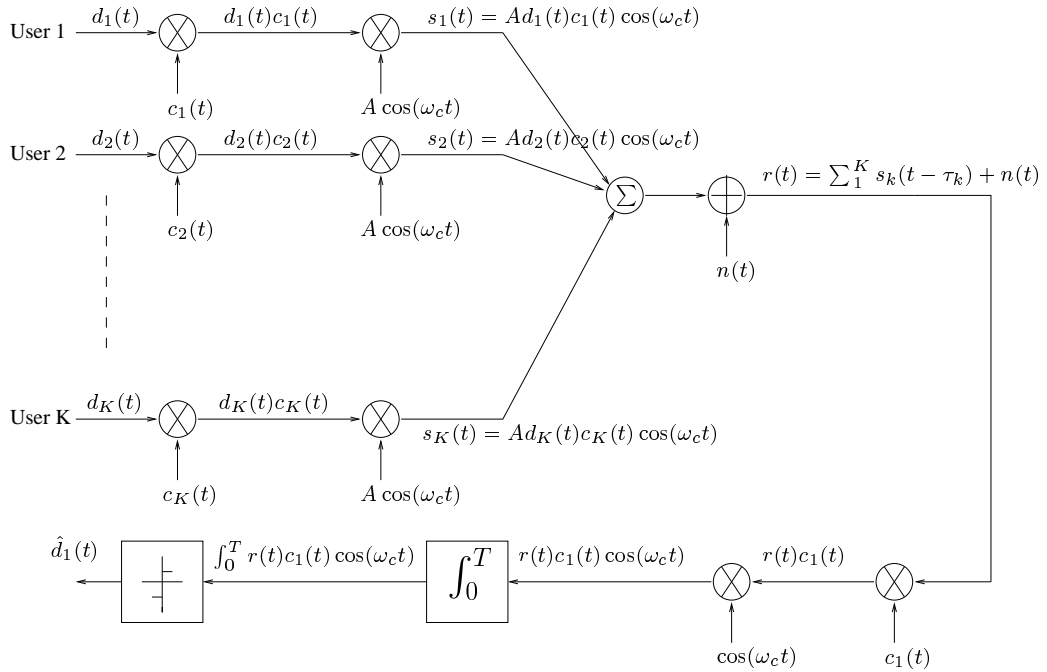


Figure 2.7: Block diagram of a simple asynchronous DS-CDMA system transmitting over a Gaussian channel. The signals from all the K users arrive at the receiver with different propagation delays, τ_k . Only the receiver for user 1 is shown. The despreading and demodulation processes shown in the figure assume perfect synchronization.

- Each information/data bit has a period of T and each chip has a period of T_c , where $T = QT_c$
- The pulse shape is rectangular and has an amplitude of ± 1 for the information signal. The pulse shape for each chip of the spreading code is also rectangular, having an amplitude of ± 1 .
- The total number of users in the system is represented by K and each user is identified by the subscript k .
- All K users are transmitting at the same bit rate.
- There is perfect power control for all K users.
- This system operates in a single cell environment.

2.7.1 Theoretical BER performance of asynchronous BPSK/DS-CDMA over Gaussian channels

In this section a BER expression is derived for a Gaussian channel, where it is assumed that for each user, all errors are caused by zero-mean Additive White Gaussian Noise (AWGN) at the receiver and multiple access interference (MAI) from the other $(K - 1)$ users. The derivation is performed at the baseband level, which greatly simplifies the analysis. However, the derivation is still valid for a bandpass system, because baseband and bandpass systems are equivalent [97].

The desired user is user 1 and all the other $(K - 1)$ users are interferers. The received signal, $r(t)$, is a sum of the transmitted signals from all K users and it is corrupted by Gaussian noise. The signal of each user arrives at a different propagation delay, given by τ_k . The received signal is formulated as :

$$r(t) = \sum_{k=1}^K \sqrt{P} d_k(t - \tau_k) c_k(t - \tau_k) + n(t). \quad (2.53)$$

This signal is then despread with a replica of the spreading code of user 1. A correlator-based receiver is used to obtain the associated decision statistic, z_1 , from which a decision is made concerning the bit transmitted. Therefore, we have :

$$z_1 = \int_0^T r(t) c_1(t - \tau_1 - \tau') dt, \quad (2.54)$$

where τ' is the code synchronization error, which degrades the demodulator's correlation properties; $\theta = -\omega_c \tau_1$, which is the delay-induced carrier-phase term; and $\varphi = -\omega_c \tau'$ is the demodulator's phase error.

If perfect synchronization is assumed for user 1, then we can set $\tau_1 = \tau' = 0$. Substituting Equation 2.53 into Equation 2.54 leads to :

$$z_1 = \int_0^T r(t) c_1(t) dt \quad (2.55)$$

$$= \int_0^T \left[\sqrt{P} d_1(t) c_1^2(t) + \sum_{k=2}^K \sqrt{P} d_k(t - \tau_k) c_k(t - \tau_k) c_1(t) + n(t) c_1(t) \right] dt \quad (2.56)$$

$$= D_1 + I + \eta, \quad (2.57)$$

where the corresponding terms are defined below, namely, D_1 is the bit transmitted by user 1 :

$$D_1 = \int_0^T \sqrt{P} d_1(t) c_1^2(t) dt, \quad (2.58)$$

and taking into account that $c_1^2(t) = 1$ and $d_1(t) = \pm 1$, this yields :

$$D_1 = \pm\sqrt{PT}. \quad (2.59)$$

The term η in Equation 2.57 is the component due to the AWGN, $n(t)$, which corresponds to the despread and demodulated term of :

$$\eta = \int_0^T n(t)c_1(t) dt. \quad (2.60)$$

Since $n(t)$ is the zero-mean AWGN having a variance of $N_0/2 = \sigma^2$, η is a Gaussian variable with zero mean and variance $\text{Var}[\eta]$, which is derived as :

$$\text{Var}[\eta] = E[\eta^2] \quad (2.61)$$

$$= E\left[\int_0^T n(t)c_1(t) dt \int_0^T n(u)c_1(u) du\right] \quad (2.62)$$

$$= \int_0^T \int_0^T E[n(t)n(u)]c_1(t)c_1(u) dt du. \quad (2.63)$$

But $E[n(t)n(u)]$ is the autocorrelation of $n(t)$, where :

$$E[n(t)n(u)] = \frac{N_0}{2}\delta(t-u). \quad (2.64)$$

Therefore, the variance $\text{Var}[\eta]$ becomes :

$$\text{Var}[\eta] = \frac{N_0}{2} \int_0^T \int_0^T \delta(t-u)c_1(t)c_1(u) dt du \quad (2.65)$$

$$= \frac{N_0}{2} \int_0^T c_1^2(u) du. \quad (2.66)$$

Since $\int_0^T c_1^2(u) du = T$, we have :

$$\text{Var}[\eta] = \frac{N_0T}{2}. \quad (2.67)$$

The middle term, I , in Equation 2.57 is the MAI component from all the other $(K-1)$ users, which is given by :

$$I = \sum_{k=2}^K \sqrt{P} \int_0^T d_k(t-\tau_k)c_k(t-\tau_k)c_1(t) dt. \quad (2.68)$$

From the central limit theorem [95], the summation of $(K-1)$ independent random vari-

ables can be modelled by the Gaussian distribution and hence in our analysis, I is approximated by a Gaussian random variable. By using the Gaussian approximation method [108] and assuming that there is perfect power control, the variance of I was derived by Pursley as follows :

$$\begin{aligned}\text{Var}[I] &= \frac{QT_c^2}{3} \sum_{k=2}^K P \\ &= \frac{QT_c^2}{3} (K-1)P.\end{aligned}\quad (2.69)$$

Substituting $T = QT_c$, we arrive at :

$$\text{Var}[I] = \frac{T^2}{3Q} (K-1)P. \quad (2.70)$$

Therefore, the equivalent SNR at the output of the correlator receiver is :

$$\text{SNR}_o = \frac{D_1^2}{\text{Var}[\eta] + \text{Var}[I]}. \quad (2.71)$$

Substituting Equations 2.59, 2.67 and 2.69 into Equation 2.71 and employing the expression $E_b = PT$, yields :

$$\text{SNR}_o = \left[\frac{PT^2}{\frac{N_0T}{2} + \frac{T^2}{3Q} (K-1)P} \right] \quad (2.72)$$

$$= \left[\frac{\frac{N_0T}{2} + \frac{T^2}{3Q} (K-1)P}{PT^2} \right]^{-1} \quad (2.73)$$

$$= \left[\frac{N_0}{2E_b} + \frac{K-1}{3Q} \right]^{-1}. \quad (2.74)$$

The second term of $(K-1)/(3Q)$ in the brackets in Equation 2.74 represents the MAI that causes an SNR degradation resulting in a degraded SNR performance for a particular value of E_b/N_0 . It can be seen that this degradation depends on the number of users, K , and the sequence length, Q . An increase in K or a decrease in Q would degrade the performance because it would increase the cross-correlation (CCL) between the received signals from all the users.

By assuming that the MAI has a Gaussian PDF, the BER of a BPSK-modulated system

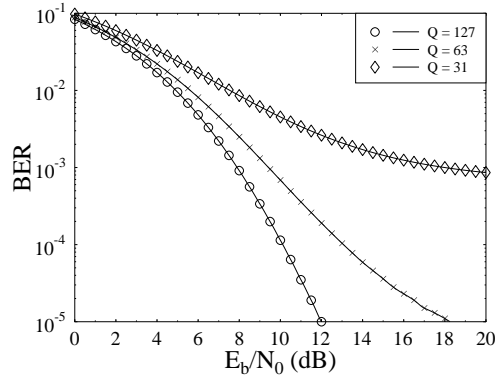


Figure 2.8: BER versus E_b/N_0 plots for an asynchronous CDMA system in a Gaussian channel. The number of users is fixed at $K = 10$, but varying values of sequence lengths, Q , are used. These graphs were plotted using Equation 2.75. As the sequence length, Q , decreases, the BER performance degrades.

in a Gaussian channel is given as $\text{BER} = Q(\sqrt{\text{SNR}_0})$, leading to :

$$\begin{aligned} \text{BER} &= Q(\sqrt{\text{SNR}_0}) \\ &= Q\left(\left[\frac{N_0}{2E_b} + \frac{K-1}{3Q}\right]^{-\frac{1}{2}}\right), \end{aligned} \quad (2.75)$$

where $Q(x)$ is the Gaussian Q-function [95].

According to Equation 2.75, if there is only one user, then $K = 1$ and the equation simplifies to $\text{BER} = Q(\sqrt{2E_b/N_0})$, which is the same as the theoretical BER performance of a BPSK system.

Figure 2.8 shows a plot of three BER versus E_b/N_0 curves. These curves were plotted using Equation 2.75 for $K = 10$ users and for sequence lengths of $Q = 31, 63$ and 127 . The curves show that as the sequence length, Q , decreased, the BER performance degraded.

Figure 2.9 shows another plot of three BER versus E_b/N_0 curves. These curves were also plotted using Equation 2.75, but for $Q = 63$ and for $K = 10, 20$ and 30 . The curves show that as the number of users, K , increased, the BER performance degraded. This was due to the increase in MAI.

Having characterized the system performance for K asynchronous users over a Gaussian channel, let us now consider synchronous users.

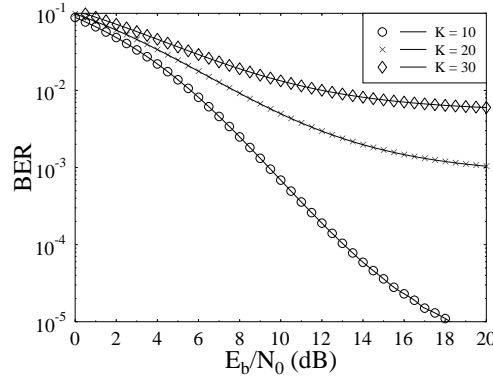


Figure 2.9: BER versus E_b/N_0 plots for an asynchronous CDMA system in a Gaussian channel. The sequence length is fixed at $Q = 63$ chips, but varying numbers of users, K , are used. These graphs were plotted using Equation 2.75. As the number of users, K , increases, the BER performance degrades.

2.7.2 Theoretical BER performance of bit-synchronous BPSK/DS-SS-CDMA systems over Gaussian channels

As stated above, the BER performance expression given in Equation 2.75 is valid for a system, where the users are asynchronous with respect to each other. Simulation studies are often conducted in a synchronous environment due to limited resources since then no oversampling of the signals is necessary. This is especially true for studies that combine Time Division Multiple Access (TDMA) and CDMA transmission. The users are allocated time slots and all the users in the same time slot transmit simultaneously, leading to synchronous reception at the receiver. Therefore, the BER performance of a perfectly synchronous system is analysed next.

Again, the output of the integrator in Figure 2.7 is often referred to as the decision statistic, z_1 , and its expression was given in Equation 2.57 as :

$$z_1 = D_1 + I + \eta,$$

where D_1 is the component representing the original bit transmitted by user 1. The expression for D_1 was given in Equation 2.59 as :

$$D_1 = \pm \sqrt{PT}.$$

The variance of the noise component η was previously derived as :

$$\text{Var}[\eta] = \frac{N_0 T}{2}. \quad (2.76)$$

Lastly, I is the interference component contributed by all the other $(K - 1)$ users, which is given by :

$$I = \int_0^T \sum_{k=2}^K \sqrt{P} d_k(t) c_k(t) c_1(t) dt. \quad (2.77)$$

The interference, I_k , from the k -th user is represented as :

$$I_k = \int_0^T \sqrt{P} d_k(t) c_k(t) c_1(t) dt \quad (2.78)$$

$$= \pm \sqrt{P} \int_0^T c_k(t) c_1(t) dt. \quad (2.79)$$

The term $\int_0^T c_k(t) c_1(t) dt$ represents the normalized periodic in-phase cross-correlation between the spreading codes of user 1 and user k , which can be rewritten as :

$$\int_0^T c_k(t) c_1(t) dt = R_{k,1} T. \quad (2.80)$$

Substituting this into Equation 2.79 leads to :

$$I_k = \sqrt{P} R_{k,1} T. \quad (2.81)$$

If we assume that the power of I , represented by S_I , is the sum of the powers of all the $K - 1$ interfering users, then we have :

$$S_I = \sum_{k=2}^K I_k^2 \quad (2.82)$$

$$= \sum_{k=2}^K [\sqrt{P} R_{k,1} T]^2 \quad (2.83)$$

$$= P T^2 \sum_{k=2}^K R_{k,1}^2. \quad (2.84)$$

The signal-to-noise ratio is given as :

$$\text{SNR}_o = \frac{D_1^2}{\text{Var}[\eta] + S_I}. \quad (2.85)$$

Q	MAI value
31	0.0593
63	0.0587
127	0.0055

Table 2.1: MAI term of Equation 2.88 for various values of Q and for $K = 10$.

Combining Equations 2.59, 2.67 and 2.84 into Equation 2.85, we arrive at :

$$\text{SNR}_o = \frac{PT^2}{\frac{N_0T}{2} + PT^2 \sum_{k=2}^K R_{k,1}^2} \quad (2.86)$$

$$= \left[\frac{\frac{N_0T}{2}}{PT^2} + \frac{PT^2 \sum_{k=2}^K R_{k,1}^2}{PT^2} \right]^{-1}. \quad (2.87)$$

Since the amplitude of each user's signal is \sqrt{P} , the energy per bit is $E_b = PT$. This leads to :

$$\text{SNR}_o = \left[\frac{1}{(2E_b/N_0)} + \sum_{k=2}^K R_{k,1}^2 \right]^{-1}. \quad (2.88)$$

The second term in Equation 2.88 represents the SNR degradation due to MAI. This term depends directly on the CCL between the spreading codes, rather than indirectly as in Equation 2.74. This is because the signals from all the users are synchronized with each other and therefore the CCL values of the spreading codes determine the amount of excess interference at the output of the integrator in Figure 2.7.

Assuming that the combined noise and interference components have a Gaussian distribution, the BER performance is given as :

$$\text{BER} = Q(\sqrt{\text{SNR}_o}) \quad (2.89)$$

$$= Q\left(\left[\frac{1}{(2E_b/N_0)} + \sum_{k=2}^K R_{k,1}^2\right]^{-\frac{1}{2}}\right), \quad (2.90)$$

where $Q(x)$ is the Gaussian Q-function [95].

Figure 2.10 shows a plot of three BER versus E_b/N_0 curves. These curves were plotted using Equation 2.90 for $K = 10$ and for Gold sequences of $Q = 31, 63$ and 127 . In general, the curves show that as the sequence length, Q , decreased, the BER performance degraded. However, there is virtually no difference between the curves for $Q = 31$ and $Q = 63$. This is because the MAI term in Equation 2.88 has very similar values for both of these sequence lengths, as shown in Table 2.1.

Figure 2.11 portrays a plot of three BER versus E_b/N_0 curves using Equation 2.90 for $Q = 63$ and for $K = 10, 20$ and 30 . In harmony with our expectations, as the number of

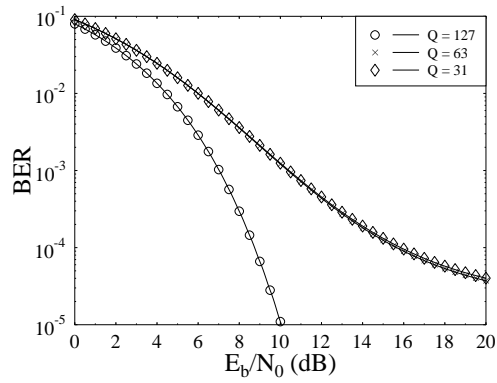


Figure 2.10: BER versus E_b/N_0 plots for a synchronous CDMA system in a Gaussian channel. Gold sequences are used with varying sequence lengths, Q , but the total number of users in the system is fixed at $K = 10$. These graphs were plotted using Equation 2.90. As the sequence length, Q , decreases, the BER performance degrades.

K	MAI value
10	0.0587
20	0.0612
30	0.0637

Table 2.2: MAI term of Equation 2.88 for various values of K and for $Q = 63$.

users, K , increased, the BER performance degraded. However, the performance degradation was small compared to the performance degradation shown in Figure 2.9. In a synchronous system, the BER performance depends directly on the CCL values between the spreading codes, which indirectly depends on the number of users. If the CCL values are small, then the increase in MAI is small, leading to a small degradation in performance. Table 2.2 shows the corresponding MAI values, i.e. the second term in Equation 2.88 for $K = 10, 20$ and 30 .

Having considered the theoretical performance of a DS-CDMA system, let us now turn our attention to the results of our simulation studies.

2.8 Simulation results and discussion

Let us now study the performance of a BPSK-modulated DS-CDMA system, quantifying :

- the effect of increasing the number of users in the system on the BER performance,
- the effect of spreading sequence length on the BER performance of the system,

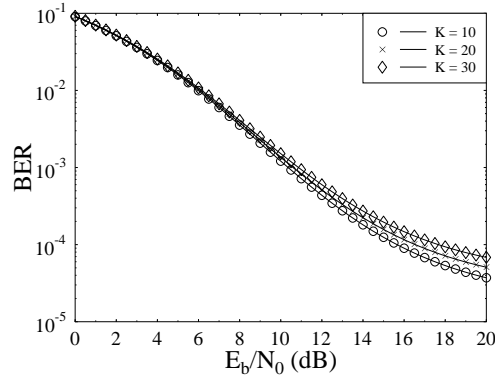


Figure 2.11: BER versus E_b/N_0 plots for a synchronous CDMA system in a Gaussian channel. Gold sequences are used with the sequence length fixed at $Q = 63$ chips, but varying numbers of users, K , are used. These graphs were plotted using Equation 2.90. As the number of users, K , increases, the BER performance degrades.

- the effect of various spreading codes having different cross-correlation values on the BER performance.

The simulation model used is shown in Figure 2.12. At the transmitter, the data bits were generated by a pseudo-random bit generator for all the K users. Each user was assigned a unique spreading code and the data bits of each user were spread using this code. Both the data bits and chips were binary. The spread signals were then summed synchronously, whereby the first chip of each bit for each user coincided with the first chip of each bit of all the other users.

At the receiver, Gaussian noise was added to the received signal. The noisy signal was then despread using a synchronous replica of the spreading code of the wanted user, i.e. it was assumed that there were no timing errors. The despread signal was fed to a so-called correlation receiver, where it was then integrated over one bit period. The output of the receiver was used to make a decision concerning the transmitted bit. The experiments were conducted under the following conditions :

- The simulations were performed at baseband, because the performance of baseband systems is equivalent to that of bandpass systems [97], but simulations carried out at baseband are more economical on computing resources.
- Perfect synchronization of the spreading codes was assumed at the receiver.
- Perfect power control was assumed.

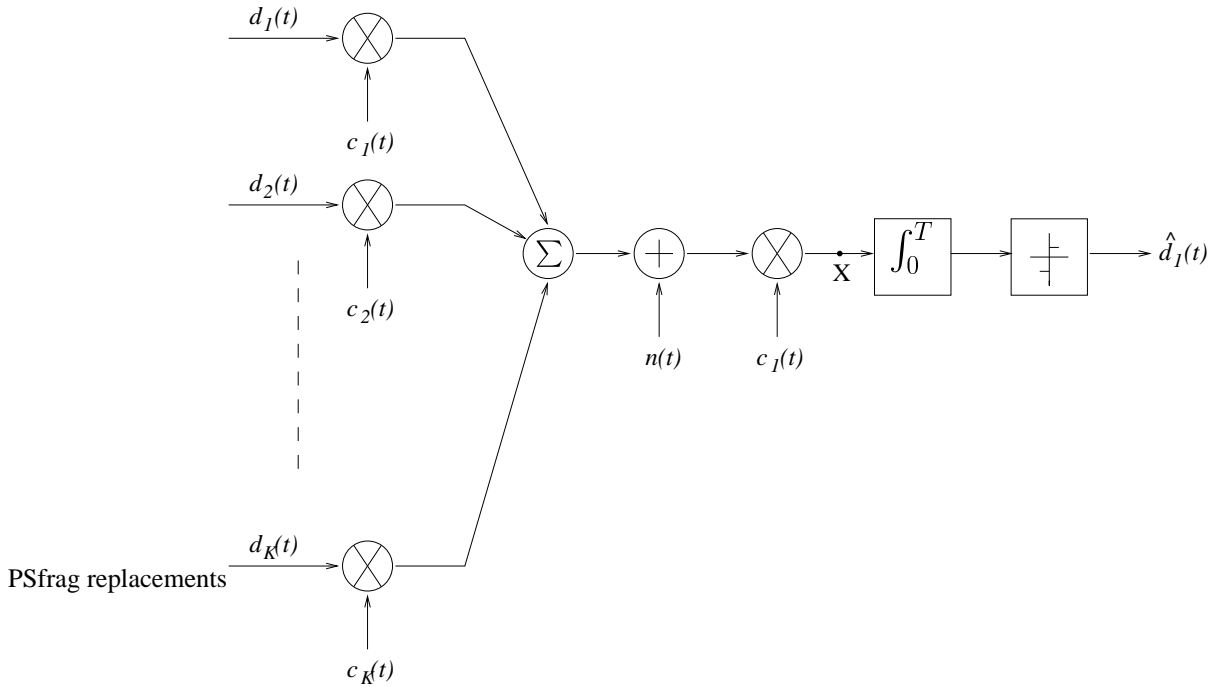


Figure 2.12: Simulation model of a synchronous BPSK DS-SS modem in a Gaussian channel

2.8.1 Estimation of E_b/N_0

The E_b/N_0 value at point X of Figure 2.13, in a communications system is estimated by first obtaining the average signal power, \bar{S} , and the average noise power, \bar{N} . The average signal-to-noise ratio, $\overline{\text{SNR}}$, is calculated as :

$$\overline{\text{SNR}} = \frac{\text{Signal power}}{\text{Noise power}} = \frac{\bar{S}}{\bar{N}}. \quad (2.91)$$

The energy per bit, E_b , is defined as $E_b = \bar{S}T$, while the noise power spectral density, N_0 , is defined as $N_0 = \bar{N}/W_b$, where W_b is the bandwidth of the noisy signal at the point where the $\overline{\text{SNR}}$ is measured. Therefore, the relationship between E_b/N_0 and $\overline{\text{SNR}}$ is :

$$\frac{E_b}{N_0} = \frac{\bar{S} \times T}{\bar{N}/W_b} \quad (2.92)$$

$$= \frac{\bar{S}}{\bar{N}} \times \frac{W_b}{R} \quad (2.93)$$

$$= \overline{\text{SNR}} \times \frac{W_b}{R}, \quad (2.94)$$

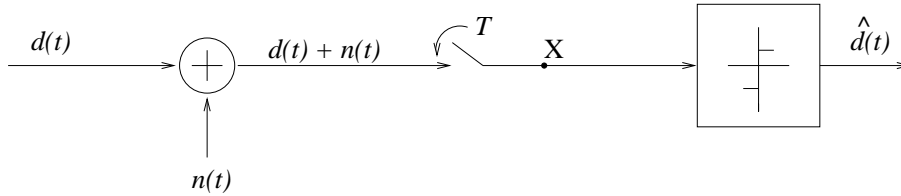


Figure 2.13: Simulation model of a BPSK modem

where T is the bit period and $R = 1/T$ is the data bit rate.

For a simple BPSK modem as shown in Figure 2.13, the bandwidth, W_b , at point X, is equal to the data bit rate, R . Therefore, at point X, we have $E_b/N_0 = \overline{\text{SNR}}$.

For the DS-CDMA system shown in Figure 2.12, at point X, the bandwidth requirement was extended due to the spreading of the signal by a factor of :

$$\frac{W_b}{R} = \frac{T}{T_c} \quad (2.95)$$

$$= Q. \quad (2.96)$$

Hence, we have :

$$\frac{E_b}{N_0} = \overline{\text{SNR}} \times \frac{T}{T_c} \quad (2.97)$$

$$= \overline{\text{SNR}} \times Q, \quad (2.98)$$

where T is the bit period and T_c is the period of one chip in the spreading code.

2.8.2 Simulated DS-CDMA BER performance over Gaussian channels for synchronous users

Our initial simulations were carried out in a synchronous environment, where all the users were perfectly synchronized at the receiver. The simulation results were compared with the analytical ones given in Equation 2.75, which exploited the Gaussian approximation and in Equation 2.90, which modelled a perfectly synchronous system. The graphs are presented in Figure 2.14, showing the BER versus E_b/N_0 curves for a synchronous BPSK/DS-CDMA system using Gold codes of length, $Q = 63$. Figures 2.14(a) and 2.14(b) have different number of users in the system, namely $K = 31$ and $K = 63$, respectively.

From the figures it can be seen that the simulation curves match the theoretical BER curves of the synchronous model quite well. Let us now consider explicitly the effect of the MAI due to different number of users.

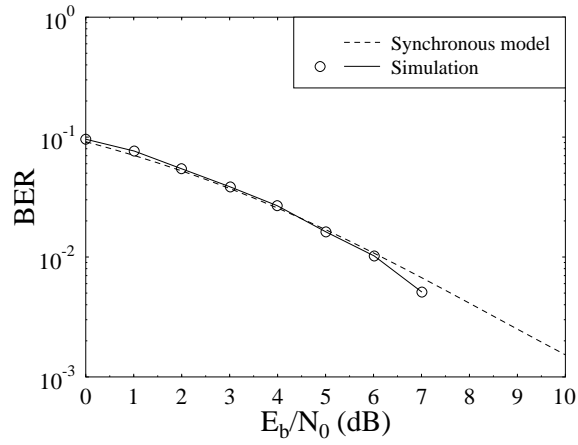
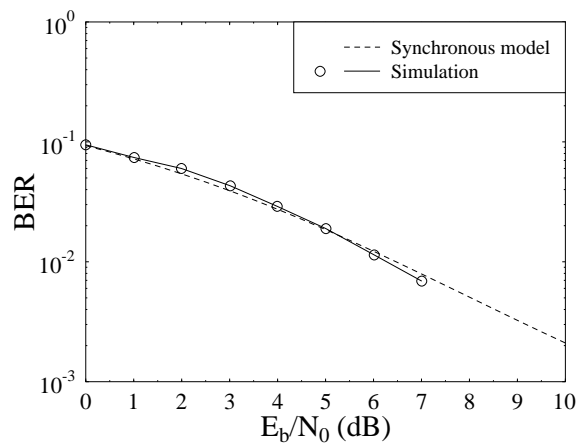
(a) $K = 31$ (b) $K = 63$

Figure 2.14: Simulated BER versus E_b/N_0 curves for a synchronous BPSK/DS-CDMA system using Gold codes of $Q = 63$ and supporting $K = 31$ users as well as $K = 63$ users as specified. The curve for the synchronous model was obtained from Equation 2.90.

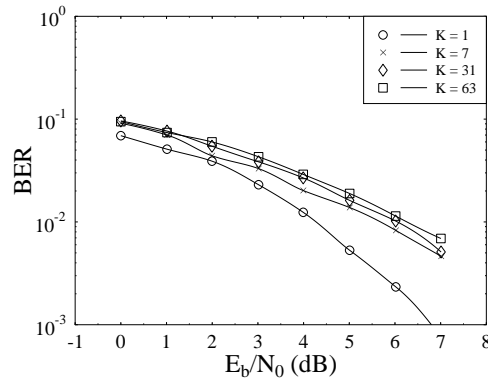


Figure 2.15: Comparison of simulation-based BER versus E_b/N_0 curves for a synchronous BPSK/DS-SS-CDMA system for various numbers of users in the system, K . The spreading codes used were Gold codes having a length of $Q = 63$.

2.8.3 Simulated DS-SS-CDMA BER performance versus the number of users over Gaussian channels

Figure 2.15 shows the plot of BER versus E_b/N_0 curves for synchronous DS-SS-CDMA simulations using different values of K . It was expected that as the number of users, K , in the system increased, the BER performance would also suffer due to the increase in multiple access interference (MAI). This was evident in the simulation results using Gold codes, as shown in Figure 2.15. However, it should be noted that the performance differences for $K = 7, 31$ and 63 are small compared to the difference between $K = 1$ and $K = 7$. This is due to the fact that the MAI term of Equation 2.90 has similar values for $K = 7, 31$ and 63 , as explained before in Section 2.7.2. We continue our elaborations by investigating the effect of the spreading code length.

2.8.4 Simulated DS-SS-CDMA BER performance versus spreading code length over Gaussian channels

Figure 2.16 shows the BER versus E_b/N_0 performance for $K = 7$ users, in conjunction with different Gold code lengths, Q . Increasing Q from 7 to 31 and to 63 decreased the BER for a given E_b/N_0 . However, there was only a slight difference between the BER curves for $Q = 31$ and $Q = 63$. This can be explained by examining the maximum in-phase cross-correlation (CCL) values, $R_{max}(0)$ of Equation 2.36, for the different values of Q in Table 2.3, where $Q = 31$ and $Q = 63$ had rather similar CCL values. Only the in-phase CCL values were considered, since the simulations were conducted in a synchronous environment, where the received signals of the different users were bit-synchronous.

From Table 2.3, $R_{max}(0)$ for $Q = 7$ is approximately three times higher than that of

Q	CCL ($R_{max}(0)$)
7	0.714
31	0.226
63	0.238
127	0.133

Table 2.3: Maximum normalised in-phase CCL values of Equation 2.36 for Gold codes of various lengths

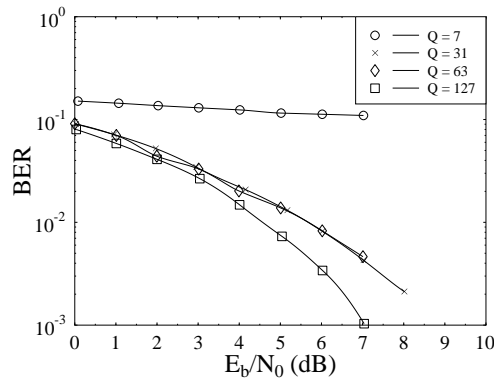


Figure 2.16: Comparison of BER versus E_b/N_0 curves for a synchronous BPSK/DS-CDMA system and for various Gold code lengths, Q , while supporting $K = 7$ users.

$Q = 31$ and $Q = 63$, which accounts for the BER curves of $Q = 31$ and $Q = 63$ showing lower BERs. However, again, the $R_{max}(0)$ values for $Q = 31$ and $Q = 63$ are similar, which results in the similarity between the BER curves despite their different code lengths. Again, for $Q = 127$, the $R_{max}(0)$ value is half as high as that of $Q = 63$, resulting in a better BER performance for $Q = 127$. Therefore, the performance of the system is dependent on the $R_{max}(0)$ values of Equation 2.36 and not specifically on Q . Let us now study the effect of various spreading codes.

2.8.5 Simulated DS-CDMA BER performance for spreading code sets having different cross-correlation values over Gaussian channels

Figure 2.17 offers a BER versus E_b/N_0 comparison for two different code sets, namely Gold codes with $Q = 63$ and Walsh codes for $Q = 64$. The number of users, $K = 15$ is the same for both code sets. The Walsh codes are perfectly orthogonal to each other. Therefore, in a perfectly synchronous environment, the BER curve matches that of the theoretical single-user BPSK curve. In comparison to the Gold codes, they perform much better. However,

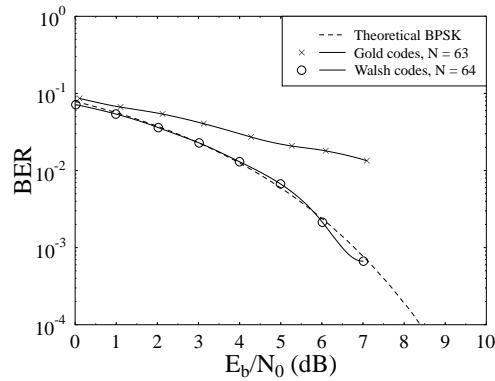
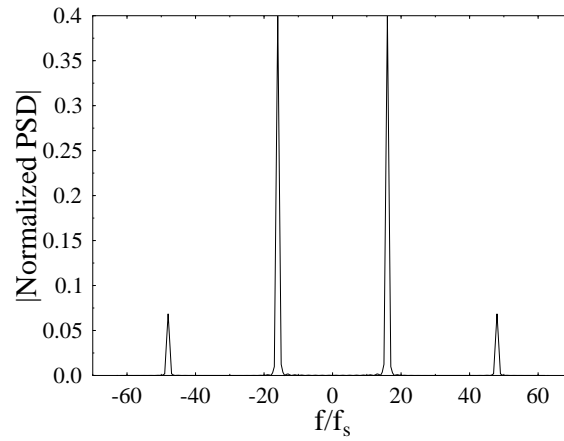


Figure 2.17: Simulated BER versus E_b/N_0 curves for synchronous BPSK/DS-CDMA supporting $K = 15$ users in the system, and comparing different types of codes, namely Gold codes and Walsh codes. Walsh codes have perfect cross-correlation properties i.e. the codes are perfectly orthogonal to each other, while Gold codes are not perfectly orthogonal codes.

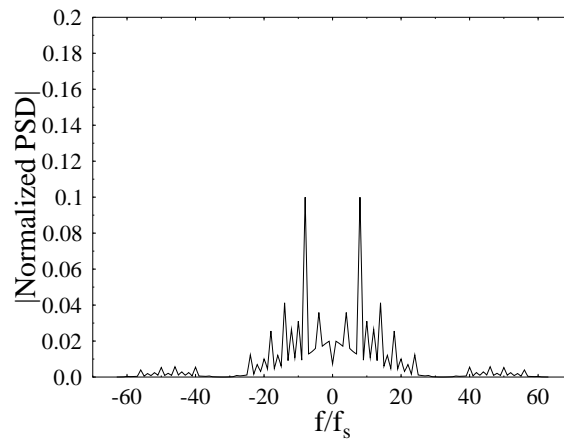
Walsh codes are not very effective as spreading codes, since they do not spread the spectrum of the signal sufficiently widely in order to cater for high multipath diversity gains, an issue to be treated in our forthcoming discussions throughout the thesis. The power spectral density (PSD) plot of a data signal spread by a Walsh code of length $Q = 64$ and the PSD of that spread by a Gold code of length $Q = 63$ are shown in Figures 2.18(a) and 2.18(b), respectively.

2.9 Discussion

In the preceding sections of this chapter, a basic portrayal of the conventional CDMA transmitter and receiver was provided. A few examples of binary sequences were presented and the effects of their cross-correlation values on the BPSK CDMA BER performance were examined. The BER performance for an asynchronous CDMA system utilizing the Gaussian approximation was presented along with a modified version for the bit-synchronous CDMA system. The theoretical and simulation performances of bit-synchronous CDMA systems in Gaussian channels employing the conventional correlation receiver were compared. It was concluded that for these simple CDMA systems, the BER performance was dependent on the cross-correlation between the spreading codes of the users and the total multiple access interference in the system. Many of our early assumptions were impractical. For instance, synchronization and timing errors at the receiver will increase the correlation between spreading codes and increase the MAI. Furthermore, synchronous transmission is difficult to achieve practically for the uplink, since the transmissions from different mobiles will commence and terminate at different times. In a wideband channel the orthogonality between spreading codes will be destroyed and this increases the cross-correlation between users and degrades



(a) PSD plot of a signal that has been spread with a Walsh code of length $Q = 64$



(b) PSD plot of a signal that has been spread with a Gold code of length $Q = 63$

Figure 2.18: Power spectral density plots of a signal that has been spread with two different codes, in order to show the difference in bandwidth spread.

the BER performance. Other propagation phenomena such as fast fading, shadowing and path loss affect the power of the received signal making it impossible to achieve perfect power control. Imperfect power control has a very significant effect, because a strong signal from one source can completely obscure a weak signal from another source. This will render the BER performance for some users to be much worse than the average. Lastly, the simulations were carried out in a single cell environment. In practice, interference arises both from users within the same cell and also from other cells.

Having gained a basic knowledge of the theoretical and simulation performance of the conventional BPSK/DS-SS receiver in a Gaussian environment, let us turn our attention to the non-conventional multiuser detection techniques in the forthcoming section.

2.10 Multiuser detection

Multiple access communications using DS-SS is interference-limited due to the multiple access interference (MAI) generated by the users transmitting within the same bandwidth simultaneously. The signals from the users are separated by means of spreading sequences that are unique to each user. These spreading sequences are usually non-orthogonal. Even if they are orthogonal, the asynchronous transmission or the time-varying nature of the mobile radio channel may partially destroy this orthogonality. The non-orthogonal nature of the codes results in MAI, which degrades the performance of the system. The frequency selective mobile radio channel also gives rise to inter-symbol interference (ISI) due to multi-path propagation. This is exacerbated by the fact that the mobile radio channel is time-varying.

Conventional CDMA detectors – such as the matched filter [95, 109] and the RAKE combiner [97] – are optimized for detecting the signal of a single desired user. RAKE combiners exploit the inherent multi-path diversity in CDMA, since they essentially consist of matched filters for each resolvable path of the multipath channel. The outputs of these matched filters are then coherently combined according to a diversity combining technique, such as maximal ratio combining, equal gain combining or selection diversity combining [97]. These conventional single-user detectors are inefficient, because the interference is treated as noise and there is no utilization of the available knowledge about the mobile channel or the spreading sequences of the interferers. The efficiency of these detectors is dependent on the cross-correlation (CCL) between the spreading codes of all the users. The higher the cross-correlation, the higher the MAI. This CCL-induced MAI is exacerbated by the multi-path channel or by asynchronous transmissions. Conventionally, this MAI is reduced by the use of voice-activity monitoring and cell sectorization [10]. The utilization of these conventional receivers results in an interference-limited system and soft hand-over capabilities are required in order to provide an acceptable grade of service [98]. Another weakness of the conventional CDMA detectors is the phenomenon known as the “near-far effect” [10, 98]. For conventional detectors to operate efficiently, the signals from all the users have to arrive at the receiver with approximately the same power. A signal that has a much weaker signal strength compared to the other signals will be “swamped” by the relatively higher powers of the other signals and the quality of the weaker signal at the output of the conventional receiver will be severely degraded. Therefore, stringent power control algorithms are needed to ensure that the signals arrive at relatively similar powers at the receiver, in order to achieve similar qualities of service for different users [10]. Using conventional detectors to detect a signal

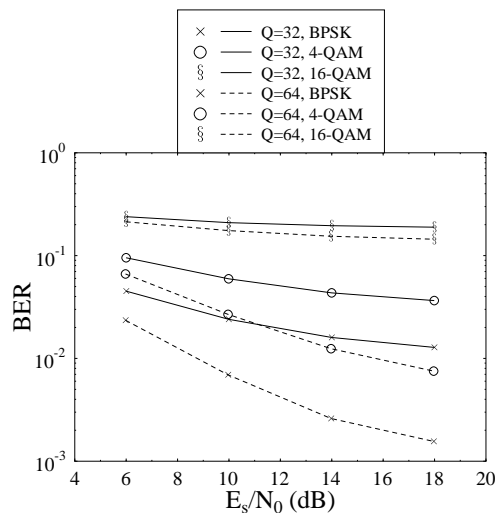


Figure 2.19: BER performance curves for the RAKE receiver with $K = 8$ users using BPSK, and over the seven-path Bad Urban channel with the impulse response shown in Figure 2.20. Different modulation modes, including BPSK, 4-QAM and 16-QAM, were investigated along with the spreading sequence lengths of $Q = 32$ and $Q = 64$.

corrupted by MAI, while encountering a hostile channel results in an irreducible BER, even if the E_s/N_0 is increased. This is because at high E_s/N_0 values the errors due to thermal noise are insignificant compared with the errors caused by the MAI and the channel. Therefore, detectors that can reduce or remove the effects of MAI and ISI are needed in order to achieve capacity gains. These detectors also have to be “near-far resistant” in order to avoid the need for stringent power control requirements. The performance of RAKE receivers for a synchronous uplink DS-CDMA system is shown in Figure 2.19 in conjunction with BPSK, 4-QAM and 16-QAM modulation, where an error floor is observed for all the different modulation modes, including BPSK. The simulations were carried out over the COST 207 [110] seven-path Bad Urban channel shown in Figure 2.20. The performance improves, however, with an increase in the spreading sequence length, Q , although the error floor still remains.

The COST 207 [110] channel profiles were developed approximately around the time, when the GSM system was standardised, in order to assist for example in GSM performance investigations. The third generation wideband CDMA systems [81] have, however, a higher bandwidth and a significantly higher chip rate than the bit rate of the GSM system [81], thus leading to a higher multipath resolution and a larger number of resolvable multipath components. Nonetheless, in our performance investigations the COST 207 channels were adopted for the sake of the comparability of our results, since these channels are widely utilized in the CDMA research community.

In order to mitigate the problem of MAI, [111] proposed and analyzed the optimum multiuser detector for asynchronous Gaussian multiple access channels. The optimum detector searches all the possible bit sequences in order to find the sequence that maximizes the

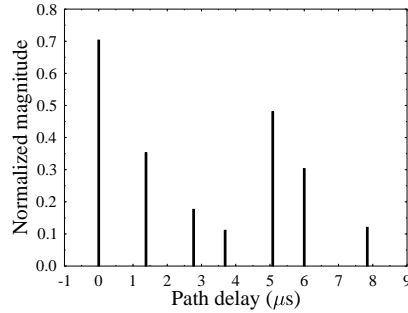


Figure 2.20: Normalized channel impulse response for the COST 207 [110] seven-path Bad Urban channel.

correlation metric given by [83] :

$$\Omega(\mathbf{r}, \mathbf{d}) = 2\mathbf{d}^T \mathbf{r} - \mathbf{d}^T \mathbf{R} \mathbf{d}, \quad (2.99)$$

where the elements in vector \mathbf{r} represent the cross-correlation of the received signal with each of the user spreading sequences, the vector \mathbf{d} consists of the bits transmitted by the users and the matrix \mathbf{R} is the correlation matrix of the spreading sequences. This optimum detector significantly outperforms the conventional detector and it is near-far resistant, but unfortunately its complexity grows exponentially in the order of $O(2^{NK})$, where N is the number of overlapping asynchronous bits considered in the detector window and K is the number of interfering users. In order to reduce the complexity of the receiver and yet provide acceptable BER performances, significant research efforts have been invested in the field of sub-optimal CDMA multiuser receivers [83]. Multiuser detection exploits the base station's knowledge of the spreading sequences and that of the estimated channel impulse response (CIR) in order to remove the MAI. These multiuser detectors can be categorized in a number of ways, such as linear versus non-linear, adaptive versus non-adaptive algorithms or burst transmission versus continuous transmission regimes. Excellent summaries of some of these sub-optimum detectors can be found in the monographs by [91], and [93] and [83]. Other MAI-mitigating techniques include the employment of adaptive antenna arrays in order to suppress the level of MAI at the receiver. Research efforts invested in this area include, amongst others, research carried out by , and [112, 113]; and [114]; [115]; as well as , , and [116]. However, the area of adaptive antenna arrays is beyond the scope of this thesis and the reader is referred to the references cited for further discussion. In the next section, a brief survey of the sub-optimal multiuser receivers will be presented.

2.10.1 Survey of multiuser receivers

Following the seminal work by [111], numerous sub-optimum multiuser detectors have been proposed for a variety of channels, data modulation schemes and transmission formats. and

[117] initially suggested a sub-optimum linear detector for symbol-synchronous transmissions and further developed it for asynchronous transmissions in a Gaussian channel [118]. This linear detector inverted the CCL matrix, which was constructed from the spreading codes of the users and was termed the decorrelating detector. It was shown that this decorrelator exhibited the same degree of near-far resistance, as the optimum multiuser detector. A further sub-optimum multiuser detector investigated was the minimum mean square error (MMSE) detector, where a biased version of the CCL matrix was inverted in order to optimize the receiver obeying the MMSE criterion. and [119] proposed a multiuser detector for a synchronous CDMA system designed for a frequency-selective Rayleigh fading channel. This approach also used a bank of matched filters followed by a whitening filter, but maximal ratio combining was used to combine the resulting signals. The decorrelating detector of [118] was further developed for differentially-encoded coherent multiuser detection in flat fading channels by Zvonar *et al* [120]. Zvonar also amalgamated the decorrelating detector with diversity combining, in order to achieve performance improvements in frequency selective fading channels [121]. A multiuser detector jointly performing decorrelating channel estimation and data detection was investigated by and [122]. Path-by-path decorrelators were employed for each user in order to obtain the input signals required for channel estimation and the channel estimates as well as the outputs of a matched filter bank were fed into a decorrelator for demodulating the data. A variant of this idea was also presented by , and [123], where training sequences and a decorrelating scheme were used for determining the channel estimate matrix. This matrix was then used in a decorrelating decision feedback scheme for obtaining the data estimates. , and [124] proposed iterative schemes for obtaining the decorrelator and linear MMSE detectors in order to reduce the complexity. and [125] advocated using a sequential estimator for minimizing the mean square error. The cross-correlations between the spreading codes and estimates of the faded amplitude of the received signal of each user were needed in order to obtain estimates of the transmitted data of each user. Duel-Hallen [126] proposed a decorrelating decision-feedback detector for removing the MAI from a synchronous system in a Gaussian channel. The outputs from a bank of filters matched to the spreading codes of the users were passed through a whitening filter. This filter was obtained by decomposing the CCL matrix of the user spreading codes through the Cholesky decomposition [127] technique. The results showed that MAI could be removed from each user successively, assuming that there was no error propagation. However, estimates of the received signal strengths of the users were needed, because the users had to be ranked in order of decreasing signal strengths so that the more reliable estimates were obtained first. The decorrelating feedback detector was improved by and [128] with a sub-optimum variant of the Viterbi algorithm, where only those metrics which were most likely were retained. Decorrelating decision feedback detection was improved with the assistance of soft-decision convolutional coding by and [129]. Soft decisions from a Viterbi decoder were fed back into the filter for signal cancellation.

The effect of MAI on the desired signal is similar to the impact of multipath propagation-induced ISI inflicted upon the same signal. Each user in a K -user system suffers from MAI due to the other $(K - 1)$ users. This MAI can also be viewed as a single-user signal perturbed by ISI from $(K - 1)$ paths in a multipath channel. Therefore, classic equalization techniques [95, 130] used to mitigate the effects of ISI can be modified for multiuser detection and these types of multiuser detectors can be classified as joint detection receivers. These joint detection receivers were developed for burst-based rather than continuous transmission.

The concept of joint detection for the uplink was proposed by and [131] for synchronous burst transmission, where the performance of a zero-forcing block linear equalizer (ZF-BLE) was investigated for frequency-selective channels. Other joint detection schemes for uplink situations were also proposed by , , , and , such as the minimum mean-square error block linear equalizer (MMSE-BLE) [132–135], the zero-forcing block decision feedback equalizer (ZF-BDFE) [134, 135] and the minimum mean-square error block decision feedback equalizer (MMSE-BDFE) [134, 135]. These joint-detection receivers were also combined with coherent receiver antenna diversity (CRAD) techniques [133–136] and turbo coding [137, 138] for performance improvement. Joint detection receivers were also proposed for downlink scenarios by , , and [139, 140]. Channel estimates were required for the joint detection receivers and some channel estimation algorithms were proposed by and [141] for employment in conjunction with joint detection. [142] extended the joint detection receiver by combining ZF-BLE and MMSE-BLE techniques with a multistage decision using soft inputs to a decoder.

Interference cancellation (IC) schemes constitute another variant of multiuser detection and they can be broadly divided into three categories, parallel cancellation, successive cancellation and a hybrid of both. and [143] proposed a multistage detector for an asynchronous system, where the outputs from a matched filter bank were fed into a detector that performed MAI cancellation using a multistage algorithm. At each stage in the detector, the estimates of all the other users from the previous stage were used for reconstructing an estimate of the MAI and this estimate was then subtracted from the interfered signal representing the wanted bit. The computational complexity of this detector was linear with respect to the number of users, K . further modified the parallel cancellation scheme in order to create a parallel group detection scheme for Gaussian channels [144] and later developed it further for frequency-selective slow Rayleigh fading channels [145]. In this scheme, K users were divided into P groups and each group was demodulated in parallel using a group detector. , and [146] then extended the applicability of the multistage interference cancellation detector to a multipath, slowly fading channel. At each cancellation stage, hard decisions generated by the previous stage were used for reconstructing the signal of each user and for cancelling its contribution from the composite signal. The effects of CIR estimation errors on the performance of the cancellation scheme were also considered. A multiuser receiver that integrated MAI rejection and channel decoding was investigated by and [147]. The MAI was cancelled via a multistage cancellation scheme and soft-outputs were fed from the Viterbi decoder of each user to each stage for improving the performance.

The parallel interference cancellation (PIC) receiver [143] was also modified for employment in multi-carrier modulation [148] by and , where convolutional coding was used in order to obtain improved estimates of the data for each user at the initial stage and these estimates were then utilized for interference cancellation in the following stages. The employment of convolutional coding improved the performance by 1.5 dB. , and [149] enhanced the performance of the parallel interference cancellation receiver by feeding back channel estimates to the signal reconstruction stage of the multistage receiver and proposed an algorithm for mitigating error propagation. , , and [150] combined multistage detection with channel estimation techniques utilizing the outputs of antenna arrays. The channel estimates obtained were fed back into the multistage detector in order to refine the data estimates. An advanced parallel cancellation receiver was also proposed by , and [151]. At each cancellation stage, only partial cancellation was carried out by weighting the regenerated signals with a less

than unity scaling factor. At each following stage, the weights were increased based on the assumption that the estimates became increasingly accurate.

A simple successive interference cancellation (SIC) scheme was analyzed by and [152]. The received signals were ranked according to their correlation values, which were obtained by utilizing the correlations between the received signal and the spreading codes of the users. The transmitted information of the strongest user was estimated enabling the transmitted signal to be reconstructed and subtracted from the received signal. This was repeated for the next strongest user, where the reconstructed signal of this second user was cancelled from the composite signal remaining after the first cancellation. The interference cancellation was carried out successively for all the other users, until eventually only the signal of the weakest user remained. It was shown that the SIC receiver improved the BER and the system's user capacity over that of the conventional matched filter for the Gaussian, narrowband Rayleigh and dispersive Rayleigh channels. Multipath diversity was also exploited by combining the SIC receiver with the RAKE correlator [152]. and [153] extended the SIC receiver by using reference symbols in order to aid the CIR estimation. The performance of the receiver was investigated in flat and frequency-selective Rayleigh fading channels, as well as in emulated multi-cell scenarios. A soft-decision based adaptive SIC scheme was proposed by and [154] where soft decisions were used in the cancellation stage and if the decision statistic did not satisfy a certain threshold, no data estimation was carried out for that particular data bit, in order to reduce error propagation.

Hybrid SIC and PIC schemes were proposed by , and [155, 156], where SIC was first performed on the received signal, followed by a multistage PIC arrangement. This work was then extended to an adaptive hybrid scheme for flat Rayleigh fading channels [157]. In this scheme, successive cancellation was performed for a fraction of the users, while the remaining users' signals were processed via a sub-parallel cancellation stage. Finally, multistage parallel cancellation was invoked. The number of serial and sub-parallel cancellations performed was varied adaptively according to BER estimates. , , and [158] proposed a pilot symbol-assisted multistage hybrid successive-parallel cancellation scheme. At each stage, data estimation was carried out successively for all the users, commencing with the user having the strongest signal and ending with the weakest signal. For each user, interference from other users was regenerated using the estimates of the current stage for the stronger users and the estimates of the previous stage for the weaker users. Channel estimates were obtained for each user by employing pilot symbols and a recursive estimation algorithm. Another hybrid successive and parallel interference cancellation receiver was proposed by , , and [159], where the users to be detected were split into a number of groups. Within each group, PIC was performed on the signals of these users belonging to the group. Between the separate groups, SIC was employed. This had the advantage of a reduced delay and improved performance compared to the SIC receiver. A further variant of the hybrid cancellation scheme was constituted by the combination of MMSE detectors with SIC receivers, as proposed by and [160]. Single-user MMSE detectors were used to obtain estimates of the data symbols, which were then fed back into the SIC stages. An adaptive interference cancellation scheme was investigated by and [161] for a multicellular scenario, where interference cancellation was performed for both in-cell interferers and out-of-cell interferers. It was shown that cancelling the estimated interference from users having weak signals actually degraded the performance, since the estimates were inaccurate. The adaptive scheme exercised interference cancellation in a discriminating manner, using only the estimates from users having strong received sig-

nals. Therefore signal power estimation was needed and the threshold for signal cancellation was adapted accordingly.

Several tree-search detection [162–164] receivers have been proposed in the literature, in order to reduce the complexity of the original maximum likelihood detection scheme proposed by [111]. Specifically, [162] investigated a tree-search detection algorithm, where a recursive, additive metric was developed in order to reduce the search complexity. Reduced tree-search algorithms, such as the well-known M-algorithms [165] and T-algorithms [165] were used by [163] in order to reduce the complexity incurred by the optimum multiuser detector. Motivated by the M-algorithm, at every node of the search algorithm, only M paths were retained, depending on certain criteria such as the highest-metric M number of paths. Alternatively, all the paths that were within a fixed threshold, T , compared to the ideal metric were retained. At the decision node, the path having the highest metric was chosen as the most likely transmitted sequence. Maximal-ratio combining was also used in conjunction with the reduced tree-search algorithms and the combining detectors outperformed the “non-combining” detectors. The T-algorithm was combined with soft-input Viterbi detectors for channel-coded CDMA multiuser detection in the work carried out by [164]. The recursive tree-search detector generated soft-outputs, which were fed into single-user Viterbi channel decoders, in order to generate the bit estimates.

Multiuser projection receivers were proposed by [166] and by Alexander, and Schlegel [167]. These receivers reduced the MAI by projecting the received signal onto a space which was orthogonal to the unwanted MAI, where the wanted signal was separable from the MAI.

In all the multiuser receiver schemes discussed earlier, all the required parameters except for the transmitted data estimates were assumed to be known at the receiver. In order to remove this constraint while reducing the complexity, adaptive receiver structures have been proposed [168]. An excellent summary of these adaptive receivers has been provided by [169]. Several adaptive algorithms have been introduced for approximating the MMSE receivers, such as the Least Mean Squares (LMS) [130] algorithm, the Recursive Least Squares (RLS) algorithm [130] and the Kalman filter [130]. [170] showed that the adaptive MMSE approach could be applied to multiuser receiver structures with a concomitant reduction in complexity. In the adaptive receivers employed for asynchronous transmission by [168], training sequences were employed, in order to obtain the estimates of the parameters required. [171] introduced a multiuser receiver for an asynchronous flat-fading channel based on the Kalman filter [171], which compared favourably with the finite impulse response MMSE detector. An adaptive decision feedback joint detection scheme was investigated by [172], where the least mean squares (LMS) algorithm was used to update the filter coefficients, in order to minimize the mean square error of the data estimates. New adaptive filter architectures for the downlink DS-SS receivers were suggested by [173], where an adaptive algorithm was employed in order to estimate the CIR, and this estimated CIR was then used by a channel equalizer. The output of the channel equalizer was finally processed by a fixed multiuser detector in order to provide the data estimates of the desired user.

The novel class of multiuser detectors, referred to as “blind” detectors, does not require explicit knowledge of the spreading codes and CIRs of the multiuser interferers. These detectors do not require the transmission of training sequences or parameter estimates for their operation. Instead, the parameters are estimated “blindly” according to certain criteria, hence the term “blind” detection. RAKE-type blind receivers have been proposed, for example

by [174] for fast-fading mobile channels, where decision-directed channel estimators were used for estimating the multipath components and the output of the RAKE fingers was combined employing various signal combining methods. [175] also proposed a RAKE-type receiver for frequency-selective fading channels. In [175], a weight vector was utilized for each RAKE finger which was calculated based on maximizing the signal-to-interference-plus-noise ratio (SINR) at the output of each RAKE finger. [176] proposed an approximate Maximum Likelihood Sequence Estimation (MLSE) solution known as the per-survivor processing (PSP) type algorithm, which combined a tree-search algorithm for data detection with the aid of the Recursive Least Squares (RLS) adaptive algorithm used for channel amplitude and phase estimation. The PSP algorithm was first proposed by [177]; as well as by [178, 179] for blind equalization in single-user ISI-contaminated channels. [180] extended their earlier work [176] in order to include the estimation of user-delays along with channel- and data-estimation [180]. [181] combined the PSP algorithm with the Kalman filter, in order to adaptively estimate the amplitudes and delays of the CDMA users. In other blind detection schemes, [182] compared the application of neural networks and LMS filters for obtaining data estimates of the CDMA users [182]. In contrast to other multiuser detectors, which required the knowledge of the spreading codes of all the users, only the spreading code of the desired user was needed for this adaptive receiver [182]. An adaptive decorrelating detector was also developed by Mitra and Poor [183], which was used to determine the spreading code of a new user entering the system. Blind equalization was combined with multiuser detection for slowly fading channels in the work published by [184]. Only the spreading sequence of the desired user was needed and a zero-forcing as well as an MMSE detector were developed for data detection. As a further solution, a sub-space approach to blind multiuser detection was also proposed by [185], where only the spreading sequence and the delay of the desired user were known at the receiver. Based on this knowledge, a blind sub-space tracking algorithm was developed for estimating the data of the desired user. Further blind adaptive algorithms were developed by [186], [187], as well as by [188]. In [186], the applicability of two adaptive algorithms to the multiuser detection problem was investigated, namely that of the stochastic gradient algorithm and the least squares algorithm; while in [188] an adaptive detector that converged to the decorrelator was analyzed.

The employment of the Kalman filter for adaptive data, CIR and delay estimation was advocated for example by [189], demonstrating that the Kalman filter gave a good performance and exhibited a high grade of flexibility. However, the Kalman filter required reliable initial delay estimates in order to initialize the algorithm. [190] modified the well-known constant modulus approach [191, 192] to blind equalization for ISI-contaminated channels in the context of multiuser interference suppression. [193] proposed an orthogonalizing matched filtering detector, which consisted of a bank of despreading filters and a signal combiner. One of the despreading filters was matched to the desired spreading sequence, while the other despreading sequences were arbitrarily chosen such that the impulse responses of the filters were linearly independent of each other. The filter outputs were adaptively weighted in the complex domain with the criterion that the average output power of the combiner was minimized. A constraint was imposed on the combining process such that the combiner's response to the desired user's signal was kept constant. In another design, an iterative scheme used to maximize the log-likelihood function was the basis of the research by [194]. RAKE correlators were employed for exploiting the multipath diversity and the outputs of

the correlators were fed to an iterative scheme for joint channel estimation and data detection using the Gauss-Seidel [195] algorithm.

Several hybrid multiuser receiver structures have also been proposed recently [196–199]. [196] advocated the hybrid multiuser detector that consisted of a decorrelator for detecting asynchronous users, followed by a maximum-SNR data combiner, an adaptive canceller and another data combiner. The decorrelator matrix was adaptively determined. A multiuser receiver employing an iterative hybrid genetic algorithm as a search technique has also been proposed by *et al* [197]. The search-space for the most likely sequence was limited to a certain population of sequences and the sequences were updated at each iteration according to certain probabilistic, aptly termed genetic operations, known as *reproduction*, *crossover* or *mutation* operations. Commencing with a population of tentative decisions, the best n sequences were selected as so-called “parent” sequences according to a fitness criterion in order to generate the “offspring” for the next generation of sequence estimates. The offspring of sequence estimates were generated by employing a uniform “crossover process” where the bits between two parent sequences were exchanged according to a random mask and a certain probability value. Finally, “mutation” was performed where the value of a bit is flipped according to a certain probability. In order to prevent the loss of “high-fitness” individuals that were not selected as parents, the worst offspring was replaced by the best non-parent individual of the earlier generation.

Neural network-type receivers have also been proposed as CDMA receivers [200, 201]. and proposed a non-linear receiver that exploited neural-network structures and employed pattern recognition techniques for data detection [200]. This work [200] was extended to a reduced complexity neural network receiver for the downlink scenario [201].

Other novel techniques employed for mitigating the multipath fading effects inflicted upon multiple users include joint transmitter-receiver optimization proposed by , and [198, 199]. In these schemes, transmitter precoding was carried out, such that the mean squared errors of the signals at all the receivers were minimized. This required the knowledge of the CIRs of all the user channels and the assumption was made that the channel fading was sufficiently slow, such that the channel prediction could be employed reliably.

Recently, there has been significant interest in iterative detection schemes where channel coding was exploited in conjunction with multiuser detection, in order to obtain a high BER performance. The spreading of the channel-coded symbols and their corruption by the wide-band channel was viewed as a serially concatenated code structure, where the CDMA channel was viewed as the inner code and the single user convolutional codes made up the outer codes. After processing the received signal in a bank of matched filters or orthogonalizing whitening matched filter, the matched filter outputs were processed using the turbo-style iterative decoding (TEQ) [202] process. In this process, a multiuser decoder was used to produce confidence measures which were used as soft inputs to the single-user channel decoders. These single-user decoders then provided similar confidence metrics for the multiuser detector. This iterative process continued, until no further performance improvement was recorded.

and [203] presented the maximum likelihood solution for the asynchronous CDMA channel, where the user data was encoded with the aid of convolutional codes. Near-single-user performance was achieved for the two-user case in conjunction with fixed-spreading codes. The decoder employed was based on the Viterbi algorithm, where the number of states increased exponentially with the product of the number of users and the constraint length of the convolutional codes. Later, a suboptimal modification of this technique was

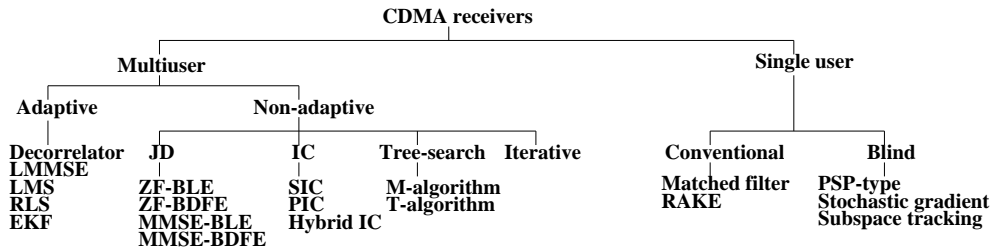


Figure 2.21: Classification of CDMA detectors

proposed [147], where the MAI was cancelled via multistage cancellation and the soft outputs from the Viterbi algorithm were fed to each stage for improving the performance. Following this, several proposals of iterative multiuser detection for channel-coded signals have been presented [204–209]. For example, , , and [206, 208] proposed the multiuser maximum a-posteriori (MAP) detectors for the decoding of the inner CDMA channel code and single-user MAP decoders for the outer convolutional codes. A reduced complexity solution employing the M-algorithm [165] was also suggested which resulted in a complexity that increased linearly – rather than exponentially, as in [203] – with the number of users [207]. and [209] employed a soft-output multiuser detector for the inner channel code, which combined soft interference cancellation and instantaneous linear MMSE filtering, in order to reduce the complexity. These iterative receiver structures showed considerable promise and near-single-user performance was achieved at high SNRs.

Figure 2.21 portrays the classification of most of the CDMA detectors that have been discussed previously. All the acronyms for the detectors have been defined in the text. Examples of the different classes of detectors are also included.

2.11 Chapter Summary and Conclusions

In this chapter we commenced our discussions with a rudimentary introduction to CDMA systems and classified the various techniques that are applicable to spreading the signal before transmissions. We then briefly considered the operation of the DS-CDMA transmitter and receiver as well as the effects of the channel and the MUI. The correlation properties of m-sequences, Gold-sequences as well as Kasami-sequences were reviewed next and a range of basic results were presented for characterising the achievable performance as a function of the various system parameters. The chapter was concluded by a brief overview of various multiuser detectors.

In conclusion, multiuser detectors reduce the error floor due to MAI and this translates into user capacity gains for the system. If the performance of multiuser detectors is independent of the spreading codes used, then the codes can be chosen in order to optimize the system’s spectral efficiency. These multiuser detectors are also near-far resistant to a certain extent and this results in less stringent power control requirements.

On the other hand, multiuser detectors are more complex than conventional detectors. Coherent detectors require knowledge of the CIR estimates, which means that a channel

estimator is needed in the receiver and training sequences have to be included in the bursts that are transmitted. These multiuser detectors also exhibit an inherent latency, which results in a delayed reception.

Multiuser detection is more suitable for uplink receivers due to its increased complexity. A hand-held mobile receiver has to be compact and lightweight, rendering multiuser detection impractical for the downlink. Recent research into blind receivers has shown that data detection for the desired user – without using the spreading sequences and channel estimates of other users – is possible, as discussed in Section 2.10.1, hence using these detectors for downlink receivers may become a reality. However, the inherent latency in convergence and the increased complexity may still remain a limiting factor in these downlink receivers. less harmful to the mobile station, because all the signals of all the users in one transmission burst are generated at the same signal strength from the base station. The near-far problem becomes serious only, when the interference from other cells is high. To mitigate the problem of MAI for the downlink, measures such as using spreading codes with good cross-correlation and auto-correlation properties can be employed. The cross-correlation property is less likely to be destroyed, as downlink transmissions can be made synchronous, especially in hybrid TDMA/CDMA systems such as the ones in the FRAMES proposal [210]. To combat fading, RAKE receivers can be employed, in order to exploit multi-path diversity.

Part II

Genetic Algorithm Assisted Multiuser Detection

Chapter 9

Genetic Algorithm-Assisted Multiuser Detection for Synchronous CDMA

9.1 Introduction

In this chapter, we will apply a GA-assisted scheme as a suboptimal multiuser detection technique in bit-synchronous CDMA systems over single-path Rayleigh fading channels. This provides a simple model for investigating the feasibility of applying GAs in CDMA multiuser detection as well as for determining the GA's configuration, in order to obtain a satisfactory performance. Based on the results obtained in this chapter, the GA-assisted CDMA multiuser detector will then be subsequently extended to an asynchronous system model incorporating multipath Rayleigh fading channels in Chapter 12.

This chapter is organised as follows. We will first highlight our system model used in this chapter in Section 9.2. The notations defined here will also be used in the subsequent chapters. An equivalent discrete-time system model is also highlighted in Section 9.3. We will then derive the optimum multiuser detector based on the Maximum Likelihood (ML) criterion for the system model adopted in this chapter in Section 9.4, which can be seen to have a computational complexity exponentially proportional to the number of users. GA-assisted multiuser detectors are then developed through a series of experiments, in order to find the GA configuration that is best suited for our application and the results will be shown in Section 9.5. Finally, using this GA configuration, the BEP performance of the GA-assisted multiuser detector based on our system model is assessed by simulations in Section 9.6. The summary of this chapter is given in Section 9.7. Before we commence our in-depth discourse, a few observations are made regarding our mathematical notations used in this dissertation. Vectors and matrices are represented in boldface, while $(\cdot)^T$ and $(\cdot)^*$ denote the

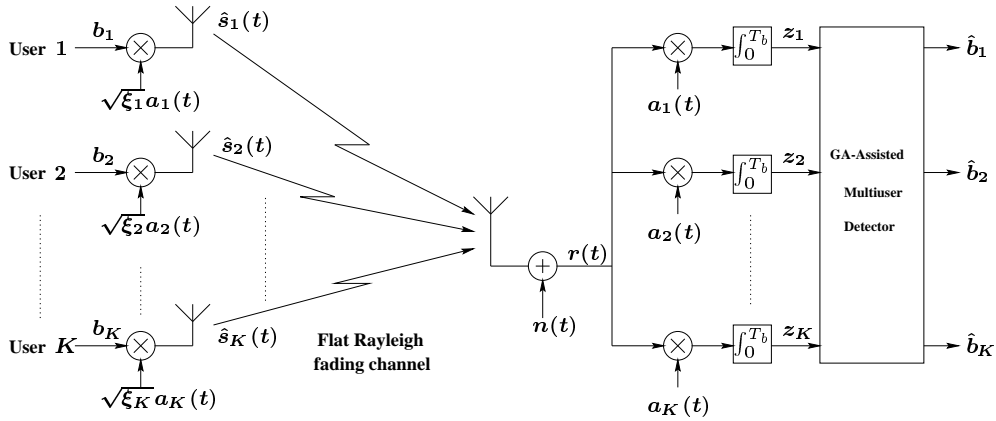


Figure 9.1: Block diagram of the K -user synchronous CDMA system model in a flat Rayleigh fading channel.

transpose matrix and the conjugate matrix of (\cdot) , respectively. Hermitian matrices, defined as the complex conjugate transpose of the matrices, are denoted as $(\cdot)^H$. Furthermore, $\text{diag}(\cdot)$ represents a diagonal matrix, where the diagonal elements correspond to the vector (\cdot) .

9.2 Synchronous CDMA System Model

We consider a bit-synchronous CDMA system as illustrated in Figure 9.1, where K users simultaneously transmit data packets of equal length to a single receiver. In this dissertation we will adopt the Binary Phase Shift Keying (BPSK) modulation technique for all the transmissions. The transmitted signal of the k th user can be expressed in an equivalent lowpass representation as :

$$\hat{s}_k(t) = \sqrt{\xi_k} \sum_{m=0}^{M-1} b_k^{(m)} a_k(t - mT_b), \quad \forall k = 1, \dots, K \quad (9.1)$$

where ξ_k is the k th user's signal energy per bit, $b_k^{(m)} \in \{+1, -1\}$ denotes the m th data bit of the k th user, $a_k(t)$ is the k th user's signature sequence, T_b is the data bit duration and M is the number of data bits transmitted in a packet. When considering a synchronous system experiencing no multipath interference, it is sufficient to observe the signal over a single bit duration T_b , since there is no interference inflicted by symbols outside this duration. Hence without loss of generality, we can omit the superscript (m) from all our equations in this chapter.

The k th user's signature sequence $a_k(t)$ may be written as :

$$a_k(t) = \sum_{h=0}^{N_c-1} a_k^{(h)} \Gamma_{T_c}(t - hT_c), \quad 0 \leq t < T_b, \quad \forall k = 1, \dots, K \quad (9.2)$$

where T_c is the chip duration, $a_k^{(h)} \in \{+1, -1\}$ denotes the h th chip, N_c is the spreading factor, which refers to the number of chips per data bit duration T_b such that $N_c = T_b/T_c$ and $\Gamma_{T_c}(t)$ is the chip pulse shape. In practical applications, $\Gamma_\tau(t)$ has a bandlimited waveform, such as a raised cosine Nyquist pulse. However, for the sake of simplicity in our analysis and simulation, we will assume that $\Gamma_\tau(t)$ is a rectangular pulse throughout this dissertation, which is defined as :

$$\Gamma_\tau(t) = \begin{cases} 1, & 0 \leq t < \tau \\ 0, & \text{otherwise.} \end{cases} \quad (9.3)$$

Without loss of generality, we assume that the signature sequence $a_k(t)$ of all K users has unit energy, as given by :

$$\int_0^{T_b} a_k^2(t) dt = 1, \quad \forall k = 1, \dots, K. \quad (9.4)$$

Each user's signal $\hat{s}_k(t)$ is assumed to propagate over a single-path frequency-nonselctive slowly Rayleigh fading channel, as shown in Figure 9.1 and the fading of each path is statistically independent for all users. The complex lowpass channel impulse response (CIR) for the link between the k th user's transmitter and the receiver, as shown in Figure 9.1, can be written as :

$$h_k(t) = \alpha_k(t) e^{j\phi_k(t)} \delta(t), \quad \forall k = 1, \dots, K \quad (9.5)$$

where the amplitude $\alpha_k(t)$ is a Rayleigh distributed random variable and the phase $\phi_k(t)$ is uniformly distributed between $[0, 2\pi)$.

Hence, when the k th user's spread spectrum signal $\hat{s}_k(t)$ given by Equation (9.1) propagates through a slowly Rayleigh fading channel having an impulse response given by Equation (9.5), the resulting output signal $s_k(t)$ over a single bit duration can be written as :

$$s_k(t) = \sqrt{\xi_k} \alpha_k b_k a_k(t) e^{j\phi_k}, \quad \forall k = 1, \dots, K \quad (9.6)$$

Upon combining Equation (9.6) for all K users, the received signal at the receiver, which is denoted by $r(t)$ in Figure 9.1, can be written as :

$$r(t) = \sum_{k=1}^K s_k(t) + n(t), \quad (9.7)$$

where $n(t)$ is the zero-mean complex Additive White Gaussian Noise (AWGN) with independent real and imaginary components, each having a double-sided power spectral density of $\sigma^2 = N_0/2$ W/Hz.

At the receiver, the output of a bank of filters matched to the corresponding set of the users' signature sequences is sampled at the end of the bit interval. The output of the l th

user's matched filter, denoted as z_l in Figure 9.1, can be written as :

$$\begin{aligned}
z_l &= \int_0^{T_b} r(t) a_l(t) dt \\
&= \int_0^{T_b} \sum_{k=1}^K \sqrt{\xi_k} \alpha_k b_k a_k(t) e^{j\phi_k} a_l(t) dt + \int_0^{T_b} n(t) a_l(t) dt \\
&= \underbrace{\sqrt{\xi_l} \alpha_l b_l e^{j\phi_l}}_{\text{Desired signal}} + \underbrace{\sum_{\substack{k=1 \\ k \neq l}}^K \sqrt{\xi_k} \alpha_k b_k \rho_{lk} e^{j\phi_k}}_{\text{Multiple Access Interference}} + \underbrace{n_l}_{\text{Noise}}, \quad (9.8)
\end{aligned}$$

where ρ_{lk} is the cross-correlation of the l th user's and the k th user's signature sequence, as given by :

$$\rho_{lk} = \int_0^{T_b} a_l(t) a_k(t) dt, \quad (9.9)$$

and

$$n_l = \int_0^{T_b} n(t) a_l(t) dt. \quad (9.10)$$

As seen in Equation (9.8), apart from the Gaussian noise n_l , the desired signal is interfered by signals transmitted by the other users. This interference due to the other users' signals is also known as Multiple Access Interference (MAI).

Assuming that the receiver has perfect knowledge of the l th user's CIR coefficients $\alpha_l e^{j\phi_l}$, the detected bit $\hat{b}_{l,MF}$ of the l th user based on the conventional coherent single-user detector will be given by the sign of the matched filter output in Equation (9.8) as :

$$\hat{b}_{l,MF} = \text{sgn} [\Re (z_l \alpha_l e^{-j\phi_l})]. \quad (9.11)$$

Multiplication by $\alpha_l e^{-j\phi_l}$ is necessary for coherent detection, because the phase rotation introduced by the channel has to be removed. By approximating the MAI as a Gaussian distributed random variable by virtue of the central limit theorem [305–307], the Bit Error Probability (BEP) of the desired user can be shown to be given by [308] :

$$P_l = \frac{1}{2} \left(1 - \sqrt{\frac{\xi_l}{N_0/2 + \sum_k \xi_k \rho_{lk}}} \right). \quad (9.12)$$

Hence from Equation (9.12), we can see that unless the signature sequences of the interfering users are orthogonal to that of the desired user, yielding $\rho_{lk} = 0$ for $k = 1, \dots, K, k \neq l$, the BEP performance of the desired user will be inferior to that achieved in a single-user

environment in conjunction with a single-user matched filter. Furthermore, since the BEP performance will deteriorate in conjunction with an increasing number of users, the conventional single-user detector is highly vulnerable to near-far effects [309].

9.3 Discrete-Time Synchronous CDMA Model

For our application, it is more convenient to express the associated signals in discrete-time format. Invoking Equation (9.6) describing the transmitted signal of each user, the sum of the transmitted signals of all users can be expressed in vector notation as :

$$\begin{aligned} s(t) &= \sum_{k=1}^K \hat{s}_k(t) \\ &= \mathbf{a} \mathbf{C} \boldsymbol{\xi} \mathbf{b}, \end{aligned} \quad (9.13)$$

where

$$\begin{aligned} \mathbf{a} &= [a_1(t), \dots, a_K(t)] \\ \mathbf{C} &= \text{diag} [\alpha_1 e^{j\phi_1}, \dots, \alpha_K e^{j\phi_K}] \\ \boldsymbol{\xi} &= \text{diag} [\sqrt{\xi_1}, \dots, \sqrt{\xi_K}] \\ \mathbf{b} &= [b_1, \dots, b_K]^T. \end{aligned} \quad (9.14)$$

Hence the received signal of Equation (9.7) can be written as :

$$r(t) = s(t) + n(t). \quad (9.15)$$

Based on Equations (9.13) and (9.15), the output vector \mathbf{Z} of the bank of matched filters portrayed in Figure 9.1 can be formulated as :

$$\begin{aligned} \mathbf{Z} &= [z_1, \dots, z_K]^T \\ &= \mathbf{R} \mathbf{C} \boldsymbol{\xi} \mathbf{b} + \mathbf{n}, \end{aligned} \quad (9.16)$$

where

$$\mathbf{R} = \begin{bmatrix} 1 & \rho_{12} & \dots & \rho_{1K} \\ \rho_{21} & 1 & \dots & \rho_{2K} \\ \vdots & \vdots & \ddots & \vdots \\ \rho_{K1} & \rho_{K2} & \dots & 1 \end{bmatrix} \quad (9.17)$$

is the $K \times K$ dimensional user signature sequence cross-correlation matrix having elements given by Equation (9.9) and

$$\mathbf{n} = [n_1, \dots, n_K]^T$$

is a zero-mean Gaussian noise vector with a covariance matrix $\mathbf{R}_n = 0.5N_0\mathbf{R}$. Based on this discrete-time model, we will next derive the optimum multiuser detector based on the maximum likelihood criterion for the synchronous CDMA system considered [310].

9.4 Optimum Multiuser Detector for Synchronous CDMA Systems

In this section we will derive the joint optimum decision rule for a K -user CDMA system based on the synchronous system model highlighted in Section 9.2. Specifically, we want to maximise the probability of jointly correct decisions of the K users supported by the system based on the received signal $r(t)$ of Equation (9.15).

From Equation (9.14) we note that there are $m = 2^K$ possible combinations of \mathbf{b} . We shall denote the i th combination as \mathbf{b}_i and the combined transmit signal of all users in Equation (9.13) corresponding to the i th combination as $\mathbf{b}_i \leftrightarrow s_i(t)$.

Based on the above notations, we can express the joint maximum *a posteriori* probability (MAP) criterion as [95] :

$$\hat{\mathbf{b}} = \arg \left\{ \max_{\mathbf{b}_i} [P(s_i(t)|r(t))] \right\}, \quad (9.18)$$

where $\hat{\mathbf{b}}$ denotes the detected bit combination. Using Bayes' rule, the *a posteriori* probability expression of Equation (9.18) can be written as [95] :

$$P(s_i(t)|r(t)) = \frac{p(r(t)|s_i(t))P(s_i(t))}{p(r(t))}, \quad (9.19)$$

where $p(r(t)|s_i(t))$ is the conditional joint probability density function (pdf) of the received signal $r(t)$ in Equation (9.15), $P(s_i(t))$ is the *a priori* probability of the signal containing the i th bit combination and $p(r(t))$ is the pdf of the received signal. Since the transmitted data bits of the K users are independent, the *a priori* probability $P(s_i(t)) = 1/2^K$ is equal for all $m = 2^K$ bit combinations. Furthermore, the received signal pdf $p(r(t))$ is independent of which of the $m = 2^K$ bit combinations is transmitted. Consequently, the decision rule based on finding the signal that maximises $P(s_i(t)|r(t))$ is equivalent to finding the signal that maximises $p(r(t)|s_i(t))$. This decision criterion based on the maximum of $p(r(t)|s_i(t))$ is termed as the Maximum Likelihood (ML) criterion and $p(r(t)|s_i(t))$ is referred to as a *likelihood function* [95].

According to Equation (9.7), the received signal $r(t)$ is a Gaussian distributed random variable having a mean equal to that of $s(t)$ given by Equation (9.13). Hence, it can be shown

that the likelihood function $p(r(t)|s_i(t))$ is given by [308] :

$$\begin{aligned} p(\mathbf{Z}|\mathbf{s}) &= \exp\left(-\frac{1}{2\sigma^2} \int_0^{T_b} |r(t) - s(t)|^2 dt\right) \\ &= \exp\left(-\frac{1}{2\sigma^2} \int_0^{T_b} \left| r(t) - \sum_{k=1}^K \sqrt{\xi_k} \alpha_k b_k a_k(t) e^{j\phi_k} \right|^2 dt\right). \end{aligned} \quad (9.20)$$

Taking the natural logarithm of the likelihood function of Equation (9.20), the resulting so-called *Log-Likelihood Function* (LLF) can be written as :

$$\begin{aligned} \ln p(\mathbf{Z}|\mathbf{s}) &= -\frac{1}{2\sigma^2} \left\{ \int_0^{T_b} |r(t)|^2 dt + \int_0^{T_b} \left| \sum_{k=1}^K \sqrt{\xi_k} \alpha_k b_k a_k(t) e^{j\phi_k} \right|^2 dt \right. \\ &\quad \left. - 2\Re \left[\int_0^{T_b} r(t) \sum_{k=1}^K \sqrt{\xi_k} \alpha_k b_k a_k(t) e^{-j\phi_k} dt \right] \right\}. \end{aligned} \quad (9.21)$$

The term $|r(t)|^2$ is common to all decision metrics, and hence it can be ignored during the optimisation. Similarly, the constant term $1/2\sigma^2$ will not influence the maximisation. Thus we can express the log-likelihood function of Equation (9.21) in the form of a correlation metric as [95] :

$$\begin{aligned} \Omega(\mathbf{b}) &= 2\Re \left[\int_0^{T_b} r(t) \sum_{k=1}^K \sqrt{\xi_k} \alpha_k b_k a_k(t) e^{-j\phi_k} dt \right] - \int_0^{T_b} \left| \sum_{k=1}^K \sqrt{\xi_k} \alpha_k b_k a_k(t) e^{j\phi_k} \right|^2 dt \\ &= 2\Re \left[\sum_{k=1}^K \sqrt{\xi_k} \alpha_k b_k e^{-j\phi_k} z_k \right] - \sum_{l=1}^K \sum_{k=1}^K \sqrt{\xi_l \xi_k} b_l b_k \alpha_l \alpha_k e^{j\phi_l} e^{-j\phi_k} \rho_{lk}, \end{aligned} \quad (9.22)$$

where z_k and ρ_{lk} are given by Equation (9.8) and Equation (9.9), respectively. Employing our discrete-time model highlighted in Section 9.3, the correlation metric of Equation (9.22) can be expressed in vector notation as [308] :

$$\Omega(\mathbf{b}) = 2\Re \left[\mathbf{b}^T \boldsymbol{\xi} \mathbf{C}^* \mathbf{Z} \right] - \mathbf{b}^T \boldsymbol{\xi} \mathbf{C} \mathbf{R} \mathbf{C}^* \boldsymbol{\xi} \mathbf{b}. \quad (9.23)$$

Hence the decision rule for the optimum CDMA multiuser detection scheme based on the maximum likelihood criterion is to choose the specific bit combination \mathbf{b} , which maximises the correlation metric of Equation (9.23). Hence,

$$\hat{\mathbf{b}} = \arg \left\{ \max_{\mathbf{b}} [\Omega(\mathbf{b})] \right\}. \quad (9.24)$$

The maximisation of Equation (9.23) is a combinatorial optimisation problem, which

requires an exhaustive search for each of the $m = 2^K$ combination of \mathbf{b} , in order to find the one that maximises the correlation metric of Equation (9.23). Explicitly, since there are $m = 2^K$ possible combinations of \mathbf{b} , the optimum multiuser detection has a complexity that grows exponentially with the number of users K .

We have mentioned in Chapter 8 that GAs have been known to solve combinatorial optimisation problems efficiently in many other applications [9]. Hence, in this dissertation, we will investigate the feasibility of invoking GAs in dealing with the CDMA multiuser detection optimisation problem as governed by Equation (9.23).

9.5 Experimental Results

As we have mentioned in Section 8.1 of Chapter 8, a GA's performance is dependent on numerous factors, such as the population size P , the choice of the selection method, the genetic operation employed, the specific parameter settings as well as the particular termination criterion used. In this section, we will attempt to find an appropriate GA setup and parameter configurations that are best suited for our optimisation problem.

Our objective function is defined by the correlation metric of Equation (9.23). Here, the legitimate solutions are the $m = 2^K$ possible combinations of the K -bit vector \mathbf{b} . Hence, each individual will take the form of a K -bit vector corresponding to the K users' bits during a single bit interval. We will denote the p th individual here as $\tilde{\mathbf{b}}_p(y) = [\tilde{b}_{p,1}(y), \dots, \tilde{b}_{p,K}(y)]$, where y denotes the y th generation. Our goal is to find the specific individual that corresponds to the highest fitness value. However, we note that the fitness values corresponding to certain combinations of \mathbf{b} evaluated from the correlation metric of Equation (9.23) will be negative. However, we have mentioned in Section 8.4.2 that some selection schemes can only operate with the aid of positive fitness values. Hence, in order to ensure that the fitness values are positive for all combinations of \mathbf{b} , we modify the correlation metric of Equation (9.23) according to [300] :

$$\exp \{ \Omega(\mathbf{b}) \} = \exp \left\{ 2\Re \left[\mathbf{b}^T \boldsymbol{\xi} \mathbf{C}^* \mathbf{Z} \right] - \mathbf{b}^T \boldsymbol{\xi} \mathbf{C} \mathbf{R} \mathbf{C}^* \boldsymbol{\xi} \mathbf{b} \right\}. \quad (9.25)$$

Our performance metric is the average Bit Error Probability (BEP) evaluated over the course of several generations. In the context of CDMA multiuser detection the three most important criteria to be satisfied by an efficient detection scheme are its BEP performance, its detection time as well as its computational complexity. The detection time of the GA is governed by the number of generations Y required, in order to obtain a reliable decision. We also mentioned in Section 8.4.6 that the computational complexity of the GA, in the context of the total number of objective function evaluations, is related to $P \times Y$. On the other hand, it is well-known that the convergence accuracy of the GA is mainly determined by the population size P , as alluded to in Section 8.1. Hence, in this section the purpose of our study is to find GA configurations that achieve a satisfactory BEP performance at the expense of an acceptable computational complexity within a reasonable time. Since our GA-assisted multiuser detector is based on optimising the modified correlation metric of Equation (9.25), the computational complexity is deemed to be acceptable, if there is a significant amount of reduction in comparison to the optimum multiuser detector, which requires $m = 2^K$ objective

Parameter	Value
Spreading factor N_c	31
Modulation mode	BPSK
Number of CDMA users, K	10 (20 for Figure 9.4)
SNR per bit ξ_k/N_0	9 dB for $k = 1, \dots, K$

Table 9.1: Simulation parameters for the experiments of Figures 9.2-9.9.

Setup/Parameter	Method/Value
Individual initialisation method	Random
Selection method	Fitness-Proportionate
Crossover operation	Single-point
Mutation operation	Standard binary mutation
Elitism	No
Incest Prevention	No
Population size P	Given in Figure 9.2
Mating pool size T	Population size P
Probability of mutation p_m	0.01

Table 9.2: Configuration of the GA used to obtain the results of Figure 9.2. Explicit description of the fitness-proportionate selection scheme and the single-point crossover operation can be found in Section 8.4.2 and Section 8.4.3, respectively.

function evaluations, in order to reach a decision, as highlighted in Section 9.4. In order to evaluate the average BEP performance of the GA-assisted multiuser detectors, randomly generated signature sequences will be used in our simulations. The simulation parameters used for our investigations in this section are presented in Table 9.1 and the following assumptions are stipulated :

- We will assume that perfect power control is invoked by all users such that, on average, their signals arrive at the receiver with the same power.
- Initially only the AWGN channel is invoked, such that $\alpha_k = 1.0$ and $\phi_k = 0$ for $k = 1, \dots, K$, i.e. there is no fading.

9.5.1 Effects of the Population Size

Let us commence our experiments by investigating the effects of the population size P on the convergence rate of the GA. Since at this moment we have no knowledge of which configuration of the GA is best suited for our optimisation problem, we shall adopt the most commonly used GA configuration found in the literature for our initial simulations. This configuration is tabulated in Table 9.2, which follows the flowchart of Figure 8.1. Basically, the individuals, which represent the candidate solutions of \mathbf{b} , are randomly created during the initialisation phase of the GA. Upon evaluating their associated fitness values based on the modified objective function of Equation (9.25), pairs of individuals found in the mating pool are selected

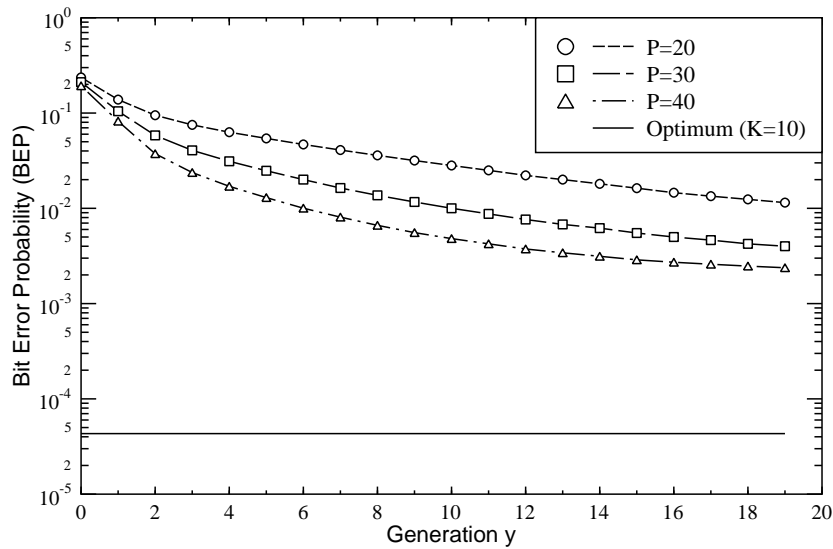


Figure 9.2: The bit error probability performance with respect to the number of generations of the GA-assisted multiuser detector for various population sizes and $K = 10$ users. The configuration of the GA used to obtain these results is tabulated in Table 9.2, while the simulation parameters are listed in Table 9.1.

for crossover and mutation operations, in order to produce offspring. The associated fitness values of these offspring are then evaluated and these offspring will form the new population of the next generation. The processes of selection, crossover, mutation and evaluation are repeated for a total of $Y - 1$ generations¹. Based on this configuration, the BEP performance of the GA-assisted multiuser detector was evaluated and the results, which showed the achievable BEP at the end of each generation are displayed in Figure 9.2. Note that the BEP at each generation, with the exception of the 0th generation, is derived by identifying the offspring associated with the highest fitness value amongst all the offspring created at that generation. The BEP at the 0th generation is derived by identifying the specific individual that exhibits the highest fitness value after the random initialisation. It is seen from the figure that the BEP performance of the GA-assisted multiuser detector improved with increasing the population size. However, the computational cost also increases as a function of the population size, as highlighted in Section 8.4.6. In order to maintain a moderate computational complexity, we shall adopt a fixed population size of $P = 30$ for all our simulations in this section. Upon closer inspection of Figure 9.2, we will notice that the BEP performance of the GA-assisted multiuser detector based on the configuration of Table 9.2 is far from promising. Furthermore, the convergence rate of the GA is very slow. Let us now study whether the per-

¹The 0th generation only consists of initialisation and evaluation.

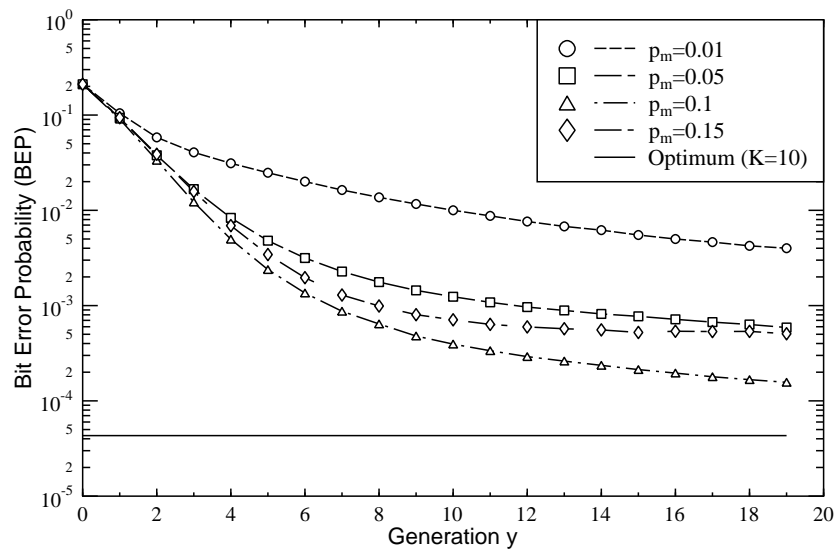


Figure 9.3: The bit error probability performance with respect to the number of generations of the GA-assisted multiuser detector for various probability of mutation values p_m and for $K = 10$ users. The configuration of the GA is specified in Table 9.3, while the simulation parameters are listed in Table 9.1.

formance can be improved by varying some of the GA parameters and the GA configuration, commencing with the probability of mutation.

9.5.2 Effects of the Probability of Mutation

As we have mentioned in Section 8.4.4, the rate of mutation plays an important role in determining the quality of convergence of a GA. A high probability of mutation p_m may disrupt schemata of potentially high fitness values and hence may lead to suboptimal solutions, while a low probability of mutation may result in premature convergence due to the lack of diversity in the population. This assertion is supported by Figure 9.3, which shows the achievable BEP performance of the GA-assisted multiuser detector over $Y = 20$ generations for various values of p_m . The configuration of the GA implemented for this simulation study is listed in Table 9.3, which is similar to the one given in Table 9.2 of Section 9.5.1. Considering the results shown in Figure 9.3, we will immediately notice that the BEP performance has improved significantly over the rather poor results obtained in the previous section for $p_m > 0.01$. Furthermore, according to Figure 9.3, $p_m = 0.1$ appears to give the best performance. All the other values of p_m have a slower convergence rate, leading to solutions far from the optimal one. On the other hand, the value of p_m is very much dependent on the

Setup/Parameter	Method/Value
Individual initialisation method	Random
Selection method	Fitness-Proportionate
Crossover operation	Single-point
Mutation operation	Standard binary mutation
Elitism	No
Incest Prevention	No
Population size P	30
Mating pool size T	Population size P
Probability of mutation p_m	Given in Figure 9.3 and Figure 9.4.

Table 9.3: Configuration of the GA used to obtain the results of Figures 9.3 and 9.4. Explicit description of the fitness-proportionate selection scheme and the single-point crossover operation can be found in Section 8.4.2 and Section 8.4.3, respectively.

length of the individual, as exemplified in Figure 9.4 for $K = 20$ users. Here, each individual will consist of 20-bit variables to be optimised. In this case, $p_m = 0.07$ gives the best performance². Since our simulations performed in this dissertation are based on a CDMA system supporting $K = 10 - 20$ users, we will adopt a probability of mutation $p_m = 0.1$ for all our subsequent simulations, since this value was shown in Figures 9.3 and 9.4 to give a good BEP performance for this user population range. However, further investigations concerning the suitable value of p_m must be performed for a higher number of users. Let us now consider, whether we can further improve the achievable BEP performance by using different crossover operations.

9.5.3 Effects of the Choice of Crossover Operation

In this section, we will investigate, whether the choice of the crossover operation will have an effect on the convergence rate of the GA. Three types of crossover operations are investigated, namely the single-point crossover, the double-point crossover and the uniform crossover, which were highlighted in Section 8.4.3. The configuration of the GA is characterised by Table 9.4 and the associated results are shown in Figure 9.5. Judging from the results displayed in Figure 9.5, there is no significant performance disparity amongst the different crossover operations. Nonetheless, the GA employing the uniform crossover can be seen to exhibit a slightly faster convergence rate, than that using the single-point and double-point crossover. This may be due to the fact that for the uniform crossover operation, every bit of the individual has an equal probability of being exchanged, unlike in the single-point crossover or the double-point crossover, where the leftmost and the rightmost bits have a lower probability of being exchanged. Hence, we shall be adopting the uniform crossover operation for all our subsequent simulations.

²The poor BEP shown in Figure 9.4 is due to the inadequate population size in handling a sizeable search space for $K = 20$.

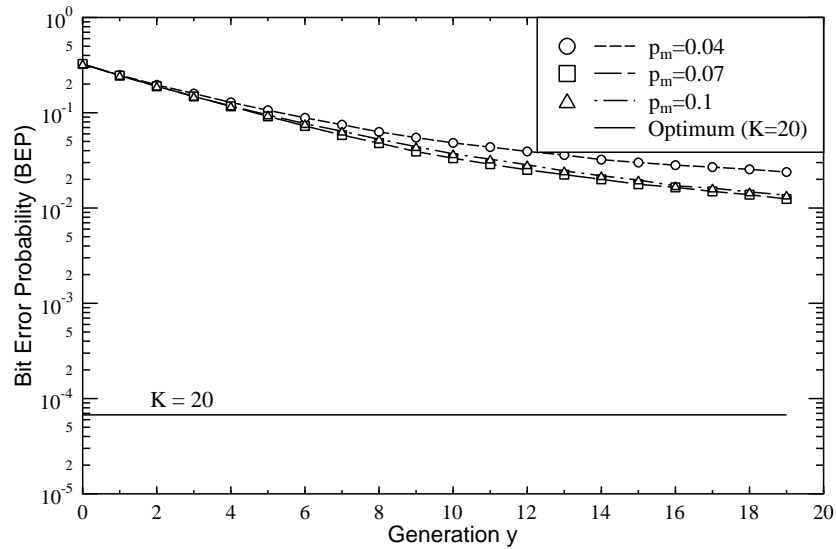


Figure 9.4: The bit error probability performance with respect to the number of generations of the GA-assisted multiuser detector for various probability of mutation value p_m and for $K = 20$ users. The configuration of the GA is specified in Table 9.3, while the simulation parameters are listed in Table 9.1.

Setup/Parameter	Method/Value
Individual initialisation method	Random
Selection method	Fitness-Proportionate
Crossover operation	Given in Figure 9.5
Mutation operation	Standard binary mutation
Elitism	No
Incest Prevention	No
Population size P	30
Mating pool size T	Population size P
Probability of mutation p_m	0.1

Table 9.4: Configuration of the GA used to obtain the results of Figure 9.5. Explicit description of the fitness-proportionate selection scheme and the various crossover operations can be found in Section 8.4.2 and Section 8.4.3, respectively.

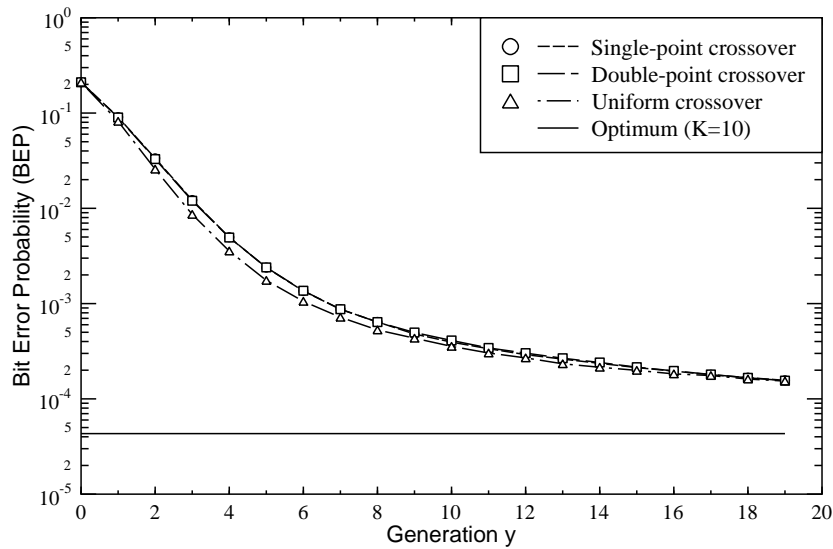


Figure 9.5: The bit error probability performance with respect to the number of generations of the GA-assisted multiuser detector employing the single-point crossover, double-point crossover and the uniform crossover for $K = 10$ users. The configuration of the GA is specified in Table 9.4, while the simulation parameters are listed in Table 9.1.

9.5.4 Effects of Incest Prevention and Elitism

Let us now investigate the effects of invoking the incest prevention and the elitism strategy, as featured in Section 8.4. In the case of the incest prevention strategy, we will ensure that the individuals in the mating pool are not identical. Hence, the mating pool size $T \leq P$ will not be fixed, because it depends on the number of non-identical individuals in the population. As for the elitism strategy, we will only replace the offspring having the lowest fitness value in the new population with the individual corresponding to the highest fitness value in the old population. The configuration of the GA for this investigation is specified by Table 9.5 and the associated results are shown in Figure 9.6. A welcome improvement that can be gleaned from Figure 9.6 is that the GA-assisted multiuser detector has finally managed to achieve the optimum performance for $K = 10$, based on the configuration of Table 9.5 in conjunction with the incest prevention and elitism strategies. Furthermore, we can see that the optimum performance is attained only, if both strategies are invoked. This can be explained as follows. Firstly, the incest prevention strategy will always ensure that a high diversity of individuals is maintained in the population, since only non-identical individuals are allowed to mate. Hence, the offspring that are produced by the crossover and mutation operations will have a high probability that they are not identical to their parents. This will ensure that new areas

Setup/Parameter	Method/Value
Individual initialisation method	Random
Selection method	Fitness-Proportionate
Crossover operation	Uniform
Mutation operation	Standard binary mutation
Elitism	Given in Figure 9.6
Incest Prevention	Given in Figure 9.6
Population size P	30
Mating pool size T	– Population size P if incest prevention is not invoked – $\leq P$ if incest prevention is invoked
Probability of mutation p_m	0.1

Table 9.5: Configuration of the GA used to obtain the results of Figure 9.6. Explicit description of the fitness-proportionate selection scheme and the incest prevention strategy can be found in Section 8.4.2 while the uniform crossover operation and the elitism strategy can be found in Section 8.4.3 and Section 8.4.5, respectively.

in the search space will be explored, which is always a good trait from an optimisation point of view. On the other hand, this will also obliterate the parents associated with high fitness values, since the offspring will constitute the new population. This is undesirable especially, if the parent is actually the optimum solution. Hence the elitism strategy can be invoked in order to counteract this effect. Since in our optimisation problem we are interested in finding only one specific individual that gives the highest fitness value and not a set of likely individuals, the elitism strategy is required to keep track of the individual having the highest fitness value found during the course of evolution. Hence by combining these two strategies, a fast convergence rate and a good performance can be achieved. Now that we know that the GA-assisted multiuser detector is capable of attaining the optimum performance within 20 generations, as shown in Figure 9.6, let us now consider, whether the detector is capable of achieving this level of performance at a faster convergence rate by invoking various selection schemes.

9.5.5 Effects of the Choice of Selection Schemes

In this section, we will attempt to identify the specific selection scheme for our GA-assisted multiuser detector that is capable of offering a fast convergence rate, while maintaining the same level of BEP performance that was attained in Figure 9.6. The selection schemes that were reviewed in Section 8.4.2, namely the fitness-proportionate selection, the sigma scaling selection, the linear ranking selection and the tournament selection, will be investigated. The configuration of the GA is listed in Table 9.6. For the linear ranking selection scheme, we set η^+ and η^- in Equation (8.11) to 1.9 and 0.1, respectively so as to place a higher emphasis on the individuals exhibiting higher fitness values. As for the tournament selection scheme, $t = 5$ individuals are selected from the population randomly with equal probability and the individual that corresponds to the highest fitness value within this group of t individuals

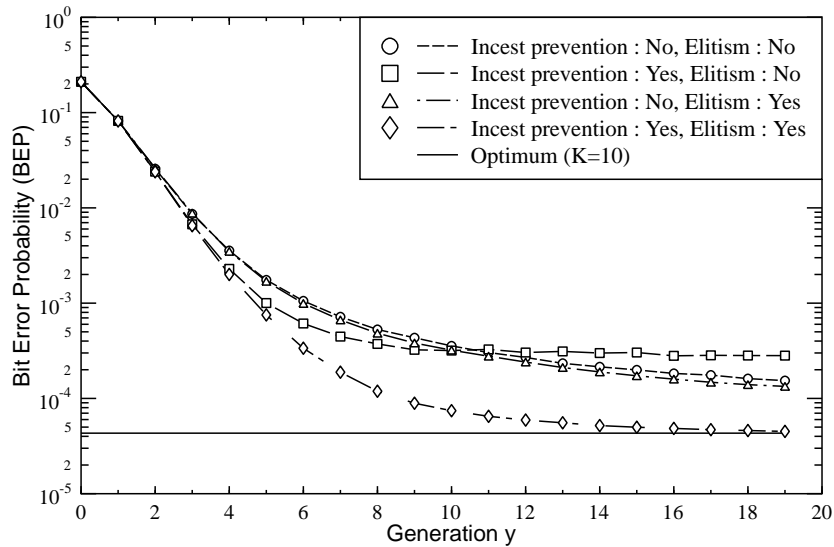


Figure 9.6: The bit error probability performance with respect to the number of generations of the GA-assisted multiuser detector employing the incest prevention strategy and/or elitism strategy, as featured in Section 8.4. The configuration of the GA is specified in Table 9.5, while the simulation parameters are listed in Table 9.1 for $K = 10$ users.

Setup/Parameter	Method/Value
Individual initialisation method	Random
Selection method	Given in Figure 9.7
Crossover operation	Uniform crossover
Mutation operation	Standard binary mutation
Elitism	Yes
Incest Prevention	Yes
Population size P	30
Mating pool size T	$T \leq P$ depending on the total number of non-identical individuals
Probability of mutation p_m	0.1

Table 9.6: Configuration of the GA used to obtain the results of Figure 9.7. Explicit description of the various selection schemes and the uniform crossover operation can be found in Section 8.4.2 and Section 8.4.3, respectively.

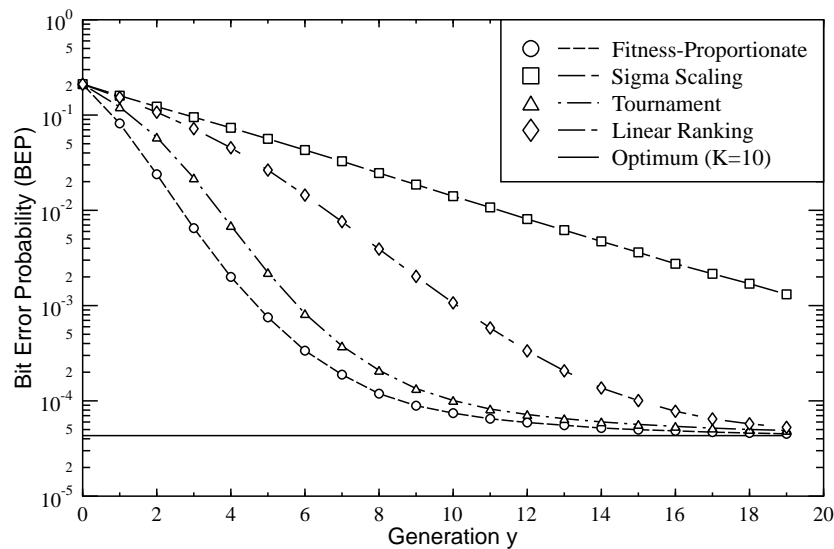


Figure 9.7: The bit error probability performance with respect to the number of generations of the GA-assisted multiuser detector employing various selection schemes. The configuration of the GA is specified in Table 9.6, while the simulation parameters are listed in Table 9.1 for $K = 10$ users.

will be chosen as the parent. Finally, for sigma scaling selection, if the probability of selection p_i corresponding to the i th individual is a negative value when calculated according to Equation (8.10), then we will set this p_i value to 0.0 and discard the associated individual from the selection process. The BEP results are shown in Figure 9.7.

As we can see, GAs utilising the fitness-proportionate selection scheme gave the best performance. On the other hand, GAs using either the sigma scaling selection scheme or the linear ranking selection scheme exhibited a slow convergence rate. A plausible explanation is due to the fact that the mating pool size T spanned over all non-identical individuals. Hence the fitness value variance of the mating pool was high. As a result, individuals having high fitness values are not given sufficient priority to be selected as a parent in the case of the sigma scaling selection. Similarly, because of the linearity of Equation (8.11), the higher-rank individuals are not assigned with a high probability of selection.

A feasible way of overcoming these shortcomings is to reduce the size T of the mating pool, such that $T \ll P$. This implies that only the $T \ll P$ number of non-identical individuals that are associated with the highest fitness values in the current population will be placed in the mating pool. If the number of non-identical individuals in the population happens to be less than T , then the value of T is set to be equivalent to the number of available non-identical individuals, in order to prevent incest mating. We set $T = 10$ and when using the GA con-

Setup/Parameter	Method/Value
Individual initialisation method	Random
Selection method	Given in Figure 9.8
Crossover operation	Uniform crossover
Mutation operation	Standard binary mutation
Elitism	Yes
Incest Prevention	Yes
Population size P	30
Mating pool size T	$T \leq 10$ depending on the number of non-identical individuals
Probability of mutation p_m	0.1

Table 9.7: Configuration of the GA used to obtain the results of Figure 9.8. Explicit description of the various selection schemes and the uniform crossover operation can be found in Section 8.4.2 and Section 8.4.3, respectively.

figuration given by Table 9.7, the corresponding simulation results are shown in Figure 9.8. Now we can see that the achievable BEP performance of the GAs employing either the sigma scaling selection scheme or the linear ranking selection scheme has improved significantly. In particular, the GA-assisted MUD employing the sigma scaling selection scheme has an almost identical performance to that using the fitness-proportionate selection scheme. From these results we conclude that the mating pool size T plays a significant part in determining the convergence rate of the GA using a particular type of selection scheme. More specifically, for the sigma scaling selection and the linear ranking selection the value of T must be set appropriately. We also have to determine the best value of t for the tournament selection scheme. On the other hand, the results obtained in Figure 9.8 for the fitness-proportionate selection scheme are similar to those shown in Figure 9.7, where no specific mating pool size T constraint was imposed, using T equal to the number of non-identical individuals in the population during the particular generation. Furthermore, the fitness-proportionate selection scheme does not involve any external parameters for it to work and judging from Figure 9.7 and Figure 9.8, GAs utilising the fitness-proportionate selection scheme gave the best performance from the range of selection schemes considered. Hence, in order to reduce the number of parameters to be optimised for the GAs to perform reliably, we will only consider the fitness-proportionate selection scheme hereafter. In most cases, the mating pool size T will also be set according to the number of non-identical individuals in the population. However, as we will see in our further discourse, there are certain situations, where a specific value of T must be set, in particular, when the population contains many non-identical individuals.

9.5.6 Effects of a Biased Generated Population

In Section 8.1, we mentioned that instead of randomly creating the initial population of individuals at the commencement of a GA-assisted search, we can invoke any useful information that is available to aid us in creating the initial population of individuals, in order to aid our search at the beginning. In our case, we can use the hard decisions offered by the matched

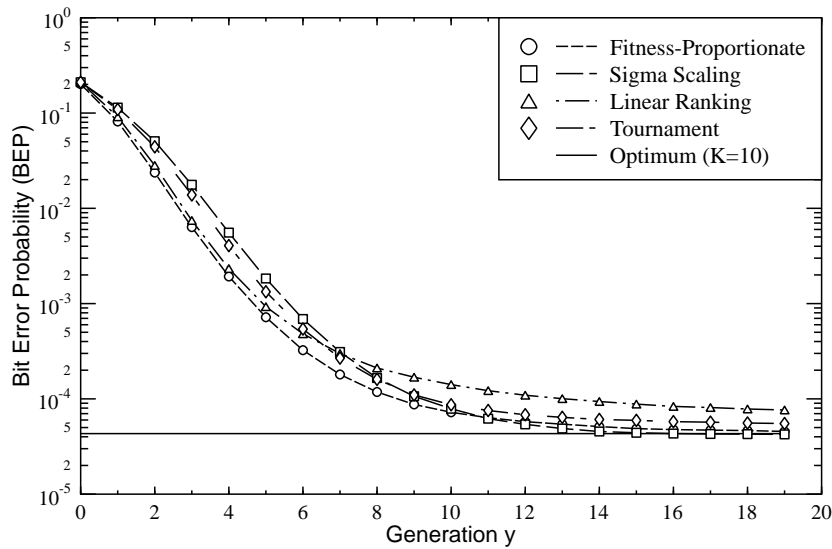


Figure 9.8: The bit error probability performance with respect to the number of generations of the GA-assisted multiuser detector employing various selection schemes. The configuration of the GA is specified in Table 9.7, while the simulation parameters are listed in Table 9.1.

filter outputs \mathbf{Z} of Equation (9.16), in order to aid our search. We shall denote these hard decisions here as :

$$\hat{\mathbf{b}}_{MF} = [\hat{b}_{1,MF}, \hat{b}_{2,MF}, \dots, \hat{b}_{K,MF}] \quad (9.26)$$

where $\hat{b}_{k,MF}$ for $k = 1, \dots, K$ is given by Equation (9.11). Two methods of biasing are proposed for our investigations. Firstly, we will assign the hard decisions of Equation (9.26) to only one individual. The remaining $P - 1$ individuals will be randomly generated. This will ensure that a high diversity of individuals are present in the population at the beginning. We shall refer to this method as M1. For our second method, we will assign a different randomly ‘mutated’ version of the hard decision vector $\hat{\mathbf{b}}_{MF}$ of Equation (9.26) to each of the individuals in the initial population. We shall adopt the same probability of mutation as p_m . In this way, the individuals in the initial population will be almost identical. Note that we cannot assign the same hard decision vector $\hat{\mathbf{b}}_{MF}$ to all the individuals, since incest prevention is invoked, which will not allow identical individuals to mate. We shall refer to this method as M2. Using the GA configuration listed in Table 9.8, the simulation results are shown in Figure 9.9. As the figure suggests, method M2 gives a better performance in terms of a faster convergence rate due to a good initial population of individuals. This fact

Setup/Parameter	Method/Value
Individual initialisation method	Given in Figure 9.9
Selection method	Fitness-proportionate
Crossover operation	Uniform crossover
Mutation operation	Standard binary mutation
Elitism	Yes
Incest Prevention	Yes
Population size P	30
Mating pool size T	$T \leq P$ depending on the number of non-identical individuals
Probability of mutation p_m	0.1

Table 9.8: Configuration of the GA used to obtain the results of Figure 9.9. Explicit description of the fitness-proportionate selection scheme and the uniform crossover operation can be found in Section 8.4.2 and Section 8.4.3, respectively.

conforms to the results obtained in [300]. Hence we shall adopt method M2 of initialising the initial population.

Based on the results gathered from our simulations, the final GA configuration that we will be utilising for most of our simulations in this dissertation, unless specified otherwise in the associated plots, is given in Table 9.9. The associated flowchart is depicted in Figure 9.10. Further useful information can be gleaned by comparing our GA configuration to the previously proposed GA-assisted multiuser detectors [300–303] in the literature, as given by Table 8.3. Notice that a low probability of mutation p_m as well as no incest prevention strategy were invoked in these proposals [300–303]. On the other hand, according to our results summarised in Section 9.5.2 and Section 9.5.4, the effects of the value of p_m and those of the incest prevention strategy can have a significant impact on the convergence rate and hence also on the BEP performance of the GA-assisted multiuser detector. As shown in Figure 9.9, our proposed GA-assisted multiuser detector is capable of reaching a near-optimal BEP performance within $Y = 10$ generations with the aid of a population size of $P = 30$ for $K = 10$ users over an AWGN channel at an SNR of 9 dB. This constitutes a total of $P \times Y = 300$ number of correlation metric evaluations according to Equation (9.25). In fact, as we have mentioned in Section 8.4.6, this number was derived based on the fact that the fitness value is calculated for every individual in the population at every generation. However in reality, certain individuals will reappear over the course of the evolution. Hence, the fitness values of these individuals need not be recalculated, if they are stored in memory. Based on our simulations for $P = 30$, $Y = 10$ and $K = 10$, we found that the average number of unique K -bit combinations that were evaluated by the GA for a single bit interval was ≈ 89 . Comparing this number to that of the optimum multiuser detector, which requires $2^{10} = 1024$ correlation metric evaluations for every b combination, our proposed GA-assisted multiuser detector is capable of attaining a significantly reduced computational complexity and yet delivering a near-optimum BEP performance up to a specific SNR value. Hence the implementation of our proposed GA-assisted multiuser detector is feasible in practical terms and offers an alternative to the implementation of the optimum multiuser detector.

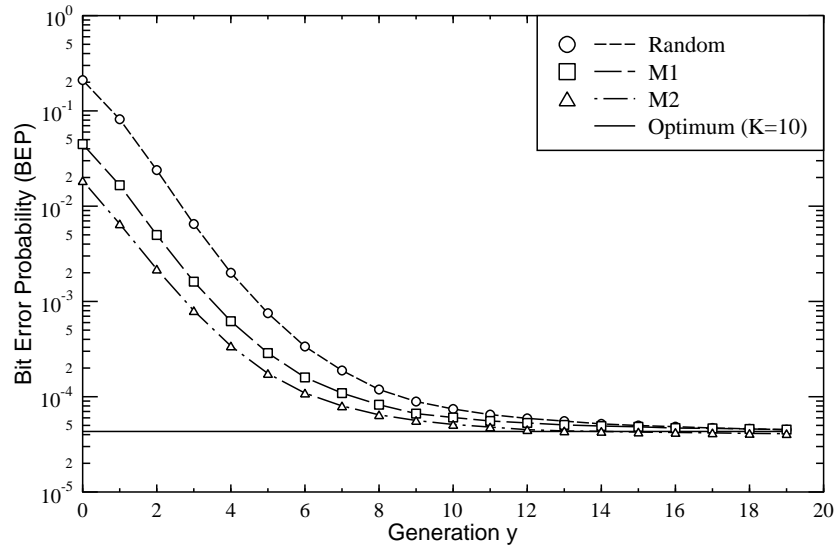


Figure 9.9: The bit error probability performance with respect to the number of generations of the GA-assisted multiuser detector employing different methods of initialising the individuals at the beginning. The configuration of the GA is specified in Table 9.8, while the simulation parameters are listed in Table 9.1 for $K = 10$ users.

Setup/Parameter	Method/Value
Individual initialisation method	Mutation of \hat{b}_{MF} of Equation (9.26)
Selection method	Fitness-proportionate
Crossover operation	Uniform crossover
Mutation operation	Standard binary mutation
Elitism	Yes
Incest Prevention	Yes
Population size P	30
Mating pool size T	$T \leq P$ depending on the number of non-identical individuals
Probability of mutation p_m	0.1
Termination generation Y	10

Table 9.9: Configuration of the GA that will be used in this dissertation hereafter, unless otherwise specified.

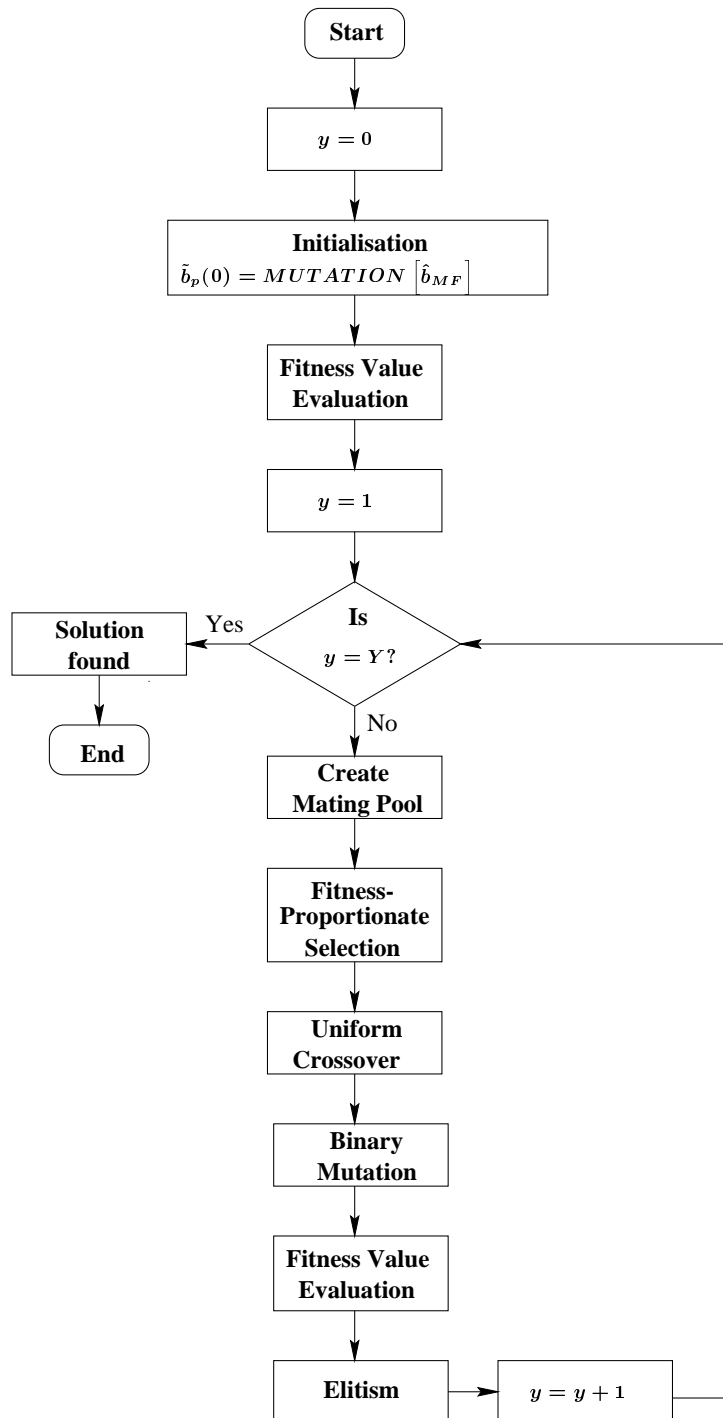


Figure 9.10: A flowchart depicting the structure of the genetic algorithm adopted for our GA-assisted multiuser detection technique, which is a specific version of Figure 8.1.

Finally, it should be stressed that we have only explored a fraction of the numerous possible configurations of GAs, a fact noted at the beginning of Chapter 8. Furthermore, the settings of certain parameters were not investigated extensively, such as the probability of mutation p_m , the ideal mutation pool size T and the population size P . These values will depend very much on the number of users K and the desired quality of detection. There are also many variants of GAs that have not been studied or indeed even highlighted in this dissertation. Hence we made no claims about the optimality of the GAs used in this dissertation for the application in CDMA multiuser detection. Hence it is possible that different GA variants, which were not covered in this dissertation, or a different set of parameters may give an even better performance. However, we will show with the aid of the following simulation results of this chapter as well as in subsequent chapters that the GA configuration of Table 9.9 together with the set of GA parameters that we have adopted is capable of offering a satisfactory trade-off between computational complexity, detection delay and an acceptable BEP performance. Using the GA configuration of Table 9.9, let us now consider the BEP performance of the GA-assisted CDMA multiuser detector in both an AWGN channel as well as in a non-dispersive-Rayleigh fading channel.

9.6 Simulation Results

9.6.1 AWGN Channel

All the results in this section were based on evaluating the BEP performance of a bit-synchronous K -user CDMA system over an AWGN channel. The signature sequences were randomly generated 31-chip per bit sequences and the transmit bit energy ξ_k was assumed to be equal for all users.

Figure 9.11 shows the average BEP as a function of the SNR per bit for the GA-assisted multiuser detector for various population sizes P and different number of generations Y for $K = 10$. The values of P and Y are assigned such that the maximum number of times the objective function of Equation (9.25) was evaluated upon detecting the bit vector $\hat{\mathbf{b}}$ during a bit interval is approximately 300. The optimum performance of the multiuser detector utilising an exhaustive search for $K = 10$ is also shown. In this case, the optimum multiuser detector has to compute the objective function of Equation (9.25) $2^{10} = 1024$ times, which corresponds to every possible combination of \mathbf{b} . Upon observing Figure 9.11, we notice that the GA-assisted multiuser detector is capable of achieving a near-optimum performance up to an SNR of 8 dB at a lower computational complexity than that of the optimum multiuser detector. Specifically, the minimum reduction in the computational complexity offered by the GA-assisted multiuser detector over its optimum counterpart is $[(1024 - 320)/1024] \times 100 = 68.75\%$. As mentioned previously in Section 9.5, this reduction in the computational complexity is expected to be higher if the repeated fitness value evaluation of the same individual is circumvented. From Figure 9.11, we can see that the BEP performance curves began to flatten at an SNR of 10 dB. This is due to the inadequate population size and/or number of generations required for the GA to converge to the optimum performance. Recall that in Section 8.1 we stated that the GAs are not guaranteed to find the optimal solution, unless a sufficiently large population size and an appropriate number of generations are guaranteed. On the other hand, it is not a prerequisite that the optimum

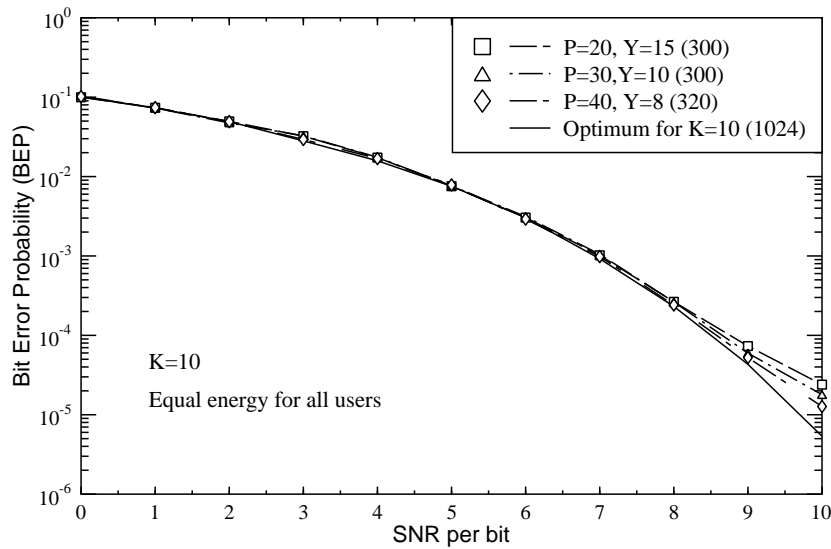


Figure 9.11: The bit error probability performance of the GA-assisted multiuser detector as a function of the SNR per bit with populations size of $P = 20, 30, 40$ using binary random signature sequences of length $N_c = 31$ for $K = 10$ users. The GA configuration used is listed in Table 9.9. The values in round brackets in the legend denote the maximum number of times the objective function of Equation (9.25) was evaluated upon detecting the bit vector $\hat{\mathbf{b}}$ during a bit interval.

performance must be achieved for every SNR value. The integrity of detection required is usually dependent on the type of service the detection scheme is intended for. For example, a speech signal may tolerate a relatively high BEP of 10^{-3} but no latency, while a data signal may require a BEP performance below 10^{-6} , but it can tolerate a higher detection delay. Hence we can immediately see that the GA-assisted multiuser detector is capable of offering this trade-off by simply adjusting the values of P and Y .

Let us now consider what happens, if the number of users K is increased to 20. In the context of the optimum multiuser detector, an exhaustive search would require a staggering $2^{20} = 1,048,576$ number of objective function evaluations, in order to obtain the optimum solution. The BEP performance of the GA-assisted multiuser detector for various values of P and Y is shown in Figure 9.12. Again, we see that by simply expanding the population size P and by extending the number of generations Y , the near-optimal BEP performance of the GA-assisted multiuser detector found for $K = 10$ can be maintained, when the number of users is increased to $K = 20$. While this will increase the associated computational complexity of the GA-assisted multiuser detector, the maximum number of objective function evaluations given by $P \times Y$ is still significantly lower, than that required by the optimum detector.

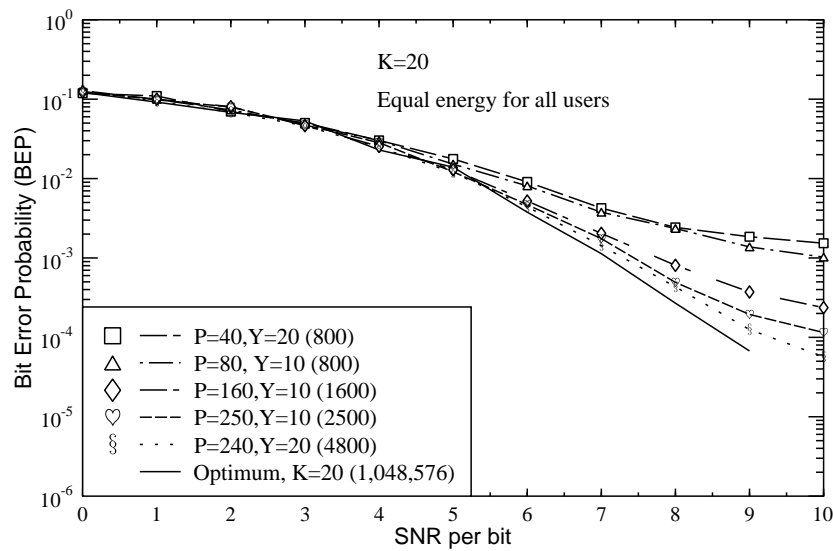


Figure 9.12: The bit error probability performance of the GA-assisted multiuser detector as a function of the SNR per bit with various populations sizes P and number of generations Y for $K = 20$ using binary random signature sequences of length $N_c = 31$. The GA configuration used is listed in Table 9.9. The values in round brackets in the legend denote the number of times the objective function of Equation (9.25) was evaluated upon detecting the bit vector $\hat{\mathbf{b}}$ during a bit interval.

Figure 9.13 shows the average BEP performance of the GA-assisted multiuser detector as a function of the number of users K for an SNR value of 7 dB. As we can see, for a given number of generations Y , the population size P must be increased, in order to maintain the same level of BEP performance as K is increased. However, the required increase in the population size P is not exponentially proportional to the number of users. Furthermore, there is a gradual degradation in the BEP performance for a given population size P and termination generation Y , as the number of users K increased.

9.6.2 Single-path Rayleigh Fading Channel

In this section, the BEP performance of the GA-assisted multiuser detector is evaluated for a bit-synchronous K -user CDMA system over a non-dispersive Rayleigh fading channel. The signature sequences were randomly generated $N_c = 31$ -chip per bit sequences and the users' CIR coefficients $\alpha_k e^{j\phi_k}$ were assumed to be known at the receiver. With the exception of Figure 9.17, the transmit bit energy ξ_k was assumed to be equal for all users.

Figure 9.14 shows the BEP performance of the GA-assisted multiuser detector for differ-

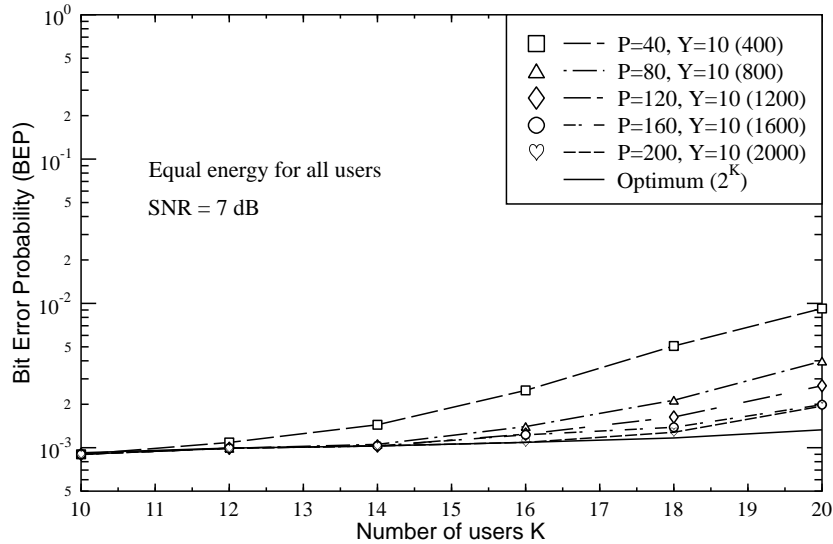


Figure 9.13: The bit error probability performance of the GA-assisted multiuser detector as a function of the number of K users with populations size of $P = 40, 80, 120, 160, 200$ and $Y = 10$ using binary random signature sequences of length $N_c = 31$. The GA configuration used is listed in Table 9.9. The values in round brackets in the legend denotes the number of times the objective function of Equation (9.25) was evaluated upon detecting the K -bit vector $\hat{\mathbf{b}}$ during a bit interval.

ent number of generations Y and for different population sizes P . The optimum performance for $K = 10$ users was also plotted for comparison. As it can be seen from the figure, the combination of $P = 40$ and $Y = 10$ – which constitutes a maximum of $40 \times 10 = 400$ number of objective function evaluations according to Equation (9.23) – was capable of achieving a near-optimal BEP performance. For SNR values beyond 40 dB, the system exhibited an error floor due to the performance limitations of the GA in conjunction with the given P and Y values studied. At lower values of Y and P , the error floor occurred at a lower SNR value. For instance, at $Y = 10$ and $P = 20$, which requires a maximum of 200 number of objective function evaluations according to Equation (9.23), the error floor occurred at an SNR value of about 32 dB, while for SNR values up to 24 dB, the detector exhibited near-optimum BEP performance. Hence, again it was shown here that the GA-assisted multiuser detector was capable of offering a trade-off between computational complexity and the optimum BEP performance.

In order to show that the computational complexity of the GA is not exponentially dependent on the number of users K , the BEP performance was evaluated in Figure 9.15 for various number of users, employing $P = 40, 80, 120, 160, 200$ in conjunction with $Y = 10$. The re-

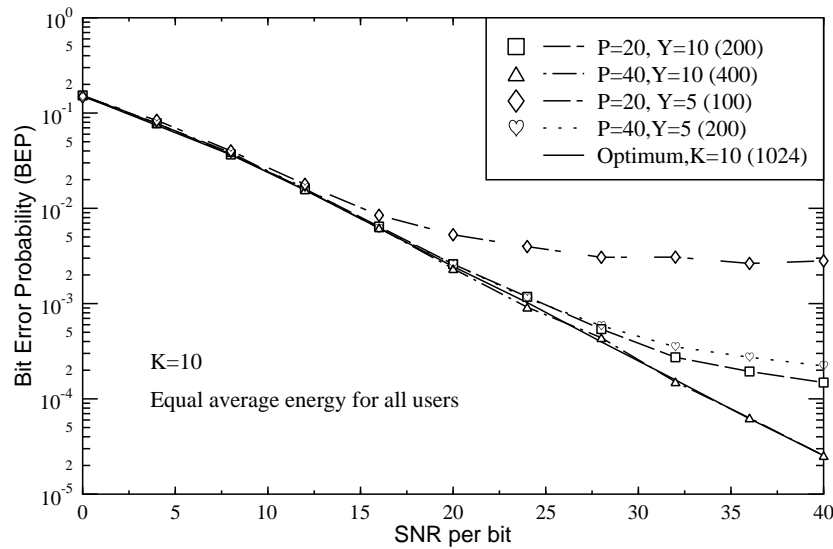


Figure 9.14: The bit error probability performance of the GA-assisted multiuser detector as a function of the SNR per bit for $K = 10$ users with various combinations of P and Y in conjunction with perfect channel estimation using binary random signature sequences of length $N_c = 31$. The GA configuration used is listed in Table 9.9. The values in round brackets in the legend denote the maximum number of times the objective function of Equation (9.25) was evaluated upon detecting the bit vector $\hat{\mathbf{b}}$ during a bit interval.

sults are shown in Figure 9.15. At $P = 40$ and $Y = 10$, we can see that the BEP performance gradually degrades upon increasing the number of users, due to the limited population size P , which was too small for adequately exploring a significantly larger search space. As the population size P is increased, the BEP improves. For a population size of $P = 160$, we can see that the GA-assisted detector is capable of attaining a near-optimal performance, while supporting $K = 20$ users. More importantly, we noted that the number of correlation metric evaluations, seen within the brackets in the legend of Figure 9.15 increases slower than exponentially as a function of the number of users. For example, when K is increased from 10 to 16, the population size P has to be increased from 40 to 120, in order to maintain the same level of performance. This constituted a factor of $1200/400 = 3$ increased computational complexity, when K was increased from 10 to 16, while maintaining a near-optimum BEP performance. By contrast, the computational complexity of the optimum multiuser detection using exhaustive search would be increased by a factor of $2^{16}/2^{10} = 64$. Similarly, when K is increased to 20, a population size of $P = 160$ is sufficient for attaining the same level of BEP performance. This constituted only a factor of $1600/400 = 4$ increased computational complexity. Furthermore, in contrast to the reduced-complexity tree-search type algo-

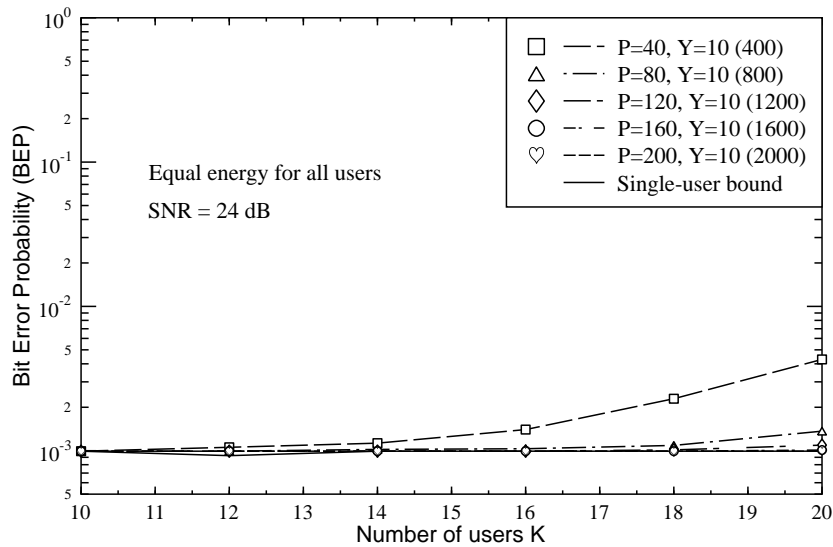


Figure 9.15: The bit error probability performance of the GA-assisted multiuser detector as a function of the number of K users with populations size of $P = 40, 80, 120, 160, 200$ and $Y = 10$ in conjunction with perfect channel estimation using binary random signature sequences of length $N_c = 31$. The GA configuration used is listed in Table 9.9. The values in round brackets in the legend denote the number of times the objective function of Equation (9.25) was evaluated upon detecting the K -bit vector $\hat{\mathbf{b}}$ during a bit interval.

rithms [311,312] – which can also achieve a near-optimum BEP performance at a complexity lower than that of the optimum detector – the detection time required by our GA-based multiuser detector to reach a decision is independent of the number of users. Additionally, for the tree-search algorithms a noise whitening filter is required. Figure 9.16 portrays the achievable complexity reduction factor of the GA-assisted multiuser detector, which was defined as $\frac{2^K}{P \times Y}$. Specifically, the numerator quantifies the number of correlation metric evaluations required by the optimum multiuser detector, while the denominator indicates the number of correlation metric evaluations required by the GA-assisted multiuser detector, in order to attain the optimum performance at an SNR value of 24 dB. This figure was extracted from the results obtained in Figure 9.15. As seen from the figure, the complexity reduction offered by the GA-assisted multiuser detector over the optimum detector becomes more significant, as the number of users is increased.

Figure 9.17 shows the near-far resistance of the proposed GA-assisted multiuser detector in conjunction with perfect CIR estimation. The average received bit energy ξ_1 of the desired user remained unchanged, while the energies of all other users ξ_k for $k = 2, \dots, K$ were either 6 dB or 10 dB higher, than that of the desired user. We can see that the GA-assisted

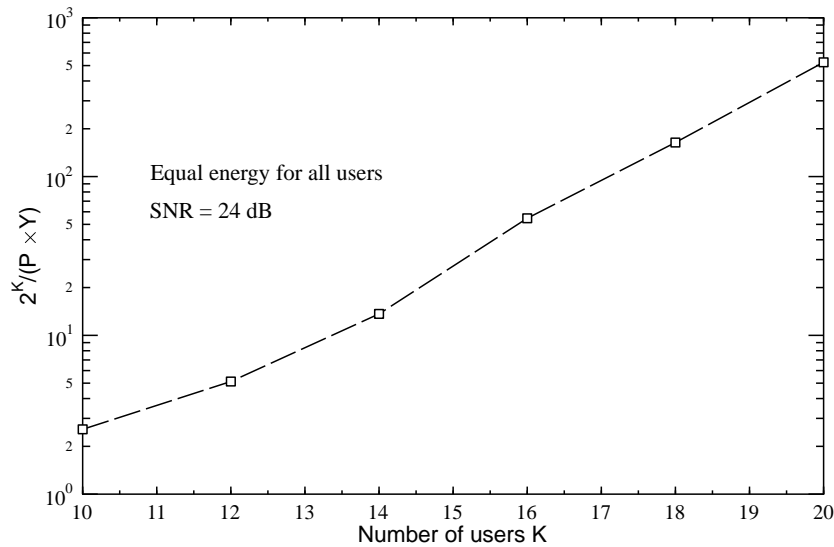


Figure 9.16: The complexity reduction factor between the optimum multiuser detector and the GA-assisted multiuser detector according to $\frac{2^K}{P \times Y}$, where the numerator denotes the number of correlation metric evaluations required by the optimum multiuser detector, while the denominator denotes that required by the GA-assisted multiuser detector, in order to attain the optimum performance at an SNR value of 24 dB, based on the results of Figure 9.15.

multiuser detector was near-far resistant.

9.7 Chapter Summary and Conclusions

In this chapter, our model of a bit-synchronous CDMA system communicating over a single-tap Rayleigh fading channel was presented in Section 9.2 and its equivalent discrete representation was considered in Section 9.3. Based on this model, the optimum multiuser detector based on the maximum likelihood criterion was derived in Section 9.4. It was shown that the correlation metric of Equation (9.23) for the optimum multiuser detection scheme is cast in the form of a combinatorial optimisation function and its computational complexity is exponentially proportional to the number of users. Thus its implementation becomes impractical, when there is a high number of users. A GA-assisted multiuser detector was proposed in this chapter, in order to circumvent the above-mentioned complexity problem. According to the results obtained from other similar GA-assisted multiuser detector proposals [300–303] found in the literature, which were summarised in Section 9.5.1, traditional GAs generally have a slow convergence rate, rendering them unsuitable for real-time data detection. In order to

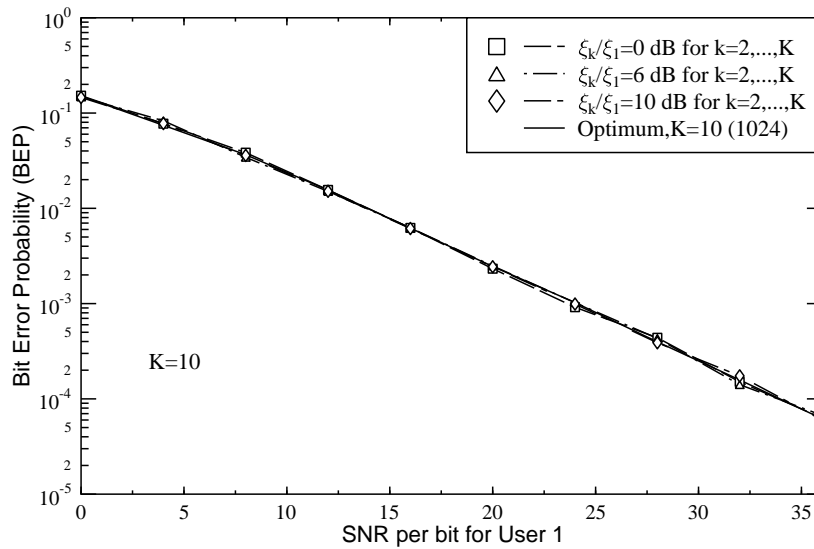


Figure 9.17: The bit error probability performance of the GA-assisted multiuser detector for $K = 10$ users with ξ_k/ξ_1 at 0 dB, 6 dB and 10 dB for $k = 2, \dots, K$ in conjunction with perfect channel estimation using binary random signature sequences of length 31. The GA configuration used is listed in Table 9.9. The values in round brackets in the legend denote the number of times the objective function of Equation (9.25) was evaluated upon detecting the K -bit vector $\hat{\mathbf{b}}$ during a bit interval.

mitigate this impediment, we conducted a series of experiments presented in Section 9.5, for finding a particular GA configuration, from the family of techniques highlighted in Chapter 8, which can offer the best trade-off between the detection delay, computational complexity and BEP performance. Based on the results obtained from our experiments, the GA configuration that we have adopted in our GA-assisted multiuser detector was given in Table 9.9. The notable differences between our favoured GA configuration and those utilised in [300–303], as shown in Table 8.3, are the probability of mutation p_m and the employment of the incest prevention strategy. As suggested by in Figure 9.3 and in Figure 9.6, these two features can have a significant impact on the convergence rate and hence on the achievable BEP performance of the GA-assisted multiuser detector. For our advocated GA configuration, the incest prevention strategy and a relatively high value of p_m were invoked, since a faster convergence and an improved BEP performance can be achieved, as illustrated in Figure 9.3 and in Figure 9.6. Last but not least, the BEP performance of the GA-assisted multiuser detector was assessed in Section 9.6 for a bit-synchronous CDMA system for transmission over an AWGN channel as well as a single-path Rayleigh fading channel. We have shown that with the aid of a sufficiently high population size P and for a reasonable number of generations

Y, the BEP performance of the GA-assisted multiuser detector approaches that of the optimum multiuser detector at the cost of a significantly lower computational complexity. Our results for a single-tap Rayleigh fading channel were obtained based on the perfect knowledge of each user's CIR coefficients at the receiver. In reality, these CIR coefficients have to be estimated by some means. In our next chapter, we will show that it is possible to extend the GA-assisted multiuser detector introduced in this chapter, such that the users' CIR coefficients can be estimated concurrently with the data detection without the assistance of any pilot signals.

Part III

M-ary Single-Carrier CDMA

Part IV

Multi-Carrier CDMA

Chapter 17

Overview of Multicarrier CDMA

17.1 Introduction

Orthogonal frequency division multiplexing (OFDM) [80, 422–424] is a parallel data transmission scheme in which high data rates can be achieved by transmitting U orthogonal subcarriers. The inter-symbol interference (ISI) and inter-channel interference (ICI) in OFDM systems are reduced by the insertion of guard intervals and code synchronization is made easier by the extended symbol period engendered by the associated serial-to-parallel conversion preceding the parallel transmission of low-rate subchannels. Recently, code-division multiple-access (CDMA) systems based on the combination of CDMA schemes and OFDM signaling, which are referred to as multicarrier CDMA systems, have attracted attention in the field of wireless communications [20, 69–71, 78, 79, 424–462]. This is mainly due to the need to support high data rate services in wireless environment characterized by highly hostile radio channels. These signals can be efficiently modulated and demodulated using Fast Fourier Transform (FFT) devices without substantially increasing the receiver's complexity. These systems also exhibit the attractive feature of high spectral efficiency, since they can operate using a low Nyquist roll-off factor [80]. Hence, OFDM systems can approach the 2 Baud/Hz maximum bandwidth efficiency associated with Nyquist sampling. The combination of code division and OFDM can combat the effects of fading channels by spreading signals over several carriers, in order to achieve frequency diversity.

Depending on whether all the subcarriers are activated on each transmission, multicarrier CDMA arrangements can be classified as the non-frequency hopping multicarrier CDMA and the frequency-hopping assisted multicarrier CDMA schemes. The family of non-frequency hopping multicarrier CDMA schemes includes multicarrier CDMA using frequency-domain spreading [447, 454, 457, 462], subchannel band-limited multicarrier direct-sequence CDMA (DS-CDMA) [448, 453], orthogonal multicarrier DS-CDMA [69, 431, 449, 460] and multitone DS-CDMA [450, 463]. The class of frequency-hopping assisted multicarrier CDMA schemes belongs to the extended family of the above multicarrier schemes, which include multicarrier DS-CDMA using adaptive frequency-hopping [461], as well as multicarrier DS-CDMA

using adaptive subchannel allocation [439] and the subclass of constant-weight code assisted multicarrier DS-CDMA using slow frequency-hopping [70, 78, 425].

Based on their signal spreading model, multicarrier schemes can also be categorized mainly into two types. In the first class of schemes, the serial data stream is first spread by a spreading code and then converted into N_p parallel chip sequences with each chip modulating a different subcarrier. The number of subcarriers is N_p , which equals the number of chips per data symbol. The spreading operation in this type of multicarrier CDMA arrangements occurs in the frequency-domain. This type of systems combine the robustness of orthogonal modulation with the flexibility of CDMA schemes [79, 440]. In the second type of multicarrier CDMA systems, the original data stream is first serial-to-parallel converted into U substreams. Then, each substream is spread using a given spreading code in the time-domain, and finally, modulates a different subcarrier with each of the data stream. In the second type of multicarrier CDMA each subcarrier's signal is similar to that of a conventional the normal single carrier DS-CDMA scheme [69]. The first class of multicarrier CDMA only includes one particular scheme, namely multicarrier CDMA using frequency-domain spreading [447, 454, 457, 462], while other known multicarrier CDMA schemes belong to the second family.

One of the main implementation disadvantages at the transmitter side of OFDM based multicarrier CDMA systems is the high peak-to-average power ratio [423, 436] of the transmitted signal. Whenever the peak transmitted power is limited by regulatory or implementational constraints - such as the minimum required transmit power or the power efficiency of the amplifier - this has the effect of reducing the average power of the transmitter and limiting the range of transmissions. Moreover, since the multicarrier signal exhibits a high amplitude variation, it is subject to nonlinear distortions inflicted by the power amplifier. This distortion inevitably results in out-of-band emissions and co-channel interference, potentially causing a significant degradation in the system's performance.

In this chapter the performance of different multicarrier CDMA systems is investigated over frequency-selective Rayleigh fading channels. Section 17.2 reviews family of the multicarrier CDMA schemes, analyzes their characteristics and discusses their advantages as well as disadvantages in terms of their transmitter and receiver structures. We will also consider their spectral efficiency and spreading gain. In Sections 17.4 to 17.8 we analyze a range of typical multicarrier CDMA schemes in depth and derive their corresponding bit error probability. Let us now commence our overview of multicarrier CDMA systems.

17.2 Overview of Multicarrier CDMA Systems

In this section we review the class of multicarrier CDMA schemes, which have been discussed in the literature. Specifically, we discuss their design parameters, spectral characteristics, advantages and disadvantages in terms of the transmitter and receiver structures as well as their spectral efficiency. The bit error rate (BER) performance analysis of these multicarrier CDMA schemes is provided in the following sections. Before considering these schemes in more detail, we first list some their common parameters.

- W_s (Hz): Overall spectral null-to-null system bandwidth;
- W_{ds} (Hz): Null-to-null transmission bandwidth of each subcarrier signal;

- W_d (Hz): null-to-null bandwidth of the binary baseband data signal;
- T_b : Binary bit duration;
- T_s : Transmitted symbol's duration;
- T_c : Chip duration of the spreading codes in the multicarrier CDMA system;
- T_{c1} : Chip duration of the spreading codes in the single-carrier CDMA system;
- f_0 : RF carrier frequency;
- $N = W_s/W_d = T_b/T_{c1}$: Spreading gain of BPSK modulated single-carrier DS-CDMA signals;
- $N_e = T_s/T_c$: Spreading gain of BPSK modulated subcarrier DS-CDMA signal, or number of chips per symbol;
- $N_b = T_b/T_c$: Number of chips per bit;
- L_1 : Number of resolvable propagation paths experienced by the single-carrier DS-CDMA signal;
- Δ : Spacing between two adjacent subcarriers;
- SG : Spectral gain, which is defined as the ratio between the bandwidth required by the multicarrier scheme without overlapping and the actual bandwidth of the corresponding multicarrier scheme.

Having defined the common multicarrier CDMA parameters, let us first highlight the concepts associated with frequency-domain spreading.

17.2.1 Frequency-Domain Spreading Assisted Multicarrier CDMA Scheme

Fig.17.1 shows the transmitter diagram of the multicarrier CDMA (MC-CDMA) scheme associated with frequency-domain spreading [447, 454, 457, 462]. The MC-CDMA transmitter spreads the original data stream over N_p subcarriers using a given spreading code of $\{c_k[0], c_k[1], \dots, c_k[N_p - 1]\}$ in the frequency domain. Observe in Fig.17.1 that this scheme does not include serial-to-parallel data conversion and there exists no spreading modulation on each subcarrier. Therefore, the data rate on each of the N_p subcarriers is the same as the input data rate. However, by spreading each data bit across all of the N_p subcarriers the fading effects of multipath channels is mitigated. With reference to Fig.17.1 the k th MC-CDMA user's transmitted signal can be expressed as:

$$s_k(t) = \sqrt{\frac{2P}{N_p}} \sum_{n=0}^{N_p-1} b_k(t) c_k[n] \cos(2\pi f_n t), \quad (17.1)$$

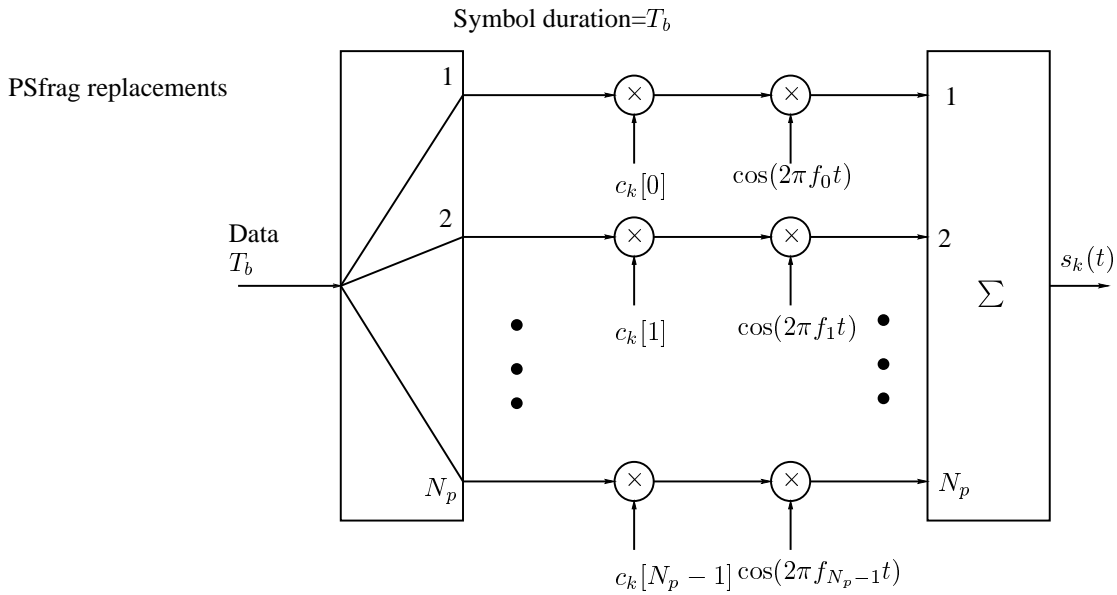


Figure 17.1: The transmitter diagram of frequency-domain spreading assisted MC-CDMA systems.

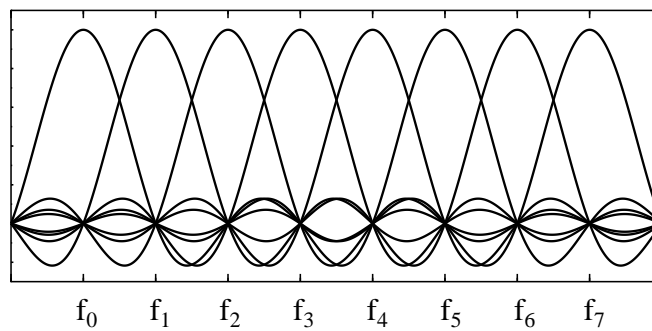


Figure 17.2: Spectrum of the frequency-domain spreading assisted MC-CDMA signal.

where P represents the transmitted power of the MC-CDMA signal, N_p is the number of subcarriers as well as the spreading gain, $\{c_k[0], c_k[1], \dots, c_k[N_p - 1]\}$ is the spreading code, $\{f_n, n = 0, 1, \dots, N_p - 1\}$ are the subcarrier frequencies, and finally, $b_k(t)$ represents the binary data sequence.

The spectrum of the transmitted MC-CDMA signal is shown in Fig.17.2, where we assume that the MC-CDMA system has eight subcarriers and that all the chip values of the spreading code of $\{c_k[0], c_k[1], \dots, c_k[N_p - 1]\}$ are +1. In this MC-CDMA system the subcarrier frequencies are chosen to be orthogonal to each other, i.e. the subcarrier frequencies satisfy the following condition:

$$\int_0^{T_b} \cos(2\pi f_i t + \phi_i) \cdot \cos(2\pi f_j t + \phi_j) dt = 0, \text{ for } i \neq j, \quad (17.2)$$

where T_b is the bit duration. Therefore, the minimum spacing Δ between two adjacent subcarriers satisfies $\Delta = \frac{1}{T_b}$, which is a widely used assumption [447, 454, 457, 462] and is also the case employed in Fig.17.2, where $f_n = f_0 + \frac{n}{T_b}$ for $n = 0, 1, \dots, N_p - 1$. If $\Delta = \frac{1}{T_b}$ associated with 50% overlap is assumed, then the bandwidth required by the MC-CDMA system is $(N_p + 1) \cdot \frac{1}{T_b}$. However, the MC-CDMA system having N_p non-overlapping subcarriers requires a total bandwidth of $N_p \cdot \frac{2}{T_b}$. Hence, the spectral gain of this MC-CDMA system is given by:

$$SG = \frac{N_p(2/T_b)}{(N_p + 1)(1/T_b)}, \quad (17.3)$$

which approaches two, as N_p increases. Thus, this MC-CDMA system exhibits an increased processing gain given by $N_p \approx 2N$, as explained by the 50% overlap of the main lobes of the adjacent MC-CDMA subcarrier spectra.

Yee [447] *et al.* have considered a MC-CDMA system, in which the subcarriers' frequency separation is higher than the coherence bandwidth of the channel, and therefore the individual subcarriers experience independent fading. As a result, the frequency diversity is maximized. However, this system requires a considerable transmission bandwidth. Nevertheless, the addition of an interleaver after the chip spreading would lessen this bandwidth requirement.

This scheme can be applied in conjunction with the same set of subcarriers, to a multiple access system by allocating each user a different spreading code. The separation of different users is provided by the spreading codes. In the receiver the fading impaired signals of the subcarriers are first equalized and then the different user's signals are separated by exploiting their different spreading codes. Due to the orthogonality of the subcarrier signals, in a downlink mobile radio communication channel, we can use the Hadamard-Walsh codes as an optimum spreading code set [79], since we do not have to pay attention to the auto-correlation characteristic of the spreading codes.

The receiver structure of the MC-CDMA scheme is shown in Fig.17.3. In this MC-CDMA receiver the received signal is combined, in a sense, in the frequency domain. Therefore the receiver can always make use of all the received signal energy scattered in the frequency domain. This is the main advantage of the MC-CDMA scheme of Fig. 17.1 and

PSfrag replacements

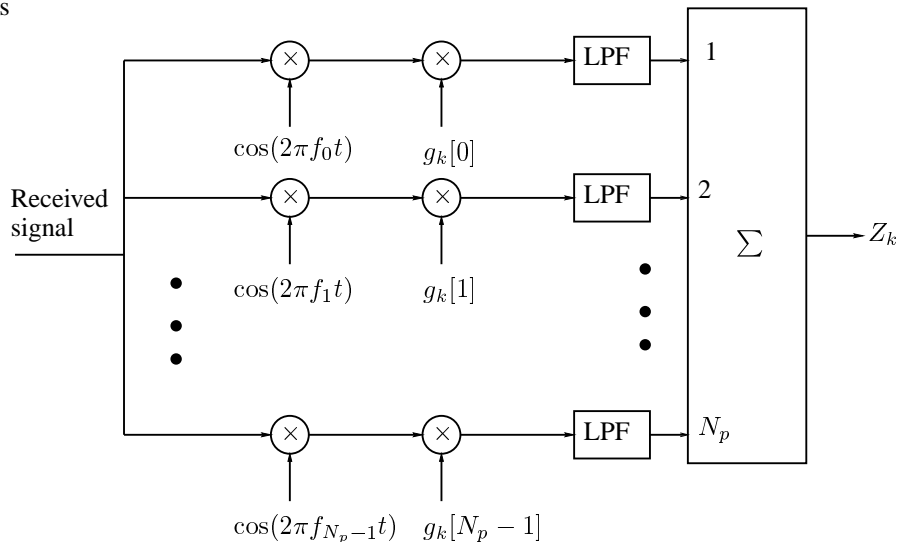


Figure 17.3: The receiver block diagram of frequency-domain spreading assisted MC-CDMA systems.

17.3 over other multicarrier CDMA schemes [79]. However, in a frequency selective fading channel different subcarriers may encounter different amplitude attenuations and phase shifts, which can consequently result in destroying the orthogonality of the subcarriers. There are many combining and detection techniques that can be employed by the MC-CDMA receiver, in order to efficiently exploit the received signal energy [79]. One of the most common approaches is Maximum Ratio Combining (MRC), where the subcarrier signals' weighting factors, $g_k[i]$, $i = 0, 1, \dots, N - 1$ in Fig.17.3, are computed as the complex conjugate of the received subcarrier signal's envelope. This approach can minimize the BER, as long as a single-user system is considered.

Note that the number of subcarriers does not have to be the same, as the processing gain. If the original symbol rate is high, the signal experiences frequency selective fading. Then the input data has to be serial-to-parallel converted, mapping the data to a number of reduced-rate streams before spreading over the frequency domain. This is because it is crucial for MC-CDMA signal transmission to have frequency non-selective fading over each subcarrier [79]. This arrangement has been studied in [435, 440].

17.2.2 Orthogonal Multicarrier DS-CDMA scheme – Type I

In [448, 453] a multicarrier DS-CDMA system has been proposed (we refer to this scheme as multicarrier DS-CDMA-I system), in which a data sequence multiplied by a spreading sequence modulates U subcarriers. The transmitter diagram of the multicarrier DS-CDMA-I system used in [453] is similar to Fig.17.4, except that band-limited subcarrier signals are employed in [453]. Similarly to Fig.17.1, this scheme does not include serial-to-parallel data conversion either. However, each subcarrier signal is direct sequence (DS) spread using a common spreading sequence $c_k(t)$, as shown in Fig.17.4. Therefore, the symbol duration of

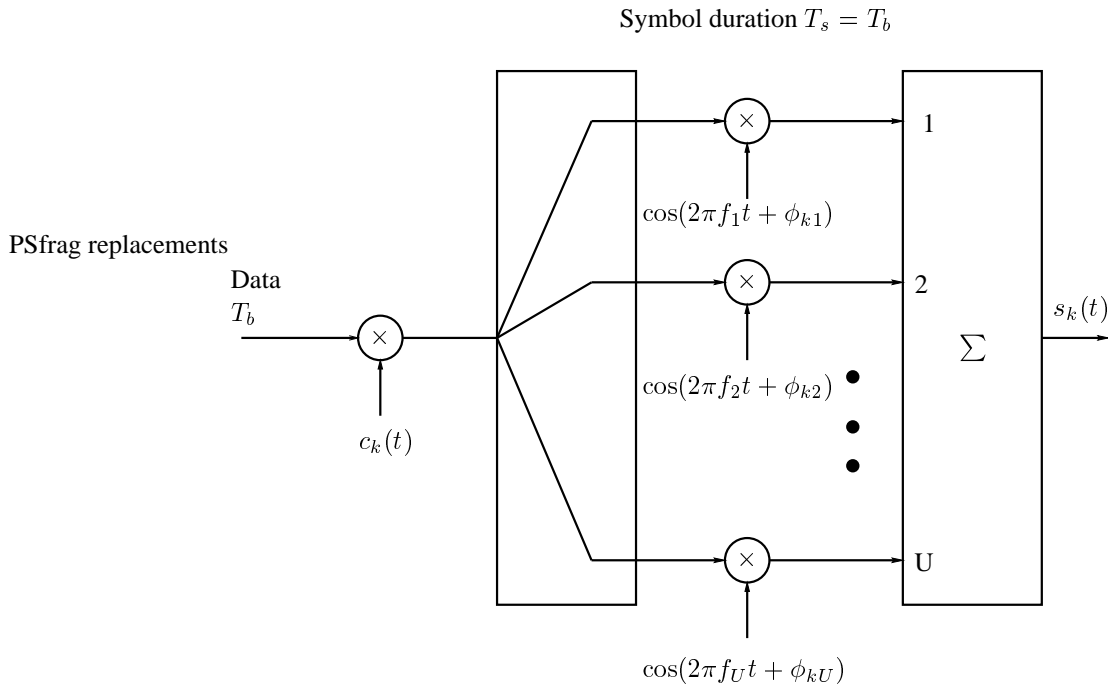


Figure 17.4: The transmitter diagram of the orthogonal multicarrier DS-SS-CDMA-I system.

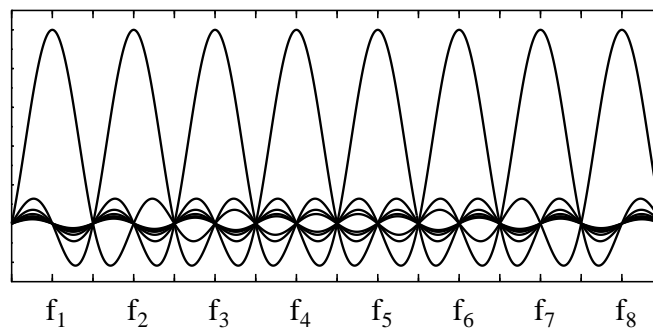


Figure 17.5: Spectrum of time-domain spreading assisted MC-SS-CDMA signals.

the multicarrier DS-CDMA signal is the same, as that of the input data bit duration. With the aid of Fig.17.4, the transmitted signal of user k in the multicarrier DS-CDMA-I system can be expressed as [453]:

$$s_k(t) = \sqrt{\frac{2P}{U}} \sum_{u=1}^U b_k(t) c_k(t) \cos(2\pi f_u t + \phi_{ku}), \quad (17.4)$$

where P is the transmitted power of the multicarrier DS-CDMA-I signal, U is the number of subcarriers, while $b_k(t)$ and $c_k(t)$ are the baseband data sequence and the spreading waveforms, respectively. Finally, f_u for $u = 1, 2, \dots, U$ are the subcarrier frequencies and ϕ_{ku} for $u = 1, 2, \dots, U$ are the initial phases introduced by the subcarrier modulation.

The spectrum of the multicarrier DS-CDMA-I signal without overlap having eight subcarriers is shown in Fig.17.5. In the multicarrier DS-CDMA-I system the subcarrier frequencies are usually chosen to be orthogonal to each other after spreading, which can be formulated as:

$$\int_0^{T_c} \cos(2\pi f_i t + \phi_i) \cdot \cos(2\pi f_j t + \phi_j) dt = 0, \text{ for } i \neq j, \quad (17.5)$$

where T_c is the chip duration. Therefore, the minimum spacing Δ between two adjacent subcarriers satisfies $\Delta = \frac{1}{T_c}$. Fig.17.5 shows the case of $\Delta = \frac{2}{T_c}$. For the case of $\Delta = \frac{2}{T_c}$, there exists no spectral overlap between the spectral main-lobes of two adjacent subcarriers and hence the spectral gain is $SG = 1$. However, if the spacing between adjacent subcarriers is assumed to be $\Delta = \frac{1}{T_c}$, the spectral gain is then given by:

$$SG = \frac{U(2/T_c)}{(U+1)(1/T_c)}, \quad (17.6)$$

that approaches two, when the number of subcarriers is high.

Let us assume that T_{c1} is the chip duration of the spreading code corresponding to a single-carrier DS-CDMA system. The processing gain of a corresponding single-carrier DS-CDMA system – which is defined as the ratio of the system's 'null-to-null' bandwidth to the binary data's 'null-to-null' bandwidth – is assumed to be $N = T_b/T_{c1}$. Hence, for the multicarrier DS-CDMA-I system using $\Delta = \frac{2}{T_c}$, the bandwidth of each subcarrier is a factor of U lower, than that of the corresponding single-carrier DS-CDMA system having identical data rate and identical system bandwidth. Therefore, the chip duration of the spreading code corresponding to the multicarrier DS-CDMA-I system of Fig.17.4 is a factor of U higher, than that of the corresponding single-carrier DS-CDMA system. Consequently, the processing gain of each subcarrier signal is $N_e = T_b/UT_{c1} = N/U$ and the system's processing gain is $N_p = U \cdot N_e = N$, which is the same as that of the corresponding single-carrier DS-CDMA system. For the case of $\Delta = \frac{1}{T_c}$, the chip duration of the spreading code corresponding to the multicarrier DS-CDMA-I system is given by $T_c = (U+1)T_{c1}/2$ and hence, the processing gain of each subcarrier signal is $N_e = T_b/T_c = 2N/(U+1)$. By contrast, the multicarrier DS-CDMA-I system's processing gain is $N_p = U \cdot N_e = 2UN/(U+1)$. The multicarrier DS-CDMA-I system increased the processing gain by about a factor two, if 50% overlap of

PSfrag replacements

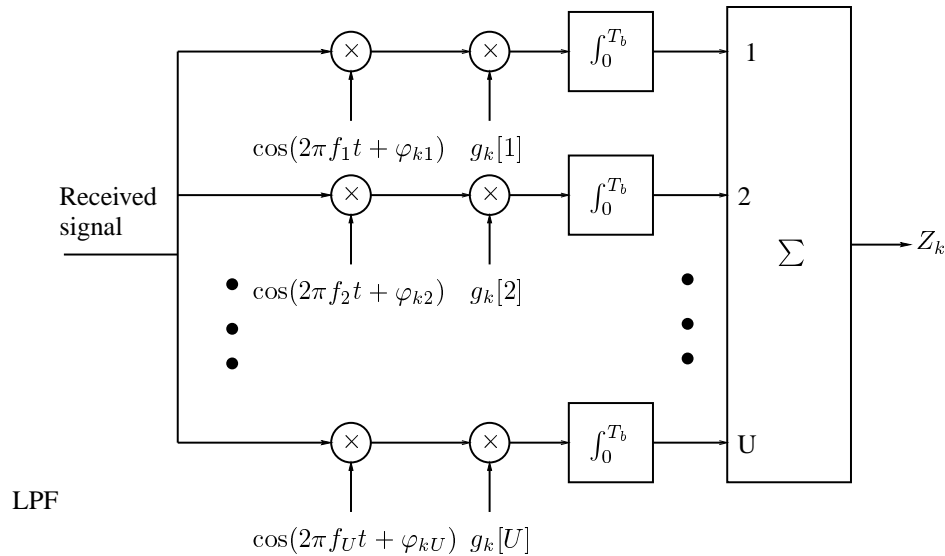


Figure 17.6: The receiver block diagram of the time-domain spreading assisted multicarrier DS-SS-CDMA-I systems.

the main lobes of the adjacent subcarrier spectra in Fig.17.5 is assumed.

The receiver block diagram of the multicarrier DS-SS-CDMA-I system is shown in Fig.17.6. In the multicarrier DS-SS-CDMA-I system frequency diversity is achieved by combining the U correlator's outputs associated with the U subcarriers. The receiver provides a correlator for each of the U subcarriers, and the outputs of the U correlators are combined to yield a processing gain comparable to that of a single-carrier DS system, provided that the spacing between two adjacent subcarriers is $\Delta = \frac{2}{T_c}$. This system has a range of advantages [453]. Firstly, the multicarrier DS-SS-CDMA-I system is robust to multipath fading due to the frequency diversity achieved over the subcarriers. Secondly, the multicarrier DS-SS-CDMA-I system exhibits narrowband interference suppression effect due to the DS spreading. Thirdly, a lower chip rate is required - which has the advantage of reduced-complexity parallel implementation - since, in a multicarrier DS-SS-CDMA-I system having U subcarriers the entire bandwidth of the system is divided into U equi-width frequency bands. Thus each subcarrier frequency is modulated by a spreading sequence having a chip duration, which is U times as long as that of the corresponding single-carrier DS-SS-CDMA system. In other words, a multicarrier system requires a lower speed, parallel-type of signal processing, in contrast to a fast, serial-type of signal processing in a single carrier RAKE [95] receiver. This, in turn, might be helpful for implementing a low power consumption device. Finally, the multicarrier DS-SS-CDMA-I system does not require a contiguous frequency band, hence available spectral gaps can be efficiently exploited.

In [453] the performance of the multicarrier DS-SS-CDMA-I system has been investigated by assuming that each subcarrier signal encounters independent non-frequency selective fading. If the DS spreading code's chip rate is high, the signal is subject to frequency selective fading. Then, RAKE receivers associated with each of the subcarriers can be implemented, in order

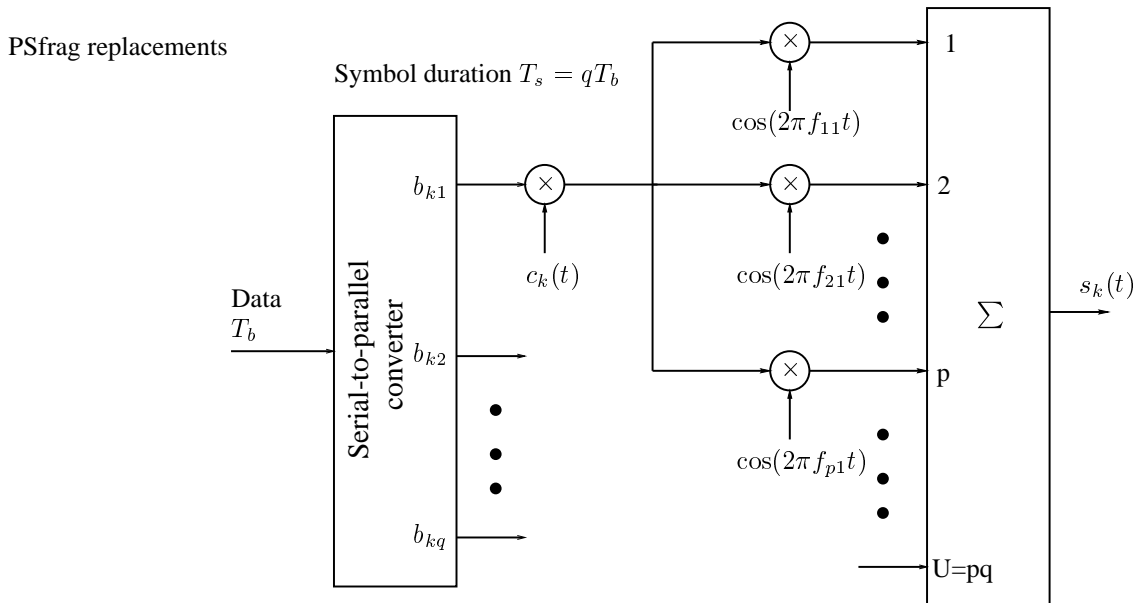


Figure 17.7: The transmitter diagram of the orthogonal multicarrier DS-CDMA-II system.

to combine the energy scattered over different paths. However, if the subcarriers are subject to correlated fading, then, interleaving over time can be employed, in order to guarantee the independence of the subcarrier signals. For example [453], suppose the first U symbols emitted by the source modulate the U subcarriers in the first time interval. In the second time interval, the same U symbols modulate the U subcarriers after a cyclic shift by one symbol. In the i th interval, $1 \leq i \leq U$, the $(i - 1)$ th shifted version of the data modulates the U subcarriers.

17.2.3 Orthogonal Multicarrier DS-CDMA Scheme – Type II

Orthogonal multicarrier DS-CDMA systems – which we refer to here as multicarrier DS-CDMA-II systems – have been studied in [69, 431, 449, 460]. The orthogonal multicarrier DS-CDMA transmitter spreads the serial-to-parallel converted data streams using a given spreading code in the time domain so that the resulting spectrum of each subcarrier can satisfy the orthogonality condition with the minimum frequency separation [69, 449]. This scheme was originally proposed for an uplink communication system, because this characteristic is effective for establishing a quasi-synchronous channel. The transmitter diagram shown in Fig. 17.7 for the multicarrier DS-CDMA-II system is the same as that used in [69], which can be interpreted as the extension of the multicarrier DS-CDMA-I system shown in Fig. 17.4. In this scheme the initial data stream is serial-to-parallel converted to a number of lower-rate streams. Each of these lower-rate streams is spread by the spreading code $c_k(t)$ of Fig. 17.7, feeding a number of parallel streams having the same rate. Each of the latter lower-rate parallel streams is bit-interleaved and these streams modulate the orthogonal subcarriers with

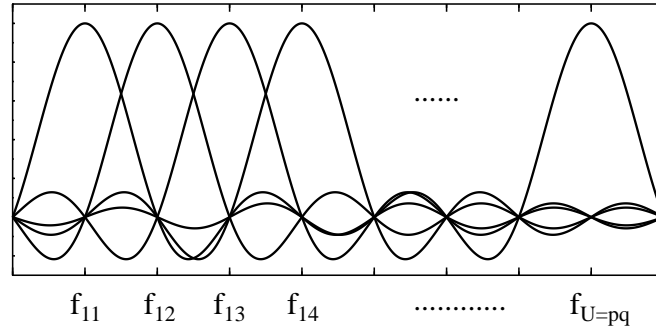


Figure 17.8: Spectrum of the orthogonal multicarrier DS-CDMA signal.

a successively overlapping bandwidth, as shown for example in Fig.17.8.

The spectrum of the multicarrier DS-CDMA-II signal is shown in Fig.17.8. In the multicarrier DS-CDMA-II system subcarrier frequencies are chosen to be orthogonal to each other with the minimum frequency separation. The orthogonality is ensured by Eq.(17.5), but the spacing between two adjacent subcarriers is chosen to be $\Delta = 1/T_c$.

Let $\{f_{11}, f_{12}, \dots, f_{U=pq}\}$ be the subcarrier frequencies, which are arranged according to Fig.17.8. These subcarrier frequencies can be written in the form of a matrix as:

$$\{f_i\} = \begin{pmatrix} f_{11} & f_{12} & \dots & f_{1q} \\ f_{21} & f_{22} & \dots & f_{2q} \\ \vdots & \vdots & \ddots & \vdots \\ f_{p1} & f_{p2} & \dots & f_{pq} \end{pmatrix}. \quad (17.7)$$

Then, according to the transmitter diagram of Fig.17.7, the bit stream having a bit duration of T_b is first serial-to-parallel converted into q parallel streams. The new bit duration on each substream, which is referred to here as the symbol duration, is $T_s = qT_b$. Each substream, b_{ki} , $k = 1, 2, \dots, K$; $i = 1, 2, \dots, q$ feeds p parallel streams and modulates p subcarriers from the same column of Eq.(17.7). It can be shown from Fig.17.8 that these subcarrier frequencies modulated by the same data bit have maximum frequency separation, which ensures the independence of the fading endured by the subcarriers modulated by the same data bit. The transmitted signal of user k is given by:

$$s_k(t) = \sum_{i=1}^q \sum_{j=1}^p \sqrt{\frac{2P}{p}} b_{ki}(t) c_k(t) \cos(2\pi f_{ji}t), \quad (17.8)$$

where P is the transmitted power of each stream, $b_{ki}(t)$ represents the data sequence of the i th stream, while $c_k(t)$ is the common spreading code in Fig.17.7.

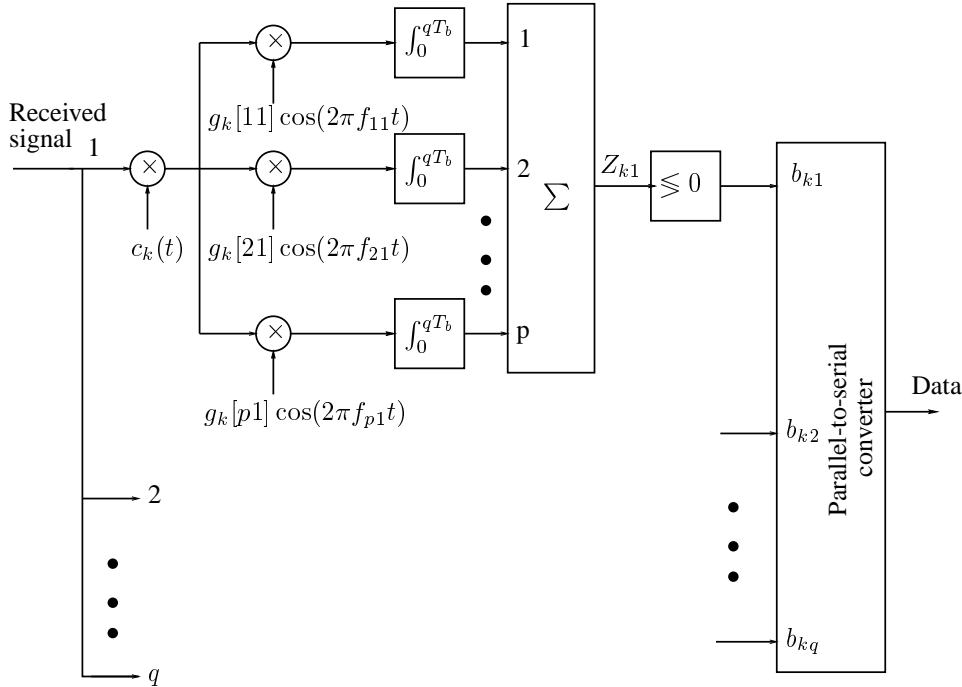


Figure 17.9: The receiver block diagram of the orthogonal multicarrier DS-CDMA systems.

The spectral gain of the multicarrier DS-CDMA-II system is given by:

$$SG = \frac{pq(2/T_c)}{(pq + 1)(1/T_c)} = \frac{2U}{U + 1}, \quad (17.9)$$

which approaches two as $U = pq$ increases. The chip duration of the spreading code $c_k(t)$ employed by the orthogonal multicarrier DS-CDMA system is $T_c = (pq + 1)T_{c1}/2 = (U + 1)T_{c1}/2$, where T_{c1} represents the chip duration of a corresponding single-carrier DS-CDMA scheme ($p = q = 1$). The spreading gain of each subcarrier signal is given by:

$$N_e = qT_b/T_c = \frac{qT_b}{(U + 1)T_{c1}/2} = \frac{2qN}{U + 1}. \quad (17.10)$$

By contrast, the multicarrier DS-CDMA-II system's spreading gain is $N_p = p \cdot N_e = 2UN/(U + 1)$. Thus, the multicarrier DS-CDMA-II system exhibits an increased processing gain, which amounts to approximately a factor of two, as explained by the 50% overlap of the main lobes of the adjacent subcarrier spectra.

The receiver block diagram of the multicarrier DS-CDMA-II system is shown in Fig. 17.9. The receiver provides a correlator for each subcarrier and the correlator outputs associated with the same data bit are combined to form a decision variable. Finally, a parallel-to-serial converter is employed to recover the serial data stream.

PSfrag replacements

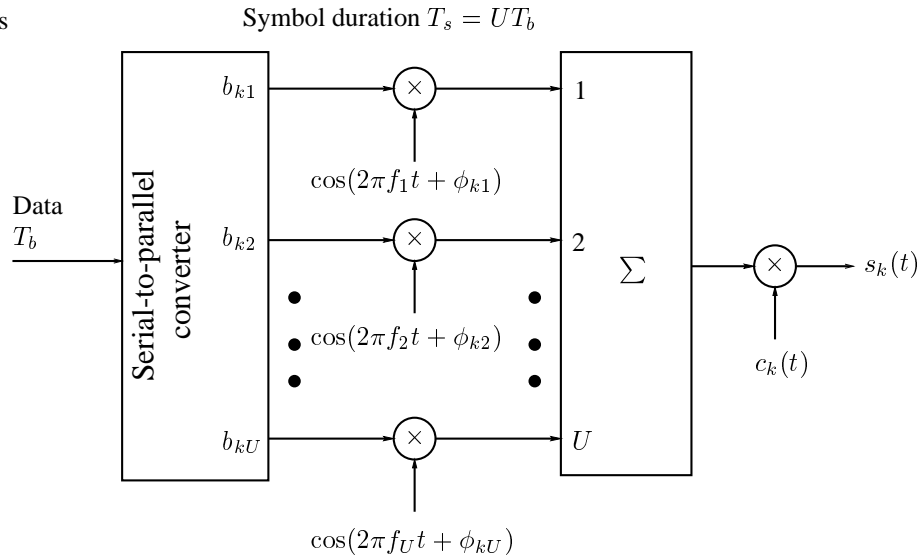


Figure 17.10: The transmitter diagram of the multitone DS-CDMA system.

In the multicarrier DS-CDMA-II system, provided that each subcarrier signal is subject to frequency selective fading, a further RAKE receiver can be employed, in order to match each subcarrier signal and combine the energy scattered by the multipath channel.

The multicarrier DS-CDMA-II scheme can provide the following advantages [69]. Firstly, the spreading processing gain is increased compared to the corresponding single-carrier DS-CDMA scheme. Secondly, the effect of multipath interference is mitigated because of DS spreading. Thirdly, frequency/time diversity can be achieved. Finally, a longer chip duration may lead to more relaxed synchronization schemes. However, a high complexity receiver has to be implemented and forward error control (FEC) techniques must be used, in order to enhance its associated performance.

17.2.4 Multitone DS-CDMA Scheme

Multitone DS-CDMA scheme was proposed by Vandendorpe in [450, 463]. The multitone DS-CDMA transmitter spreads the serial-to-parallel converted data streams using a given spreading code in the time domain, so that the spectrum of each subcarrier prior to the spreading operation can satisfy the orthogonality condition with the minimum frequency separation [463]. Therefore, there exist strong spectral overlap among the different subcarrier signals after DS spreading. The transmitter diagram and the spectrum associated with eight subcarriers for the multitone DS-CDMA signal are shown in Fig.17.10 and Fig.17.11, respectively. At the transmitter side of Fig.17.10, the binary data stream having a bit duration of T_b is serial-to-parallel converted to U parallel substreams. The new bit duration on each subcarrier, which defines the modulated symbol duration is $T_s = UT_b$. The i th substream modulates the subcarrier frequency f_i , $i = 1, 2, \dots, U$. The multitone signal is obtained by the addition of the different subcarriers' signals. Then, spectrum spreading is imposed

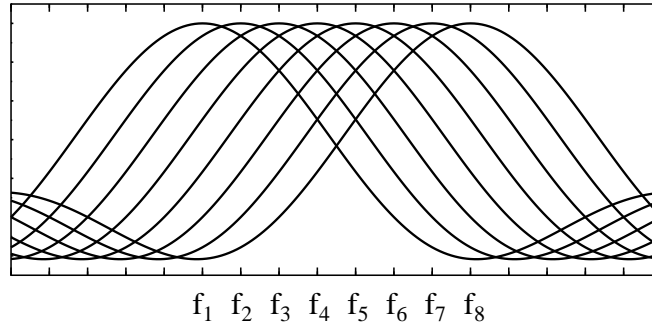


Figure 17.11: Spectrum of the multitone DS-CDMA signal.

on the multitone signal by multiplying it with a spreading code, as shown in Fig.17.10. The transmitted signal of user k can be expressed as:

$$s_k(t) = \sum_{u=1}^U \sqrt{2P} b_{ku}(t) c_k(t) \cos(2\pi f_u t + \phi_{ku}), \quad (17.11)$$

where P represents the transmitted power of each subcarrier, $b_{ku}(t)$ represents the data sequence modulating the u th subcarrier, $c_k(t)$ is the spreading code of user k , while f_u and ϕ_{ku} are the u th subcarrier frequency and modulation phase.

In the multitone DS-CDMA system the subcarrier frequencies are chosen to be orthogonal to each other with the minimum frequency separation before spreading, which can be formulated as:

$$\int_0^{T_s} \cos(2\pi f_i t + \phi_i) \cdot \cos(2\pi f_j t + \phi_j) dt = 0, \text{ for } i \neq j. \quad (17.12)$$

It can be shown that the minimum spacing of the subcarrier frequencies is $1/T_s = 1/UT_b$. Let T_{c1} represent the chip duration of the corresponding single-carrier DS-CDMA system. Referring to Fig.17.11, it can be shown that the chip duration of the spreading code for the multitone DS-CDMA system is given by:

$$T_c = \frac{2UN}{2UN - U + 1} T_{c1}, \quad (17.13)$$

where N is the spreading gain corresponding to a single-carrier DS-CDMA system. Observe that T_c approaches T_{c1} as N increases. The spreading gain of the subcarrier signal is given

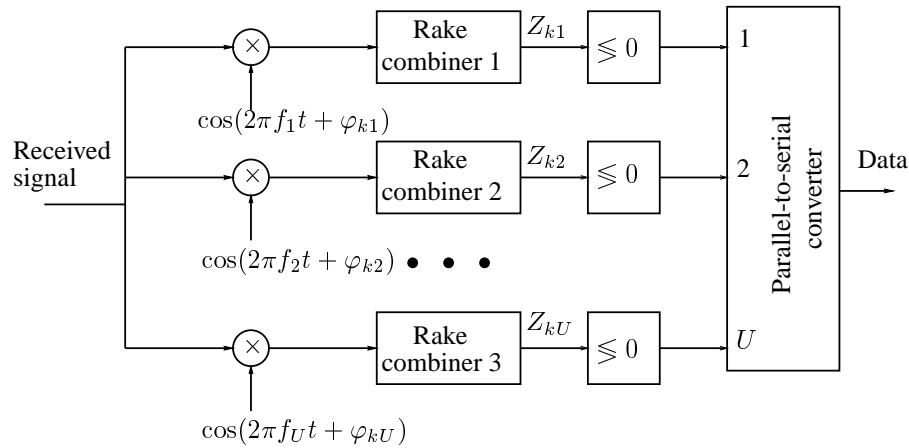


Figure 17.12: The receiver block diagram of the multitone DS-CDMA system.

by:

$$\begin{aligned}
 N_e &= T_s/T_c \\
 &= UT_b / \frac{2UN}{2UN - U + 1} T_{c1} \\
 &= \frac{2UN - U + 1}{2},
 \end{aligned} \tag{17.14}$$

which can be approximated by UN , when N is sufficiently high. Since different data bits are transmitted on different subcarriers, the overall system's processing gain is also given by Eq.(17.14).

The spectral gain of the multitone DS-CDMA system is given by:

$$\begin{aligned}
 SG &= \frac{U(2/T_c)}{2/T_c + (U - 1)/T_s} \\
 &= \frac{2N_e U}{2N_e + U - 1},
 \end{aligned} \tag{17.15}$$

that approaches U , when N_e is sufficiently high, which is the highest SG among the multi-carrier schemes considered.

The receiver block diagram of the multitone DS-CDMA system is shown in Fig.17.12. The receiver is composed of U RAKE combiners, each of which has the same structure as the single-carrier DS-CDMA RAKE receiver. This is an optimum receiver for an AWGN channel [463]. Unfortunately, the multitone DS-CDMA scheme suffers from inter-subcarrier interference and requires a high-complexity RAKE based receiver. However, the capability to use longer spreading codes results in the reduction of self-interference and multiple access interference, as compared to the spreading codes assigned to a corresponding single-carrier DS-CDMA scheme. The multitone DS-CDMA scheme uses longer spreading codes than

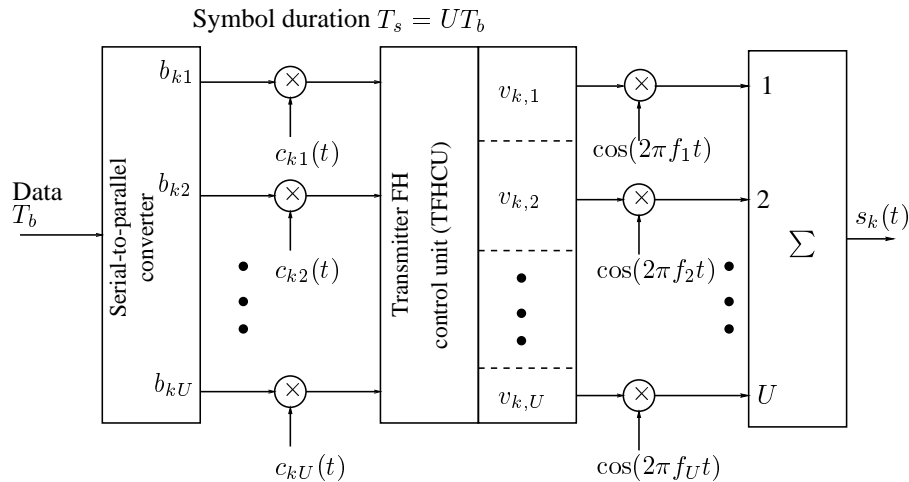


Figure 17.13: The transmitter schematic of the adaptive frequency-hopping assisted multicarrier DS-SS-CDMA system.

the corresponding single-carrier DS-SS-CDMA scheme [79], where the relative code-length extension is in proportion to the number of subcarriers. Therefore, the multitone DS-SS-CDMA system can accommodate more users.

We have reviewed the family of various multicarrier-based CDMA schemes such as MC-SS-CDMA, multicarrier DS-SS-CDMA-I, multicarrier DS-SS-CDMA-II and multitone DS-SS-CDMA in the previous four subsections. A common property of these multicarrier-based schemes is that all the subcarriers in the system are activated for each transmission. By contrast, in the following three subsections, multicarrier-based CDMA schemes are reviewed, where each transmission only exploits a fraction of the subcarriers provided by the system. In these schemes frequency-hopping techniques are employed, in order to efficiently utilize the system bandwidth available. Hence, these schemes are referred to as frequency-hopping multicarrier DS-SS-CDMA (FH/MC DS-SS-CDMA) schemes.

17.2.5 Adaptive Frequency-Hopping Assisted multicarrier DS-SS-CDMA scheme

Multicarrier DS-SS-CDMA systems using adaptive frequency-hopping (AFH/MC DS-SS-CDMA) was proposed by Chen, *et. al* [461] for uplink (mobile-to-base) transmissions. This scheme bears close resemblance to the orthogonal multicarrier DS-SS-CDMA-I or multicarrier DS-SS-CDMA-II scheme of figures 17.4 and 17.7, respectively. In the AFH/MC DS-SS-CDMA scheme the total system bandwidth is divided into U equi-width subchannels, and the serial data stream of each user is serial-to-parallel converted to U parallel substreams, where each substream is transmitted as a narrow-band DS signal over one of the subchannels. In contrast to the transmission schemes in [69, 453], where each subcarrier was used to carry part of the transmitted information, in the AFH/MC DS-SS-CDMA system data substreams can be transmitted on any of the subcarriers, depending on the severity of the fading in a subchannel.

However, in the above transmission scheme it is possible for more than one data substreams belonging to the same user to be modulated on to the same subcarrier. Hence, U number of spreading codes have to be assigned to each user, so that every data substream can be uniquely identified. The number of spreading codes required for a system supporting K users is given by KU .

The transmitter diagram of the AFH/MC DS-CDMA system using adaptive frequency-hopping is shown in Fig.17.13. The spectrum of the transmitted signal in the AFH/MC DS-CDMA system is similar to that seen in Fig.17.5 ($\Delta = 2/T_c$) or Fig.17.8 ($\Delta = 1/T_c$). Hence, the spectral gain, the spreading gain of each subcarrier signal as well as the spreading gain of the overall system are the same as that of the orthogonal multicarrier DS-CDMA-I or multicarrier DS-CDMA-II scheme. At the transmitter side the binary data stream is first converted to U parallel substreams $D_k(t) = \{b_{k1}(t), b_{k2}(t), \dots, b_{kU}(t)\}$. These substreams are then spread by the corresponding spreading codes $C_k(t) = \{c_{k1}(t), c_{k2}(t), \dots, c_{kU}(t)\}$. Let $F_k = \{f_{k1}(t), f_{k2}(t), \dots, f_{kU}(t)\}$ – where $f_{k1}(t) \leq f_{k2}(t) \leq \dots \leq f_{kU}(t)$ – be a set of subcarrier frequencies, which can be activated by the transmitter's FH control unit (TFHCU) in Fig.17.13 based on the subchannel states $V_k = \{v_{k,1}, v_{k,2}, \dots, v_{k,U}\}$ fed back from the base station receiver. Finally, after modulating each subcarrier by a spread substream according to the activated frequency set, the transmitted signal can be expressed as:

$$s_k(t) = \sum_{u=1}^U \sqrt{2P} b_{ku}(t) c_{ku}(t) \cos(2\pi f_{ku}t), \quad (17.16)$$

where P is the transmitted power per substream.

The receiver's block diagram for the AFH/MC DS-CDMA system is shown in Fig.17.14. The receiver is constituted by a conventional correlator detector. The receiver's 'channel quality estimator' of Fig.17.14 estimates the subchannel fading parameters periodically and passes the estimates to the receiver's FH control unit (RFHCU). Based on the subchannel parameters, the RFHCU generates a $K \times U$ matrix F given by [461]:

$$\mathbf{V} = \begin{pmatrix} v_{1,1} & v_{1,2} & \dots & v_{1,U} \\ v_{2,1} & v_{2,2} & \dots & v_{2,U} \\ \vdots & \vdots & \ddots & \vdots \\ v_{K,1} & v_{K,2} & \dots & v_{K,U} \end{pmatrix}, \quad (17.17)$$

where $v_{k,u} \in [0, U]$ denotes the number of substreams hopping to the u th subcarrier of the k th user. Hence, the sum of each row of the matrix \mathbf{V} is U . The k th row of \mathbf{V} is sent to the TFHCU of user k through a feedback control channel [461], in order to control the following activated subcarriers. At the same time these parameters are also used for recovering the order of the transmitted substreams, in order to complete the despreading process, as shown in Fig.17.14.

The success of the AFH/MC DS-CDMA scheme using adaptive frequency-hopping depends on the availability of a reliable channel quality estimator on providing reasonably accurate and timely estimation of the channel, on the availability of a reliable feedback control channel and on the generation of optimal frequency-hopping patterns. In [461] the water-filling algorithm has been proposed for deriving the optimal frequency hopping patterns. The

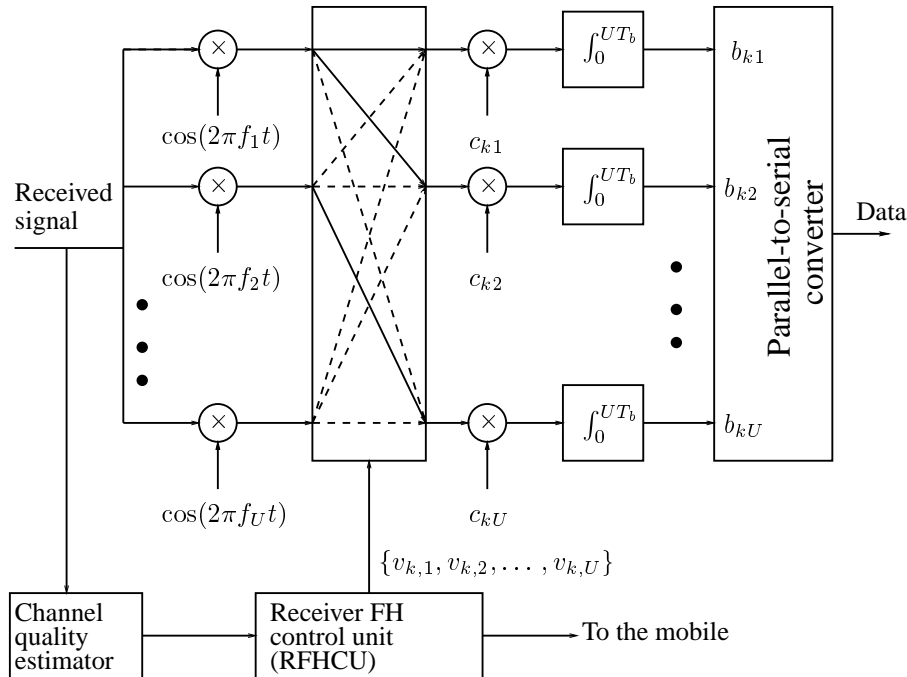


Figure 17.14: The receiver block diagram of the FH/MC DS-CDMA system using adaptive frequency-hopping.

AFH/MC DS-CDMA scheme outperforms the conventional corresponding single-carrier DS-CDMA systems using a RAKE receiver in terms of its average bit error rate (BER). However, the AFH/MC DS-CDMA scheme can only operate in a channel exhibiting slow variations versus time. Furthermore, it needs a channel quality estimator and a complex algorithm for deriving the optimal frequency-hopping patterns.

17.2.6 Adaptive Subchannel Allocation Assisted Multicarrier DS-CDMA

In contrast to the AFH/MC DS-CDMA scheme of reference [461], which was proposed for the uplink (mobile-to-base), the multicarrier DS-CDMA scheme using adaptive subchannel allocation, which is referred to here as adaptive AMC DS-CDMA, was suggested for employment in the downlink (base-to-mobile) transmission [439]. The adaptive AMC DS-CDMA scheme is based on the multicarrier DS-CDMA-I scheme of Fig.17.4 proposed in [453], where a data sequence spread by a narrowband signature sequence modulates U subcarriers. In the adaptive AMC DS-CDMA scheme of Fig.17.15, instead of transmitting the same DS waveforms over all subchannels according to Fig.17.4, each user's DS waveform is transmitted over a specific favorite subchannel for the user. This favorite subchannel is determined as follows [439]. The mobile estimates the fading amplitudes of all subchannels by exploit-

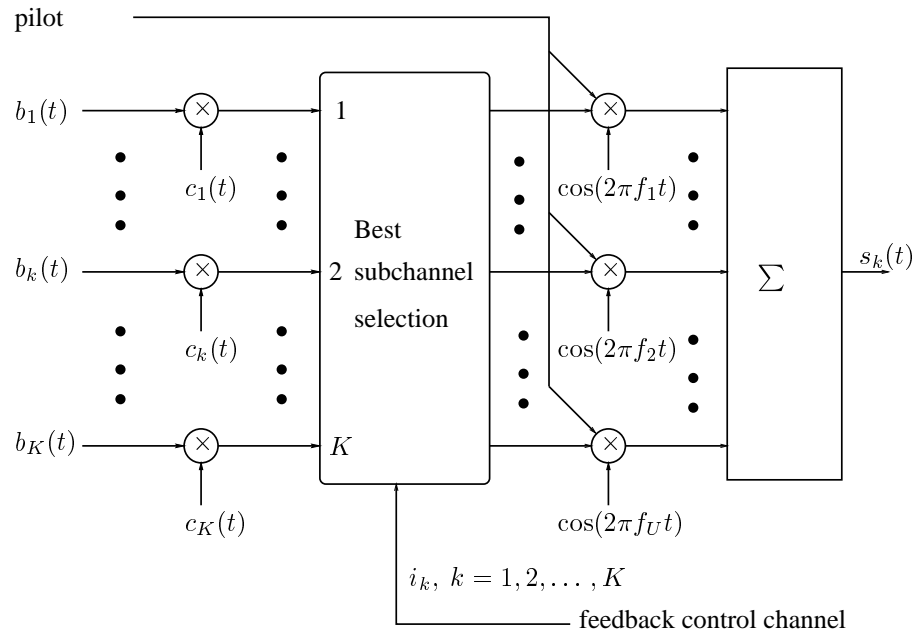


Figure 17.15: The down link transmitter's schematic for the multicarrier DS-CDMA system using adaptive subchannel allocation.

ing its received pilot signal and feeds back the index of the subchannel exhibiting the highest amplitude to the base station. With the aid of this index information, the base station allocates each user's DS waveform to the best subchannel for the user considered. This allocation scheme is optimum, provided that orthogonal spreading codes are employed.

The down link schematic of the adaptive AMC DS-CDMA system supporting K users is shown in Fig.17.15. The system model proposed in [439] is based on the multicarrier DS-CDMA scheme proposed in [453], where the total bandwidth of the system was divided into U equi-width subchannels. At the transmitter of the base station, first the favorite subchannel is selected for each user according to the channel state, and a narrowband DS waveform is transmitted through the favorite subchannel. As shown in Fig.17.15, at the base station the binary data waveform $b_k(t)$ of the k th user is first spread by the user's spreading code waveform $c_k(t)$, yielding $b_k(t)c_k(t)$. Then, the 'best subchannel selection' unit of Fig.17.15 chooses the best subchannel index denoted as i_k for the k th user, $k = 1, 2, \dots, K$. The subcarrier of the best subchannel is then modulated by $b_k(t)c_k(t)$. Finally, the K number of user signals as well as the down link pilot signal – which modulates all subcarriers – are multiplexed for transmission to the mobile receivers. The base station's transmitted signal

can be written as:

$$s_k(t) = \sum_{k=1}^K \sqrt{2P} b_k(t) c_k(t) \sum_{u=1}^U \Delta_u(i_k) \cos(2\pi f_u t) + \sum_{u=1}^U \sqrt{2P_0} c_0(t) \cos(2\pi f_u t), \quad (17.18)$$

where P represents the transmitted power of each user, P_0 denotes the identical transmitted power of the pilot signal on each subcarrier, $b_k(t)$ is the data waveform of the k th user, while $c_k(t)$ is the spreading code waveform of the k th user. Furthermore, $c_0(t)$ represents the spreading code waveform of the pilot signal. In Eq.(17.18),

$$\Delta_u(i_k) = \begin{cases} 1, & \text{for } u = i_k \\ 0, & \text{for } u \neq i_k \end{cases} \quad (17.19)$$

indicates the subcarrier activation function.

The spectrum of the adaptive AMC DS-CDMA signal using rectangular chip waveforms is the same as that of the orthogonal multicarrier DS-CDMA-I, which is shown in Fig.17.5. The spectral gain and the spreading gain corresponding to a subcarrier are the same as that of the orthogonal multicarrier DS-CDMA-I scheme using the minimum spacing of $\Delta = 2/T_c$, i.e., we have $SG = 1$ and $N_e = N/U$, respectively. The overall system's spreading gain is also N .

The receiver schematic of the multicarrier DS-CDMA mobile receiver using adaptive subchannel allocation is shown in Fig.17.16, where both the coherent demodulation phases with respect to the i th subcarrier and the despreading code are incorporated in the term $g_0[i]$, $i = 1, 2, \dots, U$ corresponding to the pilot detection. By contrast, $g_k[i_k]$ corresponds to the k th user's detection. At the mobile's receiver, the index of the best subchannel is determined by estimating the received amplitudes of the subchannels based on the mobile's received pilot signal. As shown in Fig.17.16, the received signal is first coherently demodulated using each subcarrier and then correlated with the despreading code of the pilot signal, in order to obtain the decision variables characterizing the fading amplitude. The best subchannel estimation block estimates the fading amplitudes of all the subchannels using the outputs of the pilot correlators. The index of the best subchannel corresponding to the subchannel having highest amplitude is determined, which is denoted as i_k in Fig.17.16. This favorite subchannel index information on the one hand is sent to the base station by using a feedback control channel and also preserved in the mobile over the subchannel quality update period, in order to provide the subchannel index for the k th user's data demodulation. According to the index i_k , the i_k th subchannel of user k is selected and correlated with the k th user's despreading code $c_k(t)$ – which is included in the term of $g_k[i_k]$ in Fig.17.16 – in order to form the decision variable for the transmitted data.

In [439] the performance of the adaptive AMC DS-CDMA system was studied over slow Rayleigh fading channels. It was shown that the adaptive AMC DS-CDMA scheme outperforms the multicarrier DS-CDMA scheme proposed in [453], when both orthogonal PN spreading codes and random spreading codes were considered. Since a common pilot signal

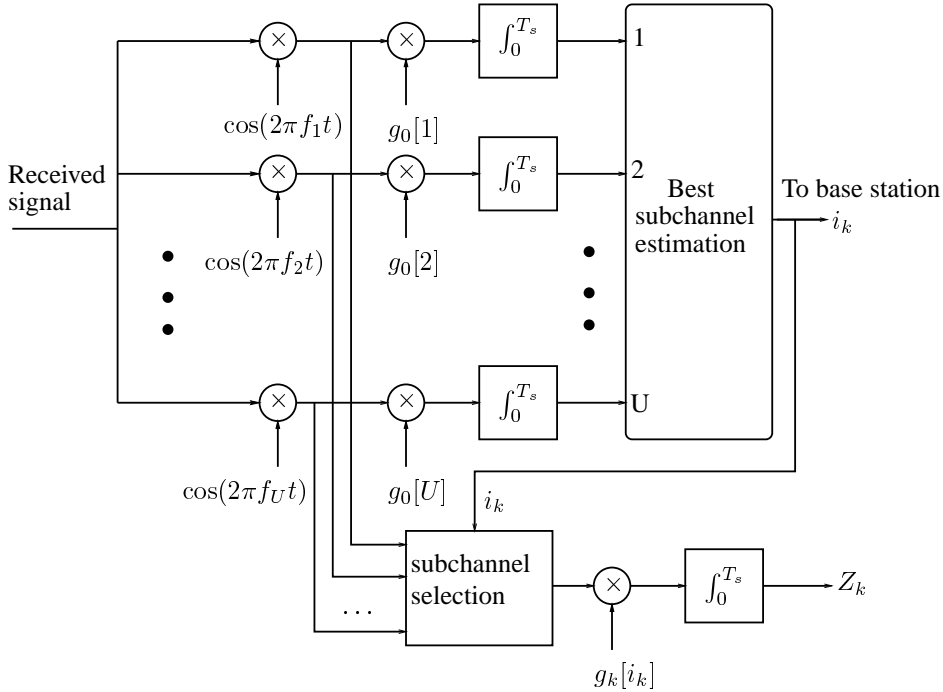


Figure 17.16: The mobile’s receiver schematic for the multicarrier DS-CDMA system using adaptive subchannel allocation.

is transmitted to all users in the down link, the complexity associated with the pilot signal’s transmission is low. However, a reliable, low-delay feedback control channel has to be assigned to each user, in order to send the index of the best subchannel provided by the mobile station’s receiver to the base station, in order to control the subcarrier activation.

The adaptive AMC DS-CDMA scheme can also be extended to allocate a number of subchannels instead of one for data transmission, in order to support variable-rate or multi-rate services.

17.2.7 Slow Frequency-Hopping Multicarrier DS-CDMA

The slow FH multicarrier DS-CDMA (SFH/MC DS-CDMA) scheme using constant-weight codes based FH patterns has been proposed in [70, 78, 425]. This scheme can efficiently amalgamate the techniques of slow FH, OFDM and DS-CDMA. In SFH/MC DS-CDMA nonlinear constant-weight codes have been introduced, in order to control the associated FH patterns and hence to activate a number of subcarriers, in order to support multi-rate services. At the same time, a set of constant-weight codes satisfying the required minimum distance conditions is employed, in order to assist in the determination and initial synchronization of the FH patterns employed.

The model of the transmitter and the multiple access channel used in the analysis of SFH/MC DS-CDMA is depicted in Fig. 17.17. Each of the K users in the system is assigned

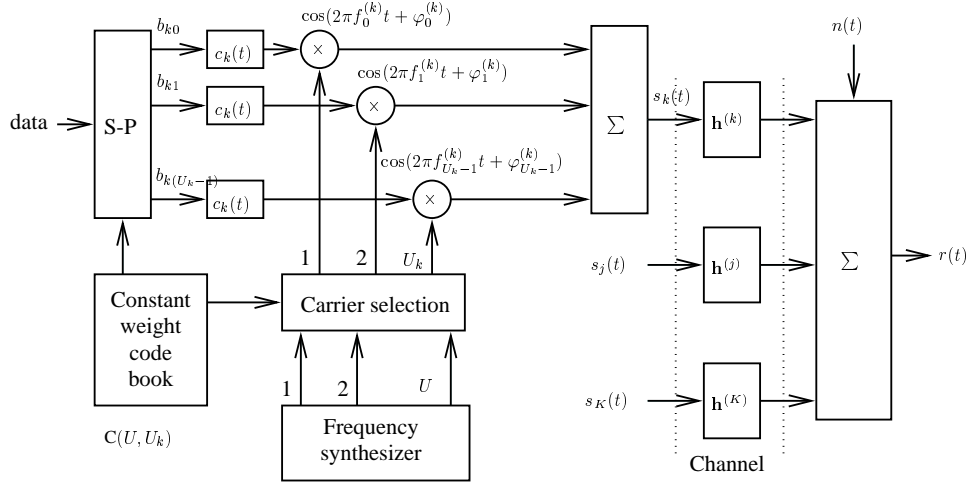


Figure 17.17: Transmitter and channel block diagram of the frequency-hopping multicarrier DS-CDMA system.

a randomly generated spreading code, which produce spread signals. In the figure, $C(U, U_k)$ represents a constant-weight code (CWC) of user k with U_k number of '1's and $(U - U_k)$ number of '0's assigned. Hence, the weight of $C(U, U_k)$ is U_k . This code is read from a so-called CWC book, which represents the frequency-hopping patterns. Theoretically, the size of the CWC book is $\binom{U}{U_k} = U! / U_k!(U - U_k)!$. The CWC $C(U, U_k)$ plays two different roles. Its first role is that its weight - namely U_k - determines the number of activated subcarriers involved, while its second function is that the positions of the U_k number of binary '1's determines the selection of a set of U_k number of activated subcarrier frequencies from the U number of outputs of the frequency synthesizer.

At the transmitter of the k th user in Fig. 17.17 the bit stream having a bit duration of T_b is first serial-to-parallel (S-P) converted, yielding U_k parallel streams, which is controlled by the CWC $C(U, U_k)$. The symbol duration, T_s , of the SFH/MC DS-CDMA signal is $T_s = U_k T_b$. Multi-rate transmission can be supported by controlling the weight of the code $C(U, U_k)$. As seen in Fig. 17.17, after serial-to-parallel conversion each stream is DS spread, in order to form the spread signal and this spread signal then modulates one of the selected subcarriers. Finally, the transmitted signal of the k th user can be expressed as:

$$s_k(t) = \sum_{u=0}^{U_k-1} \sqrt{2P} b_{ku}(t) c_k(t) \cos \left(2\pi f_u^{(k)} t + \varphi_u^{(k)} \right), \quad (17.20)$$

where P represents the transmitted power per carrier, while U_k indicates the weight of the CWC currently employed by the k th user. Furthermore, $b_{ku}(t)$ represents the current data stream's waveforms, $c_k(t)$ denotes the k th user's DS spreading waveforms, while $\{f_u^{(k)}\}$ and $\{\varphi_u^{(k)}\}$ represent the current subcarrier frequency set and modulation phase set, respectively.

The spectrum of the SFH/MC DS-CDMA signal is similar to that of the orthogonal

multicarrier DS-CDMA-I system of Fig.17.5 or orthogonal multicarrier DS-CDMA-II of Fig.17.8, depending on the spacing, Δ , between two adjacent subcarriers, which may assume $\Delta = 2/T_c$ or $\Delta = 1/T_c$, respectively.

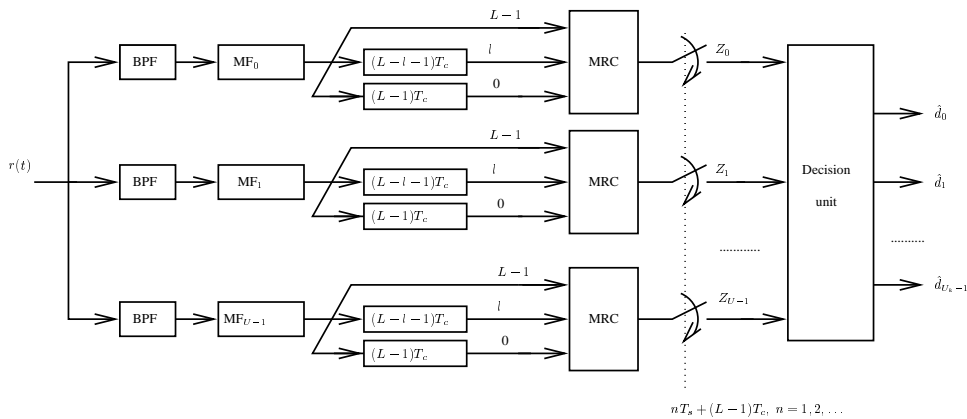


Figure 17.18: Receiver block diagram of the frequency-hopping multicarrier DS-CDMA system.

The conventional matched filter based RAKE receiver using MRC can be invoked for its detection, as shown in Fig. 17.18, where we assume that L number of diversity paths is available. In contrast to the transmitter side, where only U_k out of U activated subcarriers are transmitted by user k , at the receiver all U subcarriers are always tentatively demodulated. The information bits transmitted over the different subcarriers are detected in the decision block of Fig. 17.18. Specifically, if the receiver has the explicit knowledge of the FH patterns, the information bits conveyed by different subcarriers can be detected, as in conventional FH systems [425]. However, if no explicit *a-priori* knowledge of the FH patterns is available, the information bits can be blindly detected with the aid of the CWC codes [70]. Blind joint soft-detection based on maximum-likelihood sequence detection (MLSD) has been proposed and studied in [70] over multipath Nakagami- m fading channels. It was shown that the proposed blind joint soft-detection techniques were capable of detecting the transmitted information and simultaneously acquiring the FH patterns without explicit signalling.

In SFH/MC DS-CDMA systems the entire bandwidth of future wireless communication systems can be divided into a number of sub-bands and each sub-band can be assigned a subcarrier. According to the prevalent service requirements, the set of legitimate subcarriers can be allocated in line with the instantaneous information rate requirements. A range of FH techniques can be employed for each user, in order to occupy the whole system bandwidth and to efficiently utilize the system's frequency resources. Specifically, slow FH, fast FH or adaptive FH techniques can be introduced, in order to further improve the system's performance. In SFH/MC DS-CDMA systems the sub-bands are not required to be of equal bandwidth. Hence existing 2nd- and 3rd-generation CDMA systems can be supported using one or more subcarriers, consequently simplifying the frequency resource management and efficiently utilizing the entire bandwidth available. This regime can also remove the spectrum segmentation of existing 'legacy' systems of the past, while ensuring compatibility with future Broadband Access Networks (BRAN) and un-licensed systems. Furthermore, a number of sub-channels associated with variable processing gains can be employed, in order to

support various services requiring low- to very high-rate transmissions, for example for wireless Internet access. However, in SFH/MC DS-CDMA systems the CWC based FH patterns must be produced in the transmitter and acquired in the receiver. Furthermore, SFH/MC DS-CDMA systems benefit from using RAKE receivers in order to achieve diversity. Hence, SFH/MC DS-CDMA systems have a relatively complex transmitter and receiver.

17.2.8 Summary

In this section we have briefly outlined the features of a number of multicarrier CDMA systems, which have been studied in the literature. The advantages and disadvantages of these multicarrier CDMA schemes have been summarized. It can be shown that there are trade-offs associated with each multicarrier CDMA scheme considered. In the following sections we will focus our attention on the BER performance analysis of these schemes over frequency selective Rayleigh fading channels.

17.3 Channel Model

The channel model considered in this chapter is a frequency selective channel, where the transmitted signal is received over L independent slowly-varying flat fading channels, as shown in Fig.16.8. The complex lowpass equivalent representation of the impulse response experienced by subcarrier u of user k is given by:

$$h_{ku}(t) = \sum_{l=1}^L \alpha_{ul}^{(k)} \delta(t - \tau_{kl}) \exp(j\psi_{ul}^{(k)}), \quad (17.21)$$

where l is the index of the channel impulse response (CIR) taps, $\delta(\cdot)$ is the Dirac function, $\{\alpha_{ul}^{(k)}\}_{l=1}^L$, $\{\psi_{ul}^{(k)}\}_{l=1}^L$ and $\{\tau_{kl}\}_{l=1}^L$ are the random CIR tap amplitudes, phases and delays, respectively. However, we assume that all subcarrier signals of the same user encounter the same delay, i.e., τ_{kl} is independent of u . Note that, if $L = 1$, these terms will be represented by $\{\alpha_u^{(k)}\}$, $\{\psi_u^{(k)}\}$ and $\{\tau_{kl}\}$, respectively. We assume that $\{\alpha_{ul}^{(k)}\}_{l=1}^L$, $\{\psi_{ul}^{(k)}\}_{l=1}^L$ and $\{\tau_{kl}\}_{l=1}^L$ are mutually independent. Without loss of generality, we also assume that $\tau_{k1} < \tau_{k2} < \dots < \tau_{kL}$.

If we let $\tau_{kl} = (l - 1)T_c + \tau_k$, then Eq.(17.21) can be expressed as:

$$h_{ku}(t) = \sum_{l=1}^L \alpha_{ul}^{(k)} \delta(t - (l - 1)T_c - \tau_k) \exp(j\psi_{ul}^{(k)}), \quad (17.22)$$

which represents the widely used tap-delay line mode of the frequency-selective channel [95].

For a multipath Rayleigh fading channel the fading amplitudes $\{\alpha_{ul}^{(k)}\}_{l=1}^L$ are assumed to be statistically independent random variables having a probability density function (PDF)

expressed as [95]:

$$\begin{aligned} f(\alpha_{ul}^{(k)}) &= M(\alpha_{ul}^{(k)}, \Omega), \\ M(R, \Omega) &= \frac{2R}{\Omega} \exp\left(-\frac{R^2}{\Omega}\right), \end{aligned} \quad (17.23)$$

where $\Omega = E \left[\left(\alpha_{ul}^{(k)} \right)^2 \right]$. We assume that $\sum_{l=1}^L \left\{ E \left[\left(\alpha_{ul}^{(k)} \right)^2 \right] \right\} = 1$, hence, we have $\Omega = 1/L$. The phases $\left\{ \psi_{ul}^{(k)} \right\}_{l=1}^L$ of the different paths and of different subcarriers are assumed to be uniformly distributed random variables in $[0, 2\pi)$, while the path delays of $\left\{ \tau_{kl} \right\}_{l=1}^L$ of user k are uniformly distributed in $[0, T_s)$.

17.4 Performance of multicarrier CDMA Systems Using Frequency-Domain Spreading

In the subsection of 17.2.1 the features of the MC-CDMA scheme using frequency-domain spreading was summarized. As shown in Fig.17.1, in this MC-CDMA scheme the transmitter spreads the original signal using a given spreading code in the frequency domain. In other words, a fraction of the symbol corresponding to a chip of the spreading code is transmitted through a different subcarrier. For efficient multicarrier transmission it is crucial to have frequency non-selective fading over each subcarrier [79]. Therefore, if the original symbol rate is high, resulting in frequency selective fading, then serial-to-parallel conversion of the original data stream to a number of reduced-rate substreams may be needed, in order to increase the chip duration and hence to avoid frequency selective fading.

In this section we derive the BER for the MC-CDMA system seen in Fig.17.19 employing serial-to-parallel conversion. Specifically, we derive the BER expressions for the asynchronous MC-CDMA system [440] over frequency selective Rayleigh fading channels. The expressions derived in this section are suitable for the analysis of uplink transmissions. Let us first consider the system model.

17.4.1 System Description

17.4.1.1 The Transmitter

The transmitter schematic of the MC-CDMA system using frequency-domain spreading, which is based on Fig.17.1 but additional involves serial-to-parallel data conversion is shown in Fig.17.19. The MC-CDMA system transmits N_p chips of a data symbol in parallel on N_p different subcarriers, one chip per subcarrier, where N_p is the total number of chips per data bit or the processing gain. Hence, the chip duration is the same as the symbol duration of the transmitted MC-CDMA signal, i.e., T_s , which is given by $T_s = qT_b$, since q bits are transmitted in a symbol duration. Throughout our discussions we assume that random spreading

PSfrag replacements

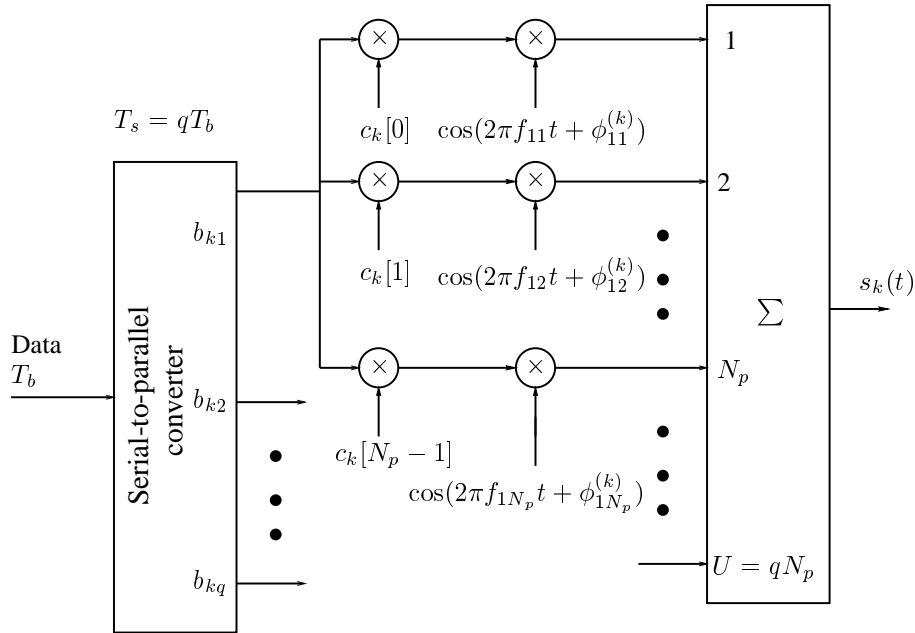


Figure 17.19: The transmitter schematic of the MC-CDMA system using frequency-domain spreading and serial-to-parallel data conversion.

codes are employed and the frequency separation between two adjacent subcarriers is $1/T_s$. Hence, the subcarriers are orthogonal over chip duration T_s . Let

$$\{f_{ij}\} = \begin{pmatrix} f_{11} & f_{12} & \cdots & f_{1N_p} \\ f_{21} & f_{22} & \cdots & f_{2N_p} \\ \vdots & \vdots & \ddots & \vdots \\ f_{q1} & f_{q2} & \cdots & f_{qN_p} \end{pmatrix} \quad (17.24)$$

be the subcarrier frequency set, which are arranged according to:

$$f_{ij} = f_0 + \frac{1}{T_s} [(i-1) + (j-1)q]. \quad (17.25)$$

Hence, according to Eq.(17.25) each column represents q number of adjacent subcarriers, while the minimum spacing between two subcarriers from the same row is q/T_s . In Fig.17.19 after the serial-to-parallel conversion stage, q data bits of user k are spread by the spreading code of user k in the frequency domain. Note that the data bits mapped to different substreams use the same spreading code. The spread signal then modulates the subcarriers mapping each chip to a subcarrier. The subcarrier frequencies modulated by the same data bit are from the same row of the matrix in Eq.(17.25), and these subcarriers are sufficiently separated in frequency to avoid correlated fading. Consequently, referring to Fig.17.19 the transmitted

signal can be expressed as:

$$s_k(t) = \sum_{n=-\infty}^{\infty} \sum_{i=1}^q \sum_{j=1}^{N_p} \sqrt{\frac{2P}{N_p}} b_{ki}[n] c_k[j-1] P_{T_s}(t - nT_s) \cos\left(2\pi f_{ij}t + \phi_{ij}^{(k)}\right), \quad (17.26)$$

where $b_{ki}[n]$ represents the i th data substream of user k and $b_{ki}[n]$ is assumed to be a random variable, assuming values of +1 or -1 with equal probability. Furthermore, $c_k[j]$ is the j th chip of the spreading code $\{c_k[1] c_k[2] \dots c_k[N_p - 1]\}$ assigned to user k , which is also assumed to be a random variable taking values +1 or -1 with equal probability of 1/2. The variable $P_{T_s}(t)$ represents the rectangular modulation waveform defined as $P_{T_s}(t) = 1$, if $0 \leq t \leq T_s$, and zero otherwise. Furthermore, f_{ij} is the subcarrier frequency associated with the i th data substream and the $(j - 1)$ th chip of the spreading code. Finally, $\phi_{ij}^{(k)}$ is the random phase introduced by the carrier modulation, which is assumed to be uniformly distributed in $[0, 2\pi)$.

We assume that frequency non-selective fading is encountered by each subcarrier signal. Hence, the following condition is satisfied:

$$1/T_s \ll (\Delta B)_c, \quad (17.27)$$

where $(\Delta B)_c$ represents the coherence bandwidth of the channel [95]. The reciprocal of $(\Delta B)_c$ is a measure of the multipath delay spread of the channel, which is denoted by T_m , $T_m \approx 1/(\Delta B)_c$. In order to guarantee independent fading of the subcarrier signals carrying chips associated with the same data bit, we assume that the following condition is satisfied:

$$(\Delta B)_c \ll q/T_s. \quad (17.28)$$

The conditions of Eq.(17.27) and Eq.(17.28), i.e., $1/T_s \ll (\Delta B)_c \ll q/T_s$ imply that the modulated subcarriers having transmission bandwidth of $1/T_s$ do not experience significant dispersion.

However, if the conditions of $1/T_s \ll (\Delta B)_c \ll q/T_s$ cannot be satisfied, the system model of Fig.17.19 can be modified, in order to satisfy this conditions. Specifically, if $1/T_s \ll (\Delta B)_c$ cannot be satisfied, we can decrease the term $1/T_s$ by transmitting more bits per symbol, i.e, by increasing the value of q in Fig.17.19. By contrast, if the condition of $(\Delta B)_c \ll q/T_s$ cannot be satisfied, the independence between the adjacent subcarriers conveying the same data bit can be further guaranteed by incorporating sufficient interleaving at the cost of an increased delay. For example, assuming that the first N_p symbols, i.e., $= N_p q$ bits, emitted by the source modulate the $N_p q$ subcarriers in the first time interval, where each symbol is modulated by the subcarrier frequencies from the same column of Eq.(17.24). In the second time interval, the same N_p symbols modulate the $N_p q$ subcarriers, but cyclically shifted by one symbol. Similarly, in the i th interval, $1 \leq i \leq N_p$, the N_p symbols after the $(i - 1)$ th cyclic shift modulate the $N_p q$ subcarriers. At the receiver, a deinterleaver is employed to recover the original ordering of the symbols. However, interleaving techniques can only be used for the transmission of delay-insensitive data.

Here, we assume that there are K asynchronous CDMA users in the system and that all of them use the same q and N_p values. The average power received from each user at the base

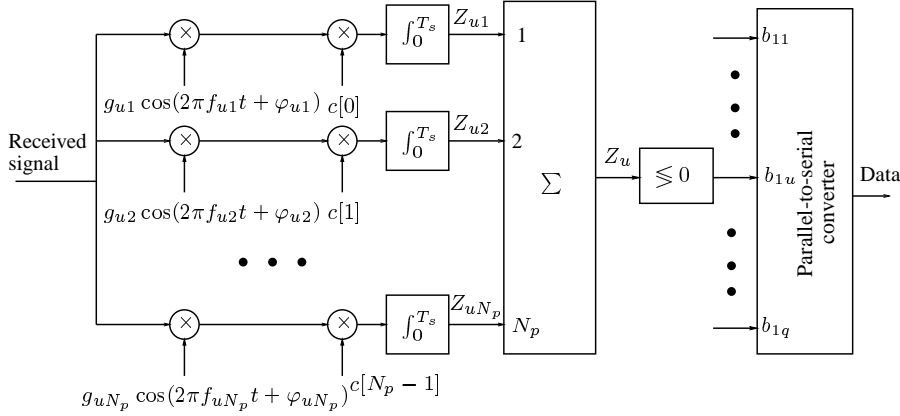


Figure 17.20: The receiver block diagram of the MC-CDMA system using frequency-domain spreading for the reference user.

station is also assumed to be the same, i.e. perfect power control is assumed. Consequently, the received signal at the base station can be expressed as:

$$r(t) = \sum_{k=1}^K \sum_{n=-\infty}^{\infty} \sum_{i=1}^q \sum_{j=1}^{N_p} \sqrt{\frac{2P}{N_p}} \alpha_{ij}^{(k)} b_{ki}[n] c_k[j-1] P_{T_s}(t - nT_s - \tau_k) \cdot \cos\left(2\pi f_{ij} t + \varphi_{ij}^{(k)}\right) + n(t), \quad (17.29)$$

where $\varphi_{ij}^{(k)} = \phi_{ij}^{(k)} + \psi_{ij}^{(k)} - 2\pi f_{ij} \tau_k$ and the random phase $\psi_{ij}^{(k)}$ corresponds to the subcarrier frequency f_{ij} of user k , which was introduced by the channel. The phase $\varphi_{ij}^{(k)}$ is a random variable uniformly distributed in $[0, 2\pi)$. In Eq.(17.29), τ_k is the misalignment of user k with respect to the reference user – we assumed that $k = 1$ and $\tau_1 = 0$ – at the receiver, which is i.i.d for different k values and uniformly distributed in $[0, T_s)$. Furthermore, $\alpha_{ij}^{(k)}$ represents the amplitude attenuation due to the fading channel, which is assumed to be a Rayleigh distributed random variable obeying the PDF given by Eq.(17.23) and $\Omega = E\left[\left(\alpha_{ij}^{(k)}\right)^2\right] = 1$. Finally, $n(t)$ is the Additive White Gaussian Noise (AWGN) with zero mean and double-sided power spectral density of $N_0/2$.

17.4.1.2 Receiver

The receiver of the first user ($k = 1$) is shown in Fig.17.20, where the superscript denoting the reference user is omitted. The MC-CDMA receiver considered is based on coherent correlator detector. As shown in Fig.17.20, the decision variable Z_u of the 0th data bit in the

u th data substream for the reference user can be expressed as:

$$Z_u = \sum_{v=1}^{N_p} Z_{uv}, \quad (17.30)$$

$$Z_{uv} = \int_0^{T_s} r(t)c[v-1]g_{uv} \cos(2\pi f_{uv}t + \varphi_{uv})dt, \quad (17.31)$$

where g_{uv} is a parameter determining which type of combining model of the chips belonging to the same data bit is used. Depending on the choice of $\{g_{uv}, v = 1, 2, \dots, N_p\}$, in our analysis there are two ways of combining the chips of the same data bit, namely MRC and equal gain combining (EGC). which we have studied in chapter XXXX. In this section the associated BER using the MRC scheme will be investigated.

Upon substituting Eq.(17.29) into Eq.(17.30), the variable Z_{uv} can be simplified to:

$$Z_{uv} = \sqrt{\frac{P}{2N_p}} T_s \left[D_{uv} + \sum_{k=2}^K I_1^{(k)} + \sum_{k=2}^K \underbrace{\sum_{i=1}^q \sum_{j=1}^{N_p} I_2^{(k)}}_{j \neq v \text{ for } i=u} \right], \quad (17.32)$$

where D_{uv} is the desired term given by:

$$D_{uv} = \alpha_{uv} g_{uv} b_u[0], \quad (17.33)$$

and $b_u[0]$ is the 0th data bit of the reference user transmitted by the uv th subcarrier. Due to the orthogonality of the subcarrier signals associated with the same user, no self-interference is inflicted by the reference signal to the v th subcarrier of the u th data stream. The multi-user interference imposed by user k can be divided into two terms. The first term is constituted by the subcarrier signal having the same subcarrier frequency, f_{uv} , as the branch considered. This term is $I_1^{(k)}$ in Eq.(17.32), which can be expressed as:

$$\begin{aligned} I_1^{(k)} &= \left(\sqrt{\frac{P}{2N_p}} T_s \right)^{-1} \int_0^{T_s} \sum_{n=-\infty}^{\infty} \sqrt{\frac{2P}{N_p}} \alpha_{uv}^{(k)} b_{ku}[n] c_k[v-1] \\ &\quad \cdot P_{T_s}(t - nT_s - \tau_k) \cos(2\pi f_{uv}t + \varphi_{uv}^{(k)}) \\ &\quad \cdot c[v-1] g_{uv} \cos(2\pi f_{uv}t + \varphi_{uv}) dt \\ &= \frac{\alpha_{uv}^{(k)} g_{uv} \cos \theta_{uv}^{(k)}}{T_s} \\ &\quad \cdot [b_{ku}[-1] c_k[v-1] c[v-1] \tau_k + b_{ku}[0] c_k[v-1] c[v-1] (T_s - \tau_k)] \end{aligned} \quad (17.34)$$

where $\theta_{uv}^{(k)} = \varphi_{uv}^{(k)} - \varphi_{uv}$. The second term of the multiuser interference imposed by user k is contributed by the other subcarrier signals associated with $\{f_{ij}, i = 1, 2, \dots, q; j = 1, 2, \dots,$

$N_P; j \neq v$ for $i = u$. The interference, $I_2^{(k)}$, arising from the subcarrier signal associated with the frequency f_{ij} of user k can be expressed as:

$$\begin{aligned}
 I_2^{(k)} &= \left(\sqrt{\frac{P}{2N_P}} T_s \right)^{-1} \int_0^{T_s} \sum_{n=-\infty}^{\infty} \sqrt{\frac{2P}{N_P}} \alpha_{ij}^{(k)} b_{ki}[n] c_k[j-1] \\
 &\quad \cdot P_{T_s}(t - nT_s - \tau_k) \cos \left(2\pi f_{ij} t + \varphi_{ij}^{(k)} \right) \\
 &\quad \cdot c[v-1] g_{uv} \cos(2\pi f_{uv} t + \varphi_{uv}) dt \\
 &= \frac{\alpha_{uv}^{(k)} g_{uv}}{T_s} \left[R_{ij}^{(k)}(\tau_k) + \hat{R}_{ij}^{(k)}(\tau_k) \right], \tag{17.35}
 \end{aligned}$$

where $R_{ij}^{(k)}(\tau_k)$ and $\hat{R}_{ij}^{(k)}(\tau_k)$ are chip-partial cross-correlation functions defined as:

$$\begin{aligned}
 R_{ij}^{(k)}(\tau_k, \theta_{ij}^{(k)}) &= \int_0^{\tau_k} b_{ki}[-1] c_k[j-1] c[v-1] \\
 &\quad \cdot \cos \left[2\pi (f_{ij} - f_{uv}) t + \theta_{ij}^{(k)} \right] dt, \tag{17.36}
 \end{aligned}$$

$$\begin{aligned}
 \hat{R}_{ij}^{(k)}(\tau_k, \theta_{ij}^{(k)}) &= \int_{\tau_k}^{T_s} b_{ki}[0] c_k[j-1] c[v-1] \\
 &\quad \cdot \cos \left[2\pi (f_{ij} - f_{uv}) t + \theta_{ij}^{(k)} \right] dt, \tag{17.37}
 \end{aligned}$$

and $\theta_{ij}^{(k)} = \varphi_{ij}^{(k)} - \varphi_{uv}$. Upon using Eq.(17.25), Eq.(17.36) and Eq.(17.37) can be written as:

$$\begin{aligned}
R_{ij}^{(k)}(\tau_k, \theta_{ij}^{(k)}) &= \int_0^{\tau_k} b_{ki}[-1]c_k[j-1]c[v-1] \\
&\quad \cdot \cos\left[\frac{2\pi[(i-u)+(j-v)q]t}{T_s} + \theta_{ij}^{(k)}\right] dt \\
&= \frac{T_s b_{ki}[-1]c_k[j-1]c[v-1]}{2\pi[(i-u)+(j-v)q]} \\
&\quad \cdot \left\{ \sin\left[\frac{2\pi[(i-u)+(j-v)q]\tau_k}{T_s} + \theta_{ij}^{(k)}\right] - \sin\theta_{ij}^{(k)} \right\} \quad (17.38) \\
\hat{R}_{ij}^{(k)}(\tau_k, \theta_{ij}^{(k)}) &= \int_{\tau_k}^{T_s} b_{ki}[0]c_k[j-1]c[v-1] \\
&\quad \cdot \cos\left[\frac{2\pi[(i-u)+(j-v)q]t}{T_s} + \theta_{ij}^{(k)}\right] dt \\
&= \frac{T_s b_{ki}[0]c_k[j-1]c[v-1]}{2\pi[(i-u)+(j-v)q]} \\
&\quad \cdot \left\{ \sin\left[\frac{2\pi[(i-u)+(j-v)q]T_s}{T_s} + \theta_{ij}^{(k)}\right] \right. \\
&\quad \left. - \sin\left[\frac{2\pi[(i-u)+(j-v)q]\tau_k}{T_s} + \theta_{ij}^{(k)}\right] \right\}, \quad (17.39)
\end{aligned}$$

where $(i-u)+(j-v)q \neq 0$. Finally, η_{uv} is the noise term engendered by the AWGN $n(t)$, which can be expressed as:

$$\eta_{uv} = \left(\sqrt{\frac{P}{2N_p}} T_s \right)^{-1} \int_0^{T_s} n(t)c[v-1]g_{uv} \cos(2\pi f_{uv}t + \varphi_{uv}) dt. \quad (17.40)$$

17.4.2 Performance Analysis

In order to derive the system's bit error probability, we have to derive the PDF of the decision variable Z_u in Eq.(17.30). First, we examine the terms in the Z_{uv} expression of Eq.(17.31).

17.4.2.1 Noise and Interference Analysis

A. Noise Analysis

The noise term η_{uv} is given by Eq.(17.40), which is a Gaussian random variable with zero mean and variance given by:

$$\text{Var}[\eta_{uv}] = \frac{N_p N_0}{2E_b} g_{uv}^2, \quad (17.41)$$

where $E_b = PT_s$ is the energy per bit.

B. Analysis of the Multiuser Interference Term $I_1^{(k)}$

The first multiuser interference term $I_1^{(k)}$ expressed by Eq.(17.34) can be modeled as a Gaussian random variable with zero mean. Its variance is given by:

$$\text{Var}[I_1^{(k)}] = E_{\tau_k, \theta_{uv}^{(k)}} \left[(I_1^{(k)})^2 \right], \quad (17.42)$$

where $E_{\tau_k, \theta_{uv}^{(k)}}[\cdot]$ represents the average associated with the random variables $\tau_k \in [0, T_s)$, $\theta_{uv}^{(k)} \in [0, 2\pi)$. Upon substituting $I_1^{(k)}$ from Eq.(17.34) into Eq.(17.42) it can be shown that the variance of $I_1^{(k)}$ can be expressed as:

$$\text{Var}[I_1^{(k)}] = \frac{1}{3} g_{uv}^2, \quad (17.43)$$

where we used $E \left[\left(\alpha_{uv}^{(k)} \right)^2 \right] = 1$, since frequency non-selective fading is assumed for each subcarrier signal, i.e. for each subcarrier signal there exists only one resolvable path.

B. Analysis of the Multiuser Interference Term $I_2^{(k)}$

The second multiuser interference term $I_2^{(k)}$ expressed by Eq.(17.35) can also be modeled as a Gaussian random variable with zero mean. Its variance is derived as follows. According to Eq.(17.35), the variance of $I_2^{(k)}$ can be expressed as:

$$\begin{aligned} \text{Var}[I_2^{(k)}] &= E_{\tau_k, \theta_{ij}^{(k)}} \left[(I_2^{(k)})^2 \right] \\ &= \frac{g_{uv}^2}{T_s^2} \left\{ E_{\tau_k, \theta_{ij}^{(k)}} \left[\left(R_{ij}^{(k)} \left(\tau_k, \theta_{ij}^{(k)} \right) \right)^2 \right] + E_{\tau_k, \theta_{ij}^{(k)}} \left[\left(\hat{R}_{ij}^{(k)} \left(\tau_k, \theta_{ij}^{(k)} \right) \right)^2 \right] \right\}, \end{aligned} \quad (17.44)$$

where $E_{\tau_k, \theta_{ij}^{(k)}} \left[\left(R_{ij}^{(k)} \left(\tau_k, \theta_{ij}^{(k)} \right) \right)^2 \right]$ and $E_{\tau_k, \theta_{ij}^{(k)}} \left[\left(\hat{R}_{ij}^{(k)} \left(\tau_k, \theta_{ij}^{(k)} \right) \right)^2 \right]$ are the variances of the chip-partial cross-correlation functions defined in Eq.(17.38) and Eq.(17.39), respectively.

Let us first derive the first term. According to Eq.(17.38), it can be shown that:

$$\begin{aligned}
E_{\tau_k, \theta_{ij}^{(k)}} \left[\left(R_{ij}^{(k)} \left(\tau_k, \theta_{ij}^{(k)} \right) \right)^2 \right] &= \frac{T_s^2}{4\pi^2 [(i-u) + (j-v)q]^2} \\
&\cdot E_{\tau_k, \theta_{ij}^{(k)}} \left\{ \sin^2 \left[\frac{2\pi [(i-u) + (j-v)q] \tau_k}{T_s} + \theta_{ij}^{(k)} \right] \right. \\
&+ \sin^2 \theta_{ij}^{(k)} \\
&\left. - 2 \sin \left[\frac{2\pi [(i-u) + (j-v)q] \tau_k}{T_s} + \theta_{ij}^{(k)} \right] \sin \theta_{ij}^{(k)} \right\}. \tag{17.45}
\end{aligned}$$

It is not difficult to shown that $E_{\tau_k, \theta_{ij}^{(k)}} \left\{ \sin^2 \left[\frac{2\pi [(i-u) + (j-v)q] \tau_k}{T_s} + \theta_{ij}^{(k)} \right] \right\} = 1/2$, $E_{\theta_{ij}^{(k)}} \left\{ \sin^2 \theta_{ij}^{(k)} \right\} = 1/2$ and $E_{\tau_k, \theta_{ij}^{(k)}} \left\{ 2 \sin \left[\frac{2\pi [(i-u) + (j-v)q] \tau_k}{T_s} + \theta_{ij}^{(k)} \right] \sin \theta_{ij}^{(k)} \right\} = 0$. By substituting these terms into the above equation, finally, we obtain that:

$$E_{\tau_k, \theta_{ij}^{(k)}} \left[\left(R_{ij}^{(k)} \left(\tau_k, \theta_{ij}^{(k)} \right) \right)^2 \right] = \frac{T_s^2}{4\pi^2 [(i-u) + (j-v)q]^2}. \tag{17.46}$$

Similarly, the second term of Eq.(17.44) can be derived and it can be shown that it is the same as Eq.(17.46)

$$E_{\tau_k, \theta_{ij}^{(k)}} \left[\left(\hat{R}_{ij}^{(k)} \left(\tau_k, \theta_{ij}^{(k)} \right) \right)^2 \right] = \frac{T_s^2}{4\pi^2 [(i-u) + (j-v)q]^2}. \tag{17.47}$$

Upon substituting Eq.(17.46) and Eq.(17.47) into Eq.(17.44), we obtain that the variance of $I_2^{(k)}$ can be expressed as:

$$\text{Var}[I_2^{(k)}] = \frac{g_{uv}^2}{2\pi^2 [(i-u) + (j-v)q]^2}. \tag{17.48}$$

17.4.2.2 Decision Statistics and Error Probability

Now we derive the PDF of the decision variable Z_u of Eq.(17.30) associated with the MRC scheme. We approximate the multiuser interference by Gaussian noise, since it is the sum of many independent random variables. Consequently, it can be shown that Z_u of Eq.(17.32)

can be approximated as a Gaussian random variable with normalized¹ mean given by:

$$E[Z_u] = \sum_{v=1}^{N_p} E[Z_{uv}] = b_u[0] \sum_{v=1}^{N_p} \alpha_{uv} g_{uv}, \quad (17.49)$$

and its normalized variance can be expressed as:

$$\sigma^2 = \left[\frac{N_p N_0}{2E_b} + \frac{(K-1)}{3} + (K-1)q(N_p-1)\bar{I}_M \right] \cdot \sum_{v=1}^{N_p} g_{uv}^2, \quad (17.50)$$

where \bar{I}_M represents the average of $\text{Var}[I_2^{(k)}]$ associated with the variables of u and v as well as i and j . For the given values of u and v , let $I(u, v)$ be expressed as:

$$\begin{aligned} I(u, v) &= E_{i,j} \left[\text{Var}[I_2^{(k)}] \right] \\ &= \frac{1}{q(N_p-1)} \underbrace{\sum_{i=1}^q \sum_{j=1}^{N_p} }_{j \neq v \text{ for } i=u} \left[\frac{1}{2\pi^2 [(i-u) + (j-v)q]^2} \right], \end{aligned} \quad (17.51)$$

then, \bar{I}_M can be expressed as:

$$\bar{I}_M = \frac{1}{qN_p} \sum_{u=1}^q \sum_{v=1}^{N_p} I(u, v). \quad (17.52)$$

Consequently, for a given set of channel attenuations α_{uv} , $v = 1, 2, \dots, N_p$, the conditional BER can be expressed as [95]:

$$P_b(\gamma) = Q\left(\sqrt{2\gamma}\right), \quad (17.53)$$

where $Q(\cdot)$ represents the Gaussian Q -function, which is defined as [95]:

$$Q(x) = \frac{1}{\sqrt{2\pi}} \int_x^\infty e^{-t^2/2} dt. \quad (17.54)$$

For the use of MRC, the channel gain associated with each subcarrier is continuously estimated and multiplied by the correlator outputs. If perfect channel gain estimation is assumed, then, $g_{uv} = \alpha_{uv}$. Consequently, the variable γ in Eq.(17.53) using MRC can be expressed

¹The normalization is obtained from Z_u divided by $\left(\sqrt{\frac{P}{2N_p}}\right)$.

as:

$$\gamma = \bar{\gamma}_c \cdot \sum_{v=1}^{N_p} \alpha_{uv}^2, \quad (17.55)$$

$$\bar{\gamma}_c = \left[\frac{2(K-1)}{3} + 2(K-1)q(N_p-1)\bar{T}_M + \left(\frac{E_b}{N_0 N_p} \right)^{-1} \right]^{-1}. \quad (17.56)$$

The unconditional BER P_b can be derived by weighting $P_b(\gamma)$ of Eq.(17.53) with its probability of occurrence expressed in terms of its PDF and then averaging, i.e., integrating it over the valid range of γ , which can be expressed as:

$$P_b = \int_0^{\infty} Q(\sqrt{2\gamma}) f(\gamma) d\gamma, \quad (17.57)$$

where $f(\gamma)$ is the PDF of γ . Since α_{uv} is a Rayleigh distributed random variable having PDF given by Eq.(17.23) and $\Omega = 1$ for the MC-CDMA scheme, $\sum_{v=1}^{N_p} \alpha_{uv}^2$ obeys the central chi-square distribution with $2N_p$ degrees of freedom [95]. Finally, γ given by Eq.(17.55) is also a random variable obeying the central chi-square distribution with $2N_p$ degrees of freedom, which can be expressed as [95]:

$$f(\gamma) = \frac{1}{\bar{\gamma}_c^{N_p} (N_p - 1)!} \gamma^{N_p - 1} \exp\left(-\frac{\gamma}{\bar{\gamma}_c}\right), \quad \gamma \geq 0. \quad (17.58)$$

Upon substituting Eq.(17.58) into Eq.(17.57) and upon simplifying the integral, it can be shown that the BER of the MC-CDMA system using MRC can be expressed as:

$$P_b = \left[\frac{(1-\mu)}{2} \right]^{N_p} \sum_{n=0}^{N_p-1} \binom{N_p-1+n}{n} \left[\frac{(1+\mu)}{2} \right]^n, \quad (17.59)$$

where, by definition:

$$\mu = \sqrt{\frac{\bar{\gamma}_c}{1 + \bar{\gamma}_c}}. \quad (17.60)$$

When the average SNR of $\bar{\gamma}_c$ satisfies the condition $\bar{\gamma}_c \gg 1$, we have $\frac{(1+\mu)}{2} \approx 1$ and $\frac{(1-\mu)}{2} \approx \frac{1}{4\bar{\gamma}_c}$ [95]. Furthermore, we have:

$$\sum_{n=0}^{N_p-1} \binom{N_p-1+n}{n} = \binom{2N_p-1}{N_p}. \quad (17.61)$$

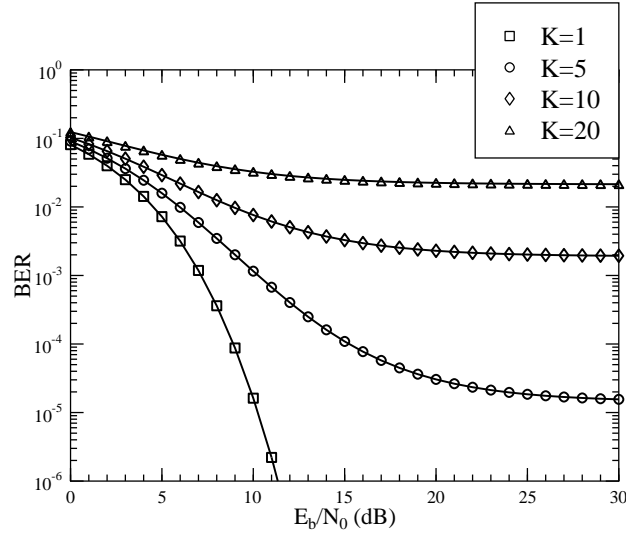


Figure 17.21: BER versus SNR per bit performance for the MC-CDMA system using frequency-domain spreading over Rayleigh fading channels with parameters $q = 4$ number of bits per symbol, processing gain of $N_p = 32$ and number of users $K = 1, 5, 10, 20$. The results were computed from Eq.(17.59).

Therefore, when $\bar{\gamma}_c$ is sufficiently high, the BER of Eq.(17.59) can be expressed as:

$$P_b \approx \left(\frac{1}{4\bar{\gamma}_c} \right)^{N_p} \binom{2N_p - 1}{N_p}. \quad (17.62)$$

According to Eq.(17.62) the probability of error for the MC-CDMA system shown in Fig.17.19 varies as $1/\bar{\gamma}_c$ raised to the N_p th power. Thus, when using frequency-domain spreading in the MC-CDMA system employing a spreading code of length N_p , the bit error rate decreases inversely proportionately with the N_p th power of the SNR.

Fig.17.21 shows the BER performance of the MC-CDMA system depicted in Fig.17.19 using frequency-domain spreading. The BER results were computed as a function of the SNR per bit, namely E_b/N_0 , using parameters of $q = 4$, $N_p = 32$ and the number of users of $K = 1, 5, 10, 20$. From the results we observe that the BER performance degrades, as the number of users increases. Furthermore, as expected, the BER decreases as the SNR per bit increases. However, when the number of users supported is sufficiently high, the BER decreases slowly, as shown by the curve associated with $K = 20$ marked by the 'triangles'. This can be also seen in Eq.(17.59) and Eq.(17.60). According to Eq.(17.60), if the number of interfering users and the SNR per bit are sufficiently high, in Eq.(17.59) we have $\mu \approx 1/\sqrt{2}$. Hence, for a given N_p , the BER remains approximately constant according to Eq.(17.59) for $\mu \approx 1/\sqrt{2}$.

17.5 Performance of Overlapping Multicarrier DS-CDMA Systems

17.5.1 Preliminaries

In Subsections 17.2.3 and 17.2.4 we have reviewed the basic characteristics of two orthogonal multicarrier DS-CDMA systems, namely those of the multicarrier DS-CDMA-II, and the multitone DS-CDMA systems seen in figures 17.7 and 17.10. In the multitone DS-CDMA system of Fig.17.10, the subcarrier frequencies are chosen to be orthogonal to each other with minimum frequency separation before the associated DS spreading, which is formulated as:

$$\int_0^{T_s} \cos(2\pi f_i t + \phi_i) \cdot \cos(2\pi f_j t + \phi_j) dt = 0, \text{ for } i \neq j. \quad (17.63)$$

Hence, the spacing Δ between two adjacent subcarrier frequencies is $\Delta = 1/T_s$, where T_s is the multitone DS-CDMA signal's symbol duration. The subcarrier frequencies, therefore, take the values of $f_0 + i/T_s$ for $i = 0, 1, \dots, U - 1$, where f_0 is the main carrier frequency. In contrast to the multitone DS-CDMA system of Fig.17.10, in the orthogonal multicarrier DS-CDMA-II system of Fig.17.7, the subcarrier frequencies are chosen to be orthogonal to each other with the minimum frequency separation after the DS spreading, which can be expressed as:

$$\int_0^{T_c} \cos(2\pi f_i t + \phi_i) \cdot \cos(2\pi f_j t + \phi_j) dt = 0, \text{ for } i \neq j, \quad (17.64)$$

implying that the spacing Δ between two adjacent subcarrier frequencies is $\Delta = 1/T_c$, as shown in Fig.17.8, where T_c is the chip duration of the DS spreading codes and the subcarrier frequencies assume the value of $f_0 + i/T_c$ for $i = 0, 1, \dots, U - 1$.

Let $N_e = T_s/T_c$ be the spreading gain of the DS spread subcarrier signals and we assume that each subcarrier signal has the same 'null-to-null' bandwidth of $2/T_c$. Then, it can be shown that the condition of Eq.(17.63), which was stipulated for the multitone DS-CDMA system of Fig.17.10, in fact, includes the orthogonality condition of Eq.(17.64) stated in the context of the multicarrier DS-CDMA-II systems of Fig.17.7. This observation can be proven by setting $f_i = f_j + N_e/T_s$ in Eq.(17.63), yielding:

$$\int_0^{T_s} \cos\left(\frac{2\pi}{T_c} t + \psi_i\right) dt = 0, \quad (17.65)$$

after a few steps, where $\psi_i = \phi_i - \phi_j$. Note that, in Eq.(17.65) we used $N_e/T_s = 1/T_c$. To proceed further, Eq.(17.65) can be extended to:

$$\sum_{l=0}^{N_e-1} \int_{lT_c}^{(l+1)T_c} \cos\left(\frac{2\pi}{T_c} t + \psi_i\right) dt = 0. \quad (17.66)$$

According to Eq.(17.66) it can be shown that each term of the sum is zero and hence we have:

$$\int_0^{T_c} \cos\left(\frac{2\pi}{T_c}t + \psi_i\right)dt = 0, \quad (17.67)$$

which reflects the orthogonality between subcarrier frequencies having minimum frequency separation after DS spreading. In other words, Eq.(17.63) constitutes the orthogonality condition of the subcarrier frequencies in the multicarrier DS-CDMA-II system of Fig.17.8.

Furthermore, it can be readily shown that the orthogonality condition of (17.63) is obeyed, whenever the spacing Δ takes the form of $\Delta = \lambda/T_s$, $\lambda = 1, 2, \dots$, where λ is referred to as the normalized spacing between two adjacent subcarriers. The multicarrier DS-CDMA scheme belongs to the family of multitone DS-CDMA arrangements having spectrum of Fig.17.11, if $\lambda = 1$, while to the class of orthogonal multicarrier DS-CDMA systems with spectrum shown in Fig.17.8, if $\lambda = N_e$. Furthermore, there exists no overlap between the main-lobes of the modulated subcarrier signals after DS spreading, when $\lambda = 2N_e$, which is the bandwidth requirement of Fig.17.11 for the multicarrier DS-CDMA system proposed in [453].

Based on the above observations both the multitone DS-CDMA system and the orthogonal multicarrier DS-CDMA system can be viewed as a member of the class of generalized multicarrier DS-CDMA systems having arbitrary subcarrier spacing of $\lambda \in \{1, 2, \dots\}$. Hence, the above generalized multicarrier DS-CDMA system model includes a number of specific multicarrier DS-CDMA schemes. Furthermore, based on the analysis of this general model, the results generated can be extended to different multicarrier DS-CDMA systems by simply varying single parameter, namely λ . Finally, the subcarrier spacing λ can be optimized according to specific design requirements tailored to the communication environments encountered, in order to achieve the optimum performance in term of λ . For example, for a given total system bandwidth, λ can be optimized, in order to minimize the multiuser interference, since λ has an influence on both the overlap of the modulated signals of the subcarriers and on the processing gain. In this context a clear trade-off exists between the overlap and the processing gain. On the one hand, if λ is low - for example $\lambda = 1$ - in the context of multitone DS-CDMA, then, a subcarrier signal will overlap with a high number of subcarrier signals of both the same user and with those of the interfering users. On the other hand, given a total bandwidth and a low value of λ , a high spreading gain can be maintained, which leads to the reduction of the multiuser interference. By contrast, if λ is high - for example $\lambda = 2N_e$ - which means that there exists no spectral overlap between the main-lobes of the subcarrier signals, then, the modulated subcarrier signals benefit from a low interference inflicted by the other subcarrier signals of both the reference and the interfering users. However, in this case the spreading gain of each subcarrier signal is low, which leads to the increase of the multiuser interference. The influence of the subcarrier spacing λ on both the spreading gain and on the spectral overlap of the subcarrier signals highlights that there exists an optimum spacing λ_{opt} , that may minimize the multiuser interference inflicted upon each of the subcarrier signals. Another example in the context of optimizing λ is that the subcarrier spacing λ can be set appropriately, in order to match the receiver requirements. For example, assuming that the receiver employs a three-finger RAKE receiver. Then a specific spacing λ can be selected such that the number of resolvable paths associated with each subcarrier becomes three in the propagation environment typically encountered, since in this case, in addition

to achieving the diversity gain, the receiver can combine all the energy scattered over the multipath components.

Hence, in the remainder of section we investigate the performance of the generalized overlapping multicarrier DS-CDMA system having an arbitrary spacing of Δ , when transmitting over frequency selective Rayleigh fading channels. We commence by first considering the system model and the parameters involved in our analysis.

17.5.2 System Description

17.5.2.1 Transmitted Signal

The transmitter schematic of the overlapping multicarrier DS-CDMA system considered is the same as that seen in Fig.17.10. Hence, the transmitted signal can be expressed as:

$$s_k(t) = \sum_{u=1}^U \sqrt{2P} b_{ku}(t) c_k(t) \cos(2\pi f_u t + \phi_{ku}), \quad (17.68)$$

where P is the transmitted power of each subcarrier signal, $b_{ku}(t)$ represents the u th data substream of user k after the serial-to-parallel conversion, $b_{ku}(t) = \sum_{i=-\infty}^{\infty} b_{ui}^{(k)} P_{T_s}(t - iT_s)$ consists of a sequence of mutually independent rectangular signalling pulses of duration T_s and of amplitude +1 or -1 with equal probability. Furthermore, $c_k(t) = \sum_{j=-\infty}^{\infty} c_j^{(k)} P_{T_c}(t - jT_c)$ denotes the random spreading code waveform of the k th user, where $P_{\tau}(t) = 1$ for $0 \leq t \leq \tau$ and equals zero otherwise, where $c_j^{(k)}$ takes values of +1 and -1 with equal probability. The variable ϕ_{ku} represents the modulation phase imposed on the u th subcarrier of user k . Finally, $\{f_u, u = 1, 2, \dots, U\}$ are the subcarrier frequencies, which are arranged according to:

$$f_u = f_0 + \frac{\lambda(u-1)}{T_s}, \quad u = 1, 2, \dots, U, \quad (17.69)$$

where $\lambda = 1, 2, \dots, 2N_e$ corresponding to $\Delta = 1/T_s, 2/T_s, \dots, 2N_e/T_s$, if we assume that the maximum spacing between two adjacent subcarriers is $2N_e$. The spectrum of the overlapping multicarrier DS-CDMA signal is shown in Fig.17.22, where W_s is the bandwidth of the system considered, T_{c1} is the chip-duration corresponding to a single-carrier DS-CDMA system, while W_{ds} represents the null-to-null bandwidth of the subcarrier signals.

According to Fig.17.22 the system's total transmission bandwidth, the subcarrier spacing Δ and the bandwidth of the subcarrier signal obey the following relationship:

$$W_s = (U-1)\Delta + W_{ds}. \quad (17.70)$$

This in turn means that:

$$\frac{2}{T_{c1}} = (U-1)\frac{\lambda}{T_s} + \frac{2}{T_c}. \quad (17.71)$$

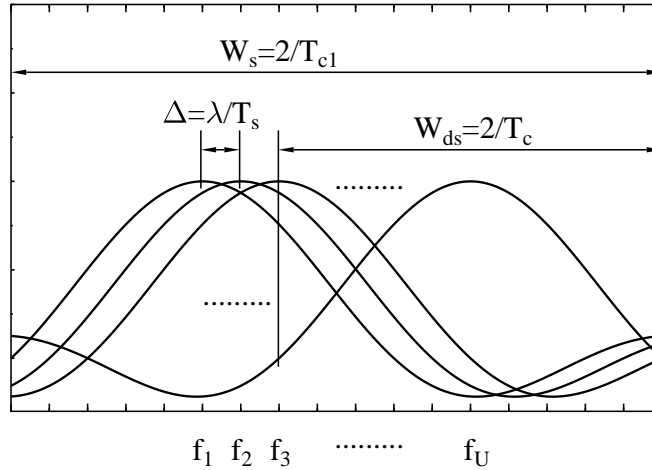


Figure 17.22: Spectrum of the overlapping multicarrier DS-CDMA signals.

Since $T_s = UT_b = UNT_{c1}$ and $T_s = N_e T_c$, after substituting these relationship into Eq.(17.71), the spreading gain associated with each subcarrier signal can be expressed as:

$$N_e = UN - \frac{(U-1)\lambda}{2}. \quad (17.72)$$

According to Eq.(17.72), it can be shown that the spreading gain of the multicarrier signal corresponding to the normalized spacing of $\lambda = 1$, i.e. that of the multitone DS-CDMA system [463], is $N_e = (UN - \frac{U-1}{2})$, as shown in Eq.(17.14). The spreading gain of the system associated with $\lambda = N_e$, i.e. that of the orthogonal multicarrier DS-CDMA system of Fig.17.7 [69], is $N_e = 2UN/(U+1)$, as shown in Eq.(17.10).

Let L_1 be the number of resolvable paths of a corresponding single-carrier DS-CDMA system. Then, the number of resolvable paths associated with the subcarrier signals in the overlapping multicarrier DS-CDMA system having spectrum shown in Fig.17.22 can be approximated by:

$$L \approx \lfloor \frac{2N_e L_1}{2N_e + (U-1)\lambda} \rfloor. \quad (17.73)$$

Let us assume that we support K asynchronous CDMA users in the system and all of them use the same parameters U and N_e . The average power received from each user at the base station is also assumed to be the same, corresponding to the perfect power control assumption. Consequently, when K signals described by Eq.(17.68) are transmitted over the frequency selective fading channels characterized by Eq.(17.21), the received signal at the

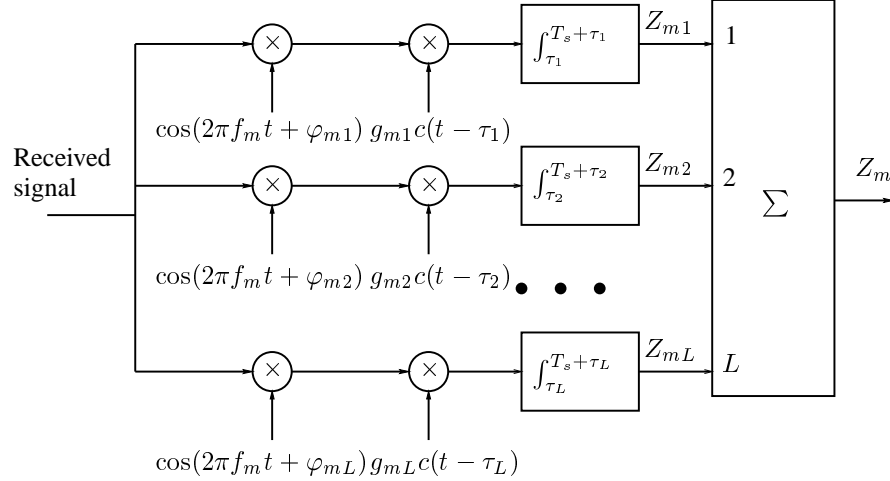


Figure 17.23: The receiver block diagram of the overlapping multicarrier DS-CDMA system.

base station can be expressed as:

$$r(t) = \sum_{k=1}^K \sum_{u=1}^U \sum_{l=1}^L \sqrt{2P} \alpha_{ul}^{(k)} b_{ku}(t - \tau_{kl}) c_k(t - \tau_{kl}) \cos(2\pi f_u t + \varphi_{ul}^{(k)}) + n(t), \quad (17.74)$$

where $\varphi_{ul}^{(k)} = \phi_{ku} + \psi_{ul}^{(k)} - 2\pi f_u \tau_{kl}$ and $\psi_{ul}^{(k)}$ is contributed by the channel.

17.5.2.2 Receiver Model

Let us assume that we want to receive the signal transmitted by the first user, which is treated as the reference user or reference signal in our analysis, and that the receiver is capable of acquiring perfect time-domain synchronization with each subcarrier signal of the reference user. The receiver considered is a conventional correlator based RAKE receiver, as shown in Fig.17.12. The m th branch of Fig.17.12 corresponding to the m th subcarrier is shown in Fig.17.23. Referring to Fig.17.23, the decision variable Z_m associated with the 0th data bit corresponding to the m th substream of the reference user can be expressed as:

$$Z_m = \sum_{v=1}^L Z_{mv}, \quad m = 1, 2, \dots, U, \quad (17.75)$$

$$Z_{mv} = \int_{\tau_v}^{T_s + \tau_v} r(t) \cdot g_{mv} c(t - \tau_v) \cos(2\pi f_m t + \varphi_{mv}) dt, \quad (17.76)$$

where g_{mv} is a parameter controlling which type of combining scheme is used, such as MRC, EGC or SC, respectively. However, in this section only the performance of the system using MRC is investigated, hence, $g_{mv} = \alpha_{mv}$ is assumed. Moreover, in Eq.(17.75) the subscripts

and superscripts associated with the reference user are omitted for notational simplicity. Furthermore, without loss any generality, we let $\tau_v = 0$ in the following analysis. Upon substituting Eq.(17.74) into Eq.(17.76), it can be shown that Z_{mv} can be written as:

$$Z_{mv} = \sqrt{\frac{P}{2}} T_s \left\{ D_{mv} + \eta_{mv} + \sum_{\substack{l=1 \\ l \neq v}}^L I_1^{(s)} + \sum_{\substack{u=1 \\ u \neq m}}^U \sum_{\substack{l=1 \\ l \neq v}}^L I_2^{(s)} + \sum_{k=2}^K \sum_{l=1}^L I_1^{(k)} + \sum_{k=2}^K \sum_{\substack{u=1 \\ u \neq m}}^U \sum_{l=1}^L I_2^{(k)} \right\}. \quad (17.77)$$

In Eq.(17.77), η_{mv} is contributed by the noise term $n(t)$ seen in Eq.(17.74), which is a Gaussian random variable with zero mean and variance $g_{mv}^2 N_0 / 2E_b$, where $E_b = PT_s$ represents the energy per bit. The variable D_{mv} in Eq.(17.77) represents the desired output given by combining Eq.(17.74), Eq.(17.76) and Eq.(17.77) upon setting $k = 1, l = v$ and $u = m$, which yields:

$$D_{mv} = b_m [0] \alpha_{mv} g_{mv}. \quad (17.78)$$

The output of the correlator matched to subcarrier m , corresponding to the v th path of the reference user contains four types of interference in Eq.(17.77). The interference of $I_1^{(s)}$ is contributed by the path $l, l = 1, 2, \dots, L, l \neq v$, on the same subcarrier m received from the reference user, which can be expressed as:

$$I_1^{(s)} = \frac{\alpha_{ml} g_{mv} \cos \theta_{ml}}{T_s} \int_0^{T_s} b_m(t - \tau_l) c(t - \tau_l) c(t) dt, \quad (17.79)$$

where $\theta_{ml} = \varphi_{ml} - \varphi_{mv}$, which is a random variable uniformly distributed in $[0, 2\pi)$. With the aid of the partial auto-correlation functions given below, Eq.(17.79) can be expressed as:

$$I_1^{(s)} = \frac{\alpha_{ml} g_{mv} \cos \theta_{ml}}{T_s} \left[b_m[-1] R_1(\tau_l) + b_m[0] \hat{R}_1(\tau_l) \right], \quad (17.80)$$

where $R_1(\tau_l)$ and $\hat{R}_1(\tau_l)$ are the partial auto-correlation functions defined as:

$$R_1(\tau_l) = \int_0^{\tau_l} c(t - \tau_l) c(t) dt, \quad (17.81)$$

$$\hat{R}_1(\tau_l) = \int_{\tau_l}^{T_s} c(t - \tau_l) c(t) dt. \quad (17.82)$$

The interference term of $I_2^{(s)}$ in Eq.(17.77) is contributed by the path $l, l = 1, 2, \dots, L, l \neq$

v , on the subcarrier u , $u = 1, 2, \dots, U$, $u \neq m$ by the reference user², which can be expressed as:

$$I_2^{(s)} = \frac{\alpha_{ul} g_{mv}}{T_s} \left[b_u[-1] R_1(\tau_l, \theta_{ul}) + b_u[0] \hat{R}_1(\tau_l, \theta_{ul}) \right], \quad (17.83)$$

where $\theta_{ul} = \varphi_{ul} - \varphi_{mv}$. Due to the difference of the frequencies associated with the subcarriers u and m , the corresponding partial auto-correlation functions are now defined as:

$$R_1(\tau_l, \theta_{ul}) = \int_0^{\tau_l} c(t - \tau_l) c(t) \cos(2\pi(f_u - f_m)t + \theta_{ul}) dt, \quad (17.84)$$

$$\hat{R}_1(\tau_l, \theta_{ul}) = \int_{\tau_l}^{T_s} c(t - \tau_l) c(t) \cos(2\pi(f_u - f_m)t + \theta_{ul}) dt. \quad (17.85)$$

With the aid of Eq.(17.69), Eq.(17.84) and Eq.(17.85) can then be written as:

$$R_1(\tau_l, \theta_{ul}) = \int_0^{\tau_l} c(t - \tau_l) c(t) \cos\left(\frac{2\pi\lambda(u - m)t}{T_s} + \theta_{ul}\right) dt, \quad (17.86)$$

$$\hat{R}_1(\tau_l, \theta_{ul}) = \int_{\tau_l}^{T_s} c(t - \tau_l) c(t) \cos\left(\frac{2\pi\lambda(u - m)t}{T_s} + \theta_{ul}\right) dt. \quad (17.87)$$

The multiuser interference term $I_1^{(k)}$ in Eq.(17.77) is due to path l , $l = 1, 2, \dots, L$ on the same subcarrier m inflicted by the interfering users for which we have $k \neq 1$. Then, $I_1^{(k)}$ in Eq.(17.77) can be expressed as:

$$I_1^{(k)} = \frac{\alpha_{ml}^{(k)} g_{mv} \cos \theta_{ml}^{(k)}}{T_s} \left[b_{km}[-1] R_k(\tau_{kl}) + b_{km}[0] \hat{R}_k(\tau_{kl}) \right], \quad (17.88)$$

where $\theta_{ml}^{(k)} = \varphi_{ml}^{(k)} - \varphi_{mv}$ is a random variable uniformly distributed in $[0, 2\pi)$, $R_k(\tau_{kl})$ and $\hat{R}_k(\tau_{kl})$ are the partial cross-correlation functions defined as:

$$R_k(\tau_{kl}) = \int_0^{\tau_{kl}} c_k(t - \tau_{kl}) c(t) dt, \quad (17.89)$$

$$\hat{R}_k(\tau_{kl}) = \int_{\tau_{kl}}^{T_s} c_k(t - \tau_{kl}) c(t) dt. \quad (17.90)$$

Finally, the multiuser interference term $I_2^{(k)}$ in Eq.(17.77) is due to path l , $l = 1, 2, \dots, L$ on the subcarrier u , $u = 1, 2, \dots, U$; $u \neq m$ imposed by the interfering users associated with

²Due to the orthogonality between the subcarrier signals from the same path and the same user, i.e., $\int_0^{T_s} \cos(2\pi f_i + \varphi_{il}) \cos(2\pi f_j + \varphi_{jl}) dt = 0$, the interference of $I_2^{(s)}$ due to the path v on the subcarrier u , $u = 1, 2, \dots, U$, $u \neq m$ from the reference user is zero. Hence, the associated terms are excluded by letting $l \neq v$ in Eq.(17.77).

$k \neq 1$. Hence, $I_2^{(k)}$ in Eq.(17.77) can be expressed as:

$$I_2^{(k)} = \frac{\alpha_{ul}^{(k)} g_{mv}}{T_s} \left[b_{ku}[-1] R_k(\tau_{kl}, \theta_{ul}^{(k)}) + b_{ku}[0] \hat{R}_k(\tau_{kl}, \theta_{ul}^{(k)}) \right], \quad (17.91)$$

where $\theta_{ul}^{(k)} = \varphi_{ul}^{(k)} - \varphi_{mv}$ is a random variable uniformly distributed in $[0, 2\pi)$. The associated partial cross-correlation functions are defined as:

$$R_k(\tau_{kl}, \theta_{ul}^{(k)}) = \int_0^{\tau_{kl}} c_k(t - \tau_{kl}) c(t) \cos \left(\frac{2\pi\lambda(u-m)t}{T_s} + \theta_{ul}^{(k)} \right) dt, \quad (17.92)$$

$$\hat{R}_k(\tau_{kl}, \theta_{ul}^{(k)}) = \int_{\tau_{kl}}^{T_s} c_k(t - \tau_{kl}) c(t) \cos \left(\frac{2\pi\lambda(u-m)t}{T_s} + \theta_{ul}^{(k)} \right) dt. \quad (17.93)$$

Having analyzed the receiver model and the decision variable, in the next subsection the multipath interference imposed by the reference user and the multiuser interference inflicted by the interfering users will be analyzed.

17.5.3 Interference Analysis

In this subsection the multipath interference engendered by the reference user itself and the multiuser interference will be evaluated by assuming that all these interference sources are Gaussian distributed and hence can be treated as independent additional noise. According to Eq.(17.80), Eq.(17.83), Eq.(17.88) and Eq.(17.91), the interference terms $I_1^{(s)}$, $I_2^{(s)}$ and $I_1^{(k)}$ constitute the special cases of the term $I_2^{(k)}$ in Eq.(17.91). Specifically, if we set $u = m$ in Eq.(17.91), we obtain Eq.(17.88). If we let $k = 1$ in Eq.(17.91), then we get Eq.(17.83). Finally, if we let $k = 1$ and $u = m$, then we obtain Eq.(17.80). Hence, we can analyze the multipath interference engendered by the reference user as well as the multiuser interference by first analyzing the multiuser interference term of Eq.(17.91). Based on the standard Gaussian approximation [108, 464], the interference term $I_2^{(k)}$ of Eq.(17.91) can be modelled as a Gaussian random variable with zero mean and a variance expressed as:

$$\text{Var} \left[I_2^{(k)} \right] = \frac{\Omega g_{mv}^2}{T_s^2} \left\{ E_{\tau_{kl}, \theta_{ul}^{(k)}} \left[R_k^2(\tau_{kl}, \theta_{ul}^{(k)}) \right] + E_{\tau_{kl}, \theta_{ul}^{(k)}} \left[\hat{R}_k^2(\tau_{kl}, \theta_{ul}^{(k)}) \right] \right\}, \quad (17.94)$$

where $\Omega = E \left[\left(\alpha_{ul}^{(k)} \right)^2 \right]$, $E_{\tau_{kl}, \theta_{ul}^{(k)}} [\]$ represents taking the expected value with respect to the random variables τ_{kl} and $\theta_{ul}^{(k)}$. In our following discourse, we analyze the partial cross-correlation functions of Eq.(17.92) and Eq.(17.93). Specifically, we will evaluate their expectations by assuming that the phase angles and time delays are modeled as mutually independent random variables, each of which is uniformly distributed over the appropriate interval. Below we only analyze the expectation of $R_k^2(\tau_{kl}, \theta_{ul}^{(k)})$, the expectation of $\hat{R}_k^2(\tau_{kl}, \theta_{ul}^{(k)})$ can be obtained following the same approach.

Eq.(17.92) can be written as [464]:

$$\begin{aligned}
 R_k(\tau, \theta) = & \sum_{j=0}^h a_i(j) a_k(N_e - h - 1 + j) \int_{jT_c}^{jT_c + \tau - hT_c} \cos\left(\frac{2\pi\lambda(u-m)t}{T_s} + \theta\right) dt \\
 & + \sum_{j=0}^{h-1} a_i(j) a_k(N_e - h + j) \int_{jT_c + \tau - hT_c}^{(j+1)T_c} \cos\left(\frac{2\pi\lambda(u-m)t}{T_s} + \theta\right) dt,
 \end{aligned} \tag{17.95}$$

where $hT_c \leq \tau_{kl} < (h+1)T_c$ and N_e represents the number of chips per symbol period or the spreading factor of the subcarrier signal. Furthermore, in Eq.(17.95) we set $\tau_{kl} = \tau$ and $\theta_{ul}^{(k)} = \theta$ for simplicity. Upon evaluating the integrals in Eq.(17.95), we find that:

$$\begin{aligned}
 R_k(\tau, \theta) = & (\tau - hT_c) \text{sinc}\left[\frac{\pi(u-m)\lambda(\tau - hT_c)}{T_s}\right] \\
 & \cdot \sum_{j=0}^h a_i(j) a_k(N_e - h - 1 + j) \cos \beta_{ka}(j, \tau) \\
 & + [(h+1)T_c - \tau] \text{sinc}\left[\frac{\pi(u-m)\lambda((h+1)T_c - \tau)}{T_s}\right] \\
 & \cdot \sum_{j=0}^{h-1} a_i(j) a_k(N_e - h + j) \cos \beta_{kb}(j, \tau),
 \end{aligned} \tag{17.96}$$

where $\text{sinc}(x) = \sin(x)/x$, and

$$\begin{aligned}
 \beta_{ka}(j, \tau) &= \frac{\pi(u-m)\lambda}{T_s} (2jT_c + \tau - hT_c) + \theta, \\
 \beta_{kb}(j, \tau) &= \frac{\pi(u-m)\lambda}{T_s} ((2j+1)T_c + \tau - hT_c) + \theta.
 \end{aligned}$$

The expression of $R^2(\tau, \varphi)$ is computed from Eq.(17.96) as:

$$\begin{aligned}
R_k^2(\tau, \theta) = & (\tau - hT_c)^2 \text{sinc}^2 \left[\frac{\pi(u-m)\lambda(\tau - hT_c)}{T_s} \right] \\
& \cdot \left[\sum_{j=0}^h a_i^2(j) a_k^2(N_e - h - 1 + j) \cos^2 \beta_{ka}(j, \tau) \right. \\
& + \sum_{r=0}^h \sum_{\substack{s=0 \\ s \neq r}}^h a_i(r) a_k(N_e - h - 1 + r) a_i(s) a_k(N_e - h - 1 + s) \\
& \left. \cdot \cos \beta_{ka}(r, \tau) \cos \beta_{ka}(s, \tau) \right] \\
& + (\tau - hT_c)[(h+1)T_c - \tau] \text{sinc} \left[\frac{\pi(u-m)\lambda(\tau - hT_c)}{T_s} \right] \\
& \cdot \text{sinc} \left[\frac{\pi(u-m)\lambda((h+1)T_c - \tau)}{T_s} \right] \\
& \cdot \left[\sum_{r=0}^h \sum_{s=0}^{h-1} a_i(r) a_k(N_e - h - 1 + r) a_i(s) a_k(N_e - h + s) \right. \\
& \cdot \cos \beta_{ka}(r, \tau) \cos \beta_{kb}(s, \tau) \\
& + \sum_{r=0}^{h-1} \sum_{s=0}^h a_i(r) a_k(N_e - h + r) a_i(s) a_k(N_e - h - 1 + s) \\
& \left. \cdot \cos \beta_{kb}(r, \tau) \cos \beta_{ka}(s, \tau) \right] \\
& + [(h+1)T_c - \tau]^2 \text{sinc}^2 \left[\frac{\pi(u-m)\lambda((h+1)T_c - \tau)}{T_s} \right] \\
& \cdot \left[\sum_{r=0}^{h-1} a_i^2(r) a_k^2(N_e - h + r) \cos^2 \beta_{kb}(r, \tau) \right. \\
& + \sum_{r=0}^{h-1} \sum_{\substack{s=0 \\ s \neq r}}^{h-1} a_i(r) a_k(N_e - h + r) a_i(s) a_k(N_e - h + s) \\
& \left. \cdot \cos \beta_{kb}(r, \tau) \cos \beta_{kb}(s, \tau) \right]. \tag{17.97}
\end{aligned}$$

Since we assumed that random spreading codes are employed in our system, $a_i(r)$ is statistically independent of $a_k(s)$ when $i \neq k$ or $r \neq s$, and takes values of +1 or -1 with equal probability. Hence, upon taking the expectation of $R_k^2(\tau, \theta)$ with respect to $a_i(r)$,

$a_k(s)$, θ and τ we arrive at:

$$\begin{aligned} \mathbf{E}_{\tau,\theta} [R_k^2(\tau, \theta)] &= \frac{1}{2T_s} \sum_{h=0}^{N_e-1} \\ &\cdot \int_{hT_c}^{(h+1)T_c} \left\{ (\tau - hT_c)^2 \operatorname{sinc}^2 \left[\frac{\pi(u-m)\lambda(\tau - hT_c)}{T_s} \right] \cdot (h+1) \right. \\ &\quad \left. + [(h+1)T_c - \tau]^2 \operatorname{sinc}^2 \left[\frac{\pi(u-m)\lambda((h+1)T_c - \tau)}{T_s} \right] \cdot h \right\} d\tau. \end{aligned} \quad (17.98)$$

Upon evaluating the resulting integral we find that:

$$\mathbf{E}_{\tau,\theta} [R_k^2(\tau, \theta)] = \frac{N_e T_s^2}{4\pi^2 (u-m)^2 \lambda^2} \left[1 - \operatorname{sinc} \left(\frac{2\pi(u-m)\lambda}{N_e} \right) \right]. \quad (17.99)$$

The corresponding expression for $\mathbf{E}_{\tau,\theta} [\hat{R}_k^2(\tau, \theta)]$ can be obtained by evaluating the expectation of $\hat{R}_k^2(\tau, \theta)$ in the same way, as for $R_k^2(\tau, \theta)$. We found that the result is the same as Eq.(17.99), i.e.:

$$\mathbf{E}_{\tau,\theta} [\hat{R}_k^2(\tau, \theta)] = \frac{N_e T_s^2}{4\pi^2 (u-m)^2 \lambda^2} \left[1 - \operatorname{sinc} \left(\frac{2\pi(u-m)\lambda}{N_e} \right) \right]. \quad (17.100)$$

Substituting Eq.(17.99) and Eq.(17.100) into Eq.(17.94), we finally found that the variance of the multiuser interference $I_2^{(k)}$ can be expressed as:

$$\operatorname{Var} [I_2^{(k)}] = \frac{\Omega g_{mv}^2 N_e}{2\pi^2 (u-m)^2 \lambda^2} \left[1 - \operatorname{sinc} \left(\frac{2\pi(u-m)\lambda}{N_e} \right) \right]. \quad (17.101)$$

Let $u - m = x$ and compute the limit $\lim_{x \rightarrow 0} \operatorname{Var} [I_2^{(k)}]$. Then we find that the variance of the interference $I_2^{(k)}$ equals to $\frac{\Omega g_{mv}^2}{3N_e}$. This is the interference variance, when a subcarrier signal of the reference user is totally overlapped by the subcarrier signal of the k th interfering user, i.e. the variance of $I_1^{(k)}$ in Eq.(17.88), which can be expressed as:

$$\operatorname{Var} [I_1^{(k)}] = \frac{\Omega g_{mv}^2}{3N_e}. \quad (17.102)$$

By using a similar approach determining the term $I_2^{(k)}$, we can derive the variance of $I_2^{(s)}$, which was found to be the same as Eq.(17.101). This result in fact is predictable, since we have assumed that random spreading codes are used, when the signal associated with each chip is assumed to be an i.i.d random variable. Moreover, it can be seen that Eq.(17.101) is

independent of the user index k . Hence, the variance of $I_2^{(s)}$ can be expressed as:

$$\text{Var} \left[I_2^{(s)} \right] = \frac{\Omega g_{mv}^2 N_e}{2\pi^2 (u-m)^2 \lambda^2} \left[1 - \text{sinc} \left(\frac{2\pi(u-m)\lambda}{N_e} \right) \right]. \quad (17.103)$$

Finally, the variance of $I_1^{(s)}$ can be obtained from Eq.(17.103) by computing the limit expressed as $\lim_{u-m=x \rightarrow 0} \left(\text{Var} \left[I_2^{(s)} \right] \right)$, which results in:

$$\text{Var} \left[I_1^{(s)} \right] = \frac{\Omega g_{mv}^2}{3N_e}. \quad (17.104)$$

Before concluding this subsection, we note that the variance of the multiuser interference in the multitone DS-CDMA system of Fig.17.10 [463] can be obtained by setting $\lambda = 1$, while that in the orthogonal multicarrier DS-CDMA system of Fig.17.7 [69] can be obtained by setting $\lambda = N_e$. It can be shown that for the case of $\lambda = N_e$, the variance of $I_2^{(k)}$ can be expressed as:

$$\text{Var} \left[I_2^{(k)} \right] = \frac{\Omega g_{mv}^2}{2\pi^2 (u-m)^2 N_e}, \quad (17.105)$$

if $u-m \neq 0$. Otherwise, if $u-m=0$, it can be shown that:

$$\text{Var} \left[I_2^{(k)} \right] = \frac{\Omega g_{mv}^2}{3N_e}. \quad (17.106)$$

IN summary, In this subsection we have analyzed the multipath interference engendered by the reference user as well as the multiuser interference inflicted by the interfering users. With the aid of the analysis in this subsection, the bit error rate performance of the overlapping multicarrier DS-CDMA system can now be derived.

17.5.4 Performance Analysis

In order to derive the BER expressions of the generalized multicarrier DS-CDMA system using overlapping subcarriers, we first have to derive the PDF of the associated decision variables. We have assumed that all the interference terms in Eq.(17.77) are independent additive Gaussian variables, hence, the variable Z_{mv} of Eq.(17.77) is a Gaussian variable with normalized mean given by Eq.(17.78), and normalized variance given by:

$$\sigma^2 = \left[\frac{KL-1}{3N_e} + (U-1)(L-1)\bar{I}_s + (K-1)(U-1)L\bar{I}_M + \left(\frac{2\Omega E_b}{N_0} \right)^{-1} \right] \cdot \Omega g_{mv}^2, \quad (17.107)$$

where \bar{I}_s and \bar{I}_M are the average associated with the value of u and m , respectively, which can be expressed as:

$$\begin{aligned}\bar{I}_s &= \bar{I}_M \\ &= \frac{1}{U(U-1)} \sum_{m=1}^U \sum_{\substack{u=1 \\ u \neq m}}^U \frac{N_e}{2\pi^2(u-m)^2\lambda^2} \left[1 - \text{sinc} \left(\frac{2\pi(u-m)\lambda}{N_e} \right) \right]\end{aligned}\quad (17.108)$$

Upon substituting Eq.(17.108) into Eq.(17.107), we obtain that:

$$\sigma^2 = \left[\frac{KL-1}{3N_e} + (U-1)(KL-1)\bar{I}_M + \left(\frac{2\Omega E_b}{N_0} \right)^{-1} \right] \cdot \Omega g_{mv}^2. \quad (17.109)$$

Since Z_m of Eq.(17.75) is the sum of L independent Gaussian variables, Z_m is also a Gaussian variable. Let $g_{mv} = \alpha_{mv}$, i.e. we assume that the correlator outputs of the same data bit are combined according to the MRC scheme. Then, the normalized mean of Z_m can be expressed as:

$$E[Z_m] = b_m[0] \sum_{v=1}^L \alpha_{mv}^2, \quad (17.110)$$

and the normalized variance of Z_m can be expressed as:

$$\sigma^2 = \left[\frac{KL-1}{3N_e} + (U-1)(KL-1)\bar{I}_M + \left(\frac{2\Omega E_b}{N_0} \right)^{-1} \right] \cdot \Omega \sum_{v=1}^L \alpha_{mv}^2. \quad (17.111)$$

Consequently, the BER conditioned on encountering the subcarrier fading attenuation $\{\alpha_{mv}\}$ can be expressed as:

$$P_b(\gamma) = Q \left(\sqrt{2\gamma} \right), \quad (17.112)$$

where

$$\gamma = \bar{\gamma}_c \cdot \frac{1}{\Omega} \sum_{v=1}^L \alpha_{mv}^2, \quad (17.113)$$

and

$$\bar{\gamma}_c = \left[\frac{2(KL-1)}{3N_e} + 2(U-1)(KL-1)\bar{I}_M + \left(\frac{\Omega E_b}{N_0} \right)^{-1} \right]^{-1}. \quad (17.114)$$

As we have shown in Section 17.4, the average BER, P_b , can be derived by the weighted

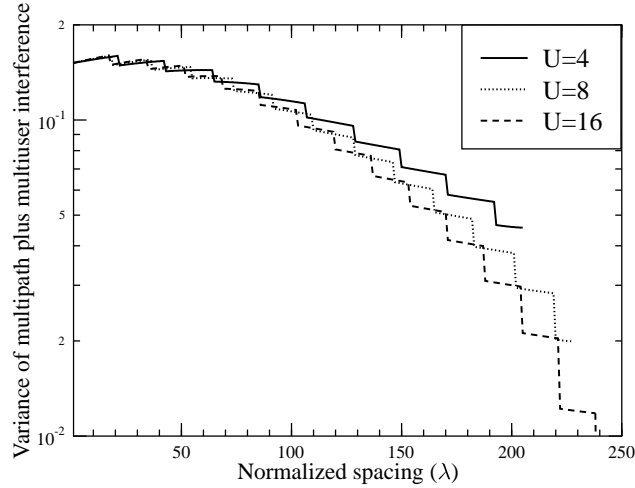


Figure 17.24: Variance of the multipath plus multiuser interference versus normalized subcarrier spacing λ performance for the overlapping multicarrier DS-CDMA system over the dispersive Rayleigh fading channels with parameters $N = 128$, $L_1 = 16$ and $K = 2$, where N and L_1 are the spreading gain and the number of resolvable paths of a corresponding single-carrier DS-CDMA system having the same data rate as well as the same system bandwidth. The results were generated by evaluating Eq.(17.111).

averaging $P_b(\gamma)$ of Eq.(17.113) over the valid range of γ , which can be expressed according to Eq.(17.57). The PDF of γ can be derived from Eq.(17.58) with N_p replaced by L . With the aid of these equations, finally, the average BER of the overlapping multicarrier DS-CDMA system using the MRC scheme can be expressed as:

$$P_b = \left[\frac{(1-\mu)}{2} \right]^L \sum_{n=0}^{L-1} \binom{L-1+n}{n} \left[\frac{(1+\mu)}{2} \right]^n, \quad (17.115)$$

where, μ is given by:

$$\mu = \sqrt{\frac{\bar{\gamma}_c}{1 + \bar{\gamma}_c}}, \quad (17.116)$$

and $\bar{\gamma}_c$ is given by Eq.(17.114).

In Fig.17.24 the variance of the multipath interference plus the multiuser interference was estimated as a function of the normalized spacing between two adjacent subcarrier frequencies. The parameters employed were $N = 128$, $L_1 = 16$, $K = 2$ and $U = 4, 8, 16$, where N and L_1 were the spreading gain and the number of resolvable paths corresponding

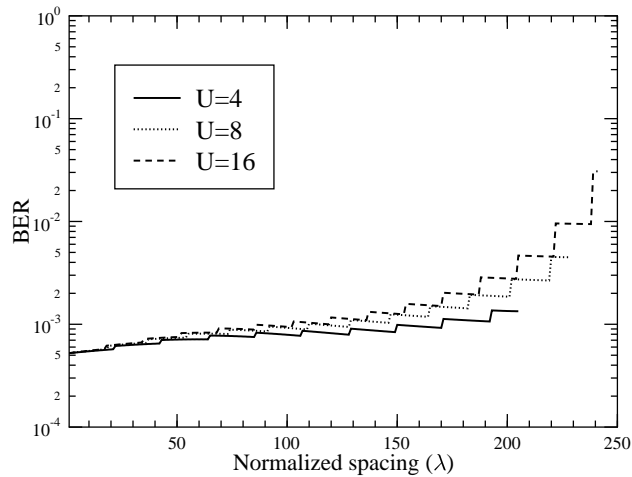


Figure 17.25: BER versus normalized subcarrier spacing λ performance for the overlapping multicarrier DS-CDMA system over the dispersive Rayleigh fading channels with parameters $N = 128$, $L_1 = 16$, $E_b/N_0 = 10dB$ and $K = 10$, where N and L_1 are the spreading gain and the number of resolvable paths of a corresponding single-carrier DS-CDMA system having the same data rate as well as the same system bandwidth. The results were computed from Eq.(17.115) by assuming that the receiver can combine all the resolvable paths.

to the single-carrier DS-CDMA system having the same data rate as well as the same system bandwidth. For a corresponding overlapping multicarrier DS-CDMA system having the same system bandwidth as the single-carrier DS-CDMA system, the spreading gain N_e , associated with each subcarrier signal and the number of resolvable paths, L of each subcarrier signal were given by Eq.(17.72) and Eq.(17.73), respectively. Note that, the system associated with $\lambda = 1$ corresponds to the multitone DS-CDMA scheme of Fig.17.10 [463], while the system using $\lambda = N_e$ corresponds to the orthogonal multicarrier DS-CDMA-II scheme of Fig.17.7 [69]. From the results seen in Fig.17.24 we find that the interference power engendered by the multipath signals and the multiuser signals decreases, as the spacing between two adjacent subcarrier frequencies becomes wider. This also implies that the multipath plus multiuser interference encountered by a given subcarrier signal in the multitone DS-CDMA scheme is higher than that experienced by a given subcarrier signal in the orthogonal multicarrier DS-CDMA-II scheme. Furthermore, observe in Fig.17.24 for a given value of λ , the variance of the multipath interference plus the multiuser interference decreases, as the number of subcarriers increases. Note that, the variance curves in Fig.17.24 appear in the shape of steps. This is because the spreading gain and the number of resolvable paths associated with each subcarrier signal only assume discrete values according to Eq.(17.72) and Eq.(17.73).

According to Eq.(17.72) and Eq.(17.73) both the spreading gain and the number of resolv-

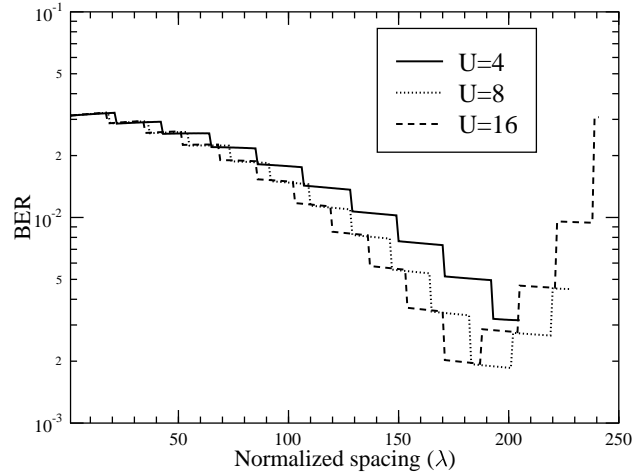


Figure 17.26: BER versus normalized subcarrier spacing λ performance for the overlapping multicarrier DS-CDMA system over the dispersive Rayleigh fading channels with parameters $N = 128$, $L_1 = 16$, $E_b/N_0 = 10dB$ and $K = 10$, where N and L_1 are the spreading gain and the number of resolvable paths of a corresponding single-carrier DS-CDMA system having the same data rate as well as the same system bandwidth. The results were computed from Eq.(17.115) by assuming that the receiver can only combine at most five paths.

able paths decreases, as the spacing between two adjacent subcarrier frequencies increases. Furthermore, according to Eq.(17.115), for a given value of $\bar{\gamma}_c$, the BER will increase, as the number of diversity branches, L that can be resolved for each subcarrier decreases. This in turn implies that the BER will increase, as the spacing between two adjacent subcarrier frequencies increases. However, according to Fig.17.24 the interference engendered by both multipath and multiuser signals becomes less severe, when increasing the normalized subcarrier spacing, λ . The resulting BER performance is determined by these two tendencies.

In Fig.17.25 the BER performance of the overlapping multicarrier DS-CDMA system was evaluated according to Eq.(17.115) as a function of the normalized subcarrier spacing λ over the dispersive Rayleigh fading channels of Section 17.3. The associated parameters were $N = 128$, $L_1 = 16$, $K = 10$, $E_b/N_0 = 10dB$ and $U = 4, 8, 16$. The subcarrier spreading gain and the number of resolvable paths of each subcarrier signal were computed with the aid of Eq.(17.72) and Eq.(17.73). With the aid of Eq.(17.73), it can be shown that the number of resolvable paths of each subcarrier decreases, as the normalized spacing, λ increases. We assumed that the receiver has the capability to combine all the resolvable paths associated with each subcarrier. From the results of Fig.17.25 we observe that, for any given number of subcarriers U , the BER increases, as the normalized spacing, λ , increases. However, the BER increase is less severe, when $\lambda < 200$. Therefore, over dispersive multipath Rayleigh

fading channels diversity reception appears more important, than the reduction of multipath and multiuser interference. According to the results of Fig.17.25, if the receiver can combine all the resolvable paths, the multitone DS-CDMA scheme of Fig.17.10 ($\lambda = 1$) outperforms the orthogonal multicarrier DS-CDMA scheme of Fig.17.7 ($\lambda = N_e$). Moreover, for any given value of λ , the overlapping multicarrier DS-CDMA scheme using a low number of subcarriers performs better than that using a high number of subcarriers.

If the complexity of the receiver is considered in terms of the diversity fingers of the RAKE receiver, it can be shown that the associated complexity of the receiver decreases, as the normalized subcarrier spacing, λ , increases. This is because, according to Eq.(17.73), the number of resolvable paths decreases, as the normalized subcarrier spacing, λ , increases. However, due to the complexity limitation of the receiver, usually the receiver cannot combine an arbitrary number of resolvable paths. Hence, in Fig.17.26 the BER of the overlapping multicarrier DS-CDMA system was estimated by assuming that the receiver can combine at most five resolvable paths for each subcarrier. If there were more than five resolvable paths, we assumed that the receiver was capable of combining five paths. However, again, if there were less than five resolvable paths for each subcarrier, we assumed that the receiver was capable of combining all the resolvable paths. The other system parameters were the same as those used in Fig.17.25 and were listed in the caption of Fig.17.26. The corresponding results of Fig.17.26 were computed from Eq.(17.115) with L replaced by the number of paths that the receiver was capable of combining. From the results of Fig.17.26 we find that, for the overlapping multicarrier DS-CDMA system having a sufficiently high number of subcarriers, both the multitone and orthogonal multicarrier DS-CDMA schemes are the suboptimum schemes. From Fig.17.26 we found that for $U = 8$ and $U = 16$, there exists an optimum normalized subcarrier spacing region in the range of $1 < \lambda < N_e$, where N_e is about 195 for $U = 8$ and 185 for $U = 16$. In this range of Fig.17.26 the overlapping multicarrier DS-CDMA scheme can achieve the minimum BER value. However, for the scheme using $U = 4$ the orthogonal multicarrier DS-CDMA system associated with $\lambda = N_e = 204$ has the best BER performance, since the number of resolvable paths at $\lambda = N_e = 204$ is still $L = 6$ according to Eq.(17.73), which is higher than the diversity combining capability of the receiver.

17.6 Performance of Multicarrier DS-CDMA-I Systems

17.6.1 Decision Variable Statistics

In this section we analyze the performance of the multicarrier DS-CDMA system of Fig.17.4 described in Subsection 17.2.2, which we referred to as the multicarrier DS-CDMA-I system. In this system a data sequence is multiplied by a spreading code and then modulates U subcarriers. Observe in Fig.17.4 that this scheme does not include serial-to-parallel data conversion. Each subcarrier signal is direct sequence (DS) spread using a common spreading sequence, as shown in Fig.17.4. Therefore, the symbol duration of the multicarrier DS-CDMA signal is the same as that of the input data bits. The transmitted signal of user k in the multicarrier

DS-CDMA-I system can be expressed as:

$$s_k(t) = \sqrt{\frac{2P}{U}} \sum_{u=1}^U b_k(t) c_k(t) \cos(2\pi f_u t + \phi_{ku}), \quad (17.117)$$

where P is the transmitted power of the multicarrier DS-CDMA-I signal, U is the number of subcarriers, while $b_k(t)$ and $c_k(t)$ are the baseband data sequence and the spreading waveforms, respectively, as we discussed previously in Section 17.5. Finally, f_u and ϕ_{ku} for $u = 1, 2, \dots, U$ are the subcarrier frequencies and modulation phases.

The users transmit over a slowly varying frequency selective Rayleigh fading channel having a delay spread of T_m and coherence bandwidth $(\Delta B)_c$, which are related by $(\Delta B)_c \approx 1/T_m$. Assuming that the spacing between two adjacent subcarrier frequencies is $\Delta = \frac{2}{T_c}$, where T_c is the chip duration of the spreading codes, no overlap exists between the mainlobes of the subcarrier signals. In this kind of multicarrier DS-CDMA systems the number of subcarriers U is chosen so as to meet the following conditions [453]:

- The subcarrier signals of the multicarrier DS-CDMA-I system experience no frequency-selectivity or no significant dispersion. Hence $T_m/T_c \leq 1$.
- All subcarrier signals are subject to independent fading, which implies that $2/T_c \geq (\Delta B)_c$.

These conditions can be expressed as:

$$\frac{1}{2} \leq \frac{T_m}{T_c} \leq 1. \quad (17.118)$$

Let T_{c1} be the chip duration of a corresponding single-carrier DS-CDMA system having the same data rate and the same bandwidth as the multicarrier DS-CDMA system considered. Then, the chip duration of the multicarrier DS-CDMA-I system considered is $T_c = UT_{c1}$. Upon substituting this into the above equation, we can see that the number of subcarriers should satisfy the condition of:

$$\frac{T_m}{T_{c1}} \leq U \leq \frac{2T_m}{T_{c1}}. \quad (17.119)$$

Since $L_1 = \lfloor T_m/T_{c1} \rfloor + 1$ represents the number of resolvable paths in the corresponding single-carrier DS-CDMA system, hence, we choose $U = L_1$.

Since in the multicarrier DS-CDMA-I system of Fig.17.4 satisfying the condition of Eq.(17.118) each subcarrier signal is subject to independent frequency non-selective fading, the received signal associated with K number of asynchronous users can be expressed as:

$$r(t) = \sum_{k=1}^K \sum_{u=1}^U \sqrt{\frac{2P}{U}} \alpha_{ku} b_k(t - \tau_k) c_k(t - \tau_k) \cos(2\pi f_u t + \varphi_{ku}) + n(t), \quad (17.120)$$

where $\varphi_{ku} = \phi_{ku} + \psi_{ku} - 2\pi f_u \tau_k$ is a random variable uniformly distributed in $[0, 2\pi)$, while

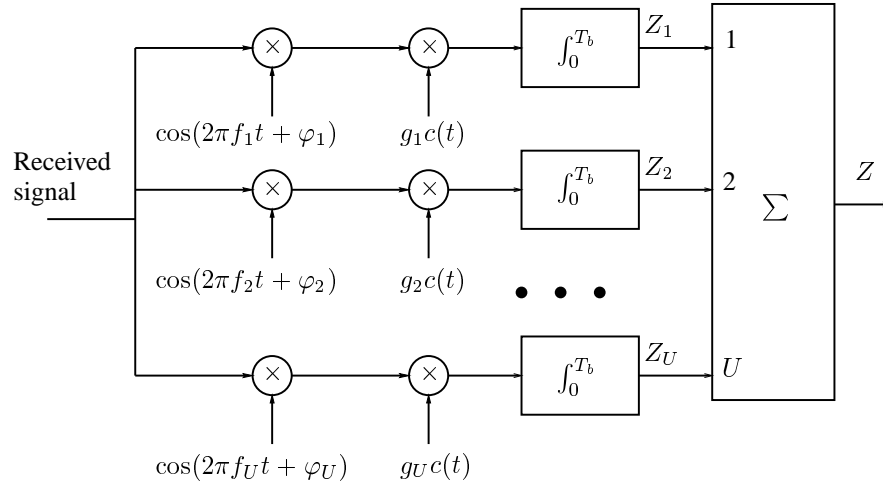


Figure 17.27: The receiver block diagram matched to the reference user $k = 1$ in the multicarrier DS-CDMA-I system.

α_{ku} , τ_k and ψ_{ku} are the channel amplitude, delay and phase, respectively, corresponding to the subcarrier u of user k . Finally, $n(t)$ represents the AWGN with double-sided power spectral density of $N_0/2$.

The receiver block diagram for the reference user is shown in Fig.17.27, where the index of $k = 1$ is omitted and $\tau_1 = 0$ is assumed for notational convenience. In the multicarrier DS-CDMA-I system, frequency diversity is achieved by combining the correlator's outputs associated with the subcarriers. The receiver provides a correlator for each subcarrier and the outputs of the correlators are combined in order to yield a processing gain comparable to that of a single-carrier DS system, provided that the spacing between two adjacent subcarriers is $\Delta = \frac{2}{T_c}$. Referring to Fig.17.27, the decision variable corresponding to the 0th data bit can be expressed as:

$$Z = \sum_{v=1}^U Z_v, \tag{17.121}$$

$$Z_v = \int_0^{T_b} r(t)g_v c(t) \cos(2\pi f_v t + \varphi_v) dt, \tag{17.122}$$

where $g_v = \alpha_v$ is assumed, associated with perfect channel estimation and a MRC diversity combining scheme. According to Eq.(17.101), in the multicarrier DS-CDMA-I system of Fig.17.4, the normalized variance of the multiuser interference engendered by an adjacent subcarrier signal is $\frac{g_v^2}{8\pi^2 N_e}$, which is derived from Eq.(17.101) by setting $u - m = 1$, $\lambda = 2N_e$, $g_{mv} = g_v$ and $\Omega = 1$. It can be shown that $\frac{g_v^2}{8\pi^2 N_e}$ is significantly lower than $g_v^2/3N_e$. Therefore, in our following analysis we ignore the interference imposed by the subcarrier

signals other than the subcarrier considered. Consequently, Z_v can be expressed as:

$$Z_v = \sqrt{\frac{P}{2U}} \left[D_v + \sum_{k=2}^K I_k + \eta_v \right], \quad (17.123)$$

where D_v is the desired output, which is given by:

$$D_v = b[0] \alpha_v^2. \quad (17.124)$$

Furthermore, I_k , $k = 2, 3, \dots, K$ represents the normalized multiuser interference inflicted by user k , which can be expressed as:

$$I_k = \frac{\alpha_{kv} \alpha_v \cos \theta_{kv}}{T_b} \left[b_k[-1] R_k(\tau_k) + b_k[0] \hat{R}_k(\tau_k) \right], \quad (17.125)$$

where $\theta_{kv} = \varphi_{kv} - \varphi_v$. The variables $R_k(\tau_k)$ and $\hat{R}_k(\tau_k)$ are the partial cross-correlation functions defined by Eqs.(17.89) and (17.90), while I_k can be approximated as a Gaussian random variable with zero mean and variance of $\alpha_v^2/3N_e$. Finally, η_v in Eq.(17.123) is a Gaussian random variable with zero mean and variance of $U \alpha_v^2 N_0/2E_b$, where $E_b = PT_b$ is the energy per bit.

Therefore, Z_v can be approximated as a Gaussian random variable having a normalized mean given by D_v and a normalized variance of $[1/3N_e + UN_0/2E_b] g_v^2$. Since Z is the sum of U independent Gaussian random variables, Z is also approximately Gaussian distributed with a mean given by:

$$E[Z] = b[0] \sum_{v=1}^U \alpha_v^2, \quad (17.126)$$

and variance of:

$$\text{Var}[Z] = \left[\frac{K-1}{3N_e} + \left(\frac{2E_b}{UN_0} \right)^{-1} \right] \sum_{v=1}^U \alpha_v^2. \quad (17.127)$$

Having obtained the statistics of the decision variable, let us now derive the BER expression for the multicarrier DS-CDMA-I system in the following subsection.

17.6.2 Performance Analysis

Since the decision variable Z can be modelled as a Gaussian variable having a normalized mean given by Eq.(17.126) and a normalized variance given by Eq.(17.127), the BER conditioned on a set of channel fading amplitudes $\{\alpha_v, v = 1, 2, \dots, U\}$ can be expressed as:

$$P_b(\gamma) = Q \left(\sqrt{2\gamma} \right), \quad (17.128)$$

where

$$\gamma = \bar{\gamma}_c \sum_{v=1}^U \alpha_v^2, \quad (17.129)$$

and

$$\bar{\gamma}_c = \left[\frac{2(K-1)}{3N_e} + \left(\frac{E_b}{UN_0} \right)^{-1} \right]^{-1}. \quad (17.130)$$

The unconditional BER can be derived by averaging Eq.(17.128) - after weighting it with the PDF of γ - over the valid range of γ using a similar approach to that in Section 17.5. Finally, the unconditional BER can be expressed as:

$$P_b = \left[\frac{(1-\mu)}{2} \right]^U \sum_{n=0}^{U-1} \binom{U-1+n}{n} \left[\frac{(1+\mu)}{2} \right]^n, \quad (17.131)$$

where, μ is given by:

$$\mu = \sqrt{\frac{\bar{\gamma}_c}{1+\bar{\gamma}_c}}, \quad (17.132)$$

and $\bar{\gamma}_c$ is given by Eq.(17.130).

17.7 Performance of Multicarrier DS-CDMA Systems Using Adaptive Subchannel Allocation

The multicarrier DS-CDMA scheme using adaptive subchannel allocation – which was portrayed in Fig.17.15 and referred to as the adaptive AMC DS-CDMA scheme – has been proposed and studied in [439]. The adaptive AMC DS-CDMA scheme represents the extension of the multicarrier DS-CDMA scheme [453] of Fig.17.4 for the forward links. In contrast to the multicarrier DS-CDMA scheme of [453], where identical DS waveforms are transmitted over each of the subchannels, in adaptive AMC DS-CDMA each user's DS waveform is transmitted over the user's favorite subchannel exhibiting the highest amplitude [439]. The channel's fading amplitudes are estimated at the mobile for all subchannels and the index of the best subchannel is fed back to the base station.

In this section, we investigate the performance of the adaptive AMC DS-CDMA system of Fig.17.15 discussed in Subsection 17.2.6. Again, this scheme can be viewed as the extension of the multicarrier DS-CDMA scheme investigated in Section 17.6. In our investigations we assume that random spreading codes are employed and the channel is frequency-selective Rayleigh fading, but each subchannel's fading amplitude is an i.i.d random variable obeying the Rayleigh distribution. We assume, for simplicity that the channel's fading amplitudes are

perfectly estimated and fed back from the mobile station to the base station without delay and feedback transmission errors. This assumption has often been used in the literature in order to derive the best-case performance estimate of systems with the aid of perfect channel quality side-information [75]. Furthermore, we assume that the multiuser interference can be approximated by an additive Gaussian random variable having zero mean, as we assumed in the previous sections.

In the adaptive AMC DS-CDMA system of Fig.17.15 the signal transmitted on the down link by the base station can be expressed as in Eq.(17.18), which can be rewritten as:

$$\begin{aligned} s_k(t) &= \sum_{k=1}^K \sqrt{2P} b_k(t) c_k(t) \sum_{u=1}^U \Delta_u(i_k) \cos(2\pi f_u t + \phi_{ku}) \\ &+ \sum_{u=1}^U \sqrt{2P_0} c_0(t) \cos(2\pi f_u t + \phi_u), \end{aligned} \quad (17.133)$$

where P represents the power transmitted by the base station to each user, P_0 represents the transmitted power of the pilot signal that is transmitted by the base station on each subcarrier, in order to facilitate the selection of the best subchannel for the transmission of the useful data to the mobiles, $b_k(t)$ and $c_k(t)$ represent the data waveform and spreading code waveform of the k th user, while $c_0(t)$ represents the spreading code waveform of the pilot signal. Finally,

$$\Delta_u(i_k) = \begin{cases} 1, & \text{for } u = i_k \\ 0, & \text{for } u \neq i_k, \end{cases} \quad (17.134)$$

indicating that only one subcarrier is activated by each user.

Assuming that frequency non-selective fading is experienced by the U subcarrier signals and that the K number of down link user signals plus the associated pilot signal used for estimating the down link subchannel quality are transmitted synchronously, the signal received by the mobile can be expressed as:

$$\begin{aligned} r(t) &= \sum_{k=1}^K \sqrt{2P} \alpha_{i_k} b_k(t) c_k(t) \cos(2\pi f_{i_k} t + \varphi_{ki_k}) \\ &+ \sum_{u=1}^U \sqrt{2P_0} \alpha_u c_0(t) \cos(2\pi f_u t + \varphi_u) \\ &+ n(t), \end{aligned} \quad (17.135)$$

where $\varphi_{ki_k} = \phi_{ki_k} + \psi_{ki_k}$, $\varphi_u = \phi_u + \psi_u$, $n(t)$ is the AWGN.

The mobile's receiver block diagram for the AMC DS-CDMA scheme was shown in Fig.17.16, where the coherent demodulation phases associated with the i th subchannel and the despreading code are incorporated in the term of $g_0[i]$, $i = 1, 2, \dots, U$ corresponding to the detection of the pilot signal used for the estimation of the subchannel quality. Similarly, the term of $g_k[i_k]$ corresponds to the k th user's data detection. Explicitly, at the mobile, the

index of the best subchannel is determined by estimating the fading amplitudes of the subchannels with the aid of the known pilot signal. We assume that the first user is the reference user and ignore the user index related to the reference user associated with $k = 1$. Let i_1 be the best subchannel, which is being used for the 0th data bit's transmission. We assume that there are K_h out of $K - 1$ active interfering users who share the i_1 th subchannel with the reference user. Therefore, assuming perfect estimation of the subchannels' amplitudes and phases, the decision variable, Z seen at the output of the mobile's receiver schematic, can be expressed in the form of:

$$\begin{aligned} Z &= \int_0^{T_b} r(t) \alpha_{i_1} c_1(t) \cos(2\pi f_{i_1} t + \varphi_{i_1}) dt \\ &= \sqrt{\frac{P}{2}} T_b \left[D_{i_1} + \sum_{k_h=1}^{K_h} I_{k_h} + I_0 + \eta_{i_1} \right], \end{aligned} \quad (17.136)$$

where D_{i_1} represents the term associated with the desired user, which can be expressed as:

$$D_{i_1} = b[0] \alpha_{i_1}^2, \quad (17.137)$$

and I_{k_h} is the multiuser interference imposed by from the k th user, which can be expressed as:

$$\begin{aligned} I_{k_h} &= \frac{\alpha_{i_k} \alpha_{i_1} \cos(\theta_{i_k})}{T_b} \int_0^{T_b} b_{k_h}(t) c_k(t) c_1(t) dt \\ &= \frac{\alpha_{i_k} \alpha_{i_1} \cos(\theta_{i_k}) b_{k_h}[0]}{N_e} \sum_{n=0}^{N_e-1} c_n^{(k)} c_n^{(1)}. \end{aligned} \quad (17.138)$$

The multiuser interference term I_{k_h} can be approximated by a Gaussian random variable with mean zero and variance of:

$$\text{Var}[I_{k_h}] = \frac{\Omega_M \alpha_{i_1}^2}{2N_e}, \quad (17.139)$$

where $\Omega_M = E[\alpha_M^2]$, while α_M represents the fading amplitude corresponding to the best subchannel of user k . Since $\{\alpha_{ki}, i = 1, 2, \dots, U\}$ are Rayleigh distributed random variables obeying a PDF given by Eq.(17.23), $\{\alpha_{ki}^2, i = 1, 2, \dots, U\}$ obey exponential distributions having a PDF given by:

$$f_{\alpha_{ki}^2}(R) = \frac{1}{\Omega} \exp\left(-\frac{R}{\Omega}\right), \quad R \geq 0. \quad (17.140)$$

The PDF of $\alpha_M^2 = \max \{ \alpha_{k1}^2, \alpha_{k2}^2, \dots, \alpha_{kU}^2 \}$ can be derived using the following formula:

$$f_{\alpha_M^2}(r) = \frac{d}{dr} \left[\int_0^r f_{\alpha_{ki}^2}(R) dR \right]^U. \quad (17.141)$$

Upon substituting Eq.(17.140) into Eq.(17.141), we obtain:

$$f_{\alpha_M^2}(r) = \frac{U}{\Omega} \exp\left(-\frac{r}{\Omega}\right) \left[1 - \exp\left(-\frac{r}{\Omega}\right)\right]^{U-1}, \quad r \geq 0. \quad (17.142)$$

With the aid of Eq.(17.142) Ω_M is given by:

$$\begin{aligned} \Omega_M &= E[\alpha_M^2] \\ &= \int_0^\infty r \cdot f_{\alpha_M^2}(r) dr \\ &= \int_0^\infty r \frac{U}{\Omega} \exp\left(-\frac{r}{\Omega}\right) \left[1 - \exp\left(-\frac{r}{\Omega}\right)\right]^{U-1} dr \\ &= U\Omega \sum_{n=0}^{U-1} \binom{U-1}{n} \frac{(-1)^n}{(n+1)^2}. \end{aligned} \quad (17.143)$$

In Eq.(17.136) I_0 represents the interference engendered by the pilot signal. Assuming that the interference due to the subcarriers other than subcarrier i_1 of interest can be ignored, I_0 can be expressed as:

$$\begin{aligned} I_0 &= \left(\sqrt{\frac{P}{2}} T_b \right)^{-1} \int_0^{T_b} \sqrt{2P_0} \alpha'_{i_1} c_0(t) \cos(2\pi f_{i_1} t + \varphi_{i_1}) \\ &\quad \alpha_{i_1} c_1(t) \cos(2\pi f_{i_1} t + \varphi_{1i_1}) dt \\ &= \frac{\sqrt{\rho} \alpha'_{i_1} \alpha_{i_1} \cos \theta_{i_1}}{N_e} \sum_{n=0}^{N_e-1} c_n^{(0)} c_n^{(1)}, \end{aligned} \quad (17.144)$$

where $\rho = P_0/P$ represents the ratio between the power of the pilot signal transmitted by the base station on each subcarrier and that of the reference signal. The fading amplitude of the pilot signal on subcarrier i_1 is denoted by α'_{i_1} . For a given value of α_{i_1} , I_0 can also be approximated a Gaussian random variable with zero mean and variance of:

$$\text{Var}[I_0] = \frac{\rho \Omega_M \alpha_{i_1}^2}{2N_e}. \quad (17.145)$$

Finally, η_{i_1} is a Gaussian random variable with mean zero and variance given by $N_0/2E_b$.

Consequently, for a given fading amplitude of α_{i_1} , the decision variable Z at the output of the mobile's receiver schematic seen in Fig.17.16 can be approximated by a Gaussian random variable having a normalized mean given by Eq.(17.137), and a normalized variance given

by:

$$\text{Var}[Z] = \left[\frac{K_h + \rho}{2N_e} + \left(\frac{2\Omega_M E_b}{N_0} \right)^{-1} \right] \Omega_M \alpha_{i_1}^2. \quad (17.146)$$

The bit error probability for a given fading amplitude of α_{i_1} and for K_h number of users activating the i_1 th subcarrier can be expressed as:

$$P_b(\alpha_{i_1}^2, K_h) = Q \left(\sqrt{\bar{\gamma}_c \cdot \frac{2\alpha_{i_1}^2}{\Omega_M}} \right), \quad (17.147)$$

where

$$\bar{\gamma}_c = \left[\frac{K_h + \rho}{N_e} + \left(\frac{\Omega_M E_b}{N_0} \right)^{-1} \right]^{-1}. \quad (17.148)$$

Since the i_1 th subchannel was assumed to be the best subchannel during the 0th bit's transmission, i.e., $\alpha_{i_1}^2 = \max \{\alpha_1^2, \alpha_2^2, \dots, \alpha_U^2\}$, $\alpha_{i_1}^2$ has the same PDF as α_M^2 which was given by Eq.(17.142). Therefore, the conditioning of $P_b(\alpha_{i_1}^2, K_h)$ on $\alpha_{i_1}^2$ can be removed by the weighted averaging of Eq.(17.147) according to its PDF $f_{\alpha_{i_1}^2}(r)$ of Eq.(17.142) over the valid range of $\alpha_{i_1}^2$, which can be expressed as:

$$\begin{aligned} P_b(K_h) &= \int_0^\infty P_b(r, K_h) f_{\alpha_{i_1}^2}(r) dr \\ &= \int_0^\infty Q \left(\sqrt{\bar{\gamma}_c \cdot \frac{2r}{\Omega_M}} \right) \times \frac{U}{\Omega} \exp \left(-\frac{r}{\Omega} \right) \left[1 - \exp \left(-\frac{r}{\Omega} \right) \right]^{U-1} dr \\ &= \sum_{n=0}^{U-1} \frac{(-1)^n}{\sqrt{2\pi}} \binom{U-1}{n} \frac{U}{\Omega} \int_0^\infty \int_{\sqrt{\frac{2r}{\bar{\gamma}_c \Omega_M}}}^\infty \exp \left(-\frac{t^2}{2} \right) \exp \left(-\frac{(n+1)r}{\Omega} \right) dt dr. \end{aligned} \quad (17.149)$$

Interchanging the order of integration associated with t and r , Eq.(17.149) can be written as:

$$P_b(K_h) = \sum_{n=0}^{U-1} \frac{(-1)^n}{\sqrt{2\pi}} \binom{U-1}{n} \frac{U}{\Omega} \int_0^\infty \int_0^{\frac{\Omega_M t^2}{2\bar{\gamma}_c}} \exp \left(-\frac{t^2}{2} \right) \exp \left(-\frac{(n+1)r}{\Omega} \right) dt dr. \quad (17.150)$$

Upon evaluating out the above integrals, Eq.(17.150) can be simplified to:

$$P_b(K_h) = \frac{U}{2} \sum_{n=0}^{U-1} \frac{(-1)^n}{(n+1)} \binom{U-1}{n} \left[1 - \sqrt{\frac{\bar{\gamma}_c \Omega}{\bar{\gamma}_c \Omega + (n+1)\Omega_M}} \right]. \quad (17.151)$$

Since

$$U \sum_{n=0}^{U-1} \frac{(-1)^n}{(n+1)} \binom{U-1}{n} = 1, \quad (17.152)$$

Eq.(17.151) can be rewritten as:

$$\begin{aligned} P_b(K_h) &= \frac{1}{2} + \frac{U}{2} \sum_{n=0}^{U-1} \frac{(-1)^{n+1}}{(n+1)} \binom{U-1}{n} \sqrt{\frac{\bar{\gamma}_c \Omega}{\bar{\gamma}_c \Omega + (n+1)\Omega_M}} \\ &= \frac{1}{2} + \frac{1}{2} \sum_{n=1}^U (-1)^n \binom{U}{n} \sqrt{\frac{\bar{\gamma}_c \Omega}{\bar{\gamma}_c \Omega + n\Omega_M}}. \end{aligned} \quad (17.153)$$

If we assume that the channel attenuation for a given mobile is independent of the channel quality for any other mobile and that the probability of choosing any specific subchannel as the best subchannel from the set of U subchannels is equiprobable, the probability that there are K_h out of $K-1$ number of interfering users activating the i_1 th subchannel can be expressed as:

$$P(K_h) = \binom{K-1}{K_h} \left(\frac{1}{U}\right)^{K_h} \left(1 - \frac{1}{U}\right)^{K-1-K_h}. \quad (17.154)$$

The unconditional BER, consequently, can be expressed as [439]:

$$\begin{aligned} P_b &= \sum_{K_h=0}^{K-1} P(K_h) P_b(K_h) \\ &= \sum_{K_h=0}^{K-1} \binom{K-1}{K_h} \left(\frac{1}{U}\right)^{K_h} \left(1 - \frac{1}{U}\right)^{K-1-K_h} P_b(K_h), \end{aligned} \quad (17.155)$$

where $P_b(K_h)$ is given by Eq.(17.153).

In Fig.17.28 and Fig.17.29 we compared the down link BER performance of the multicarrier DS-CDMA-I system of Fig.17.4, which was analyzed in Section 17.6, and that of the adaptive AMC DS-CDMA system of Fig.17.15 and Fig.17.16 investigated in this section. In Fig.17.28 the BER was evaluated as a function of the SNR per bit E_b/N_0 by assuming that the spreading gain of a corresponding single-carrier DS-CDMA system was $N = N_e U = 256$ and the number of active users was $K = 20$. By contrast, in Fig.17.29 the BER was evaluated as a function of the number of active users K by assuming that the spreading gain of the corresponding single-carrier DS-CDMA system was also $N = N_e U = 256$ and the SNR per bit was $E_b/N_0 = 8$ dB. Therefore, the spreading gain of each subcarrier signal was $N_e = 64$ for $U = 4$ and $N_e = 32$ for $U = 8$. The results for the adaptive AMC DS-CDMA scheme were computed according to Eq.(17.155) with $\bar{\gamma}_c$ given by Eq.(17.148), while the results for the multicarrier DS-CDMA-I scheme were computed from Eq.(17.131) with $\bar{\gamma}_c$ given by Eq.(17.130). However, since synchronous transmissions are usually employed in

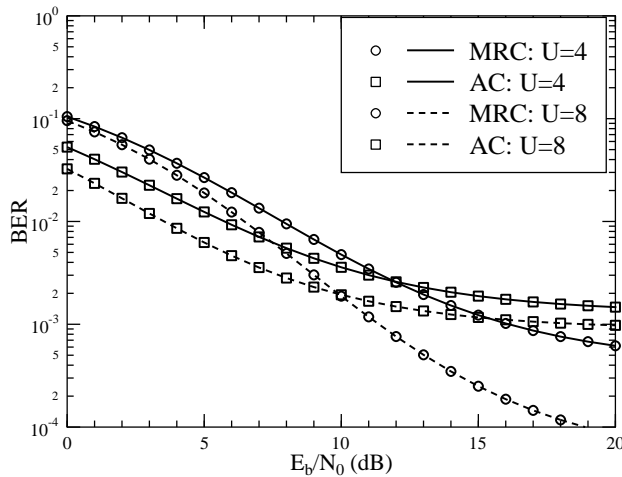


Figure 17.28: Down link BER versus SNR per bit, E_b/N_0 , performance comparison for the multicarrier DS-CDMA-I system of Fig.17.4 and the adaptive AMC DS-CDMA system of Fig.17.15 over dispersive Rayleigh fading channels with parameters of $N = 256$, $K = 20$ and $U = 4, 8$, where N is the spreading gain of a corresponding single-carrier DS-CDMA system. The results were computed from Eq.(17.131) for the multicarrier DS-CDMA-I scheme, while from Eq.(17.155) for the AMC DS-CDMA scheme.

the down link, the term $3N_e$ in Eq.(17.130) should be replaced by $2N_e$, according to the derivation of Eq.(17.148) in this section. From the results of Fig.17.28 we observe that for low to moderate SNR per bit value, the adaptive AMC DS-CDMA scheme outperforms the multicarrier DS-CDMA-I scheme, as long as the receiver can maintain near-perfect channel estimation with the aid of the pilot signals and provided that there are no feedback errors concerning the choice of the best subchannel. However, if the SNR per bit in excess of $E_b/N_0 > 14dB$ for $U = 4$ and $E_b/N_0 > 12dB$ for $U = 8$, the above-mentioned trend is reversed, in other words, the adaptive AMC DS-CDMA scheme is outperformed by the multicarrier DS-CDMA-I scheme. In Fig.17.29 the adaptive AMC DS-CDMA scheme outperforms the multicarrier DS-CDMA-I scheme over the entire range of the number of active users investigated, namely from $K = 1$ to $K = 50$, when SNR per bit of $E_b/N_0 = 8dB$ was assumed. Furthermore, since multicarrier systems using a high number of subcarriers can achieve a high diversity order, we infer from the results of both Fig.17.28 and Fig.17.29 that for any given value of E_b/N_0 or any given number of active users, K , the BER performance of the system using a high number of subcarriers, such as $U = 8$, is better than that of the system employing a low number of subcarriers, such as $U = 4$.

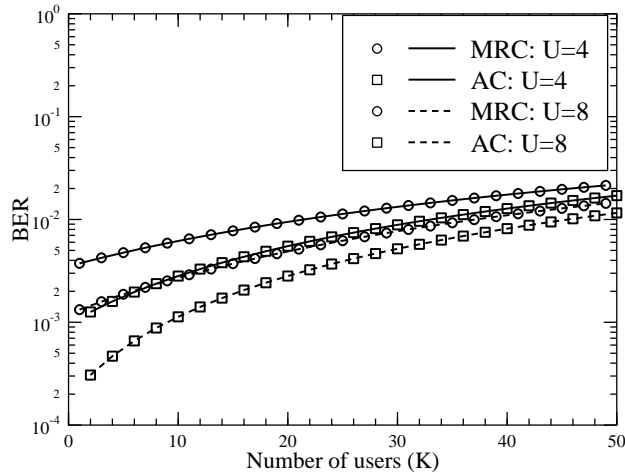


Figure 17.29: Down link BER versus number of users, K , performance comparison for the multicarrier DS-CDMA-I of Fig.17.4 system and the adaptive AMC DS-CDMA system of Fig.17.15 over dispersive Rayleigh fading channels with parameters of $N = 256$, $E_b/N_0 = 8dB$ and $U = 4, 8$, where N is the spreading gain of a corresponding single-carrier DS-CDMA system. The results were computed from Eq.(17.131) for the multicarrier DS-CDMA-I scheme, while from Eq.(17.155) for the AMC DS-CDMA scheme.

17.8 Performance of Slow Frequency-Hopping Multicarrier DS-CDMA Systems

In this section we investigate the performance of the SFH/MC DS-CDMA system seen in Fig.17.17, when using BPSK data modulation. Its performance is evaluated over a range of multipath Rayleigh fading channels. Two detection schemes are investigated in conjunction with the receiver having perfect knowledge or no knowledge of the FH patterns employed. When the receiver invokes the explicit knowledge of the FH patterns used, then conventional hard-detection - which is often applied in direct-sequence, slow frequency-hopping CDMA (DS/SFH CDMA) [408, 465] systems - is employed for the sake of simplifying the receiver. By contrast, when the receiver does not have any knowledge concerning the FH pattern used, then the joint soft-detection techniques are used, in order to simultaneously accomplish both demodulation and FH pattern acquisition.

17.8.1 System Description

17.8.1.1 The Transmitted Signal

The SFH/MC DS-CDMA system has been reviewed in Subsection 17.2.7, where the model of the transmitter and the multiple access channel was depicted in Fig. 17.17. Referring to Fig. 17.17, the transmitted signal of user k can be expressed as:

$$s_k(t) = \sum_{u_k=0}^{U_k-1} \sqrt{2P} b_{ku_k}(t) c_k(t) \cos \left(2\pi f_{u_k}^{(k)} t + \varphi_{u_k}^{(k)} \right), \quad (17.156)$$

where P represents the transmitted power per subcarrier, while U_k indicates the weight of the constant-weight code currently employed by the k th user, and $c_k(t)$ represents the spreading waveform. Furthermore, $\{b_{ku_k}(t)\}$, $\{f_{u_k}^{(k)}\}$ and $\{\varphi_{u_k}^{(k)}\}$ represent the current data stream's waveforms, the subcarrier frequency set and the phase angles introduced in the carrier modulation process. The data stream's waveform $b_{ku_k}(t) = \sum_{i=-\infty}^{\infty} b_{ku_k}^{(i)} P_{T_s}(t - iT_s)$ consists of a sequence of mutually independent rectangular pulses of duration T_s and of amplitude +1 or -1 with equal probability. The spreading sequence $c_k(t) = \sum_{j=-\infty}^{\infty} c_k^{(j)} P_{T_c}(t - jT_c)$ denotes

the signature sequence waveform of the k th user, where $c_k^{(j)}$ assumes values of +1 or -1 with equal probability, while $P_{T_c}(t)$ is the common chip waveform for all signals. In our analysis for the sake of simplicity we assume that there exists no spectral overlap between the spectral main-lobes of two adjacent subcarriers, and also assume that there exists no interference between subcarriers. More explicitly, interference is inflicted only, when an interfering user activates the same subcarrier, as the reference user. Let $N_b = T_b/T_c$ be the number of chips per bit, where T_b is the bit duration before the serial-to-parallel conversion stage of Fig.17.17. Let the processing gain of each subcarrier signal be N_e , which can be expressed as $N_e = T_s/T_c$. Furthermore, we assume that the frequency hopping duration is T_h , and that the number of data bits $N_h = T_h/T$ transmitted per hop is a positive integer, which is strictly larger than 1, i.e. we assume using slow frequency hopping.

17.8.1.2 Channel Description

The channel model considered in this section is the finite-length tapped delay line model of a frequency-selective multipath channel [95], whose complex low-pass impulse response for subcarrier u_k of user k is given by:

$$h_{u_k}^{(k)}(t) = \sum_{l_p=0}^{L_p-1} \alpha_{u_k, l_p}^{(k)} e^{j\phi_{u_k, l_p}^{(k)}} \delta(t - l_p T_c). \quad (17.157)$$

In Eq.(17.157) $l_p T_c$ is the relative delay of the l_p -th path of user k with respect to the main path, the phases $\{\phi_{u_k, l_p}^{(k)}\}$ are i.i.d random variables uniformly distributed in the interval

$[0, 2\pi)$, whilst the L_p tap weights $\{\alpha_{u_k, l_p}^{(k)}\}$ are independent Rayleigh distributed random variables with a PDF given by Eq.(17.23). Consequently, for an asynchronous CDMA system supporting K users, the received signal takes the form of:

$$\begin{aligned} r(t) &= n(t) \\ &+ \sqrt{2P} \cdot \sum_{k=1}^K \sum_{u_k=0}^{U_k-1} \sum_{l_p=0}^{L_p-1} \alpha_{u_k, l_p}^{(k)} b_{ku}^{(k)}(t - l_p T_c - \tau_k) \\ &\quad \cdot c_k(t - l_p T_c - \tau_k) \cos\left(2\pi f_{u_k}^{(k)} t + \psi_{u_k, l_p}^{(k)}\right), \end{aligned} \quad (17.158)$$

where $n(t)$ represents the AWGN with zero mean and double-sided power spectral density of $N_0/2$, $\psi_{u_k, l_p}^{(k)} = \left[\varphi_{u_k}^{(k)} + \phi_{u_k, l_p}^{(k)} - 2\pi f_{u_k}^{(k)}(\tau_k + l_p T_c)\right] \pmod{2\pi}$, which is assumed to be an i.i.d random variable having a uniform distribution in $[0, 2\pi)$, and τ_k represents the propagation delay of user k .

17.8.1.3 Receiver Model

Let the first user be the user-of-interest and consider the conventional matched filter based RAKE receiver using MRC, as shown in Fig. 17.18, where the superscript and subscript of the reference user's signal has been omitted for notational convenience. In Fig. 17.18 L - the number of diversity branches used by the receiver - $1 \leq L \leq L_p$ is a variable, allowing us to study the effect of different diversity orders. In contrast to the transmitter side of Fig.17.17, where only U_k out of U subcarriers are transmitted by the user k , at the receiver of Fig. 17.18 all U subcarriers are always tentatively demodulated. Furthermore, the information bits transmitted over the different subcarriers might be detected using hard-detection separately, or using blind soft-detection jointly for all subcarriers. The choice of soft-detection depends on whether the receiver is capable of acquiring the FH patterns blindly, i.e., without their explicit signalling. This important issue will be discussed in the forthcoming Sections. Consequently, from the point of view of the receiver, each subcarrier can be viewed as an On-Off type signalling scheme. When a subcarrier is actively used for signalling and hence it is in the On-state, the MRC output samples give +1 or -1 information. Otherwise, while passive and hence in the Off-state, the MRC stage outputs noise.

The U number of matched filters in Fig. 17.18 are matched to the reference user's spreading code, and are assumed to have achieved time synchronization. Let us assume that perfect estimates of the channel tap weights and phases are available. Then - after appropriately delaying the individual matched filter outputs, in order to coherently combine the L number of path signals used by the RAKE combiner - the q th MRC output sampled at $t = T + (L-1)T_c$, in order to detect the first symbol can be expressed as:

$$Z_q = D_q[0] + I_q, \quad (17.159)$$

where $D_q[0]$ represents the desired direct component, which can be expressed as:

$$D_q[0] = \sqrt{\frac{P}{2}} T_s b_q[0] \sum_{l=0}^{L-1} \alpha_{q,l}^2. \quad (17.160)$$

In Eq.(17.160) $b_q[0]$ is the first bit transmitted on subcarrier q by the reference user and $b_q[0] \in \{+1, -1, 0\}$ with '0' representing the Off-state. Since we have assumed that there exists no interference amongst the subcarriers, interference is inflicted only, when an interfering user activates the same subcarrier, as the reference user. Hence, the interference plus noise term I_q in Eq.(17.159) can be expressed as:

$$I_q = I_q[S] + I_q[M] + N_q, \quad (17.161)$$

where $I_q[S]$ represents the multipath interference imposed by the q -th subcarrier of the user-of-interest, which can be expressed as:

$$\begin{aligned} I_q[S] = & \left(\sqrt{\frac{P}{2}} T_s \right) \sum_{l=0}^{L-1} \alpha_{q,l} \sum_{\substack{l_p=0 \\ l_p \neq l}}^{L_p-1} \frac{\alpha_{q,l_p} \cos \theta_{q,l_p}}{T_s} \\ & \cdot \int_{(L-1)T_c}^{T_s+(L-1)T_c} b_q[t - (L + l_p - l - 1)T_c] \\ & \cdot c[t - (L + l_p - l - 1)T_c] c[t - (L - 1)T_c] dt, \end{aligned} \quad (17.162)$$

where $I_q[M]$ represents the multiuser interference inflicted the q -th subcarriers of the interfering users. Let us assume that there exists K_h , ($0 \leq K_h \leq K - 1$) number of interfering signals, all of which activate the q -th subcarrier during the first symbol's transmission of the reference signal. The event, when an interferer activates the same subcarrier as the reference user, is often referred to in the literature as a so-called *hit* - an event that will be discussed in detail in the next Subsection. Then, $I_q[M]$ can be expressed as:

$$\begin{aligned} I_q[M] = & \left(\sqrt{\frac{P}{2}} T_s \right) \sum_{l=0}^{L-1} \alpha_{q,l} \sum_{h=1}^{K_h} \sum_{l_p=0}^{L_p-1} \frac{\alpha_{q,l_p}^{(h)} \cos \theta_{q,l_p}^{(h)}}{T} \\ & \cdot \int_{(L-1)T_c}^{T_s+(L-1)T_c} b_q^{(h)}[t - (L + l_p - l - 1)T_c - \tau_h] \\ & \cdot c_h[t - (L + l_p - l - 1)T_c - \tau_h] c[t - (L - 1)T_c] dt. \end{aligned} \quad (17.163)$$

In Eq.(17.162) and (17.163) the $\cos(\cdot)$ terms are contributed by the phase differences between the incoming subcarriers and the locally generated subcarrier used in the demodulation. Fi-

nally, the noise term of Eq.(17.161) can be expressed as:

$$N_q = \sum_{l=0}^{L-1} \alpha_{q,l} \int_{(L-1)T_c}^{T_s+(L-1)T_c} n(t)c[t - (L-1)T_c] \cos(2\pi f_q t + \psi_{q,l}) dt, \quad (17.164)$$

which is a Gaussian random variable with zero mean and variance of $\frac{N_0 T_s}{4} \sum_{l=0}^{L-1} \alpha_{q,l}^2$, where $\{\alpha_{q,l}\}$ represents the path attenuations.

We have obtained the decision variables of the MRC output samples. Let us now analyze the BER performance of the SFH/MC DS-CDMA system using hard-detection by invoking the often-used Gaussian approximation.

17.8.2 Performance of the SFH/MC DS-CDMA Receiver with Explicit Knowledge of the FH Patterns: Hard-Detection

17.8.2.1 Probability of Error

In the analysis of this section, we employ the Gaussian approximation and hence model the multiuser interference and the self-interference terms of Eq.(17.161) as an AWGN process having zero mean and a variance equal to the corresponding variances. Consequently, for a set of given channel amplitudes $\{\alpha_{q,l}\}$ – according to the analysis of the previous sections – the q -th MRC output sample can be approximated as an AWGN variable having a mean value given by Eq.(17.160) and a variance of:

$$\sigma^2 = \frac{PT_s^2}{2} \left[\frac{K_h L_p + L_p - 1}{3N_e} + \left(\frac{2\Omega E_b}{N_0} \right)^{-1} \right] \cdot \Omega \sum_{l=0}^{L-1} \alpha_{q,l}^2, \quad (17.165)$$

where $E_b = PT_s$ is the energy per bit and $\Omega = E[(\alpha_{q,l})^2]$.

Since the receiver has the explicit knowledge of the FH pattern employed by the transmitter, the information transmitted on the U_k number of activated subcarriers can be detected without taking into account the Off-state carriers. Hence, the average bit error probability can be expressed as [408, 465]:

$$P_b = \sum_{K_h=0}^{K-1} \binom{K-1}{K_h} P_h^{K_h} (1 - P_h)^{K-1-K_h} P_b(K_h, \bar{\gamma}_c), \quad (17.166)$$

where $0 \leq K_h \leq K-1$ and P_h is the probability of a *hit* - as defined above - imposed by an interfering signal. In an asynchronous system, if we assume that the FH pattern is determined randomly by a constant-weight code chosen from the set of $\binom{U}{U_k}$ codes, then

the probability of a *hit* engendered by the interfering user k can be approximated by:

$$P_h(k) = \frac{\binom{U-1}{U_k-1}}{\binom{U}{U_k}} = \frac{U_k}{U}. \quad (17.167)$$

The average probability of a hit, P_h , can be computed by averaging Eq.(17.167), taking into account the weights of the constant-weight codes used and the number of users, K , which yields:

$$P_h = \frac{\bar{U}}{Q}, \quad (17.168)$$

where \bar{U} represents the average weight of the constant-weight codes used. The probability of $P_b(K_h, \bar{\gamma}_c)$ in Eq.(17.166) denotes the conditional bit error probability of the hard-detections, given that K_h hits were inflicted by the other $K - 1$ interfering users, i.e., K_h out of $K - 1$ users in the system activated the same subcarrier as the reference user.

Before proceeding to the evaluation of the average probability of $P_b(K_h, \bar{\gamma}_c)$ for a given K_h , we first have to determine the error probability conditioned on the multipath component attenuations $\{\alpha_{q,l}\}$. Following from our previous discussions, for the receiver having an explicit knowledge of the FH pattern, only the case, when $b_q[0] \in \{+1, -1\}$ has to be considered in deriving the error probability. The associated conditional bit error probability of the BPSK modulated bits may be written as:

$$P_b(K_h, \gamma) = Q(\sqrt{2\gamma}), \quad (17.169)$$

where

$$\gamma = \bar{\gamma}_c \cdot \frac{1}{\Omega} \sum_{l=0}^{L-1} \alpha_{q,l}^2 \quad (17.170)$$

$$\bar{\gamma}_c = \left[\frac{2(K_h L_p + L_p - 1)}{3N_e} + \left(\frac{\Omega E_b}{N_0} \right)^{-1} \right]^{-1}, \quad (17.171)$$

where $\bar{\gamma}_c$ represents the average SNR per path.

The average bit error probability for K_h number of hits is calculated from the conditional error probability upon weighting $P_b(K_h, \gamma)$ by the PDF of γ , $f(\gamma)$, and then averaging or integrating the weighted product over its legitimate range, as shown in Eq.(17.57). According to our analysis in Section 17.4, the average BER for a given number of interfering users can be expressed with the aid of Eq.(17.57) - Eq.(17.59) as:

$$P_b(K_h, \bar{\gamma}_c) = \left[\frac{(1-\mu)}{2} \right]^L \sum_{n=0}^{L-1} \binom{L-1+n}{n} \left[\frac{(1+\mu)}{2} \right]^n, \quad (17.172)$$

where, by definition:

$$\mu = \sqrt{\frac{\bar{\gamma}_c}{1 + \bar{\gamma}_c}}, \quad (17.173)$$

with $\bar{\gamma}_c$ given by Eq.(17.171).

Consequently, the average BER of the receiver using hard-detection can be computed by substituting Eq.(17.168) and Eq.(17.172) into Eq.(17.166).

17.8.2.2 Numerical Results

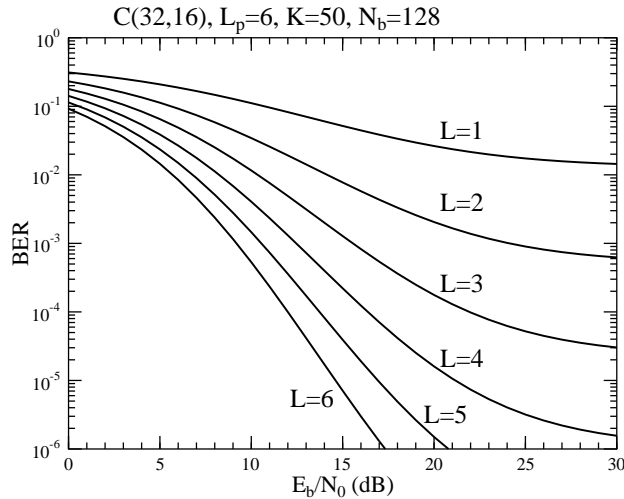


Figure 17.30: BER versus SNR per bit performance for constant-weight code based SFH/MC DS-CDMA systems using hard-detection over multipath Rayleigh fading channels upon varying the diversity order L , using the constant-weight code $C(32,16)$ for FH patterns, $L_p = 6$ resolvable paths, $K = 50$ users and a bit-duration to chip-duration ratio $N_b = 128$. For the receiver using maximum ratio combining (MRC), the optimum diversity order L is its maximum possible value of $L = L_p$, corresponding to combining all the resolvable multipath components.

In order to quantify the system's performance improvements due to diversity, Fig.17.30 depicts the BER as a function of the SNR per bit, namely E_b/N_0 . The individual curves in each figure are parameterized by the diversity order $L = 1, 2, \dots, 6$. We assumed that the FH patterns were designed from the constant-weight code $C(32,16)$, there were $L_p = 6$ resolvable paths, the number of active users was $K = 50$ and the spreading gain of each subcarrier signal was $N_e = 128U$, i.e., the bit-duration to chip-duration ratio was $N =$

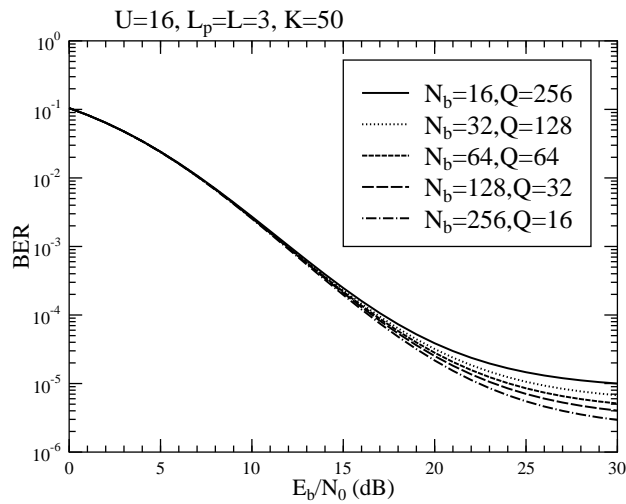


Figure 17.31: BER versus SNR per bit performance for constant-weight code based SFH/MC DS-CDMA systems using hard-detection and $L_p = L = 3$ upon varying the value of N and Q . For a constant bandwidth associated with $N_b Q = 2^{12}$, the combination of $N_b = 256$ and $Q = 16$ provides the best performance while also imposing the highest complexity, requiring a high bit/chip duration ratio N_b .

128. From the results it is seen that the system's BER performance is dramatically improved by increasing the diversity order L . For MRC, the value of L has to be maximized. The corresponding choice of $L = L_p$ implies combining all the resolvable multipath components, irrespective of the receiver's associated complexity.

In Fig.17.31 SFH/MC DS-CDMA systems having a constant system bandwidth associated with the product $N_b Q = 2^{12}$, but using various combinations of the number of subcarriers Q and bit-duration to chip-duration ratio of N_b were considered. In this system, increasing the number of subcarriers implies decreasing the 'hit' probability inflicted by the interfering users and simultaneously, decreasing the direct-sequence spread bandwidth of each subcarrier. The parameters used are shown in the figure. For a constant system bandwidth and for $L_p = L = 3$, we observe that although Q and N_b change over a wide range, the BER performance remains indistinguishable for relatively low SNR per bit values, namely below 15dB. However, for higher SNR per bit values, in excess of 21dB, the BER performance improves upon increasing N_b .

Since increasing the value of N_b implies increasing the DS spread bandwidth and results in decreasing the chip-duration, consequently, for a given multipath fading environment having an average delay spread of T_m , the number of resolvable paths $L_p = T_m/T_c$, increases upon decreasing T_c . Hence, the assumption of $L_p = L = 3$ in Fig.17.31 is impractical. Therefore, in Fig.17.32 the performance of a SFH/MC DS-CDMA system using

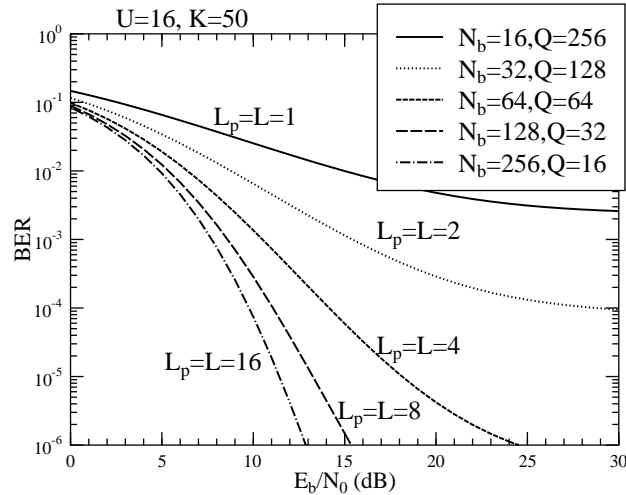


Figure 17.32: BER versus SNR per bit performance for constant-weight code based SFH/MC DS-CDMA systems using hard-detection and $L_p = L = 1, 2, 4, 8, 16$ upon varying the value of N_b and Q . Best BER performance is achieved for a high diversity order of $L_p = L = 16$, combining all associated multipath components, regardless of the associated receiver complexity.

hard-detection over a given multipath fading environment having an average delay spread of T_m was considered, as a function of $L_p = L = 1, 2, 4, 8$ and 16 . More explicitly, here we assumed that there was one resolvable path at the receiver for the system associated with $N_b = 16$. Consequently, the number of resolvable paths was $L_p = 2, 4, 8, 16$ for the systems using $N_b = 32, 64, 128, 256$, respectively. Furthermore, we assumed that the receiver was capable of combining all the resolvable paths regardless of the associated complexity. Other parameters related to the computations were the same, as in Fig.17.31, which are shown in the figure. The results indicate that the BER performance is significantly improved, when increasing N_b . Hence, for signals undergoing severe fading, a high number of independent subchannels are required, in order to enhance the system's performance.

For the systems considered in Fig.17.32 to achieve the best BER performance the receiver has to have a high diversity order. For example, for the system with $N_b = 256$ to achieve the best BER performance, the receiver has to combine all the 16 multipath signals. However, at the time of writing the implementation of such a complex receiver is impractical. Hence, in Fig.17.33 we considered a receiver with a maximum diversity order of $L = 3$, although a higher number of resolvable paths, L_p , was available at the receiver. From the results we infer that the curve associated with $Q = 64$, $N_b = 64$, or $L_p = 4$, $L = 3$ achieves the best BER performance.

From the results of Fig.17.31 to Fig.17.33 we conclude that, for a SFH/MC DS-CDMA

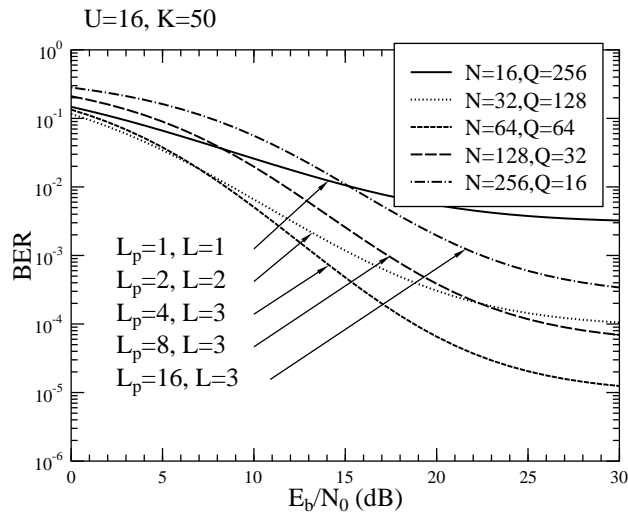


Figure 17.33: BER versus SNR per bit performance for constant-weight code based SFH/MC DS-CDMA systems using hard-detection upon varying the value of N_b and Q for a maximum diversity order of $L = 3$ and $L_p = 1, 2, 4, 8, 16$. Given the complexity constraint of $L = 3$, the system associated with $N_b = 64$, $Q = 64$, $L_p = 4$, $L = 3$ achieved the best performance.

system having a constant system bandwidth and using hard-detection, from a system optimization point of view, the DS spread bandwidth of each subchannel has to be adjusted, so that the resulting number of resolvable paths, L_p , is as close to L as possible. Then the receiver can efficiently utilize the energy dispersed over the multipath components. The required number of subchannels, consequently, can be obtained by dividing the system bandwidth by the required DS spread bandwidth.

17.8.3 Detection of SFH/MC DS-CDMA Signals without Knowledge of the FH Patterns: Blind Joint Soft-Detection

In the previous subsection, we studied the detection of the SFH/MC DS-CDMA signals, when the receiver employed the explicit knowledge of the FH pattern of the transmitter used, whilst the perfect estimation of the channel impulse response (CIR) was also assumed. Often, however, the receiver is not supplied with the explicit knowledge of the FH patterns. This happens for example at the commencement of communications before the receiver detected this information, or in case of soft hand-overs to other base stations. However, the loss of information under these circumstances is unacceptable and hence more powerful detection algorithms are required, than the hard-detection techniques of the last subsection.

If we assume that the transmitted signals are equally probable, symbol-by-symbol

Maximum-Likelihood Sequence Detection (MLSD) is considered to be the optimum receiver scheme [83, 95, 466]. In this subsection we investigate the MLSD of SFH/MC DS-CDMA signals under the assumption that all symbols (vectors) are transmitted with equal probability. We assume furthermore that the MRC output samples are mutually independent random variables having mean value given by Eq.(17.160) and, for simplicity, a common variance given by Eq.(17.165). Hence the PDF of the q -th sampled subchannel output of Fig. 17.18 can be expressed as:

$$p_q(z) = \frac{1}{\sqrt{2\pi}\sigma} e^{-\frac{(z-D_q[0])^2}{2\sigma^2}}, \quad (17.174)$$

where $D_q[0]$ is given by Eq.(17.160) with $b_q[0] \in \{+1, -1, 0\}$, and σ^2 is given by Eq.(17.165).

17.8.3.1 Maximum Likelihood Detection

Since the receiver is only aware of the weight of the transmitted constant-weight code, but not the positions of the binary '1's, the receiver now has to detect not only the positions of the '1's, which indicate the subcarriers used, but also the antipodal binary modulated information conveyed by the activated subcarriers. Let us express the input data of the scheme seen in Fig.17.18 in the vectorial form of $\mathbf{D}_i = \{d_{i,0}, d_{i,1}, \dots, d_{i,U-1}\}$, where $0 \leq i \leq M-1$ represents the constant-weight code set of weight U_1 and M is the number of constant-weight codes included in this set. Then a set of U MRC samples $\mathbf{Z} = \{Z_1, Z_2, \dots, Z_{U-1}\}$ in Fig. 17.18 - which we refer to here as a received symbol or vector - are input to the 'decision unit' invoking a joint ML detection rule, which is based on the determination of the probabilities defined as:

$$p(\mathbf{Z}|\mathbf{D}_i) = \frac{1}{(2\pi\sigma^2)^{U/2}} \exp \left(-\frac{\sum_{q=0}^{U-1} \left(Z_q - \sqrt{\frac{P}{2}} T_s d_{i,q} \sum_{l=0}^{L-1} \alpha_l^2 \right)^2}{2\sigma^2} \right), \quad (17.175)$$

$i = 0, 1, \dots, M-1.$

The decision criterion is based on selecting the signal corresponding to the maximum of the set of probabilities $\{p(\mathbf{Z}|\mathbf{D}_i)\}$.

Upon taking the logarithm of both sides of the above equation we arrive at:

$$\ln(p(\mathbf{Z}|\mathbf{D}_i)) = -\frac{U}{2} \ln(2\pi\sigma^2) - \frac{1}{2\sigma^2} D(\mathbf{Z}, \mathbf{D}_i), \quad (17.176)$$

where

$$D(\mathbf{Z}, \mathbf{D}_i) = \sum_{q=0}^{U-1} \left| Z_q - \sqrt{\frac{P}{2}} T_s d_{i,q} \sum_{l=1}^{L-1} \alpha_l^2 \right|^2 \quad (17.177)$$

represents the Euclidean distance between the decision variable vector of \mathbf{Z} and the transmitted data vector of \mathbf{D}_i . Finding the maximum of $\ln(p(\mathbf{Z}|\mathbf{D}_i))$ over the whole set of legitimate transmitted data vectors \mathbf{D}_i is equivalent to finding the vector \mathbf{D}_i that minimizes the Euclidean distance of $D(\mathbf{Z}, \mathbf{D}_i)$, $i = 0, 1, \dots, M - 1$. Furthermore, by extending Eq.(17.177) we arrive at:

$$\begin{aligned} D(\mathbf{Z}, \mathbf{D}_i) &= \sum_{q=0}^{U-1} Z_q^2 - \left(\sqrt{\frac{P}{2}} T_s \sum_{l=0}^{L-1} \alpha_l^2 \right) \sum_{q=0}^{U-1} Z_q d_{i,q} \\ &\quad + \left(\sqrt{\frac{P}{2}} T_s \sum_{l=0}^{L-1} \alpha_l^2 \right)^2 \sum_{q=0}^{U-1} d_{i,q}^2, \end{aligned} \quad (17.178)$$

where the first term on the right-hand side is a constant for all i values, i.e., for all transmitted data vectors. Furthermore, since we assumed that the constant-weight code is from the code set $\{\mathbf{D}_i\}$, the third term is also constant for $i = 0, 1, \dots, M - 1$. Consequently, the minimization of $D(\mathbf{Z}, \mathbf{D}_i)$ is equivalent to the maximisation of the correlation metrics of:

$$C(\mathbf{Z}, \mathbf{D}_i) = \sum_{q=0}^{U-1} Z_q d_{i,q}, \quad i = 0, 1, \dots, M - 1, \quad (17.179)$$

which defines the corresponding decision rule based on selecting the signal corresponding to the maximum of the set of correlation metrics $C(\mathbf{Z}, \mathbf{D}_i)$ over the set of M legitimate data vectors may be input to the transmitter schematic of Fig.17.17.

The detection complexity of a received symbol or vector is determined by both the length and the weight of the constant-weight code. For a constant-weight code $C(U, U_k)$, the detection complexity is proportional to $O\left(\binom{U}{U_k} 2^{U_k}\right)$ - where O indicates the 'order' of complexity - since each activated subcarrier associated a binary '1' in the constant-weight code $C(U, U_k)$ may convey a +1 or -1 data bit. However, if U number of different-rate transmission schemes are supported, and each rate is invoked with an equal *a-priori* probability, then the average detection complexity can be expressed as $O(3^U/U)$. This detection complexity becomes excessive, when evaluating Eq.(17.179) for all possible code words, if the value of U is high. In the next two sections we impose some limitations on the transmission scheme by limiting the minimum distance of the constant-weight codes representing the FH patterns, in order to simplify the detection process.

17.8.3.2 Approach I

To this effect, let us assume that the synthesizer of the reference user in Fig 17.17 generates a total of $U = 2^m$ subcarriers. This design choice conveniently coincides with the practical implementational constraints of invoking the Fast Fourier Transform (FFT) for modulation. Assume furthermore that $U_1 = 2^n$, $n = 0, 1, \dots, m$, number of subcarriers are activated. Then the U number of subcarriers can be divided into U_1 number of groups, each group having $W = U/U_1 = 2^{m-n}$ subcarriers. A U_1 -bit symbol or vector now can be transmitted by U_1 number of subcarriers randomly selected from the U_1 groups, where each group contributes one activated subcarrier. Under the above constraints, each of the U_1 groups of W subcarriers can be independently detected. This reduces the number of combinations to be considered by the detector and hence the correlation metrics of Eq.(17.179) can be reformulated as:

$$C(\mathbf{Z}, \mathbf{D}_i) = \sum_{q=0}^{W-1} Z_q d_{i,q} + \sum_{q=W}^{2W-1} Z_q d_{i,q} + \dots + \sum_{q=(U_1-1)W}^{U_1W-1} Z_q d_{i,q}, \quad (17.180)$$

where $C_j = \{d_{i,jW}, d_{i,jW+1}, \dots, d_{i,(j+1)W-1}\}$ for $j = 0, 1, \dots, U_1 - 1$ represents a constant-weight code $C(W, 1)$ having a weight of one. Since the MRC outputs in Fig. 17.18 are mutually independent random variables, the U_1 terms in Eq.(17.180) can be computed in a parallel fashion, which implies that each of the U_1 bits can be detected separately by simply considering the W number of MRC output samples. Consequently, the detection complexity of the U_1 -bit symbol is now proportional to $O(2U_1W) \equiv O(2U)$, which is linearly dependent on the total number of subcarriers, but independent of the information rate.

Although the complexity of the above detection approach is low, it results in a reduced detection performance. In order to enhance the detection performance and at the same time simplify the computations, the FH patterns can be designed by selecting a subset of codes having a minimum distance of d from the constant-weight codes $C(U, U_1)$, which is discussed in the next subsection.

17.8.3.3 Approach II

Let $C(U, d, U_1)$ represent a constant-weight code set having a code length of U and weight of U_1 , as discussed previously. Furthermore, let the minimum distance between any pair of codes from $C(U, d, U_1)$ be d . Then, this code constitutes a specific subset of the constant-weight code $C(U, U_1)$, where the number of codewords was $M = \binom{U}{U_1}$. By contrast, let $A(U, d, U_1)$ represent the number of codewords of the constant-weight code $C(U, d, U_1)$. Then, if the frequency hopping patterns are determined now by all the $A(U, d, U_1)$ codewords, the detection complexity will be reduced from $O\left[\binom{U}{U_1}2^{U_1}\right]$ to $O[A(U, d, U_1)2^{U_1}]$. In fact, from our numerical results in Subsection 17.8.4.3, we will see that, if the value of the minimum distance d is sufficiently high and the SNR is also sufficiently high, then the BER performance will be very close to that of the receiver having an explicit knowledge of the FH pattern. This allows the receiver to blindly acquire a restricted set of FH patterns exhibiting a minimum distance of d , during the call-initiation process. This limited set of FH codes can be used by the transmitter to signal the actual FH code used for the transmission of 'payload'

information to the receiver. According to the above philosophy a set of constant-weight code-words having a minimum distance of d is used to convey the side-information constituted by the index of the FH code in the fixed weight codebook to be used by the receiver. During the consecutive information transmission phase then the the whole set of $\binom{U}{U_1}$ number of FH codes or patterns can be used without imposing any minimum distance limitations.

The nonlinear constant-weight code $C(U, d, U_1)$, where $d = 2v$ with v being a positive integer, has some well-known properties. Specifically, The constant-weight codes constitute a class of efficient codes suitable for error-correction or error-detection over both binary symmetrical and asymmetrical channels [467–469]. For completeness, some of them, which are related to the forthcoming analysis are characterised below.

Proposition 1 *Johnson bound [468]:*

$$A(U, 2v, U_1) \leq \frac{Uv}{Uv - U_1(U - U_1)}, \quad (17.181)$$

provided that $Uv > U_1(U - U_1)$.

Proposition 2 [469][pp.528]: *Given that q is the integer power of a prime number, we have:*

$$\begin{aligned} A(q^2 + 1, 2q - 2, q + 1) &= q(q^2 + 1), \\ A(q^3 + 1, 2q, q + 1) &= q^2(q^2 - q + 1). \end{aligned} \quad (17.182)$$

Proposition 3 [469][pp.528]: *Assuming that a $4r \times 4r$ Hadamard matrix exists, we have:*

$$\begin{aligned} A(4r - 2, 2r, 2r - 1) &= 2r, \\ A(4r - 1, 2r, 2r - 1) &= 4r - 1, \\ A(4r, 2r, 2r) &= 8r - 2. \end{aligned} \quad (17.183)$$

Based on the above limitations in the context of Approach I and II, we can exploit a range of further properties of the code $C(U, 2v, U_1)$. Let us now derive the expressions of the error probability for the SFH/MC DS-CDMA system using blind joint soft-detection.

17.8.4 Performance of the SFH/MC DS-CDMA receiver without Knowledge of the FH Patterns: Blind Joint Soft-Detection

Fig. 17.34 portrays an example of the previously discussed constant-weight codes. The SFH/MC DS-CDMA system of Fig.17.17 uses a constant-weight code $C(U, 2v, U_1)$ for activating the subcarriers. In this section we employ receiver relying on no knowledge of the FH pattern itself. However, the receiver is aware of the number of the active subcarriers. The receiver's task is then to evaluate the previously derived correlation metrics seen in Eq.(17.179).

These metrics must be evaluated for two different scenarios in order to demodulate a parallel U_1 -bit symbol or vector.

Specifically, we have to consider those codes, which have identical '1' positions in the FH code, corresponding to identical activated subcarriers, but potentially conveying different data symbols on these active subcarriers. We refer to these as *intra-set codes* or *intra-codes*, for short, which are exemplified in Fig.17.34. Explicitly, the above intra-codes are derived from the same constant-weight code and activate the same subcarriers. By contrast, the so-called *inter-codes* of Fig.17.34 are derived from different constant-weight codes, which have the same number of '1' FH code positions, but activate different subcarriers.

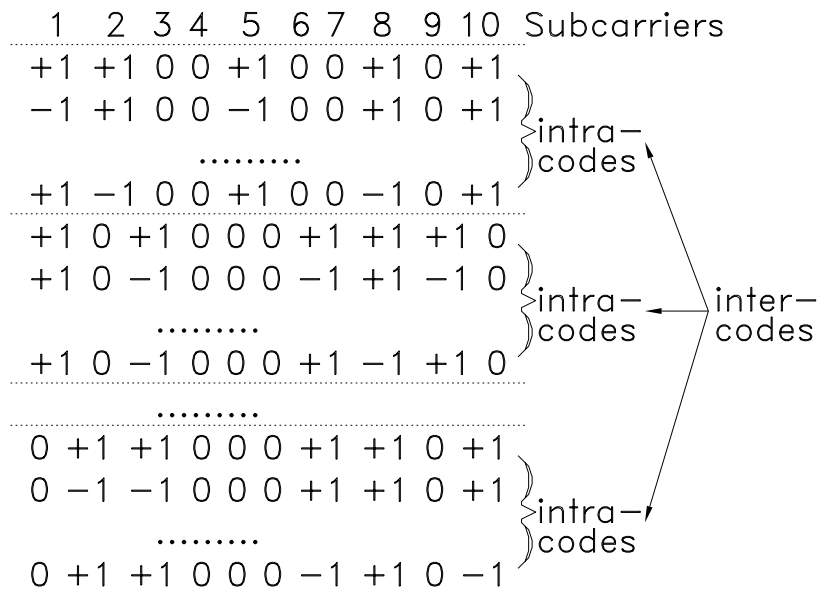


Figure 17.34: Example of intra-codes and inter-codes of a constant-weight code $C(10, 4, 5)$ for SFH/MC DS-CDMA system using 10 subcarriers.

Consequently, in our proposed blind joint soft-detection scheme two different types of errors exist, the intra-code errors and the inter-code errors. The probability of these errors is denoted by $P_{intra}(\cdot)$ and $P_{inter}(\cdot)$, respectively. The intra-code errors do not result in opting for a code other than the transmitter's code and hence do not inflict a constant-weight FH code decision error, they simply result in some bits being demodulated erroneously. By contrast, the inter-code errors may lead not only to erroneous bit decisions, but also to opting for another constant-weight code and hence to potentially more severe bit decision error events. The derivation of the exact expression for the probability of correct vector or symbol decoding is arduous, since the error probabilities depend on all the $A(U, 2v, U_1)2^{U_1}$ number of correlation metrics evaluated according to Eq.(17.179). Hence below we derive the union upper-bound of the error probability.

Let us divide the entire set of $A(U, 2v, U_1)2^{U_1}$ number of information vectors or symbols into $A(U, 2v, U_1)$ number of sets, where the vectors from the same set activate the same subcarriers. Hence the vectors of the different sets constitute 'inter-codes', which were exemplified in Fig.17.34. Hence each set has 2^{U_1} vectors, since the information transmitted by an active subcarrier might be +1 or -1 and there are U_1 active subcarriers. Let the first vector in the first set, which is denoted by X_{11} be transmitted. Then the union upper-bound probability of an intra-code error can be expressed as [95,466]:

$$P_{intra}(Up) = \sum_{j=2}^{2^{U_1}} Q \left(\sqrt{\frac{|X_{11} - X_{1j}|^2}{4\sigma^2}} \right), \quad (17.184)$$

where X_{1j} is the j th vector of the first set, $|X_{11} - X_{1j}|^2$ represents the distance between X_{11} and X_{1j} , and σ^2 is the common variance of the MRC output samples, which is given by Eq.(17.165). By contrast, the union upper-bound probability of an inter-code error can be written as:

$$P_{inter}(Up) = \sum_{i=2}^{A(U,2v,U_1)} \sum_{j=1}^{2^{U_1}} Q \left(\sqrt{\frac{|X_{11} - X_{ij}|^2}{4\sigma^2}} \right), \quad (17.185)$$

where again, $|X_{11} - X_{ij}|^2$ represents the distance between X_{11} and X_{ij} .

Consequently, the union upper-bound probability of error is the sum of Eq.(17.184) and Eq.(17.185), yielding:

$$P(Up) = P_{intra}(Up) + P_{inter}(Up). \quad (17.186)$$

Furthermore, the joint probability of a correct detection plus that of an intra-code decision error represents the probability of the event that the receiver selected the correct constant-weight code matched to the transmitted one. This event corresponds to the correct FH pattern detection probability, which can be interpreted as the *correct acquisition - or acquisition success - probability* expressed as:

$$\lambda = 1 - P_{inter}(Up). \quad (17.187)$$

With the aid of Eqs.(17.184) to (17.187), we can now approximate the union upper-bound bit error probability performance of the SFH/MC DS-CDMA scheme. For the previously introduced Approach II of subsection 17.8.3.3 we will also consider a more accurate error probability expression.

17.8.4.1 Approach I

Recall from our previous discussions that according to our Approach I in subsection 17.8.3.2 each group of $W = U/U_1$ subcarriers of the U_1 groups can be separately detected, since each hosts one active subcarrier. The codes utilized by the W subcarriers of a group are equivalent to a class of $C(W, 2, 1)$ code with $A(W, 2, 1) = W$. This class of constant-weight

codes includes W number of orthogonal inter-codes, each activating a single carrier in one of the W possible positions. In other words, this scenario can be viewed as considering the independent detection of U_1 number of length W codes, which have a weight of 1 and a minimum distance of 2. Reduced detection complexity is attained due to decomposing the original detection problem into U_1 number of low-complexity detection steps.

Since the cross-correlation between two intra-codes is -1, hence, the intra-code error probability conditioned on the CIR tap attenuations can be expressed using Eq.(17.184) as:

$$P_{intra}(U_p, \gamma) = Q\left(\sqrt{2\gamma}\right), \quad (17.188)$$

where γ is given by Eq.(17.171). By contrast, the union upper-bound of an inter-code FH sequence error conditioned on the CIR tap attenuations can be written as:

$$P_{inter}(U_p, \gamma) = 2(W - 1)Q(\sqrt{\gamma}). \quad (17.189)$$

Hence the union upper-bound probability of intra- or inter-code FH pattern errors conditioned on the CIR tap attenuations is the sum of Eq.(17.188) and Eq.(17.189), as we have seen in Eq.(17.186). The average union upper-bound error probability per bit for a given number of hits, K_h , is calculated from the conditional union upper-bound probability by weighting it with the aid of its probability of occurrence expressed in terms of the PDF of γ , $f(\gamma)$, which is given by Eq.(17.58) with N_p replaced by L and $\bar{\gamma}_c$ being given by Eq.(17.171). It can be shown that:

$$P^I(K_h, \bar{\gamma}_c) = P(K_h, \bar{\gamma}_c) + 2(W - 1)P\left(K_h, \frac{\bar{\gamma}_c}{2}\right), \quad (17.190)$$

where $P(K_h, x)$ is given by Eq.(17.172).

The average union upper-bound bit error probability for the receiver using the previously introduced blind soft-detection Approach I of Subsection 17.8.3.2 can be computed by substituting Eq.(17.168) and Eq.(17.190) into Eq.(17.166) with $P(K_h, \bar{\gamma}_c)$ replaced by $P^I(K_h, \bar{\gamma}_c)$.

The acquisition success probability for the case of potential hits inflicted by the $K - 1$ interfering users is expressed as:

$$\lambda(K_h) = 1 - 2(W - 1)P_b(K_h, \bar{\gamma}_c). \quad (17.191)$$

Then the *average* acquisition probability for the proposed blind joint soft-detection Approach I of Subsection 17.8.3.2 can be computed by averaging Eq.(17.191) over the distribution of the number of hits, yielding:

$$\lambda = \sum_{K_h=0}^{K-1} \binom{K-1}{K_h} P_h^{K_h} (1 - P_h)^{K-1-K_h} \lambda(K_h). \quad (17.192)$$

17.8.4.2 Approach II

For the previously introduced blind joint soft-decision Approach II of Subsection 17.8.3.3, the knowledge of the distance between any pairs of constant-weight codewords is required. Explicitly, this distance information is necessary for the computation of the union upper-bounds for the probability of intra-code and inter-code FH pattern detection errors in Eq.(17.184) and Eq.(17.185), as well as for the determination of the union upper-bound of the FH pattern detection error probability in Eq.(17.186). For specific sets of constant-weight codes exhibiting an equal distance in the context of arbitrary pairs, the exact union upper-bound can be determined from the above mentioned equations.

Note that for intra-codes and for sufficiently high SNRs, the probability of a single bit error in a U_1 -bit symbol is significantly higher, than that of two bit errors, assuming that the MRC outputs are i.i.d random variables. Hence the union upper-bound probability of an intra-code error in Eq.(17.184) can be approximated by:

$$P_{intra}(Up) \approx P_{intra}(II) = \sum_{j=2}^{U_1} Q \left(\sqrt{\frac{|X_{11} - X_{1j}|^2}{4\sigma^2}} \right), \quad (17.193)$$

where we replaced Up by II , in order to indicate that this probability is now not the union-upper bound of an intra-code error according to Approach II. Furthermore, X_{11} and X_{1j} are two intra-codes activating the same subcarrier, but having a distance of 'one' between them, representing a one-bit error. Hence, the cross-correlation of X_{11} and X_{1j} is $(1 - \frac{2}{U_1})$, and consequently the error probability of Eq.(17.193) can be written as [95]:

$$P_{intra}(II, \gamma) = (U_1 - 1)Q \left(\sqrt{2\gamma} \right). \quad (17.194)$$

By contrast, for an inter-code error under sufficiently high SNRs, according to Fig.17.34, the metrics computed from Eq.(17.179) for the specific data vectors \mathbf{D}_i other than the transmitted vector are maximized, if the bits of \mathbf{D}_i in the positions corresponding to the activated subcarriers of the transmitter were identical to the transmitted bits. These cases constitute the most probable events of inter-code errors and hence Eq.(17.185) can be approximated by:

$$P_{inter}(Up) \approx P_{inter}(II) = 2^v [A(U, 2v, U_1) - 1] Q \left(\sqrt{\frac{|X_{11} - X_{ij}|^2}{4\sigma^2}} \right), \quad (17.195)$$

where again, Up was replaced by II , in order to avoid confusion with the union upper-bound of the inter-code error probability. Furthermore, X_{11} and X_{ij} are two inter-codes having a minimum distance of $d = 2v$. The conditional probability of error in Eq.(17.195) can be hence simplified to:

$$P_{inter}(II, \gamma) = 2^v [A(U, 2v, U_1) - 1] Q \left(\sqrt{v\gamma} \right). \quad (17.196)$$

Note that in deriving Eq.(17.196), according to Fig.17.34, the cross-correlation between X_{11} and X_{ij} is $1 - \frac{v}{U_1}$, since the '0' elements (Off-state) of the constant-weight code are included

in the correlation computations.

The total bit error probability conditioned on the CIR tap attenuations is constituted by both intra- and inter-code errors, which can be approximated as:

$$P(II, \gamma) = \frac{1}{U_1} P_{intra}(II, \gamma) + \frac{1}{2} P_{inter}(II, \gamma) \quad (17.197)$$

according to the above analysis. The average bit error probability for a given number of hits, K_h , is calculated from the conditional bit error probability of Eq.(17.197) by averaging it with respect to the PDF of γ , $f(\gamma)$, which is given by Eq.(17.58) with N_p replaced by L and $\bar{\gamma}_c$ being given by Eq.(17.171). Following this averaging or integration we have:

$$P^{II}(K_h, \bar{\gamma}_c) = \frac{U_1 - 1}{U_1} P(K_h, \bar{\gamma}_c) + \frac{2^v [A(U, 2v, U_1) - 1]}{2} P\left(K_h, \frac{v\bar{\gamma}_c}{2}\right), \quad (17.198)$$

where $P(K_h, x)$ is given by Eq.(17.172).

The average bit error probability of the receiver using the blind soft-detection Approach II of Subsection 17.8.3.3 can be computed by substituting Eq.(17.168) and Eq.(17.198) into Eq.(17.166) with $P(K_h, \bar{\gamma}_c)$ replaced by $P^{II}(K_h, \bar{\gamma}_c)$.

The acquisition success probability for the given number of hits inflicted by the $K - 1$ interfering users can be expressed as:

$$\lambda(K_h) = 1 - 2^v [A(U, 2v, U_1) - 1] P\left(K_h, \frac{v\bar{\gamma}_c}{2}\right). \quad (17.199)$$

Finally, the average acquisition success probability of the blind joint soft-detection Approach II can be computed by averaging Eq.(17.199) over the distribution of the number of hits, which was given in Eq.(17.192) with $\lambda(K_h)$ replaced by Eq.(17.199). Let us now characterized the performance of the blind soft detection Approach I and Approach II.

17.8.4.3 Numerical Results

In Fig.17.35 we estimated the upper-bound BER of Approach I upon combining $L = 1, 3, 5$ paths in the receiver. The BER of hard-detection based on the approach of Subsection 17.8.2 was also plotted as a benchmarker, assuming that the receiver exploited the explicit knowledge of the FH patterns. The parameters related to the computations were shown in the figures. The results demonstrate that the system provides dramatic BER improvements, when the number of combined diversity paths, L , increases. However, the results also demonstrate that opting for the blind joint soft-detection Approach I of Subsection 17.8.3.2 increased the BER with respect to hard-detection.

In Fig.17.36 we evaluated the intra-code Word Error Rate (WER) and the inter-code word error rate, as well as their sum for the SFH/MC DS-CDMA system using the blind joint soft-detection Approach II of Subsection 17.8.3.3. We employed the FH description code of C(16,12,8), having a minimum distance of $d = 12$ between the constant-weight codes, which corresponded to $v = 6$. Since the intra-code word error probability is the codeword error probability of the soft-detection technique proposed, when the receiver has the *a-priori*

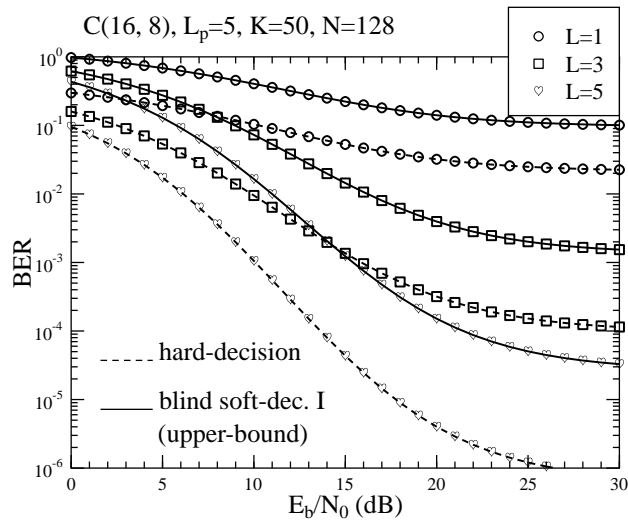


Figure 17.35: Comparison of the BER versus bit-SNR performance between the hard-detection technique of Subsection 17.8.2 and blind soft-detection using Approach I evaluated from Eqs.(17.190), (17.166) and (17.168) for the constant-weight code C(16,8), $L_p = 5$ resolvable paths, diversity combining orders $L = 1, 3, 5$, $K = 50$ users and a bit-duration to chip-duration ratio of $N_b = 128$. The remaining parameters are explicitly stated at the top of the illustration. The BER performance of hard-detection is superior to that of the blind joint soft-detection using Approach I.

knowledge of the FH patterns, the results shown in this figure explicitly illustrate the comparison of the word error rate performance between the SFH/MC DS-CDMA system using blind joint soft-detection and that using soft-detection with *a-priori* knowledge of the FH patterns. From the results we concluded that under various SNR conditions the total WER was dominated by one of its contributing factors. Namely, for very low SNR per bit values or very low number of diversity fingers, such as $L = L_p = 1$, the performance was dominated by the word error rate of the inter-code decisions. By contrast, for moderate to high SNRs per bit and for high diversity orders $L = L_p = 5$, the word error rate of the intra-code errors was more dominant. However, for the case of $L = L_p = 3$ and for sufficiently high SNRs per bit, the resultant word error rate was dependent on both the intra-code and the inter-code error events. Based on the fact that the word error rate of blind joint soft-detection is the sum of the intra-code and inter-code WER, the blind joint soft-detection approach is outperformed by the soft-detection technique using the *a-priori* knowledge of the FH patterns. This becomes explicit for $L = 1$, $L = 3$ and for $L = 5$ at relatively low SNR per bit values in Figure 17.36. However, for $L = 5$ at sufficiently high SNR per bit values there is effectively very little difference between the word error rate performance curves of the blind joint soft-detection scheme (Intra+Inter-code curve) and the soft-detection arrangement using the *a-priori* knowl-

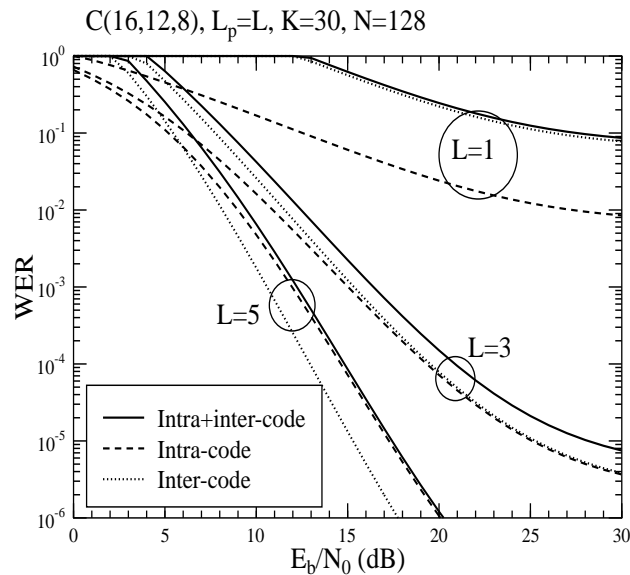


Figure 17.36: Word error rate (WER) versus SNR per bit performance of the constant-weight code based SFH/MC DS-CDMA system using the blind soft-detection Approach II. For $v > 2$, sufficiently high SNR per bit values and sufficiently high diversity orders, the average error probability of blind joint soft-detection using Approach II is dominated by the intra-code errors.

edge of the FH patterns (Intra-code curve). Since the inter-code word error rate is a function of v , we infer from Eq.(17.194) and Eq.(17.196) that if $v > 2$, the total word error rate will be dominated by Eq.(17.194), provided that the SNR per bit is sufficiently high and the channel fading is sufficiently benign or the diversity order is sufficiently high. This property suggests that for $v > 2$ intra-code error-control techniques can be introduced, in order to correct the intra-code errors by increasing the minimum distance between the intra-codes and hence decreasing the intra-code word error rate of Eq.(17.194). This would decrease the total word error rate of the blind soft-detection using Approach II.

Finally, in Fig.17.37 we characterised the probability of the successful FH code acquisition for the blind soft-detection Approach I and that of the blind soft-detection Approach II for the multi-rate transmission scenario discussed previously, under the assumption that all the interfering users employed the same constant-weight codes, namely C(32,16). From the results we observe that for Approach I the probability of successful FH code acquisition becomes higher, when the constant-weight codes associated with higher information rates are used. By contrast, for Approach II and for the specific set of constant-weight codes we used, C(32,8,4) achieved the best performance. Nevertheless, if the SNR per bit is sufficiently high, the curves corresponding to the constant-weight codes of C(32,4,2), C(32,8,4) and C(32,14,8)

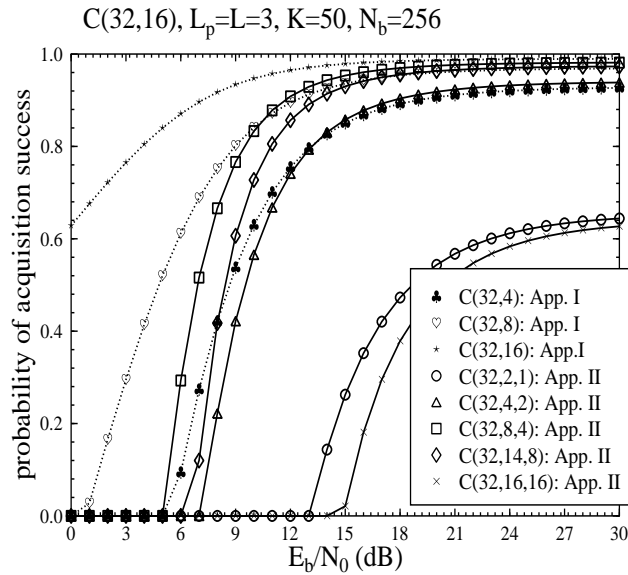


Figure 17.37: Acquisition success probability of the constant-weight code based SFH/MC DS-CDMA system using the blind soft-detection Approach I and II, under the assumption of constant spreading gain for multi-rate based systems. If the SNR per bit is sufficiently high, blind joint soft-detections can acquire the FH patterns used with a high probability, while also detecting the transmitted information bits.

will tend to a successful acquisition probability of unity.

This allows the receiver to blindly acquire a restricted set of FH patterns exhibiting a minimum distance of d . This restricted set of FH patterns can then be used by the transmitter to signal the index of the actual FH codes used for the transmission of ‘payload’ information to the receiver. During the information transmission phase then a randomly selected set of FH patterns from the $\binom{Q}{U}$ number of FH codes can be used without imposing any minimum distance limitations. In other words, following the blind detection of the ‘side-information’ constituted by the FH codes used by the transmitter, successive communications can be based on the explicit knowledge of the FH patterns.

17.9 Chapter Summary and Conclusions

Following a brief classification of the most popular MC-CDMA systems in this chapter we introduced slow frequency hopping for improving the system’s performance and flexibility. The proposed SFH/MC DS-CDMA system is capable of efficiently amalgamating the techniques of slow FH, OFDM and DS-CDMA. Nonlinear constant-weight codes have been introduced,

in order to control the associated FH patterns, and hence to activate a number of subcarriers, in order to support multi-rate services. Hard-detection or blind joint soft-detection have been proposed for signal detection. The hard-detection exploits the explicit knowledge of the FH pattern employed, while the soft-detection assumes no a priori knowledge of the FH patterns used. The properties of the constant-weight FH codes have been investigated in conjunction with specific system parameters, and the performance of the proposed SFH/MC DS-CDMA systems using either hard-detection or blind joint soft-detection has been evaluated, under the conditions of supporting constant-rate or multi-rate services. From the results we concluded that the blind joint soft-detection techniques are capable of detecting the transmitted information and simultaneously acquiring the FH patterns.

Part V

Standards and Networking

Glossary

ACL	Auto-correlation of a sequence
adaptive-rate	a term applied to techniques that adapt the bit rate according to certain criteria
AQAM	Adaptive Quadrature Amplitude Modulation, a transmission scheme where the modulation mode is adapted according to certain criteria
ARIB	Association of Radio Industries and Businesses in Japan
AWGN	Additive White Gaussian Noise
BCH	Bose-Chaudhuri-Hocquenghem, A class of forward error correcting codes (FEC)
BER	Bit error rate, the number of the bits received incorrectly
blind detection	A data or parameter estimation technique that does not require reference sequences to be transmitted or parameter estimation to be carried out separately
BPS	Bits Per Symbol, indicates the throughput performance
BPSK	Binary Phase Shift Keying, a type of data modulation scheme
BS	A common abbreviation for Base Station
CATT	Chinese Academy of Telecommunication Technology
CCL	Cross-correlation, usually of two different sequences
CDMA	Code Division Multiple Access, a multiple access scheme where multiple users transmit simultaneously within the same bandwidth and are separated through the use of a unique spreading code for each user
CIR	Channel Impulse Response
CRAD	Coherent Receiver Antenna Diversity, where the received signals from more than one antenna are coherently combined to obtain signal gain.
DBPSK	Differential Binary Phase Shift Keying, a type of data modulation scheme
decorrelator	A detector that removes the correlation of all the interferer signals with the signal of the desired user

diversity	A technique employed to obtain performance gain where different received versions of the same source signal are combined in order to improve the system performance
DS-CDMA	Direct Sequence Code Division Multiple Access, a sub-class of CDMA where each transmitted bit is directly multiplied with a spreading sequence in order to spread its bandwidth.
ETSI	European Telecommunications Standards Institute
FDMA	Frequency Division Multiple Access, a multiple access scheme where different users transmit in different bandwidths in order not to interfere with each other
FFH	Fast Frequency Hopping
FH-CDMA	Frequency Hopping Code Division Multiple Access, a sub-class of CDMA where the carrier frequency of the CDMA user is switched according to a pattern determined by its unique code
IC	Interference Cancellation, a type of multiuser receiver for CDMA where the received signal is regenerated from previous data estimates and cancelled from the composite received signal, in order to provide more reliable estimates after the cancellation stages
IMT-2000	International Mobile Telecommunications 2000
interleaving	A technique employed to randomize burst errors caused by fading in the mobile channel. The transmitted bits are arranged according to a known order before transmission and at the receiver the received symbols are re-arranged into the pre-transmission order so that the bursty errors can be separated. This helps improve the performance of the channel decoder.
IS-95	Interim Standard 95, the definition of the cellular (800 MHz) CDMA Common Air Interface
ISI	Inter-symbol Interference, interference caused by the time dispersion of the wideband channel where the transmitted symbols interfere with each other
JD	Joint Detection or Joint Detector, a type of multiuser receiver that uses equalization techniques to detect jointly detect the symbols of multiple users
JD-CDMA	Joint Detection CDMA system, a CDMA system that employs joint detection receivers
LMS	Least Mean Square algorithm, a linear adaptive filtering algorithm that recursively optimizes the filter tap weights in order to obtain the minimum mean square error at the output of the filter
MAI	Multiple Access Interference, the interference caused by multiple users transmitting simultaneously within the same bandwidth and is usually used in the context of CDMA systems
MAP	Maximum A Posteriori, the maximum a posteriori probability criterion maximizes the probability of making a correct decision
matched filter	A filter that has an impulse response that is matched to the waveform of the desired signal and maximizes the SNR at the output of the filter

MC-CDMA	Multi-Carrier Code Division Multiple Access, a sub-class of CDMA where a data symbol is spread with a spreading sequence into say, Q chips and each chip of the spread data symbol is transmitted over a narrowband subcarrier in the frequency domain.
MLSE	Maximum Likelihood Sequence Estimation, a sequence estimation technique that produces the most likely transmitted sequence based on a metric that is optimized for a certain criterion
MMSE	Minimum Mean Square Error
MMSE-BDFE	Minimum Mean Square Error Block Decision Feedback Equalizer, a type of joint detection receiver that minimizes the mean square error and feeds back already detected symbols to improve the reliability of the output estimates
MMSE-BLE	Minimum Mean Square Error Block Linear Equalizer, a type of joint detection receiver that linearly minimizes the mean square error
MRC	Maximal Ratio Combining, a diversity combining technique where multiple received signals are coherently combined
MS	A common abbreviation for Mobile Station
multipath diversity	Multiple versions of the transmitted signal are obtained at the receiver due to the different multipaths in a channel and the signals of these paths can be combined in order to provide performance gain
multiuser receiver	A receiver that employs available knowledge on the properties of all the transmitting users in order to detect the data symbols of all the users
near-far effect	The phenomenon that occurs when the signals from different users arrive at the base station with different signal strengths. The stronger signals swamp out the weaker signals, thus severely degrading the performance of the weaker signals.
PDF	Probability Density Function
PIC	Parallel Interference Cancellation, an interference cancellation receiver where the received signals of all the interferers are cancelled from the received composite signal at each cancellation stage in order to generate a more reliable signal for the data estimation of the desired user
PN sequence	Pseudo-noise sequence, or pseudo-random sequence, which is a generated sequence that exhibits noise-like properties
power control	A technique used to combat the near-far effect where the power control algorithm attempts to regulate the transmitted powers of all the users such that the signals of all the users arrive with similar strengths at the receiver.
PSD	Power Spectral Density
PSP	Per Survivor Processing, a trellis-decoding algorithm, where the required parameters, for example CIR estimates, are unknown. The parameter estimation is carried out in a "per-survivor" fashion, which means that a parameter estimator is assigned to each surviving data sequence of the trellis.
QAM	Quadrature Amplitude Modulation

RAKE	A multipath diversity combiner, that inherited its name from the way it “rakes” in all the incoming pulses to form an equalized signal. The signal energy from different multipaths are combined according to the chosen diversity combining technique.
RLS	Recursive Least Squares, an adaptive filtering technique where a recursive method is used to adapt the filter tap weights such that the square of the error between the filter output and the desired response is minimized
SFH	Slow Frequency Hopping
SIC	Successive Interference Cancellation, an interference cancellation receiver where only the received signals of all the interferers that are more reliable than the desired signal are cancelled from the received composite signal in order to generate a more reliable signal for the data estimation of the desired user
SINR	Signal to Interference plus Noise ratio, same as signal to noise ratio (SNR) when there is no interference.
SNR	Signal to Noise Ratio, noise energy compared to the signal energy
SOVA	Soft Output Viterbi Algorithm, a trellis algorithm that generates the most likely sequence in soft decisions according to the constraints of the trellis and the received signal
SSMA	Spread Spectrum Multiple Access
TDD	Time Division Duplex, a transmission protocol where the uplink and downlink transmissions are carried out in the same frequency but separated in time
TDD-CDMA	Time Division Duplex Code Division Multiple Access, a multiple access scheme that combines TDD and CDMA
TDMA	Time Division Multiple Access, a multiple access technique where multiple users transmit in the same bandwidth but are separated in time through user-designated timeslots
TH-CDMA	Time Hopping Code Division Multiple Access, a sub-class of CDMA where each user transmits in the timeslots determined by its spreading sequence
TIA	Telecommunications Industry Association in USA
UMTS	Universal Mobile Telecommunications Systems
UTRA	UMTS Terrestrial Radio Access
Viterbi algorithm	A trellis algorithm that generates the most likely sequence according to the constraints of the trellis and the received signal
VSF	Variable Spreading Factor, an adaptive rate transmission scheme for CDMA, where the bit rate is adapted by varying the spreading factor but keeping the chip rate constant
W-CDMA	Wideband Code Division Multiple Access, a high chip-rate and bit-rate CDMA air interface, where the mobile channel bandwidth is very wide and the fading within the channel is frequency-selective. In general, the minimum bandwidth of wideband CDMA is 5 MHz.

WMF	Whitening Matched Filter, a filter that whitens the received noise and maximizes the SNR at the output of the filter
ZF-BDFE	Zero Forcing Block Decision Feedback Equalizer, a type of joint detection receiver that eliminates all the interference at the expense of noise enhancement and feeds back already detected symbols to improve the reliability of the output estimates
ZF-BLE	Zero Forcing Block Linear Equalizer, a type of linear joint detection receiver that eliminates all the interference at the expense of noise enhancement

Bibliography

- [1] J. Mitola, "The software radio architecture," *IEEE Communications Magazine*, pp. 26–38, May 1995.
- [2] J. Mitola, "Technical challenges in the globalization of software radio," *IEEE Communications Magazine*, pp. 84–89, February 1999.
- [3] W. Tuttlebee, ed., *Software Defined Radio, Volumes I and II*. John Wiley, 2002.
- [4] L. Hanzo, C. Wong, and M. Yee, *Adaptive Wireless Transceivers*. John Wiley, IEEE Press, 2002. (For detailed contents, please refer to <http://www-mobile.ecs.soton.ac.uk>).
- [5] L. Hanzo, T. Liew, and B. Yeap, *Turbo Coding, Turbo Equalisation and Space-Time Coding*. John Wiley, IEEE Press, 2002. (For detailed contents, please refer to <http://www-mobile.ecs.soton.ac.uk>).
- [6] J. Holland, *Adaptation in Natural and Artificial Systems*. Ann Arbor, Michigan: University of Michigan Press, 1975.
- [7] T.-J. Lim, L. K. Rasmussen, and H. Sugimoto, "An asynchronous multiuser CDMA detector based on the kalman filter," *IEEE Journal of Selected Areas in Communications*, vol. 16, pp. 1711–1722, December 1998.
- [8] X. Wang and H. V. Poor, "Adaptive joint multiuser detection and channel estimation in multipath fading CDMA," *Wireless Networks*, vol. 4, pp. 453–470, June 1998.
- [9] D. E. Goldberg, *Genetic Algorithms in Search, Optimization, and Machine Learning*. Reading, Massachusetts: Addison-Wesley, 1989.
- [10] K. S. Gilhousen, I. M. Jacobs, R. Padovani, A. J. Viterbi, L. A. Weaver, and C. E. Wheatley, "On the capacity of a cellular CDMA system design," *IEEE Transactions on Vehicular Technology*, vol. 40, pp. 303–312, May 1991.
- [11] Telecomm. Industry Association (TIA), Washington, DC, *Mobile station - Base station compatibility standard for dual-mode wideband spread spectrum cellular system, EIA/TIA Interim Standard IS-95*, 1993.
- [12] J. Holtzman, "A simple, accurate method to calculate spread-spectrum multiple-access error probabilities," *IEEE Transactions on Communications*, vol. 40, pp. 461–464, March 1992.
- [13] T. Eng, N. Kong, and L. Milstein, "Comparison of diversity combining techniques for Rayleigh-fading channels," *IEEE Transactions on Communications*, vol. 44, pp. 1117–1129, September 1996.
- [14] R. E. Ziemer and R. L. Peterson, *Digital Communications and Spread Spectrum Systems*. New York: Macmillan Publishing Company, 1985.

- [15] A. Polydoros and C. Weber, "A unified approach to serial search spread-spectrum code acquisition-Part I: general theory," *IEEE Transactions on Communications*, vol. 32, pp. 542–549, May 1984.
- [16] D. Sarwate, "Acquisition of direct-sequence spread-spectrum signals," in *Wireless Communication - TDMA versus CDMA* (S. G. Glisic and P. L. Leppanen, eds.), pp. 121–145, Kluwer Academic Publishers, 1997.
- [17] U. Madhow, "MMSE interference suppression for timing acquisition and demodulation in direct-sequence CDMA systems," *IEEE Transactions on Communications*, vol. 46, pp. 1065–1075, August 1998.
- [18] K. Chugg, "Blind acquisition characteristics of PSP-based sequence detectors," *IEEE Journal on Selected Areas in Communications*, vol. 16, pp. 1518–1529, October 1998.
- [19] R. Rick and L. Milstein, "Optimal decision strategies for acquisition of spread-spectrum signals in frequency-selective fading channels," *IEEE Transactions on Communications*, vol. 46, pp. 686–694, May 1998.
- [20] D.-W. Lee and L. Milstein, "Analysis of a multicarrier DS-CDMA code-acquisition system," *IEEE Transactions on Communications*, vol. 47, pp. 1233–1244, August 1999.
- [21] S. Bensley and B. Aazhang, "Maximum-likelihood synchronization of a single user for code-division multiple-access communication systems," *IEEE Transactions on Communications*, vol. 46, pp. 392–399, March 1998.
- [22] W. R. Braun, "PN acquisition and tracking performance in DS/CDMA systems with symbol-length spreading sequences," *IEEE Transactions on Communications*, vol. 45, pp. 1595–1601, December 1997.
- [23] R. Rick and L. Milstein, "Parallel acquisition in mobile DS-CDMA systems," *IEEE Transactions on Communications*, vol. 45, pp. 1466–1476, November 1997.
- [24] U. Cheng, "Performance of a class of parallel spread-spectrum code acquisition schemes in the presence of data modulation," *IEEE Transactions on Communications*, vol. 36, pp. 596–604, May 1988.
- [25] E. Sourour and S. Gupta, "Direct-sequence spread-spectrum parallel acquisition in nonselective and frequency-selective Rician fading channels," *IEEE Journal on Selected Areas in Communications*, vol. 10, pp. 535–544, April 1992.
- [26] P.-T. Sun and C.-Y. Chu, "Hidden preamble detector for acquisition of frequency hopping multiple-access communication system," *IEE Proceedings Communications*, vol. 144, pp. 161–165, June 1997.
- [27] Y.-H. You, T.-H. Moon, J.-H. Kim, and C.-E. Kang, "Threshold decision technique for direct sequence code synchronisation in a fading mobile channel," *IEE Proceedings Communications*, vol. 144, pp. 155–1160, June 1997.
- [28] J. Holmes and C.-C. Chen, "Acquisition time performance of PN spread-spectrum systems," *IEEE Transactions on Communications*, vol. 25, pp. 778–784, August 1977.
- [29] V. Jovanovic and E. Sousa, "Analysis of non-coherent correlation in DS/BPSK spread spectrum acquisition," *IEEE Transactions on Communications*, vol. 43, pp. 565–573, February/March/April 1995.
- [30] A. Polydoros and C. Weber, "A unified approach to serial search spread-spectrum code acquisition-Part II: a matched-filter receiver," *IEEE Transactions on Communications*, vol. 32, pp. 550–560, May 1984.
- [31] E. Sourour and S. Gupta, "Direct-sequence spread-spectrum parallel acquisition in a fading mobile channel," *IEEE Transactions on Communications*, vol. 38, pp. 992–998, July 1990.
- [32] S. Glisic, T. Poutanen, W. Wu, G. Petrovic, and Z. Stefanovic, "New PN code acquisition scheme for CDMA networks with low signal-to-noise ratios," *IEEE Transactions on Communications*, vol. 47, pp. 300–310, February 1999.

- [33] C.-J. Kim, H.-J. Lee, and H.-S. Lee, "Adaptive acquisition of PN sequences for DSSS communications," *IEEE Transactions on Communications*, vol. 46, pp. 993–996, August 1998.
- [34] B.-H. Kim and B.-G. Lee, "DSA: a distributed sample-based fast DS/CDMA acquisition technique," *IEEE Transactions on Communications*, vol. 47, pp. 754–765, May 1999.
- [35] B.-H. Kim and B.-G. Lee, "Performance analysis of DSA-based DS/CDMA acquisition," *IEEE Transactions on Communications*, vol. 47, pp. 817–822, June 1999.
- [36] M. Salih and S. Tantarana, "A closed-loop coherent PN acquisition system with a pre-loop estimator," *IEEE Transactions on Communications*, vol. 47, pp. 1394–1405, September 1999.
- [37] R. Smith and S. Miller, "Acquisition performance of an adaptive receiver for DS-CDMA," *IEEE Transactions on Communications*, vol. 47, pp. 1416–1424, September 1999.
- [38] D. Dicarlo and C. Weber, "Statistical performance of single dwell serial synchronization systems," *IEEE Transactions on Communications*, vol. 28, pp. 1382–1388, August 1980.
- [39] Y.-T. Su, "Rapid code acquisition algorithms employing PN matched filters," *IEEE Transactions on Communications*, vol. 36, pp. 724–732, June 1988.
- [40] U. Madhow and M. Pursley, "Acquisition in direct-sequence spread-spectrum communication networks: an asymptotic analysis," *IEEE Transactions on Information Theory*, vol. 39, pp. 903–912, May 1993.
- [41] P. Baier, K. Dostert, and M. Pandit, "A novel spread-spectrum receiver synchronization scheme using a saw-tapped delay line," *IEEE Transactions on Communications*, vol. 30, pp. 1037–1047, May 1982.
- [42] C.-D. Chung, "Differentially coherent detection technique for direct-sequence code acquisition in a rayleigh fading mobile channel," *IEEE Transactions on Communications*, vol. 43, pp. 1116–1126, February/March/April 1995.
- [43] D. Dicarlo and C. Weber, "Multiple dwell serial search: performance and application to direct sequence code acquisition," *IEEE Transactions on Communications*, vol. 31, pp. 650–659, May 1983.
- [44] B. Ibrahim and A. Aghvami, "Direct sequence spread spectrum matched filter acquisition in frequency-selective Rayleigh fading channels," *IEEE Journal on Selected Areas in Communications*, vol. 12, pp. 885–890, June 1994.
- [45] J. Li and S. Tantarana, "Optimal and suboptimal coherent acquisition schemes for PN sequences with data modulation," *IEEE Transactions on Communications*, vol. 43, pp. 554–564, February/March/April 1995.
- [46] H.-R. Park and B.-J. Kang, "On the performance of a maximum-likelihood code-acquisition technique for preamble search in a CDMA reverse link," *IEEE Transactions on Vehicular Technology*, vol. 47, pp. 65–74, February 1998.
- [47] M. Zarrabizadeh and E. Sousa, "A differentially coherent PN code acquisition receiver for CDMA systems," *IEEE Transactions on Communications*, vol. 45, pp. 1456–1465, November 1997.
- [48] U. Cheng, W. Hurd, and J. Statman, "Spread-spectrum code acquisition in the presence of doppler shift and data modulation," *IEEE Transactions on Communications*, vol. 38, pp. 241–250, February 1990.
- [49] K. K. Chawla and D. V. Sarwate, "Parallel acquisition of PN sequences in DS/SS systems," *IEEE Transactions on Communications*, vol. 42, pp. 2155–2164, May 1994.
- [50] L.-L. Yang and J. Simsa, "Performance evaluation of spread-spectrum code acquisition system using four-state Markov process," in *Proceedings IEEE ISSSTA '98*, (Sun City: South Africa), pp. 848–852, September 1998.

- [51] L.-L. Yang and L. Hanzo, "Serial acquisition techniques for DS-CDMA signals in frequency-selective multi-user mobile channels," in *Proceedings of IEEE VTC'99*, (Houston, USA), pp. 2398–2402, May 1999.
- [52] M. Katz and S. Glisic, "Modeling of code acquisition process in CDMA networks - quasi-synchronous systems," *IEEE Transactions on Communications*, vol. 46, pp. 1564–1568, December 1998.
- [53] W.-H. Sheen, J.-K. Tzeng, and C.-K. Tzou, "Effects of cell correlations in a matched-filter PN code acquisition for direct-sequence spread-spectrum systems," *IEEE Transactions on Vehicular Technology*, vol. 48, pp. 724–732, May 1999.
- [54] D. Zheng, J. Li, S. Miller, and E. Strom, "An efficient code-timing estimator for DS-CDMA signals," *IEEE Transactions on Signal Processing*, vol. 45, pp. 82–89, January 1997.
- [55] E. Strom, S. Parkvall, S. Miller, and B. Ottersten, "Propagation delay estimation in asynchronous direct-sequence code-division multiple access systems," *IEEE Transactions on Communications*, vol. 44, pp. 84–93, January 1996.
- [56] L.-C. Chu and U. Mitra, "Analysis of MUSIC-based delay estimators for direct-sequence code-division multiple-access systems," *IEEE Transactions on Communications*, vol. 47, pp. 133–138, January 1999.
- [57] J. Blogh and L. Hanzo, *3G Systems and Intelligent Networking*. John Wiley and IEEE Press, 2002. (For detailed contents, please refer to <http://www-mobile.ecs.soton.ac.uk>.)
- [58] M. Zeng, A. Annamalai, and V. K. Bhargava, "Recent advances in cellular wireless communications," *IEEE Communications Magazine*, pp. 128–138, September 1999.
- [59] P. Chaudhury, W. Mohr, and S. Onoe, "The 3GPP proposal for IMT-2000," *IEEE Communications Magazine*, pp. 72–81, December 1999.
- [60] M. Proglor, C. Evci, and M. Umehira, "Air interface access schemes for broadband mobile systems," *IEEE Communications Magazine*, pp. 106–115, September 1999.
- [61] L. Kleinrock, "On some principles of nomadic computing and multi-access communications," *IEEE Communications Magazine*, pp. 46–50, July 2000.
- [62] P. Bender, P. Black, M. Grob, R. Padovani, N. Sindhushayana, and A. Viterbi, "CDMA/HDR: A bandwidth-efficient high-speed wireless data service for nomadic users," *IEEE Communications Magazine*, pp. 70–77, July 2000.
- [63] J. Chuang and N. Sollenberger, "Beyond 3G: wideband wireless data access based on OFDM and dynamic packet assignment," *IEEE Communications Magazine*, pp. 78–87, July 2000.
- [64] N. Dimitriou, R. Tafazolli, and G. Sfikas, "Quality of service for multimedia CDMA," *IEEE Communications Magazine*, pp. 88–94, July 2000.
- [65] H. Tsurumi and Y. Suzuki, "Broadband RF stage architecture for software-defined radio in handheld terminal applications," *IEEE Communications Magazine*, pp. 90–95, February 1999.
- [66] R. H. Walden, "Performance trends for analog-to-digital converters," *IEEE Communications Magazine*, pp. 96–101, February 1999.
- [67] S. Srikanteswara, J. H. Reed, P. Athanas, and R. Boyle, "A soft radio architecture for reconfigurable platforms," *IEEE Communications Magazine*, pp. 140–147, February 2000.
- [68] D. Murotake, J. Oates, and A. Fuchs, "Real-time implementation of a reconfigurable IMT-2000 base station channel modem," *IEEE Communications Magazine*, pp. 148–152, February 2000.

- [69] E. Sourour and M. Nakagawa, "Performance of orthogonal multicarrier CDMA in a multipath fading channel," *IEEE Transactions on Communications*, vol. 44, pp. 356–367, March 1996.
- [70] L.-L. Yang and L. Hanzo, "Blind soft-detection assisted frequency-hopping multicarrier DS-CDMA systems," in *Proceedings of IEEE GLOBECOM'99*, (Rio de Janeiro, Brazil), pp. 842–846, December:5-9 1999.
- [71] S. Slimane, "MC-CDMA with quadrature spreading for wireless communication systems," *European Transactions on Telecommunications*, vol. 9, pp. 371–378, July–August 1998.
- [72] L.-L. Yang and L. Hanzo, "Slow frequency-hopping multicarrier DS-CDMA for transmission over Nakagami multipath fading channels," *IEEE Journal on Selected Areas in Communications (Accepted for publication)*, vol. 19, no. 7, pp. 1211–1221, 2001.
- [73] S. Verdu, "Wireless bandwidth in the making," *IEEE Communications Magazine*, pp. 53–58, July 2000.
- [74] S. Nanda, K. Balachandran, and S. Kumar, "Adaptation techniques in wireless packet data services," *IEEE Communications Magazine*, pp. 54–64, January 2000.
- [75] A. J. Goldsmith and S. G. Chua, "Variable-rate variable-power MQAM for fading channels," *IEEE Transactions on Communications*, vol. 45, pp. 1218–1230, October 1997.
- [76] M. S. Alouini and A. J. Goldsmith, "Capacity of Rayleigh fading channels under different adaptive transmission and diversity-combining techniques," *IEEE Transactions on Vehicular Technology*, vol. 48, pp. 1165–1181, July 1999.
- [77] A. Duel-Hallen, S. Hu, and H. Hallen, "Long-range prediction of fading signals," *IEEE Signal Processing Magazine*, pp. 62–75, May 2000.
- [78] L.-L. Yang and L. Hanzo, "Blind joint soft-detection assisted slow frequency-hopping multicarrier DS-CDMA," *IEEE Transactions on Communications*, vol. 48, pp. 1520–1529, September 2000.
- [79] R. Prasad and S. Hara, "Overview of multi-carrier CDMA," *IEEE Communications Magazine*, vol. 35, pp. 126–133, Dec. 1997.
- [80] L. Hanzo, W. Webb, and T. Keller, *Single- and Multi-carrier Quadrature Amplitude Modulation: Principles and Applications for Personal Communications, WLANs and Broadcasting*. London: IEEE Press, and John Wiley & Sons, 2nd ed., 1999.
- [81] R. Steele and L. Hanzo, *Mobile Radio Communications*. IEEE Press-John Wiley, 2 ed., 1999.
- [82] L.-L. Yang and L. Hanzo, "Parallel code-acquisition for multicarrier DS-CDMA systems communicating over multipath Nakagami fading channels," in *Proceedings of IEEE GLOBECOM'2000*, (San Francisco, California), November 27 - December 1 2000.
- [83] S. Verdú, *Multuser Detection*. Cambridge University Press, 1998.
- [84] C. Berrou and A. Glavieux, "Near optimum error correcting coding and decoding: turbo-codes," *IEEE Transactions on Communications*, vol. 44, pp. 1261–1271, Oct. 1996.
- [85] Y. Li and N. R. Sollenberger, "Adaptive antenna arrays for OFDM systems with cochannel interference," *IEEE Trans. on. Comms.*, vol. 47, pp. 217–229, Feb 1999.
- [86] V. Tarokh, N. Seshadri, and A. R. Calderbank, "Space-time codes for high data rate wireless communication: performance criterion and code construction," *IEEE Transactions on Information Theory*, vol. 44, pp. 744–765, March 1998.
- [87] M. K. Simon, J. K. Omura, R. A. Scholtz, and B. K. Levitt, *Spread Spectrum Communications Handbook*. McGraw Hill, 1994.

- [88] A. J. Viterbi, *CDMA: Principles of Spread Spectrum Communication*. Addison-Wesley Publishing Company, 1995.
- [89] L. E. Miller and J. S. Lee, *CDMA Systems Engineering Handbook*. Boston: Artech House, 1998.
- [90] J. S. Lee, "Overview of the technical basis of QUALCOMM's CDMA cellular telephone system design : A view of North American TIA/EIA IS-95," in *International Conference on Communications Systems (ICCS)*, (Singapore), pp. 353–358, 1994.
- [91] R. Prasad, *CDMA for Wireless Personal Communications*. Artech House, Inc., 1996.
- [92] S. G. Glisic and P. A. Leppänen, *Wireless Communications TDMA versus CDMA*. Kluwer Academic Publishers, 1997.
- [93] S. Glisic and B. Vucetic, *Spread Spectrum CDMA Systems for Wireless Communications*. Artech House, Inc., 1997.
- [94] P. W. Baier, "A critical review of CDMA," in *Proceedings of the IEEE Vehicular Technology Conference (VTC)*, (Atlanta, USA), pp. 6–10, Apr. 28-May 1 1996.
- [95] J. G. Proakis, *Digital Communications*. Mc-Graw Hill International Editions, 3rd ed., 1995.
- [96] G. Stüber, *Principles of Mobile Communication*. Kluwer Academic Publishers, 1996.
- [97] L. Hanzo, W. Webb, and T. Keller, *Single and Multicarrier Quadrature Amplitude Modulation*. John-Wiley IEEE Press, 2000.
- [98] R. L. Pickholtz, L. B. Milstein, and D. L. Schilling, "Spread spectrum for mobile communications," *IEEE Transactions on Vehicular Technology*, vol. 40, pp. 313–322, May 1991.
- [99] A. J. Viterbi, "Wireless digital communication : a view based on three lessons learned," *IEEE Communications Magazine*, pp. 33–36, Sep. 1991.
- [100] A. Klein, B. Steiner, and A. Steil, "Known and novel diversity approaches as powerful means to enhance the performance of cellular mobile radio systems," *IEEE Journal on Selected Areas in Communications*, vol. 14, pp. 1784–1795, Dec. 1996.
- [101] A. Baier, U.-C. Fiebig, W. Granzow, W. Koch, P. Teder, and J. Thielecke, "Design study for a CDMA-based third-generation mobile radio system," *IEEE Journal on Selected Areas in Communications*, vol. 12, pp. 733–743, May 1994.
- [102] T. Ottosson and A. Svensson, "On schemes for multirate support in DS-CDMA systems," *Wireless Personal Communications (Kluwer)*, vol. 6, pp. 265–287, Mar. 1998.
- [103] S. Ramakrishna and J. M. Holtzman, "A comparison between single code and multiple code transmission schemes in a CDMA system," in *Proceedings of the IEEE Vehicular Technology Conference (VTC)*, (Ottawa, Canada), pp. 791–795, May 18-21 1998.
- [104] R. E. Blahut, *Theory and Practice of Error Control Codes*. Addison-Wesley Publishing Company, 1983.
- [105] M. P. Lötter and L. P. Linde, "A comparison of three families of spreading sequences for CDMA applications," in *Proceedings of IEEE South African Symposium on Communications and Signal Processing (COMSIG)*, (Stellenbosch, South Africa), pp. 68–75, Oct. 4 1994.
- [106] R. Gold, "Optimal binary sequences for spread spectrum multiplexing," *IEEE Transactions on Information Theory*, vol. 13, pp. 619–621, Oct. 1967.
- [107] T. Kasami, *Combinatorial Mathematics and its Applications*. University of North Carolina Press, 1969.

- [108] M. Pursley, "Performance evaluation for phase-coded SSMA communication - part 1 : System analysis," *IEEE Transactions on Communications*, vol. 25, pp. 795–799, Aug. 1977.
- [109] A. D. Whalen, *Detection of signals in noise*. Academic Press, 1971.
- [110] M. Failli, "Digital land mobile radio communications COST 207," tech. rep., European Commission, Luxembourg, 1989.
- [111] S. Verdú, "Minimum probability of error for asynchronous Gaussian multiple access channels," *IEEE Transactions on Information Theory*, vol. 32, pp. 85–96, Jan. 1986.
- [112] J. S. Thompson, P. M. Grant, and B. Mulgrew, "Smart antenna arrays for cdma systems," *IEEE Personal Communications Magazine*, vol. 3, pp. 16–25, Oct. 1996.
- [113] J. S. Thompson, P. M. Grant, and B. Mulgrew, "Performance of antenna array receiver algorithms for CDMA," in *Proceedings of the IEEE Global Telecommunications Conference (GLOBECOM)*, (London, UK), pp. 570–574, Nov. 18–22 1996.
- [114] A. F. Naguib and A. Paulraj, "Performance of wireless CDMA with m-ary orthogonal modulation and cell site antenna arrays," *IEEE Journal on Selected Areas in Communications*, vol. 14, pp. 1770–1783, Dec. 1996.
- [115] L. C. Godara, "Application of antenna arrays to mobile communications, part I: Performance improvement, feasibility, and system considerations," *Proceedings of the IEEE*, vol. 85, pp. 1031–1060, Aug. 1997.
- [116] R. Kohno, H. Imai, M. Hatori, and S. Pasupathy, "Combination of adaptive array antenna and a canceller of interference for direct-sequence spread-spectrum multiple-access system," *IEEE Journal on Selected Areas in Communications*, vol. 8, pp. 675–681, May 1998.
- [117] R. Lupas and S. Verdú, "Linear multiuser detectors for synchronous code division multiple access channels," *IEEE Transactions on Information Theory*, vol. 35, pp. 123–136, Jan. 1989.
- [118] R. Lupas and S. Verdú, "Near-far resistance of multiuser detectors in asynchronous channels," *IEEE Transactions on Communications*, vol. 38, pp. 509–519, Apr. 1990.
- [119] Z. Zvonar and D. Brady, "Suboptimal multiuser detector for frequency selective Rayleigh fading synchronous CDMA channels," *IEEE Transactions on Communications*, vol. 43, pp. 154–157, Feb.-Apr. 1995.
- [120] Z. Zvonar and D. Brady, "Differentially coherent multiuser detection in asynchronous CDMA flat Rayleigh fading channels," *IEEE Transactions on Communications*, vol. 43, pp. 1252–1255, Feb.-Apr. 1995.
- [121] Z. Zvonar, "Combined multiuser detection and diversity reception for wireless CDMA systems," *IEEE Transactions on Vehicular Technology*, vol. 45, pp. 205–211, Feb. 1996.
- [122] T. Kawahara and T. Matsumoto, "Joint decorrelating multiuser detection and channel estimation in asynchronous cdma mobile communications channels," *IEEE Transactions on Vehicular Technology*, vol. 44, pp. 506–515, Aug. 1995.
- [123] M. Hosseinian, M. Fattouche, and A. B. Sesay, "A multiuser detection scheme with pilot symbol-aided channel estimation for synchronous CDMA systems," in *Proceedings of the IEEE Vehicular Technology Conference (VTC)*, (Ottawa, Canada), pp. 796–800, May 18–21 1998.
- [124] M. J. Juntti, B. Aazhang, and J. O. Lilleberg, "Iterative implementation of linear multiuser detection for dynamic asynchronous CDMA systems," *IEEE Transactions on Communications*, vol. 46, pp. 503–508, Apr. 1998.
- [125] P.-A. Sung and K.-C. Chen, "A linear minimum mean square error multiuser receiver in Rayleigh fading channels," *IEEE Journal on Selected Areas in Communications*, vol. 14, pp. 1583–1594, Oct. 1996.

- [126] A. Duel-Hallen, "Decorrelating decision-feedback multiuser detector for synchronous code-division multiple-access channel," *IEEE Transactions on Communications*, vol. 41, pp. 285–290, Feb. 1993.
- [127] G. H. Golub and C. F. van Loan, *Matrix Computations*. North Oxford Academic, 1983.
- [128] L. Wei and C. Schlegel, "Synchronous DS-SSMA system with improved decorrelating decision-feedback multiuser detection," *IEEE Transactions on Vehicular Technology*, vol. 43, pp. 767–772, Aug. 1994.
- [129] A. Hafeez and W. E. Stark, "Combined decision-feedback multiuser detection/soft-decision decoding for CDMA channels," in *Proceedings of the IEEE Vehicular Technology Conference (VTC)*, (Atlanta, USA), pp. 382–386, Apr. 28-May 1 1996.
- [130] S. Haykin, *Adaptive Filter Theory*. Prentice-Hall International, Inc., 1996.
- [131] A. Klein and P. W. Baier, "Linear unbiased data estimation in mobile radio systems applying CDMA," *IEEE Journal on Selected Areas in Communications*, vol. 11, pp. 1058–1066, Sep. 1993.
- [132] A. Klein, G. K. Kaleh, and P. W. Baier, "Zero forcing and minimum mean square error equalization for multiuser detection in code division multiple access channels," *IEEE Transactions on Vehicular Technology*, vol. 45, pp. 276–287, May 1996.
- [133] J. Blanz, A. Klein, M. Nasshan, and A. Steil, "Performance of a cellular hybrid C/TDMA mobile radio system applying joint detection and coherent receiver antenna diversity," *IEEE Journal on Selected Areas in Communications*, vol. 12, pp. 568–579, May 1994.
- [134] P. Jung and J. Blanz, "Joint detection with coherent receiver antenna diversity in CDMA mobile radio systems," *IEEE Transactions on Vehicular Technology*, vol. 44, pp. 76–88, Feb. 1995.
- [135] P. Jung, J. Blanz, M. Nasshan, and P. W. Baier, "Simulation of the uplink of the JD-CDMA mobile radio systems with coherent receiver antenna diversity," *Wireless Personal Communications (Kluwer)*, vol. 1, no. 1, pp. 61–89, 1994.
- [136] A. Steil and J. J. Blanz, "Spectral efficiency of JD-CDMA mobile radio systems applying coherent receiver antenna diversity," in *Proceedings of the International Symposium on Spread Spectrum Techniques and Applications (ISSSTA)*, (Mainz, Germany), pp. 313–319, Sep. 22-25 1996.
- [137] P. Jung, M. Nasshan, and J. Blanz, "Application of turbo codes to a CDMA mobile radio system using joint detection and antenna diversity," in *Proceedings of the IEEE Vehicular Technology Conference (VTC)*, (Stockholm, Sweden), pp. 770–774, Jun. 8-10 1994.
- [138] P. Jung and M. Nasshan, "Results on turbo-codes for speech transmission in a joint detection CDMA mobile radio system with coherent receiver antenna diversity," *IEEE Transactions on Vehicular Technology*, vol. 46, pp. 862–870, Nov. 1997.
- [139] M. M. Nasshan, A. Steil, A. Klein, and P. Jung, "Downlink cellular radio capacity of a joint detection CDMA mobile radio system," in *Proceedings of the 45th IEEE Vehicular Technology Conference (VTC)*, (Chicago, USA), pp. 474–478, Jul. 25-28 1995.
- [140] A. Klein, "Data detection algorithms specially designed for the downlink of CDMA mobile radio systems," in *Proceedings of the IEEE Vehicular Technology Conference (VTC)*, (Phoenix, USA), pp. 203–207, May 4-7 1997.
- [141] B. Steiner and P. Jung, "Optimum and suboptimum channel estimation for the uplink of CDMA mobile radio systems with joint detection," *European Transactions on Telecommunications*, vol. 5, pp. 39–50, 1994.

- [142] M. Werner, "Multistage joint detection with decision feedback for CDMA mobile radio applications," in *Proceedings of the IEEE International Symposium on Personal, Indoor and Mobile Radio Communications (PIMRC)*, pp. 178–183, 1994.
- [143] M. K. Varanasi and B. Aazhang, "Multistage detection in asynchronous code-division multiple-access communications," *IEEE Transactions on Communications*, vol. 38, pp. 509–519, Apr. 1990.
- [144] M. K. Varanasi, "Group detection for synchronous Gaussian code-division multiple-access channels," *IEEE Transactions on Information Theory*, vol. 41, pp. 1083–1096, July 1995.
- [145] M. K. Varanasi, "Parallel group detection for synchronous CDMA communication over frequency-selective Rayleigh fading channels," *IEEE Transactions on Information Theory*, vol. 42, pp. 116–128, Jan. 1996.
- [146] Y. C. Yoon, R. Kohno, and H. Imai, "A SSMA system with cochannel interference cancellation with multipath fading channels," *IEEE Journal on Selected Areas in Communications*, vol. 11, pp. 1067–1075, Sep. 1993.
- [147] T. R. Giallorenzi and S. G. Wilson, "Suboptimum multiuser receivers for convolutionally coded asynchronous DS-CDMA systems," *IEEE Transactions on Communications*, vol. 44, pp. 1183–1196, Sep. 1996.
- [148] Y. Sanada and M. Nakagawa, "A multiuser interference cancellation technique utilizing convolutional codes and multicarrier modulation for wireless indoor communications," *IEEE Journal on Selected Areas in Communications*, vol. 14, pp. 1500–1509, Oct. 1996.
- [149] M. Latva-aho, M. Juntti, and M. Heikkilä, "Parallel interference cancellation receiver for DS-CDMA systems in fading channels," in *Proceedings of the IEEE International Symposium on Personal, Indoor and Mobile Radio Communications (PIMRC)*, (Helsinki, Finland), pp. 559–564, Sep. 1-4 1997.
- [150] D. Dahlhaus, A. Jarosch, B. H. Fleury, and R. Heddergott, "Joint demodulation in DS/CDMA systems exploiting the space and time diversity of the mobile radio channel," in *Proceedings of the IEEE International Symposium on Personal, Indoor and Mobile Radio Communications (PIMRC)*, (Helsinki, Finland), pp. 47–52, Sep. 1-4 1997.
- [151] D. Divsalar, M. K. Simon, and D. Raphaeli, "Improved parallel interference cancellation for CDMA," *IEEE Transactions on Communications*, vol. 46, pp. 258–267, Feb. 1998.
- [152] P. Patel and J. Holtzman, "Analysis of a simple successive interference cancellation scheme in a DS/CDMA system," *IEEE Journal on Selected Area in Communications*, vol. 12, pp. 796–807, June 1994.
- [153] A. C. K. Soong and W. A. Krzymien, "A novel CDMA multi-user interference cancellation receiver with reference symbol aided estimation of channel parameters," *IEEE Journal on Selected Areas in Communications*, vol. 14, pp. 1536–1547, Oct. 1996.
- [154] A. L. C. Hui and K. B. Letaief, "Successive interference cancellation for multiuser asynchronous DS/CDMA detectors in multipath fading links," *IEEE Transactions on Communications*, vol. 46, pp. 384–391, Mar. 1998.
- [155] Y. Li and R. Steele, "Serial interference cancellation method for CDMA," *Electronics Letters*, vol. 30, pp. 1581–1583, Sep. 1994.
- [156] T. B. Oon, R. Steele, and Y. Li, "Cancellation frame size for a quasi-single-bit detector in asynchronous CDMA channel," *Electronics Letters*, vol. 33, pp. 258–259, Feb. 1997.
- [157] T.-B. Oon, R. Steele, and Y. Li, "Performance of an adaptive successive serial-parallel CDMA cancellation scheme in flat Rayleigh fading channels," in *Proceedings of the IEEE Vehicular Technology Conference (VTC)*, (Phoenix, USA), pp. 193–197, May 4-7 1997.

- [158] M. Sawahashi, Y. Miki, H. Andoh, and K. Higuchi, "Pilot symbol-assisted coherent multistage interference canceller using recursive channel estimation for DS-CDMA mobile radio," *IEICE Transactions on Communications*, vol. E79-B, pp. 1262–1270, Sep. 1996.
- [159] S. Sun, L. K. Rasmussen, H. Sugimoto, and T. J. Lim, "Hybrid interference canceller in CDMA," in *Proceedings of the IEEE International Symposium on Spread Spectrum Techniques and Applications (ISSSTA)*, (Sun City, South Africa), pp. 150–154, Sep. 2-4 1998.
- [160] Y. Cho and J. H. Lee, "Analysis of an adaptive SIC for near-far resistant DS-CDMA," *IEEE Transactions on Communications*, vol. 46, pp. 1429–1432, Nov. 1998.
- [161] P. Agashe and B. Woerner, "Interference cancellation for a multicellular CDMA environment," *Wireless Personal Communications (Kluwer)*, vol. 3, no. 1-2, pp. 1–14, 1996.
- [162] L. K. Rasmussen, T. J. Lim, and T. M. Aulin, "Breadth-first maximum likelihood detection in multiuser CDMA," *IEEE Transactions on Communications*, vol. 45, pp. 1176–1178, Oct. 1997.
- [163] L. Wei, L. K. Rasmussen, and R. Wyrwas, "Near optimum tree-search detection schemes for bit-synchronous multiuser CDMA systems over Gaussian and two-path Rayleigh-fading channels," *IEEE Transactions on Communications*, vol. 45, pp. 691–700, June 1997.
- [164] M. Nasiri-Kenari, R. R. Sylvester, and C. K. Rushforth, "Efficient soft-in-soft-out multiuser detector for synchronous CDMA with error-control coding," *IEEE Transactions on Vehicular Technology*, vol. 47, pp. 947–953, Aug. 1998.
- [165] J. B. Anderson and S. Mohan, "Sequential coding algorithms: a survey and cost analysis," *IEEE Transactions on Communications*, vol. 32, pp. 169–176, Feb. 1984.
- [166] C. Schlegel, S. Roy, P. D. Alexander, and Z.-J. Xiang, "Multiuser projection receivers," *IEEE Journal on Selected Areas in Communications*, vol. 14, pp. 1610–1618, Oct. 1996.
- [167] P. D. Alexander, L. K. Rasmussen, and C. B. Schlegel, "A linear receiver for coded multiuser CDMA," *IEEE Transactions on Communications*, vol. 45, pp. 605–610, May 1997.
- [168] P. B. Rapajic and B. S. Vucetic, "Adaptive receiver structures for asynchronous CDMA systems," *IEEE Journal on Selected Areas in Communications*, vol. 12, pp. 685–697, May 1994.
- [169] G. Woodward and B. S. Vucetic, "Adaptive detection for DS-CDMA," *Proceedings of the IEEE*, vol. 86, pp. 1413–1434, July 1998.
- [170] Z. Xie, R. T. Short, and C. K. Rushforth, "Family of suboptimum detectors for coherent multiuser communications," *IEEE Journal on Selected Areas in Communications*, vol. 8, pp. 683–690, May 1990.
- [171] T. J. Lim, L. K. Rasmussen, and H. Sugimoto, "An asynchronous multiuser CDMA detector based on the kalman filter," *IEEE Journal on Selected Areas in Communications*, vol. 16, pp. 1711–1722, Dec. 1998.
- [172] P. Seite and J. Tardivel, "Adaptive equalizers for joint detection in an indoor CDMA channel," in *Proceedings of the IEEE Vehicular Technology Conference (VTC)*, (Chicago, USA), pp. 484–488, Jul. 25-28 1995.
- [173] S. M. Spangenberg, D. G. M. Cruickshank, S. McLaughlin, G. J. R. Povey, and P. M. Grant, "Advanced multiuser detection techniques for downlink CDMA, version 2.0," tech. rep., Virtual Centre of Excellence in Mobile and Personal Communications Ltd (Mobile VCE), July 1999.
- [174] G. J. R. Povey, P. M. Grant, and R. D. Pringle, "A decision-directed spread-spectrum RAKE receiver for fast-fading mobile channels," *IEEE Transactions on Vehicular Technology*, vol. 45, pp. 491–502, Aug. 1996.

- [175] H. Liu and K. Li, "A decorrelating RAKE receiver for CDMA communications over frequency-selective fading channels," *IEEE Transactions on Communications*, vol. 47, pp. 1036–1045, Jul. 1999.
- [176] Z. Xie, C. K. Rushforth, R. T. Short, and T. K. Moon, "Joint signal detection and parameter estimation in multiuser communications," *IEEE Transactions on Communications*, vol. 41, pp. 1208–1216, Aug. 1993.
- [177] N. Seshadri, "Joint data and channel estimation using blind trellis search techniques," *IEEE Transactions on Communications*, vol. 42, pp. 1000–1011, Feb/Mar/Apr 1994.
- [178] R. Raheli, A. Polydoros, and C.-K. Tzou, "Per-survivor-processing: A general approach to MLSE in uncertain environments," *IEEE Transactions on Communications*, vol. 43, pp. 354–364, Feb/Mar/Apr 1995.
- [179] R. Raheli, G. Marino, and P. Castoldi, "Per-survivor processing and tentative decisions: What is in between?," *IEEE Transactions on Communications*, vol. 44, pp. 127–129, Feb. 1998.
- [180] T. K. Moon, Z. Xie, C. K. Rushforth, and R. T. Short, "Parameter estimation in a multi-user communication system," *IEEE Transactions on Communications*, vol. 42, pp. 2553–2560, Aug. 1994.
- [181] R. Iltis and L. Mailaender, "Adaptive multiuser detector with joint amplitude and delay estimation," *IEEE Journal on Selected Areas in Communications*, vol. 12, pp. 774–785, June 1994.
- [182] U. Mitra and H. V. Poor, "Adaptive receiver algorithms for near-far resistant CDMA," *IEEE Transactions on Communications*, vol. 43, pp. 1713–1724, Feb-Apr 1995.
- [183] U. Mitra and H. V. Poor, "Analysis of an adaptive decorrelating detector for synchronous CDMA," *IEEE Transactions on Communications*, vol. 44, pp. 257–268, Feb. 1996.
- [184] X. Wang and H. V. Poor, "Blind equalization and multiuser detection in dispersive CDMA channels," *IEEE Transactions on Communications*, vol. 46, pp. 91–103, Jan. 1998.
- [185] X. D. Wang and H. V. Poor, "Blind multiuser detection: a subspace approach," *IEEE Transactions on Information Theory*, vol. 44, pp. 677–690, Mar. 1998.
- [186] M. Honig, U. Madhow, and S. Verdú, "Blind adaptive multiuser detection," *IEEE Transactions on Information Theory*, vol. 41, pp. 944–960, July 1995.
- [187] N. B. Mandayam and B. Aazhang, "Gradient estimation for sensitivity analysis and adaptive multiuser interference rejection in code division multiple access systems," *IEEE Transactions on Communications*, vol. 45, pp. 848–858, July 1997.
- [188] S. Ulukus and R. D. Yates, "A blind adaptive decorrelating detector for CDMA systems," *IEEE Journal on Selected Areas in Communications*, vol. 16, no. 8, pp. 1530–1541, 1998.
- [189] T. J. Lim and L. K. Rasmussen, "Adaptive symbol and parameter estimation in asynchronous multiuser CDMA detectors," *IEEE Transactions on Communications*, vol. 45, pp. 213–220, Feb. 1997.
- [190] J. Miguez and L. Castedo, "A linearly constrained constant modulus approach to blind adaptive multiuser interference suppression," *IEEE Communications Letters*, vol. 2, pp. 217–219, Aug. 1998.
- [191] D. N. Godard, "Self-recovering equalization and carrier tracking in two-dimensional data communication systems," *IEEE Transactions on Communications*, vol. 28, pp. 1867–1875, Nov. 1980.
- [192] K. Wesolowsky, "Analysis and properties of the modified constant modulus algorithm for blind equalization," *European Transactions on Telecommunications and Related Technologies*, vol. 3, pp. 225–230, May-Jun. 1992.
- [193] K. Fukawa and H. Suzuki, "Orthogonalizing matched filtering (OMF) detector for DS-CDMA mobile communication systems," *IEEE Transactions on Vehicular Technology*, vol. 48, pp. 188–197, Jan. 1999.

- [194] U. Fawer and B. Aazhang, "Multiuser receiver for code division multiple access communications over multipath channels," *IEEE Transactions on Communications*, vol. 43, pp. 1556–1565, Feb-Apr 1995.
- [195] W. H. Press, S. A. Teukolsky, W. T. Vetterling, and B. P. Flannery, *Numerical Recipes in C: The Art of Scientific Computing*. Cambridge University Press, 1993.
- [196] Y. Bar-Ness, "Asynchronous multiuser CDMA detector made simpler: Novel decorrelator, combiner, canceller, combiner (dc^3) structure," *IEEE Transactions on Communications*, vol. 47, pp. 115–122, Jan. 1999.
- [197] K. Yen and L. Hanzo, "Hybrid genetic algorithm based multi-user detection schemes for synchronous CDMA systems," in *Proceedings of the IEEE Vehicular Technology Conference (VTC)*, (Tokyo, Japan), May 15-18 2000.
- [198] W. M. Jang, B. R. Vojčić, and R. L. Pickholtz, "Joint transmitter-receiver optimization in synchronous multiuser communications over multipath channels," *IEEE Transactions on Communications*, vol. 46, pp. 269–278, Feb. 1998.
- [199] B. R. Vojčić and W. M. Jang, "Transmitter precoding in synchronous multiuser communications," *IEEE Transactions on Communications*, vol. 46, pp. 1346–1355, Oct. 1998.
- [200] R. Tanner and D. G. M. Cruickshank, "Receivers for nonlinearly separable scenarios in DS-CDMA," *Electronics Letters*, vol. 33, pp. 2103–2105, Dec. 1997.
- [201] R. Tanner and D. G. M. Cruickshank, "RBF based receivers for DS-CDMA with reduced complexity," in *Proceedings of the IEEE International Symposium on Spread Spectrum Techniques and Applications (ISSSTA)*, (Sun City, South Africa), pp. 647–651, Sep. 2-4 1998.
- [202] C. Berrou, P. Adde, E. Angui, and S. Faudeil, "A low-complexity soft-output Viterbi decoder architecture," in *Proceedings of IEEE International Conference on Communications (ICC)*, (Geneva, Switzerland), pp. 737–740, May 23-26 1993.
- [203] T. R. Giallorenzi and S. G. Wilson, "Multiuser ML sequence estimator for convolutionally coded asynchronous DS-CDMA systems," *IEEE Transactions on Communications*, vol. 44, pp. 997–1008, Aug. 1996.
- [204] M. Moher, "An iterative multiuser decoder for near-capacity communications," *IEEE Transactions on Communications*, vol. 46, pp. 870–880, July 1998.
- [205] M. Moher and P. Guinaud, "An iterative algorithm for asynchronous coded multiuser detection," *IEEE Communications Letters*, vol. 2, pp. 229–231, Aug. 1998.
- [206] P. D. Alexander, A. J. Grant, and M. C. Reed, "Iterative detection in code-division multiple-access with error control coding," *European Transactions on Telecommunications*, vol. 9, pp. 419–426, Sep.-Oct. 1998.
- [207] P. D. Alexander, M. C. Reed, J. A. Asenstorfer, and C. B. Schlegel, "Iterative multiuser interference reduction: Turbo CDMA," *IEEE Transactions on Communications*, vol. 47, pp. 1008–1014, Jul. 1999.
- [208] M. C. Reed, C. B. Schlegel, P. D. Alexander, and J. A. Asenstorfer, "Iterative multiuser detection for CDMA with FEC: Near-single-user performance," *IEEE Transactions on Communications*, vol. 46, pp. 1693–1699, Dec. 1998.
- [209] X. D. Wang and H. V. Poor, "Iterative (turbo) soft interference cancellation and decoding for coded CDMA," *IEEE Transactions on Communications*, vol. 47, pp. 1046–1061, Jul. 1999.
- [210] T. Ojanperä, A. Klein, and P.-O. Anderson, "FRAMES multiple access for UMTS," *IEE Colloquium (Digest)*, pp. 7/1–7/8, May 1997.
- [211] E. A. Lee and D. G. Messerschmitt, *Digital Communication*. Kluwer Academic Publishers, 1988.

- [212] D. F. Mix, *Random Signal Processing*. Prentice-Hall International, Inc., 1995.
- [213] H. R. Karimi and N. W. Anderson, "A novel and efficient solution to block-based joint-detection using approximate Cholesky factorization," in *Proceedings of the IEEE International Symposium on Personal, Indoor and Mobile Radio Communications (PIMRC)*, (Boston, USA), pp. 1340–1344, Sep 8-11 1998.
- [214] R. Karimi, "Efficient multi-rate multi-user detection for the asynchronous WCDMA uplink," in *Proceedings of the IEEE Vehicular Technology Conference (VTC Fall)*, (Amsterdam, The Netherlands), pp. 593–597, Sep. 19-22 1999.
- [215] N. Benvenuto and G. Sostrato, "Joint detection with low computational complexity for hybrid TD-CDMA systems," in *Proceedings of the IEEE Vehicular Technology Conference (VTC Fall)*, (Amsterdam, The Netherlands), pp. 618–622, Sep. 19-22 1999.
- [216] P. A. Bello, "Sample size required in error-rate measurement on fading channels," *Proceedings of the IEEE*, vol. 86, July 1998.
- [217] A. S. Barbulescu and S. S. Pietrobon, "Interleaver design for turbo codes," *IEE Electronics Letters*, vol. 30, pp. 2107–2108, Dec 1994.
- [218] J. Hagenauer and P. Hoeher, "A Viterbi algorithm with soft-decision outputs and its applications," in *Proceedings of IEEE Global Telecommunications Conference*, (Dallas, USA), pp. 1680–1686, Nov. 27-30 1989.
- [219] E. Papproth and G. K. Kaleh, "Near-far resistant channel estimation for the DS-CDMA uplink," in *Proceedings of the IEEE International Symposium on Personal, Indoor and Mobile Radio Communications (PIMRC)*, (Toronto, Canada), pp. 758–762, Sep. 27-29 1995.
- [220] T. Ojanperä and R. Prasad, *Wideband CDMA for Third Generation Mobile Communications*. Artech House, Inc., 1998.
- [221] W. T. Webb and R. Steele, "Variable rate QAM for mobile radio," *IEEE Transactions on Communications*, vol. 43, pp. 2223 – 2230, July 1995.
- [222] S. W. Kim, "Adaptive rate and power DS/CDMA communications in fading channels," *IEEE Communications Letters*, vol. 3, pp. 85–87, Apr. 1999.
- [223] F. Adachi, K. Ohno, A. Higashi, T. Dohi, and Y. Okumura, "Coherent multicode DS-CDMA mobile radio access," *IEICE Transactions on Communications*, vol. E79-B, pp. 1316–1325, Sep. 1996.
- [224] T. Dohi, Y. Okumura, A. Higashi, K. Ohno, and F. Adachi, "Experiments on coherent multicode DS-CDMA," *IEICE Transactions on Communications*, vol. E79-B, pp. 1326–1332, Sep. 1996.
- [225] H. D. Schotten, H. Elders-Boll, and A. Busboom, "Adaptive multi-rate multi-code CDMA systems," in *Proceedings of the IEEE Vehicular Technology Conference (VTC)*, (Ottawa, Canada), pp. 782–785, May 18-21 1998.
- [226] M. Saquib and R. Yates, "Decorrelating detectors for a dual rate synchronous DS/CDMA channel," *Wireless Personal Communications (Kluwer)*, vol. 9, pp. 197–216, May 1999.
- [227] M. J. Juntti, "Multiuser detector performance comparisons in multirate CDMA systems," in *Proceedings of the IEEE Vehicular Technology Conference (VTC)*, (Ottawa, Canada), pp. 36–40, May 18-21 1998.
- [228] S. Abeta, S. Sampei, and N. Morinaga, "Channel activation with adaptive coding rate and processing gain control for cellular DS/CDMA systems," in *Proceedings of the IEEE Vehicular Technology Conference (VTC)*, (Atlanta, USA), pp. 1115–1119, Apr. 28-May 1 1996.

- [229] M. Hashimoto, S. Sampei, and N. Morinaga, "Forward and reverse link capacity enhancement of DS/CDMA cellular system using channel activation and soft power control techniques," in *Proceedings of the IEEE International Symposium on Personal, Indoor and Mobile Radio Communications (PIMRC)*, (Helsinki, Finland), pp. 246–250, Sep. 1-4 1997.
- [230] V. K. N. Lau and S. V. Maric, "Variable rate adaptive modulation for DS-CDMA," *IEEE Transactions on Communications*, vol. 47, pp. 577–589, Apr. 1999.
- [231] S. Tateesh, S. Atungsiri, and A. M. Kondo, "Link adaptive multi-rate coding verification system for CDMA mobile communications," in *Proceedings of the IEEE Global Telecommunications Conference (GLOBECOM)*, (London, UK), pp. 1969–1973, Nov. 18-22 1996.
- [232] Y. Okumura and F. Adachi, "Variable data rate transmission with blind rate detection for coherent DS-CDMA mobile radio," *Electronics Letters*, vol. 32, pp. 1865–1866, Sep. 1996.
- [233] J. S. Blough, P. Cherriman, and L. Hanzo, "Adaptive beamforming assisted, power controlled dynamic channel allocation for adaptive modulation," in *Proceedings of the IEEE Vehicular Technology Conference (VTC Fall)*, (Amsterdam, The Netherlands), pp. 2348–2352, Sep. 19-22 1999.
- [234] K. Miya, O. Kato, K. Homma, T. Kitade, M. Hayashi, and T. Ue, "Wideband CDMA systems in TDD-mode operation for IMT-2000," *IEICE Transactions on Communications*, vol. E81-B, pp. 1317–1326, July 1998.
- [235] O. Kato, K. Miya, K. Homma, T. Kitade, M. Hayashi, and M. Watanabe, "Experimental performance results of coherent wideband DS-CDMA with TDD scheme," *IEICE Transactions on Communications*, vol. E81-B, pp. 1337–1344, July 1998.
- [236] I. Jeong and M. Nakagawa, "A novel transmission diversity system in TDD-CDMA," *IEICE Transactions on Communications*, vol. E81-B, pp. 1409–1416, July 1998.
- [237] T. Keller and L. Hanzo, "Adaptive orthogonal frequency division multiplexing schemes," in *Proceedings of the ACTS Mobile Communications Summit*, (Rhodes, Greece), pp. 794–799, June 1998.
- [238] T. Keller and L. Hanzo, "Blind-detection assisted sub-band adaptive turbo-coded OFDM schemes," in *Proceedings of the IEEE Vehicular Technology Conference (VTC Spring)*, (Houston, USA), pp. 489–493, May 16-20 1999.
- [239] S. Sampei, S. Komaki, and N. Morinaga, "Adaptive modulation/TDMA scheme for large capacity personal multimedia communications systems," *IEICE Transactions on Communications*, vol. E77-B, pp. 1096–1103, September 1994.
- [240] J. M. Torrance, *Adaptive Full Response Digital Modulation for Wireless Communications Systems*. PhD thesis, University of Southampton, 1997.
- [241] M. S. Yee and L. Hanzo, "Multi-level Radial Basis Function network based equalisers for Rayleigh channel," in *Proceedings of the IEEE Vehicular Technology Conference (VTC Spring)*, (Houston, USA), pp. 707–711, May 16-20 1999.
- [242] A. J. Goldsmith and S. G. Chua, "Variable rate variable power MQAM for fading channels," *IEEE Transactions on Communications*, vol. 45, pp. 1218 – 1230, October 1997.
- [243] C. H. Wong and L. Hanzo, "Upper-bound of a wideband burst-by-burst adaptive modem," in *Proceedings of the IEEE Vehicular Technology Conference (VTC Spring)*, (Houston, USA), pp. 1851–1855, May 16-20 1999.
- [244] T. Eyceoz, A. Duel-Hallen, and H. Hallen, "Deterministic channel modeling and long range prediction of fast fading mobile radio channels," *IEEE Communications Letters*, vol. 2, pp. 254–256, Sep. 1998.

- [245] F. Adachi, M. Sawahashi, and K. Okawa, "Tree-structured generation of orthogonal spreading codes with different lengths for forward link of DS-CDMA mobile radio," *Electronics Letters*, vol. 33, pp. 27–28, Jan. 1997.
- [246] A.-L. Johansson and A. Svensson, "Successive interference cancellation schemes in multi-rate DS/CDMA systems," in *Wireless Information Networks (Baltzer)*, pp. 265–279, 1996.
- [247] A. Toskala, J. P. Castro, E. Dahlman, M. Latva-aho, and T. Ojanperä, "FRAMES FMA2 Wideband-CDMA for UMTS," *European Transactions on Telecommunications*, vol. 9, pp. 325–335, Jul.-Aug. 1998.
- [248] T. Ue, S. Sampei, and N. Morinaga, "Symbol rate and modulation level controlled adaptive modulation/TDMA/TDD for personal communication systems," in *Proceedings of the IEEE Vehicular Technology Conference (VTC)*, (Chicago, USA), pp. 306–310, Jul. 25–28 1995.
- [249] S. M. Alamouti, "A simple transmit diversity technique for wireless communications," *IEEE Journal on Selected Areas in Communications*, vol. 16, pp. 1451–1458, Oct. 1998.
- [250] V. Tarokh, N. Seshadri, and A. R. Calderbank, "Space-time codes for high data rate wireless communication: Performance analysis and code construction," *IEEE Transactions on Information Theory*, vol. 44, pp. 744–765, Mar. 1998.
- [251] S. R. Kim, J. G. Lee, and H. Lee, "Interference cancellation scheme with simple structure and better performance," *Electronics Letters*, vol. 32, pp. 2115–2117, Nov. 1996.
- [252] D. Koulakiotis and A. H. Aghvami, "Evaluation of a DS/CDMA multiuser receiver employing a hybrid form of interference cancellation in Rayleigh-fading channels," *IEEE Communications Letters*, vol. 2, pp. 61–63, Mar. 1998.
- [253] A. L. Johansson and A. Svensson, "Multistage interference cancellation in multirate DS/CDMA on a mobile radio channel," in *Proceedings of the IEEE Vehicular Technology Conference (VTC)*, (Atlanta, USA), pp. 666–670, Apr. 28–May 1 1996.
- [254] M. E. Rollins and S. J. Simmons, "Simplified per-survivor Kalman processing in fast frequency-selective fading channels," *IEEE Transactions on Communications*, vol. 45, pp. 544–553, May 1997.
- [255] W. Koch and A. Baier, "Optimum and sub-optimum detection of coded data disturbed by time-varying inter-symbol interference," in *Proceedings of IEEE Global Telecommunications Conference (GLOBECOM)*, pp. 1679–1684, 1990.
- [256] J. A. Erfanian, S. Pasupathy, and G. Gulak, "Reduced complexity symbol detectors with parallel structures for ISI channels," *IEEE Transactions on Communications*, vol. 42, pp. 1661–1671, Feb.-Apr. 1994.
- [257] V. Tarokh, H. Jafarkhani, and A. R. Calderbank, "Space-time block coding for wireless communications: performance results," *IEEE Journal on Selected Areas in Communications*, vol. 17, pp. 451–460, March 1999.
- [258] A. F. Naguib, V. Tarokh, N. Seshadri, and A. R. Calderbank, "A space-time coding modem for high-data-rate wireless communications," *IEEE Journal on Selected Areas in Communications*, vol. 16, pp. 1459–1478, October 1998.
- [259] S. M. Alamouti, "A simple transmit diversity technique for wireless communications," *IEEE Journal on Selected Areas in Communications*, vol. 16, pp. 1451–1458, October 1998.
- [260] Proposed TDOC: 662/98 to ETSI SMG2 UMTS Standards, *Space-time block coded transmit antenna diversity for WCDMA*, December 1998.

- [261] Telcomm. Industry Association (TIA), *TIA/EIA Interim Standard: Physical Layer Standard for cdma2000 Standards for Spread Spectrum Systems*, 2000.
- [262] B. Hochwald, T. L. Marzetta, and C. B. Papadias, "A transmitter diversity scheme for wideband CDMA systems based on space-time spreading," *IEEE Journal on Selected Areas in Communications*, vol. 19, pp. 48–60, January 2001.
- [263] T. Eng and L. Milstein, "Coherent DS-CDMA performance in Nakagami multipath fading," *IEEE Transactions on Communications*, vol. 43, pp. 1134–1143, Feb./Mar./Apr. 1995.
- [264] W. Lee, *Mobile Communications Engineering*. New York: McGraw-Hill, 2nd ed., 1998.
- [265] N. Nakagami, "the m -distribution, a general formula for intensity distribution of rapid fading," in *Statistical Methods in Radio Wave Propagation* (W. G. Hoffman, ed.), Oxford, England: Pergamon, 1960.
- [266] V. Aalo, O. Ugweje, and R. Sudhakar, "Performance analysis of a DS/CDMA system with noncoherent M -ary orthogonal modulation in nakagami fading," *IEEE Transactions on Vehicular Technology*, vol. 47, pp. 20–29, February 1998.
- [267] M.-S. Alouini and A. Goldsmith, "A unified approach for calculating error rates of linearly modulated signals over generalized fading channels," *IEEE Transactions on Communications*, vol. 47, pp. 1324–1334, September 1999.
- [268] M. Simon and M.-S. Alouini, "A unified approach to the probability of error for noncoherent and differentially coherent modulation over generalized fading channels," *IEEE Transactions on Communications*, vol. 46, pp. 1625–1638, December 1998.
- [269] M. Simon and M.-S. Alouini, "A unified approach to the performance analysis of digital communication over generalized fading channels," *Proceedings of the IEEE*, vol. 86, pp. 1860–1877, September 1998.
- [270] L. E. Millera and J.-S. Lee, *CDMA Systems Engineering Handbook*. Artech House Pubs., 1998.
- [271] C. Darwin, *On the Origin of Species*. London: John Murray, 1859.
- [272] I. Rechenberg, "Cybernetic solution path of an experimental problem," tech. rep., Ministry of Aviation, Royal Aircraft Establishment, U.K., 1965.
- [273] H.-P. Schwefel, *Evolutionsstrategie und numerische Optimierung*. PhD thesis, Technische Universität Berlin, 1975.
- [274] L. Fogel, A. J. Owens, and M. J. Walsh, *Artificial Intelligence through Simulated Evolution*. New York: John Wiley, 1966.
- [275] T. Bäck, U. Hammel, and H.-P. Schwefel, "Evolutionary computation: Comments on the history and current state," *IEEE Transactions on Evolutionary Computation*, vol. 1, pp. 3–17, April 1997.
- [276] M. Mitchell, *An Introduction to Genetic Algorithms*. Cambridge, Massachusetts: MIT Press, 1996.
- [277] K. S. Tang, K. F. Man, S. Kwong, and Q. He, "Genetic algorithms and their applications," *IEEE Signal Processing Magazine*, vol. 13, pp. 22–37, November 1996.
- [278] D. Whitley, "A genetic algorithm tutorial," *Statistics and Computing*, vol. 4, pp. 65–85, June 1994.
- [279] S. Forrest, "Genetic algorithms: Principles of natural selection applied to computation," *Science*, vol. 261, pp. 872–878, August 1993.
- [280] H. Mühlenbein, *Foundations of Genetic Algorithms*, ch. Evolution in time and space – The Parallel Genetic Algorithm, pp. 316–337. California, USA: G. Rawlins, ed., Morgan Kaufmann, 1991.

- [281] J. J. Grefenstette and J. E. Baker, "How genetic algorithms work: A critical look at implicit parallelism," in *Proceedings of the Third International Conference on Genetic Algorithms* (J. D. Schaffer, ed.), (California, USA), pp. 20–27, Morgan Kaufmann, 1989.
- [282] B. L. Miller and D. E. Goldberg, "Genetic algorithms, selection schemes, and the varying effects of noise," *Evolutionary Computation*, vol. 4, pp. 113–131, Summer 1996.
- [283] G. Harik, E. Cantú-Paz, D. E. Goldberg, and B. L. Miller, "The gambler's ruin problem, genetic algorithms, and the sizing of populations," in *Proceedings of the 1997 IEEE Conference on Evolutionary Computation* (T. Bäck, ed.), (New York), pp. 7–12, IEEE Press, 1997.
- [284] M. D. Vose and G. E. Liepins, "Punctuated equilibria in genetic search," *Complex Systems*, vol. 5, pp. 31–44, January/February 1991.
- [285] A. E. Nix and M. D. Vose, "Modeling genetic algorithms with Markov chains," *Annals of Mathematics and Artificial Intelligence*, vol. 5, pp. 79–88, January/February/March 1992.
- [286] M. D. Vose, *Foundations of Genetic Algorithms 2*, ch. Modeling Simple Genetic Algorithms, pp. 63–73. California, USA: L. D. Whitley, ed., Morgan Kaufmann, 1993.
- [287] A. H. Wright, *Foundations of Genetic Algorithms*, ch. Genetic Algorithms for Real Parameter Optimization, pp. 205–218. California, USA: G. Rawlins, ed., Morgan Kaufmann, 1991.
- [288] C. Z. Janikow and Z. Michalewicz, "An experimental comparison of binary and floating point representations in genetic algorithms," in *Proceedings of the Fourth International Conference on Genetic Algorithms* (R. K. Belew and L. B. Booker, eds.), (California, USA), pp. 31–36, Morgan Kaufmann, 1991.
- [289] R. Tanese, *Distributed Genetic Algorithms for Function Optimization*. PhD thesis, University of Michigan, 1989.
- [290] J. E. Baker, "Adaptive selection methods for genetic algorithms," in *Proceedings of the First International Conference on Genetic Algorithms and Their Applications* (J. J. Grefenstette, ed.), (New Jersey, USA), pp. 101–111, Lawrence Erlbaum Associates, 1985.
- [291] T. Blickle and L. Thiele, "A comparison of selection schemes used in evolutionary algorithms," *Evolutionary Computation*, vol. 4, pp. 361–394, Winter 1996.
- [292] D. E. Goldberg and K. Deb, *Foundations of Genetic Algorithms*, ch. A Comparative Analysis of Selection Schemes Used in Genetic Algorithms, pp. 69–93. California, USA: G. Rawlins, ed., Morgan Kaufmann, 1991.
- [293] L. Eshelman and J. Schaffer, "Preventing premature convergence in genetic algorithms by preventing incest," in *Proceedings of the Fourth International Conference on Genetic Algorithms* (R. K. Belew and L. B. Booker, eds.), (California, USA), pp. 115–122, Morgan Kaufmann, 1991.
- [294] G. Syswerda, "Uniform crossover in genetic algorithms," in *Proceedings of the Third International Conference on Genetic Algorithms* (J. D. Schaffer, ed.), (California, USA), pp. 2–9, Morgan Kaufmann, 1989.
- [295] W. Spears and K. De Jong, *Foundations of Genetic Algorithms*, ch. An Analysis of Multi-Point Crossover, pp. 301–315. California, USA: G. Rawlins, ed., Morgan Kaufmann, 1991.
- [296] J. D. Schaffer, R. A. Caruana, L. J. Eshelman, and R. Das, "A study of control parameters affecting on-line performance of genetic algorithms for function optimization," in *Proceedings of the Third International Conference on Genetic Algorithms* (J. D. Schaffer, ed.), (California, USA), pp. 51–60, Morgan Kaufmann, 1989.

- [297] J. J. Grefenstette, "Optimization of control parameters for genetic algorithms," *IEEE Transactions on Systems, Man and Cybernetics*, vol. SMC-16, pp. 122–128, January 1986.
- [298] T. Bäck, "Optimal mutation rates in genetic search," in *Proceedings of the Fifth International Conference on Genetic Algorithms* (S. Forrest, ed.), (California, USA), pp. 2–8, Morgan Kaufmann, 1993.
- [299] T. Bäck, "Self adaptation in genetic algorithms," in *Proceedings of the First European Conference on Artificial Life* (F. J. Varela and P. Bourguine, eds.), (Massachusetts, USA), pp. 263–271, MIT Press, 1992.
- [300] M. J. Juntti, T. Schlösser, and J. O. Lilleberg, "Genetic algorithms for multiuser detection in synchronous CDMA," in *IEEE International Symposium on Information Theory – ISIT'97*, (Ulm, Germany), p. 492, 1997.
- [301] X. F. Wang, W. S. Lu, and A. Antoniou, "A genetic algorithm-based multiuser detector for multiple-access communications," in *IEEE International Symposium on Circuits and System – ISCAS'98*, (Monterey, California, USA), pp. 534–537, 1998.
- [302] C. Ergün and K. Hacioglu, "Application of a genetic algorithm to multi-stage detection in CDMA systems," in *Proceedings of the 9th Mediterranean Electrotechnical Conference – MELECON'98*, (Tel-Aviv, Israel), pp. 846–850, 1998.
- [303] C. Ergün and K. Hacioglu, "Multiuser detection using a genetic algorithm in CDMA communications systems," *IEEE Transactions on Communications*, vol. 48, pp. 1374–1383, August 2000.
- [304] S. Abedi, *Genetic Multiuser Detection for Code Division Multiple Access Systems*. PhD thesis, University of Surrey, 2000.
- [305] M. B. Pursley, "Performance evaluation for phase-coded spread-spectrum multiple-access communication-part i: System analysis," *IEEE Transactions on Communications*, vol. COM-25, pp. 795–799, August 1977.
- [306] R. K. Morrow, Jr., "Bit-to-bit error dependence in slotted DS/SSMA packet systems with random signature sequences," *IEEE Transactions on Communications*, vol. 37, pp. 1052–1061, October 1989.
- [307] J. M. Holtzman, "A simple, accurate method to calculate spread-spectrum multiple-access error probabilities," *IEEE Transactions on Communications*, vol. 40, pp. 461–464, March 1992.
- [308] S. Verdú, *Multiuser Detection*. New York, USA: Cambridge University Press, 1998.
- [309] M. K. Varanasi and B. Aazhang, "Near-optimum detection in synchronous code-division multiple-access systems," *IEEE Transactions on Communications*, vol. 39, pp. 725–736, May 1991.
- [310] S. Verdú, "Minimum probability of error for asynchronous Gaussian multiple-access channel," *IEEE Transactions on Communications*, vol. 32, pp. 85–96, January 1986.
- [311] L. Wei, L. K. Rasmussen, and R. Wyrwas, "Near optimum tree-search detection schemes for bit-synchronous multiuser CDMA systems over Gaussian and two-path Rayleigh-fading channels," *IEEE Transactions on Communications*, vol. 45, pp. 691–700, June 1997.
- [312] L. K. Rasmussen, T. J. Lim, and T. M. Aulin, "Breadth-first maximum likelihood detection in multiuser CDMA," *IEEE Transactions on Communications*, vol. 45, pp. 1176–1178, October 1997.
- [313] J. S. Lee and L. E. Miller, *CDMA Systems Engineering Handbook*. Boston, USA: Artech House Publishers, 1998.
- [314] J. Cavers, "An analysis of pilot symbol assisted modulation for rayleigh fading channels," *IEEE Transactions on Vehicular Technology*, vol. 40, pp. 686–693, November 1991.
- [315] T. Ojanperä and R. Prasad, *Wideband CDMA for Third Generation Mobile Communications*. Boston, USA: Artech House Publishers, 1998.

- [316] Z. Xie, C. K. Rushforth, R. T. Short, and T. K. Moon, "Joint signal detection and parameter estimation in multiuser communications," *IEEE Transactions on Communications*, vol. 41, pp. 1208–1215, August 1993.
- [317] U. Fawer and B. Aazhang, "A multiuser receiver for code division multiple access communications over multipath channels," *IEEE Transactions on Communications*, vol. 43, pp. 1556–1565, February/March/April 1995.
- [318] T. Kawahara and T. Matsumoto, "Joint decorrelating multiuser detection and channel estimation in asynchronous CDMA mobile communication channels," *IEEE Transactions on Vehicular Technology*, vol. 44, pp. 506–515, August 1995.
- [319] S. Chen and Y. Wu, "Maximum likelihood joint channel and data estimation using genetic algorithms," *IEEE Transactions on Signal Processing*, vol. 46, pp. 1469–1473, May 1998.
- [320] Z. Zvonar and M. Stojanovic, "Performance of antenna diversity multiuser receivers in CDMA channels with imperfect fading estimation," *Wireless Personal Communications*, vol. 3, no. 1-2, pp. 91–110, 1996.
- [321] D. N. Kalofonos, M. Stojanovic, and J. G. Proakis, "Analysis of the impact of channel estimation errors on the performance of a MC-CDMA system in a Rayleigh fading channel," in *IEEE Global Telecommunications Conference*, vol. 4, (Phoenix, Arizona, USA), pp. 213–217, November 1997.
- [322] M. Omid, P. Gulak, and S. Pasupathy, "Parallel structures for joint channel estimation and data detection over fading channels," *IEEE Journal of Selected Areas in Communications*, vol. 16, pp. 1616–1629, December 1998.
- [323] M. Stojanovic and Z. Zvonar, "Performance of multiuser detection with adaptive channel estimation," *IEEE Transactions on Communications*, vol. 47, pp. 1129–1132, August 1999.
- [324] P. Schramm, "Differentially coherent demodulation for differential bpsk in spread spectrum systems," *IEEE Transactions on Vehicular Technology*, vol. 48, pp. 1650–1656, September 1999.
- [325] H. Liu and Z. Siveski, "Differentially coherent decorrelating detector for cdma single-path time-varying Rayleigh fading channels," *IEEE Transactions on Communications*, vol. 47, pp. 590–597, April 1999.
- [326] M. Juntti, *Multiuser Demodulation for DS-CDMA Systems in Fading Channels*. PhD thesis, University of Oulu, 1997.
- [327] A. Klein, B. Steiner, and A. Steil, "Known and novel diversity approaches as a powerful means to enhance the performance of cellular mobile radio systems," *IEEE Journal of Selected Areas in Communications*, vol. 14, pp. 1784–1795, December 1996.
- [328] P. Díaz and R. Agustí, "The use of coding and diversity combining for mitigating fading effects in a DS/CDMA system," *IEEE Transactions on Vehicular Technology*, vol. 47, pp. 95–102, February 1998.
- [329] P. Jung and J. Blanz, "Joint detection with coherent receiver antenna diversity in CDMA mobile radio systems," *IEEE Transactions on Vehicular Technology*, vol. 44, pp. 76–88, February 1995.
- [330] A. Naguib and A. Paulraj, "Performance of wireless CDMA with M -ary orthogonal modulation and cell site antenna arrays," *IEEE Journal of Selected Areas in Communications*, vol. 14, pp. 1770–1783, December 1996.
- [331] P. van Rooyen, R. Kohno, and I. Oppermann, "DS-CDMA performance with maximum ratio combining and antenna arrays," *Wireless Networks*, vol. 4, pp. 479–488, June 1998.
- [332] N. Srinivas and K. Deb, "Multiobjective optimization using nondominated sorting in genetic algorithms," *Evolutionary Computation*, vol. 2, pp. 221–248, Autumn 1994.

- [350] K. Cheun, "Performance of direct-sequence spread-spectrum RAKE receivers with random spreading sequences," *IEEE Transactions on Communications*, vol. 45, pp. 1130–1143, September 1997.
- [351] R. S. Lunayach, "Performance of a direct sequence spread-spectrum system with long period and short period code sequences," *IEEE Transactions on Communications*, vol. COM-31, pp. 412–419, March 1983.
- [352] L.-L. Yang and L. Hanzo, "Performance of a residue number system based orthogonal signalling scheme in AWGN channels." Yet to be published.
- [353] L.-L. Yang and L. Hanzo, "Performance of a residue number system based orthogonal signalling scheme over frequency-nonsselective, slowly fading channel." Yet to be published.
- [354] L.-L. Yang and L. Hanzo, "Performance of Residue Number System Based DS-CDMA over Multipath Fading Channels Using Orthogonal Sequences," *European Transactions on Telecommunications*, vol. 9, pp. 525–535, November/December 1998.
- [355] L.-L. Yang and L. Hanzo, "Residue number system arithmetic assisted M -ary modulation," *IEEE Communications Letters*, vol. 3, pp. 28–30, February 1999.
- [356] L.-L. Yang and L. Hanzo, "Residue number system based multiple code DS-CDMA systems," in *Proceedings of IEEE VTC'99*, (Houston, USA), pp. 1450–1454, May 1999.
- [357] L.-L. Yang and L. Hanzo, "Ratio statistic test assisted residue number system based parallel communication systems," in *Proceedings of IEEE VTC'99*, (Houston, USA), pp. 894–898, May 1999.
- [358] K. Yen, L.-L. Yang, and L. Hanzo, "Residual number system assisted CDMA – a new system concept," in *Proceedings of 4th ACTS Mobile Communications Summit'99*, (Sorrento, Italy), pp. 177–182, June 8–11 1999.
- [359] S. Haykin, *Digital Communications*. New York: John Wiley and Sons, 1988.
- [360] R. Pickholtz, D. Schilling, and L. Milstein, "Theory of spread-spectrum communications — a tutorial," *IEEE Transactions on Communications*, vol. COM-30, pp. 855–884, May 1982.
- [361] S. Rappaport and D. Grieco, "Spread-spectrum signal acquisition: Methods and technology," *IEEE Communications Magazine*, vol. 22, pp. 6–21, June 1984.
- [362] E. Ström, S. Parkvall, S. Miller, and B. Ottersten, "Propagation delay estimation in asynchronous direct-sequence code division multiple access systems," *IEEE Transactions on Communications*, vol. 44, pp. 84–93, January 1996.
- [363] R. Rick and L. Milstein, "Optimal decision strategies for acquisition of spread-spectrum signals in frequency-selective fading channels," *IEEE Transactions on Communications*, vol. 46, pp. 686–694, May 1998.
- [364] R. D. Gaudenzi, T. Garde, F. Giannetti, and M. Luise, "A performance comparison of orthogonal code division multiple-access techniques for mobile satellite communications," *IEEE Journal on Selected Areas in Communications*, vol. 13, pp. 325–332, February 1995.
- [365] M. Chase and K. Pahlavan, "Performance of DS-CDMA over measured indoor radio channels using random orthogonal codes," *IEEE Transactions on Vehicular Technology*, vol. 42, pp. 617–624, November 1993.
- [366] S.-W. Kim and W. Stark, "Performance limits of Reed-Solomon coded CDMA with orthogonal signaling in a Rayleigh-fading channel," *IEEE Transactions on Communications*, vol. 46, pp. 1125–1134, September 1998.
- [367] S. Lin and J. Costello, *Error Control Coding: Fundamentals and Applications*. Englewood Cliffs, NJ: Prentice-Hall, 1983.
- [368] R. E. Blahut, *Fast Algorithms for digital Signal Processing*. Addison Wesley Publishing Company, 1984.

- [369] C. Keller and M. Pursley, "Diversity combining for channels with fading and partial-band interference," *IEEE Journal on Selected Areas in Communications*, vol. SAC-5, pp. 248–259, February 1987.
- [370] G. Chyi, G. Proakis, and C. M. Keller, "On the symbol error probability of maximum-selection diversity reception schemes over a Rayleigh fading channel," *IEEE Transactions on Communications*, vol. COM-37, pp. 79–83, January 1989.
- [371] L.-L. Yang and L. Hanzo, "Performance analysis of m -ary orthogonal signaling using errors-and-erasures decoding over frequency-selective rayleigh fading channels," *IEEE Journal on Selected Areas of Communications*, vol. 19, pp. 211–221, February 2001.
- [372] R. W. Watson and C. W. Hastings, "Self-checked computation using residue arithmetic," *Proceedings of the IEEE*, vol. 54, pp. 1920–1931, December 1966.
- [373] N. S. Szabo and R. I. Tanaka, *Residue Arithmetic and Its Applications to Computer Technology*. New York: McGraw-Hill Book Company, 1967.
- [374] E. D. Claudio, G. Orlandi, and F. Piazza, "A systolic redundant residue arithmetic error correction circuit," *IEEE Transactions on Computers*, vol. 42, pp. 427–432, April 1993.
- [375] H. Krishna, K.-Y. Lin, and J.-D. Sun, "A coding theory approach to error control in redundant residue number systems - Part I: theory and single error correction," *IEEE Trans. Circuits Syst.*, vol. 39, pp. 8–17, January 1992.
- [376] J.-D. Sun and H. Krishna, "A coding theory approach to error control in redundant residue number systems - Part II: multiple error detection and correction," *IEEE Trans. Circuits Syst.*, vol. 39, pp. 18–34, January 1992.
- [377] H. Krishna and J.-D. Sun, "On theory and fast algorithms for error correction in residue number system product codes," *IEEE Transactions on Computer*, vol. 42, pp. 840–852, July 1993.
- [378] W. Jenkins and E. Altman, "Self-checking properties of residue number error checkers based on mixed radix conversion," *IEEE Transactions on Circuit and Systems*, vol. 35, pp. 159–167, February 1988.
- [379] F. Barsi and P. Maestrini, "Error correction properties of redundant residue number systems," *IEEE Transactions on Computers*, vol. 22, pp. 307–315, March 1973.
- [380] S.-S. Yau and Y.-C. Liu, "Error correction in redundant residue number systems," *IEEE Transactions on Computers*, vol. 22, pp. 5–11, January 1973.
- [381] D. Mandelbaum, "Error correction in residue arithmetic," *IEEE Transactions on Computers*, vol. 21, pp. 538–545, June 1972.
- [382] M. Etzel and W. Jenkins, "Redundant residue number systems for error detection and correction in digital filters," *IEEE Transactions on Acoustics, Speech, and Signal Processing*, vol. 28, pp. 538–545, October 1980.
- [383] W. Jenkins, "The design of error checkers for self-checking residue number arithmetic," *IEEE Transactions on Computers*, vol. 32, pp. 388–396, April 1983.
- [384] F. Barsi and P. Maestrini, "Improved decoding algorithms for arithmetic residue codes," *IEEE Transactions on Information Theory*, vol. 24, pp. 640–644, September 1978.
- [385] V. Ramachandran, "Single residue error correction in residue number systems," *IEEE Transactions on Computers*, vol. 32, pp. 504–507, May 1983.
- [386] L.-L. Yang and L. Hanzo, "Coding theory and performance of redundant residue number system codes." submitted to *IEEE Transactions on Information Theory*, 1999.

- [387] L.-L. Yang and L. Hanzo, "Performance of residue number system based DS-CDMA over multipath fading channels using orthogonal sequences," *European Trans. on Telecommunications*, vol. 9, pp. 525–536, November - December 1998.
- [388] M. A. Soderstrand, W. K. Jenkins, and G. A. Jullien, *Residue Number System Arithmetic: Modern Applications in Digital Signal Processing*. New York, USA: IEEE Press, 1986.
- [389] M. A. Soderstrand, "A high-speed, low-cost, recursive digital filter using residue number arithmetic," *Proceeding IEEE*, vol. 65, pp. 1065–1067, July 1977.
- [390] W. K. Jenkins and B. J. Leon, "The use of residue number system in the design of finite impulse response filters," *IEEE Transactions on Circuits Systems*, vol. CAS-24, pp. 191–201, April 1977.
- [391] R. Krishnan, G. Jullien, and W. Miller, "Complex digital signal processing using quadratic residue number systems," *IEEE Transactions on Acoustics, Speech and Signal Processing*, vol. 34, pp. 166–176, February 1986.
- [392] G. Alia and E. Martinelli, "A vlsi modulo m multiplier," *IEEE Transactions on Computers*, vol. 40, pp. 873–878, July 1991.
- [393] T. Vu, "Efficient implementations of the chinese remainder theorem for sign detection and residue decoding," *IEEE Transactions on Computers*, vol. 34, pp. 646–651, July 1985.
- [394] R. Cosentino, "Fault tolerance in a systolic residue arithmetic processor array," *IEEE Transactions on Computers*, vol. 37, pp. 886–889, July 1988.
- [395] B.-D. Tseng, G. Jullien, and W. Miller, "Implementation of fft structure using the residue number system," *IEEE Transactions on Computers*, vol. 28, pp. 831–844, November 1979.
- [396] F. Barsi and P. Maestrini, "Error detection and correction by product codes in residue number system," *IEEE Transactions on Computers*, vol. 23, pp. 915–924, September 1974.
- [397] A. P. Shenoy and R. Kumaresan, "Fast base extension using a redundant modulus in rns," *IEEE Transactions on Computers*, vol. 38, pp. 292–296, February 1989.
- [398] D. Radhakrishnan and Y. Yuan, "Novel approaches to the design of vlsi rns multipliers," *IEEE Transactions on Circuit and Systems-II*, vol. 39, pp. 52–57, January 1992.
- [399] G. Alia and E. Martinelli, "On the lower bound to the vlsi complexity of number conversion from weighted to residue representation," *IEEE Transactions on Computers*, vol. 42, pp. 962–967, August 1993.
- [400] G. Alia and E. Martinelli, "A vlsi algorithm for direct and reverse conversion from weighted binary number system to residue number system," *IEEE Transactions on circuits and Systems*, vol. 31, pp. 1033–1039, December 1984.
- [401] K. Elleithy and M. Bayoumi, "Fast and flexible architectures for rns arithmetic decoding," *IEEE Transactions on Circuits and Systems-II*, vol. 39, pp. 226–235, April 1992.
- [402] S. G. Glisic and P. A. Leppanen, *Wireless Communications: TDMA versus CDMA*. Kluwer Academic Publishers, Boston, 1997.
- [403] P. Enge and D. Sarwate, "Spread spectrum multiple access performance of orthogonal code: impulse noise," *IEEE Transactions on Communications*, vol. COM-36, pp. 98–105, January 1988.
- [404] L.-L. Yang and C.-S. Li, "DS-CDMA performance of random orthogonal codes over nakagami multipath fading channels," in *Proceedings of IEEE ISSSTA'96*, (Mainz, Germany), pp. 68–72, IEEE, Sept 1996.

- [405] R. V. Nee and A. D. Wild, "Reducing the peak-to-average power ratio of OFDM," in *Proceedings of IEEE Vehicular Technology Conference (VTC'98)* [554], pp. 2072–2076.
- [406] W. G. Jeon, K. H. Chang, and Y. S. Cho, "An adaptive data predistorter for compensation of nonlinear distortion in OFDM systems," *IEEE Transactions on Communications*, vol. 45, pp. 1167–1171, October 1997.
- [407] L. B. Milstein, T. S. Rappaport, and R. Barghouti, "Performance evaluation for cellular CDMA," *IEEE Journal on Selected Areas in Communications*, vol. 10, no. 4, pp. 680–689, 1992.
- [408] T. Vlachus and E. Geraniotis, "Performance study of hybrid spread-spectrum random-access communications," *IEEE Transactions on Communications*, vol. 39, pp. 975–985, June 1991.
- [409] G. D. Forney, "Exponential error bounds for erasure, list, and decision feedback scheme," *IEEE Transactions on Information Theory*, vol. 14, pp. 206–220, March 1968.
- [410] A. J. Viterbi, "A robust ratio-threshold technique to mitigate tone and partial band jamming in coded MFSK systems," in *Proceedings of IEEE Military Communications Conferences Rec.*, pp. 22.4.1–22.4.5, IEEE, October 1982.
- [411] L.-F. Chang and R. McEliece, "A study of Viterbi's ratio threshold AJ technique," in *Proceedings of IEEE Military Communications Conferences Rec.*, pp. 182–186, IEEE, October 1984.
- [412] C. Baum and M. Pursley, "Bayesian methods for erasure insertion in frequency-hop communication system with partial-band interference," *IEEE Transactions on Communications*, vol. 40, pp. 1231–1238, July 1992.
- [413] C. Baum and M. Pursley, "A decision-theoretic approach to the generation of side information in frequency-hop multiple-access communications," *IEEE Transactions on Communications*, vol. 43, pp. 1768–1777, February/March/April 1995.
- [414] C. Baum and M. Pursley, "Bayesian generation of dependent erasures for frequency-hop communications and fading channels," *IEEE Transactions on Communications*, vol. 44, pp. 1720–1729, December 1996.
- [415] C. Baum and M. Pursley, "Erasure insertion in frequency-hop communications with fading and partial-band interference," *IEEE Transactions on Vehicular Technology*, vol. 46, pp. 949–956, November 1997.
- [416] G. Forney, *Concatenated codes*. MIT Press, Cambridge, Massachusetts, 1966.
- [417] T. Kasami, T. Takata, T. Fujiwara, and S. Lin, "A concatenated coded modulation scheme for error control," *IEEE Transactions on Communications*, vol. 38, pp. 752–763, June 1990.
- [418] T. Kasami, T. Takata, K. Yamashita, T. Fujiwara, and S. Lin, "On bit-error probability of a concatenated coding scheme," *IEEE Transactions on Communications*, vol. 45, pp. 536–543, May 1997.
- [419] L. B. Milstein, R. B. Pickholtz, and D. L. Schilling, "Optimization of the processing gain of an fsk-fh system," *IEEE Transactions on Communications*, vol. 28, pp. 1062–1069, July 1980.
- [420] C. W. Helstrom, *Probability and Stochastic Processes for Engineering*. New York: Macmillan Publishing Company, 2nd ed., 1991.
- [421] *Consultative Committee for Space Data System: Recommendation for Space Data System Standard: Telemetry Channel Coding "Blue Book"*, May 1984.
- [422] S. B. Weinstein and P. Ebert, "Data transmission by frequency-division multiplexing using the discrete Fourier transform," *IEEE Transactions on Communication Technology*, vol. 19, pp. 628–634, October 1971.
- [423] J. Bingham, "Multicarrier modulation for data transmission: An idea whose time has come," *IEEE Communications Magazine*, pp. 5–14, May 1990.

- [424] I. Kalet, "The multitone channel," *IEEE Transactions on Communications*, vol. 37, pp. 119–124, February 1989.
- [425] L.-L. Yang and L. Hanzo, "Slow frequency-hopping multicarrier DS-SS," in *International Symposium on Wireless Personal Multimedia Communications (WPMC'99)*, (Amsterdam, The Netherlands), pp. 224–229, September:21–23 1999.
- [426] R. Li and G. Stette, "Time-limited orthogonal multicarrier modulation schemes," *IEEE Transactions on Communications*, vol. 43, pp. 1269–1272, February/March/April 1995.
- [427] L. Goldfeld and D. Wulich, "Multicarrier modulation system with erasures-correcting decoding for nakagami fading channels," *European Trans. on Telecommunications*, vol. 8, pp. 591–595, November–December 1997.
- [428] E. Sousa, "Performance of a direct sequence spread spectrum multiple access system utilizing unequal carrier frequencies," *IEICE Transactions on Communications*, vol. E76-B, pp. 906–912, August 1993.
- [429] B. Saltzberg, "Performance of an efficient parallel data transmission system," *IEEE Transactions on Communication Technology*, vol. 15, pp. 805–811, December 1967.
- [430] C. Baum and K. Conner, "A multicarrier transmission scheme for wireless local communications," *IEEE Journal on Selected Areas in Communications*, vol. 14, pp. 512–529, April 1996.
- [431] V. Dasilva and E. Sousa, "Multicarrier orthogonal CDMA signals for quasi-synchronous communication systems," *IEEE Journal on Selected Areas in Communications*, vol. 12, pp. 842–852, June 1994.
- [432] L. Vandendorpe and O. V. de Wiel, "MIMO DFE equalization for multitone DS/SS systems over multipath channels," *IEEE Journal on Selected Areas in Communications*, vol. 14, pp. 502–511, April 1996.
- [433] N. Al-Dhahir and J. Cioffi, "A bandwidth-optimized reduced-complexity equalized multicarrier transceiver," *IEEE Transactions on Communications*, vol. 45, pp. 948–956, August 1997.
- [434] P. Jung, F. Berens, and J. Plechinger, "A generalized view on multicarrier CDMA mobile radio systems with joint detection (Part i)," *FREQUENZ*, vol. 51, pp. 174–184, July–August 1997.
- [435] S. Hara and R. Prasad, "Design and performance of multicarrier CDMA system in frequency-selective Rayleigh fading channels," *IEEE Transactions on Vehicular Technology*, vol. 48, pp. 1584–1595, September 1999.
- [436] V. Tarokh and H. Jafarkhani, "On the computation and reduction of the peak-to-average power ratio in multicarrier communications," *IEEE Transactions on Communications*, vol. 48, pp. 37–44, January 2000.
- [437] D. Wulich and L. Goldfeld, "Reduction of peak factor in orthogonal multicarrier modulation by amplitude limiting and coding," *IEEE Transactions on Communications*, vol. 47, pp. 18–21, January 1999.
- [438] H.-W. Kang, Y.-S. Cho, and D.-H. Youn, "On compensating nonlinear distortions of an OFDM system using an efficient adaptive predistorter," *IEEE Transactions on Communications*, vol. 47, pp. 522–526, April 1999.
- [439] Y.-H. Kim, I. Song, S. Seokho, and S. R. Park, "A multicarrier CDMA system with adaptive subchannel allocation for forward links," *IEEE Transactions on Vehicular Technology*, vol. 48, pp. 1428–1436, September 1999.
- [440] X. Gui and T.-S. Ng, "Performance of asynchronous orthogonal multicarrier CDMA system in frequency selective fading channel," *IEEE Transactions on Communications*, vol. 47, pp. 1084–1091, July 1999.
- [441] T. Lok, T. Wong, and J. Lehnert, "Blind adaptive signal reception for MC-SS systems in Rayleigh fading channels," *IEEE Transactions on Communications*, vol. 47, pp. 464–471, March 1999.

- [442] B. Rainbolt and S. Miller, "Multicarrier CDMA for cellular overlay systems," *IEEE Journal on Selected Areas in Communications*, vol. 17, pp. 1807–1814, October 1999.
- [443] S.-M. Tseng and M. Bell, "Asynchronous multicarrier DS-CDMA using mutually orthogonal complementary sets of sequences," *IEEE Transactions on Communications*, vol. 48, pp. 53–59, January 2000.
- [444] D. Rowitch and L. Milstein, "Convolutionally coded multicarrier DS-CDMA systems in a multipath fading channel – Part I: Performance analysis," *IEEE Transactions on Communications*, vol. 47, pp. 1570–1582, October 1999.
- [445] D. Rowitch and L. Milstein, "Convolutionally coded multicarrier DS-CDMA systems in a multipath fading channel – Part II: Narrow-band interference suppression," *IEEE Transactions on Communications*, vol. 47, pp. 1729–1736, November 1999.
- [446] D.-W. Lee and L. Milstein, "Comparison of multicarrier DS-CDMA broadcast systems in a multipath fading channel," *IEEE Transactions on Communications*, vol. 47, pp. 1897–1904, December 1999.
- [447] N. Yee, J.-P. Linnartz, and G. Fettweis, "Multi-carrier CDMA in indoor wireless radio network," *IEICE Transactions on Communications*, vol. E77-B, pp. 900–904, July 1994.
- [448] S. Kondo and L. Milstein, "On the use of multicarrier direct sequence spread spectrum systems," in *Proceedings of IEEE MILCOM'93*, (Boston, MA), pp. 52–56, Oct. 1993.
- [449] V. M. DaSilva and E. S. Sousa, "Performance of orthogonal CDMA codes for quasi-synchronous communication systems," in *Proceedings of IEEE ICUPC'93*, (Ottawa, Canada), pp. 995–999, Oct. 1993.
- [450] L. Vandendorpe, "Multitone direct sequence CDMA system in an indoor wireless environment," in *Proceedings of IEEE First Symposium of Communications and Vehicular Technology in the Benelux, Delft, The Netherlands*, pp. 4.1–1–4.1–8, Oct. 1993.
- [451] B. Steiner, "Time domain uplink channel estimation in multicarrier-CDMA mobile radio system concepts," in *Multi-Carrier Spread-Spectrum* (K. Fazel and G. P. Fettweis, eds.), pp. 153–160, Kluwer Academic Publishers, 1997.
- [452] K.-W. Yip and T.-S. Ng, "Tight error bounds for asynchronous multicarrier CDMA and their application," *IEEE Communications Letters*, vol. 2, pp. 295–297, November 1998.
- [453] S. Kondo and L. Milstein, "Performance of multicarrier DS CDMA systems," *IEEE Transactions on Communications*, vol. 44, pp. 238–246, February 1996.
- [454] B. Popović, "Spreading sequences for multicarrier CDMA systems," *IEEE Transactions on Communications*, vol. 47, pp. 918–926, June 1999.
- [455] P. Jung, P. Berens, and J. Plechinger, "Uplink spectral efficiency of multicarrier joint detection code division multiple access based cellular radio systems," *Electronics Letters*, vol. 33, no. 8, pp. 664–665, 1997.
- [456] D.-W. Lee, H. Lee, and J.-S. Kim, "Performance of a modified multicarrier direct sequence CDMA system," *Electronics and Telecommunications Research Institute Journal*, vol. 19, pp. 1–11, April 1997.
- [457] A. Chouly, A. Brajal, and S. Jourdan, "Orthogonal multicarrier techniques applied to direct sequence spread spectrum CDMA systems," in *Proceedings of the IEEE GLOBECOM '93*, (Houston, USA), pp. 1723–1728, November 1993.
- [458] L. Rasmussen and T. Lim, "Detection techniques for direct sequence and multicarrier variable rate for broadband CDMA," in *Proceedings of the ICCS/ISPACS '96*, pp. 1526–1530, 1996.

- [459] P. Jung, F. Berens, and J. Plechinger, "Joint detection for multicarrier CDMA mobile radio systems-Part II: Detection techniques," in *Proceedings of the IEEE ISSSTA*, vol. 3, (Mainz, Germany), pp. 996–1000, September 1996.
- [460] Y. Sanada and M. Nakagawa, "A multiuser interference cancellation technique utilizing convolutional codes and multicarrier modulation for wireless indoor communications," *IEEE Journal on Selected Areas in Communications*, vol. 14, pp. 1500–1509, October 1996.
- [461] Q. Chen, E. S. Sousa, and S. Pasupathy, "Multicarrier CDMA with adaptive frequency hopping for mobile radio systems," *IEEE Journal on Selected Areas in Communications*, vol. 14, pp. 1852–1857, December 1996.
- [462] N. Yee, J.-P. Linnartz, and G. Fettweis, "Multicarrier CDMA in indoor wireless radio networks," in *Proceedings of PIMRC'93*, pp. 109–113, 1993.
- [463] L. Vandendorpe, "Multitone spread spectrum multiple access communications system in a multipath Rician fading channel," *IEEE Transactions on Vehicular Technology*, vol. 44, no. 2, pp. 327–337, 1995.
- [464] L.-L. Yang and L. Hanzo, "Overlapping M -ary frequency shift keying spread-spectrum multiple-access systems using random signature sequences," *IEEE Transactions on Vehicular Technology*, vol. 48, pp. 1984–1995, November 1999.
- [465] J. Wang and M. Moeneclaey, "Hybrid DS/SFH-SSMA with predetection diversity and coding over indoor radio multipath Rician-fading channels," *IEEE Transactions on Communications*, vol. 40, pp. 1654–1662, October 1992.
- [466] A. J. Viterbi and J. K. Omura, *Principle of Digital Communication and Coding*. New York: McGraw-Hill, 1979.
- [467] T. R. N. Rao and E. Fujiwara, *Error-Control Coding for Computer Systems*. New Jersey: Prentice Hall, 1989.
- [468] S. M. Johnson, "A new upper bound for error-correcting codes," *IRE Transactions on Information Theory*, vol. 8, no. 2, pp. 203–207, 1962.
- [469] F. J. Macwilliams and N. J. A. Sloane, *The Theory of Error-Correcting Codes*. New York: North-Holland, 1977.
- [470] L.-L. Yang and L. Hanzo, "Performance of generalized multicarrier DS-CDMA over Nakagami- m fading channels," *Submitted for publication (<http://www-mobile.ecs.soton.ac.uk/lly>)*, 2000.
- [471] L.-L. Yang and L. Hanzo, "A space-time spreading assisted broadband multicarrier DS-CDMA scheme: System design and performance analysis," *Submitted for Possible Publication (<http://www-mobile.ecs.soton.ac.uk/lly>)*, July 2001.
- [472] L.-L. Yang and L. Hanzo, "Performance analysis of space-time spreading assisted wideband CDMA systems communicating over multipath Nakagami fading channels," *Submitted for Possible Publication (<http://www-mobile.ecs.soton.ac.uk/lly>)*, May 2001.
- [473] M. S. Alouini and M. K. Simon, "Performance of coherent receiver with hybrid SC/MRC over Nakagami- m fading channels," *IEEE Transactions on Vehicular Technology*, vol. 48, pp. 1155–1164, July 1999.
- [474] H. Xiang, "Binary code-division multiple-access systems operating in multipath fading, noise channels," *IEEE Transactions on Communications*, vol. 33, pp. 775–784, August 1985.
- [475] M. Simon and M.-S. Alouini, "A unified performance analysis of digital communication with dual selective combining diversity over correlated Rayleigh and Nakagami- m fading channels," *IEEE Transactions on Communications*, vol. 47, pp. 33–43, January 1999.

- [476] M.-S. Alouini and M. Simon, "Application of the dirichlet transformation to the performance evaluation of generalized selection combining over Nakagami- m fading channels," *Journal of Communications and Networks*, vol. 47, pp. 5–13, March 1999.
- [477] Q. T. Zhang, "Exact analysis of postdetection combining for DPSK and NKSF systems over arbitrarily correlated Nakagami channels," *IEEE Transactions on Communications*, vol. 46, pp. 1459–1467, November 1998.
- [478] S.-W. Kim and Y.-H. Lee, "Combined rate and power adaption in DS/CDMA communications over Nakagami fading channels," *IEEE Transactions on Communications*, vol. 48, pp. 162–168, January 2000.
- [479] M. Simon and D. Divsalar, "Some new twists to problems involving the gaussian probability integral," *IEEE Transactions on Communications*, vol. 46, pp. 200–210, February 1998.
- [480] G. Efthymoglou, V. Aalo, and H. Helmken, "Performance analysis of coherent DS-CDMA system in a Nakagami fading channel with arbitrary parameters," *IEEE Transactions on Vehicular Technology*, vol. 46, pp. 289–296, May 1997.
- [481] M. Katz, *Code Acquisition in Advanced CDMA Networks*. Acta Universitatis Ouluensis Technica, Oulu, C 175, 2002.
- [482] A. J. Viterbi, *CDMA: Principles of Spread Spectrum Communications*. New York: Addison-Wesley Publishing Company, 1995.
- [483] J. Rapeli, "UMTS: Targets, system concept, and standardization in a global framework," *IEEE Personal Communications*, vol. 2, pp. 20–28, February 1995.
- [484] P.-G. Andermo and L.-M. Ewerbring, "A CDMA-based radio access design for UMTS," *IEEE Personal Communications*, vol. 2, pp. 48–53, February 1995.
- [485] E. Nikula, A. Toskala, E. Dahlman, L. Girard, and A. Klein, "FRAMES multiple access for UMTS and IMT-2000," *IEEE Personal Communications Magazine*, vol. 5, pp. 16–25, Apr. 1998.
- [486] T. Ojanperä and R. Prasad, ed., *Wideband CDMA for 3rd Generation Mobile Communications*. Artech House Publishers, 1998.
- [487] E. Berruto, M. Gudmundson, R. Menolascino, W. Mohr, and M. Pizarroso, "Research activities on UMTS radio interface, network architectures, and planning," *IEEE Communications Magazine*, vol. 36, pp. 82–95, February 1998.
- [488] M. Callendar, "Future public land mobile telecommunication systems," *IEEE Personal Communications*, vol. 12, no. 4, pp. 18–22, 1994.
- [489] *The 3GPP1 website*. <http://www.3gpp.org>.
- [490] *The 3GPP2 website*. <http://www.3gpp2.org>.
- [491] T. Ojanperä and R. Prasad, *Wideband CDMA for Third Generation Mobile Communications*. London: Artech House, 1998.
- [492] E. Dahlman, B. Gudmundson, M. Nilsson, and J. Sköld, "UMTS/IMT-2000 based on wideband CDMA," *IEEE Communications Magazine*, vol. 36, pp. 70–80, Sep. 1998.
- [493] T. Ojanperä, "Overview of research activities for third generation mobile communications," in Glisic and Leppänen [92], ch. 2 (Part 4), pp. 415–446.
- [494] European Telecommunications Standards Institute, *The ETSI UMTS Terrestrial Radio Access (UTRA) ITU-R RTT Candidate Submission*, June 1998. ETSI/SMG/SMG2.

- [495] Association of Radio Industries and Businesses, *Japan's Proposal for Candidate Radio Transmission Technology on IMT-2000: W-CDMA*, June 1998.
- [496] F. Adachi, M. Sawahashi, and H. Suda, "Wideband DS-CDMA for next-generation mobile communications systems," *IEEE Communications Magazine*, vol. 36, pp. 56–69, September 1998.
- [497] F. Adachi and M. Sawahashi, "Wideband wireless access based on DS-CDMA," *IEICE Transactions on Communications*, vol. E81-B, pp. 1305–1316, July 1998.
- [498] A. Sasaki, "Current situation of IMT-2000 radio transmission technology study in Japan," *IEICE Transactions on Communications*, vol. E81-B, pp. 1299–1304, July 1998.
- [499] P. Baier, P. Jung, and A. Klein, "Taking the challenge of multiple access for third-generation cellular mobile radio systems — a European view," *IEEE Communications Magazine*, vol. 34, pp. 82–89, February 1996.
- [500] J. Schwarz da Silva, B. Barani, and B. Arroyo-Fernández, "European mobile communications on the move," *IEEE Communications Magazine*, vol. 34, pp. 60–69, February 1996.
- [501] F. Ovesjö, E. Dahlman, T. Ojanperä, A. Toskala, and A. Klein, "FRAMES multiple access mode 2 - wideband CDMA," in *Proceedings of the IEEE International Symposium on Personal, Indoor and Mobile Radio Communications (PIMRC)*, (Helsinki, Finland), pp. 42–48, Sep. 1-4 1997.
- [502] *The UMTS Forum website*. <http://www.umts-forum.org/>.
- [503] E. L. Kuan, C. H. Wong, and L. Hanzo, "Burst-by-burst adaptive joint detection CDMA," in *Proceedings of the IEEE Vehicular Technology Conference (VTC Spring)*, (Houston, USA), pp. 1628–1632, May 16-20 1999.
- [504] M. Sunay, Z.-C. Honkasalo, A. Hottinen, H. Honkasalo, and L. Ma, "A dynamic channel allocation based TDD DS CDMA residential indoor system," in *IEEE 6th International Conference on Universal Personal Communications, ICUPC'97*, (San Diego, CA), pp. 228–234, October 1997.
- [505] J. Lee, *CDMA Systems Engineering Handbook*. London: Artech House Publishers, 1998.
- [506] L. Hanzo, C. Wong, and P. Cherriman, "Channel-adaptive wideband video telephony," *IEEE Signal Processing Magazine*, vol. 17, pp. 10–30, July 2000.
- [507] P. Cherriman and L. Hanzo, "Programmable H.263-based wireless video transceivers for interference-limited environments," *IEEE Trans. on Circuits and Systems for Video Technology*, vol. 8, pp. 275–286, June 1998.
- [508] A. Fujiwara, H. Suda, and F. Adachi, "Turbo codes application to DS-CDMA mobile radio," *IEICE Transactions on Communications*, vol. E81A, pp. 2269–2273, November 1998.
- [509] M. Juntti, "System concept comparison for multirate CDMA with multiuser detection," in *Proceedings of IEEE Vehicular Technology Conference (VTC'98)* [554], pp. 18–21.
- [510] T. Kasami, *Combinational Mathematics and its Applications*. University of North Carolina Press, 1969.
- [511] A. Brand and A. Aghvami, "Multidimensional PRMA with prioritized Bayesian broadcast — a MAC strategy for multiservice traffic over UMTS," *IEEE Transactions on Vehicular Technology*, vol. 47, pp. 1148–1161, November 1998.
- [512] R. Ormondroyd and J. Maxey, "Performance of low rate orthogonal convolutional codes in DS-CDMA," *IEEE Transactions on Vehicular Technology*, vol. 46, pp. 320–328, May 1997.
- [513] E. L. Kuan and L. Hanzo, "Joint detection CDMA techniques for third-generation transceivers," in *Proceedings of the ACTS Mobile Communications Summit*, (Rhodes, Greece), pp. 727–732, June 1998.

- [514] A. Chockalingam, P. Dietrich, L. Milstein, and R. Rao, "Performance of closed-loop power control in DS-CDMA cellular systems," *IEEE Transactions on Vehicular Technology*, vol. 47, pp. 774–789, August 1998.
- [515] R. Gejji, "Forward-link-power control in CDMA cellular-systems," *IEEE Transactions on Vehicular Technology*, vol. 41, pp. 532–536, November 1992.
- [516] K. Higuchi, M. Sawahashi, and F. Adachi, "Fast cell search algorithm in DS-CDMA mobile radio using long spreading codes," in *Proceedings of IEEE VTC'97*, vol. 3, (Phoenix, AZ), pp. 1430–1434, IEEE, 4–7 May 1997.
- [517] M. Golay, "Complementary series," *IRE Transactions on Information Theory*, vol. IT-7, pp. 82–87, 1961.
- [518] V. Tarokh, H. Jafarkhani, and A. Calderbank, "Space-time block codes from orthogonal designs," *IEEE Transactions on Information Theory*, vol. 45, pp. 1456–1467, May 1999.
- [519] W. Lee, *Mobile Communications Engineering*. New York: McGraw-Hill, 2nd ed., 1997.
- [520] H. Wong and J. Chambers, "Two-stage interference immune blind equaliser which exploits cyclostationary statistics," *Electronics Letters*, vol. 32, pp. 1763–1764, September 1996.
- [521] C.-C. Lee and R. Steele, "Effect of soft and softer handoffs on cdma system capacity," *IEEE Transactions on Vehicular Technology*, vol. 47, pp. 830–841, August 1998.
- [522] M. Gustafsson, K. Jamal, and E. Dahlman, "Compressed mode techniques for inter-frequency measurements in a wide-band DS-CDMA system," in *Proceedings of IEEE International Symposium on Personal, Indoor and Mobile Radio Communications, PIMRC'97*, (Marina Congress Centre, Helsinki, Finland), pp. 231–235, IEEE, 1–4 September 1997.
- [523] D. Knisely, S. Kumar, S. Laha, and S. Nanda, "Evolution of wireless data services : IS-95 to cdma2000," *IEEE Communications Magazine*, vol. 36, pp. 140–149, October 1998.
- [524] Telecommunications Industry Association (TIA), *The cdma2000 ITU-R RTT Candidate Submission*, 1998.
- [525] D. Knisely, Q. Li, and N. Rames, "cdma2000: A third generation radio transmission technology," *Bell Labs Technical Journal*, vol. 3, pp. 63–78, July–September 1998.
- [526] Y. Okumura and F. Adachi, "Variable-rate data transmission with blind rate detection for coherent DS-CDMA mobile radio," *IEICE Transactions on Communications*, vol. E81B, pp. 1365–1373, July 1998.
- [527] M. Raitola, A. Hottinen, and R. Wichman, "Transmission diversity in wideband CDMA," in *Proceeding of VTC'99 (Spring)* [555], pp. 1545–1549.
- [528] J. Liberty Jr. and T. Rappaport, "Analytical results for capacity improvements in CDMA," *IEEE Transactions on Vehicular Technology*, vol. 43, pp. 680–690, August 1994.
- [529] J. Winters, "Smart antennas for wireless systems," *IEEE Personal Communications*, vol. 5, pp. 23–27, February 1998.
- [530] S. Moshavi, "Multiuser detection for DS-CDMA communications," *IEEE Communications Magazine*, vol. 34, pp. 124–136, Oct. 1996.
- [531] T. Lim and S. Roy, "Adaptive filters in multiuser (MU) CDMA detection," *Wireless Networks*, vol. 4, pp. 307–318, June 1998.
- [532] L. Wei, "Rotationally-invariant convolutional channel coding with expanded signal space, part I and II," *IEEE Transactions on Selected Areas in Comms*, vol. SAC-2, pp. 659–686, September 1984.

- [533] T. Lim and M. Ho, "LMS-based simplifications to the kalman filter multiuser CDMA detector," in *Proceedings of IEEE Asia-Pacific Conference on Communications/International Conference on Communication Systems*, (Singapore), November 1998.
- [534] D. You and T. Lim, "A modified blind adaptive multiuser CDMA detector," in *Proceedings of IEEE International Symposium on Spread Spectrum Techniques and Application (ISSSTA'98)* [556], pp. 878–882.
- [535] S. Sun, L. Rasmussen, T. Lim, and H. Sugimoto, "Impact of estimation errors on multiuser detection in CDMA," in *Proceedings of IEEE Vehicular Technology Conference (VTC'98)* [554], pp. 1844–1848.
- [536] Y. Sanada and Q. Wang, "A co-channel interference cancellation technique using orthogonal convolutional codes on multipath rayleigh fading channel," *IEEE Transactions on Vehicular Technology*, vol. 46, pp. 114–128, February 1997.
- [537] P. Tan and L. Rasmussen, "Subtractive interference cancellation for DS-CDMA systems," in *Proceedings of IEEE Asia-Pacific Conference on Communications/International Conference on Communication Systems*, (Singapore), November 1998.
- [538] K. Cheah, H. Sugimoto, T. Lim, L. Rasmussen, and S. Sun, "Performance of hybrid interference canceller with zero-delay channel estimation for CDMA," in *Proceeding of Globecom'98*, (Sydney, Australia), pp. 265–270, IEEE, 8–12 November 1998.
- [539] S. Sun, L. Rasmussen, and T. Lim, "A matrix-algebraic approach to hybrid interference cancellation in CDMA," in *Proceedings of IEEE International Conference on Universal Personal Communications '98*, (Florence, Italy), pp. 1319–1323, October 1998.
- [540] A. Johansson and L. Rasmussen, "Linear group-wise successive interference cancellation in CDMA," in *Proceedings of IEEE International Symposium on Spread Spectrum Techniques and Application (ISSSTA'98)* [556], pp. 121–126.
- [541] D. Guo, L. Rasmussen, S. Sun, T. Lim, and C. Cheah, "MMSE-based linear parallel interference cancellation in CDMA," in *Proceedings of IEEE International Symposium on Spread Spectrum Techniques and Application (ISSSTA'98)* [556], pp. 917–921.
- [542] L. Rasmussen, D. Guo, Y. Ma, and T. Lim, "Aspects on linear parallel interference cancellation in CDMA," in *Proceedings of IEEE International Symposium on Information Theory*, (Cambridge, MA), p. 37, August 1998.
- [543] L. Rasmussen, T. Lim, H. Sugimoto, and T. Oyama, "Mapping functions for successive interference cancellation in CDMA," in *Proceedings of IEEE Vehicular Technology Conference (VTC'98)* [554], pp. 2301–2305.
- [544] S. Sun, T. Lim, L. Rasmussen, T. Oyama, H. Sugimoto, and Y. Matsumoto, "Performance comparison of multi-stage SIC and limited tree-search detection in CDMA," in *Proceedings of IEEE Vehicular Technology Conference (VTC'98)* [554], pp. 1854–1858.
- [545] H. Sim and D. Cruickshank, "Chip based multiuser detector for the downlink of a DS-CDMA system using a folded state-transition trellis," in *Proceeding of VTC'99 (Spring)* [555], pp. 846–850.
- [546] G. L. Turin, "Introduction to spread-spectrum antimultipath techniques and their application to urban digital radio," *Proceedings of IEEE*, vol. 68, pp. 328–353, March 1980.
- [547] B. Lu and X. D. Wang, "Iterative receivers for multiuser space-time coding systems," *IEEE Journal on Selected Areas in Communications*, vol. 18, pp. 2322–2335, November 2000.
- [548] D. Bertsekas and R. Gallager, *Data Networks*. Englewood Cliffs, N.J. : Prentice Hall, 2nd ed., 1992.

- [549] E. L. Kuan and L. Hanzo, "Comparative study of adaptive-rate CDMA transmission employing joint-detection and interference cancellation receivers," in *Proceedings of the IEEE Vehicular Technology Conference (VTC) 2000, Spring conference*, (Tokyo, Japan), May 15-18 2000.
- [550] E. L. Kuan, C. H. Wong, and L. Hanzo, "Burst-by-burst adaptive joint detection CDMA," in *Proceedings of the IEEE Vehicular Technology Conference (VTC Spring)*, (Houston, USA), pp. 1628–1632, May 1999.
- [551] L. Hanzo, P. Cherriman, and E. Kuan, "Interactive cellular and cordless video telephony: State-of-the-art, system design principles and expected performance," *Proceedings of the IEEE*, pp. 1388–1413, September 2000.
- [552] J. M. Torrance and L. Hanzo, "On the upper bound performance of adaptive QAM in a slow Rayleigh fading channel," *IEE Electronics Letters*, pp. 169 – 171, April 1996.
- [553] H. J. Larson and B. O. Shubert, *Probabilistic Models in Engineering Sciences, Volume I: Random Variables and Stochastic Processes*. New York: John Wiley & Sons, 1979.
- [554] IEEE, *Proceedings of IEEE Vehicular Technology Conference (VTC'98)*, (Ottawa, Canada), 18–21 May 1998.
- [555] IEEE, *Proceeding of VTC'99 (Spring)*, (Houston, TX), 16–20 May 1999.
- [556] IEEE, *Proceedings of IEEE International Symposium on Spread Spectrum Techniques and Application (ISSSTA'98)*, (Sun City, South Africa), September 1998.